In Vitro Anti-skin Cancer Properties and Mechanisms of Action of Xanthones from the Mangosteen Pericarp

A thesis submitted in fulfillment of the requirement for the degree of

Doctor of Philosophy

By

Jing Jing WANG

Bachelor of Clinical Medicine

Department of Medical Biotechnology

School of Medicine

Faculty of Health Sciences

Flinders University of South Australia

September 2012

Candidate's Declaration

This work contains no material which has been accepted for the award of any other degree or diploma in any university or other tertiary institution and, to the best of my knowledge and belief, contains no material previously published or written by another person, except where due reference has been made in the text.

Jing Jing Wang

September 2012

Thesis Summary

The incidence of skin cancer has increased more than 600% worldwide since the 1940s, and Australians have the highest incidence in the world, with at least 2 in 3 Australians diagnosed with skin cancer before the age of 70. The current chemotherapy is not effective, with new drugs in high demand. Plants are important sources for anti-cancer drugs. Mangosteen (*Garcinia mangostana* Linn.) is a tropical tree from South East Asia and its fruit pericarp is a well-known traditional medicine.

This study investigated the potential anti-skin cancer activity of the crude extract and major xanthone compounds from the pericarp of mangosteen by investigating the cytotoxicity and underlying cellular and molecular mechanisms. Two types of human skin cancer cell lines were used as *in vitro* models: melanoma SK-MEL-28 and squamous cell carcinoma A-431.

There were five major research outcomes. (i) Development of a methodology for extraction of mangosteen based on chemical composition and antioxidant activity. (ii) Demonstration of anti-proliferative activity towards skin cancer cell lines. The crude extract and six xanthone compounds tested had significant anti-cancer activities, with IC_{50} values ranging from 2.39 to 7.61 µg/ml. The activity was selective against skin cancer cells with less effect on human normal skin fibroblast CCD-1064Sk and the keratinocyte HaCaT cell lines. IC_{50} values of the xanthones were similar to, or much lower than, those of two most commonly used commercial drugs (5-fluorouracil and dacarbazine). (iii) Identification of cellular and molecular pathways. The anti-cancer action of xanthone compounds was found to be via activation of caspases together with the loss of mitochondrial membrane potential

and inhibition of Akt and NFκB survival pathways. In melanoma SK-MEL-28 cells, downregulation of BRAF V600E mutation expression was observed after treatment with some xanthones, e.g. a maximum 6.8-fold decrease in the level of BRAF V600E relative to the untreated control. (iv) Identification of synergistic effects. Synergistic effects between α-mangostin and the other individual compounds were observed. However, no synergistic effect was found between xanthone compounds and commercial drugs under the tested conditions in the current study. (v) Evaluation of anti-metastatic activity of α-mangostin. Skin cancers, especially melanoma, have a high potential to metastasise. α-Mangostin exhibited significant inhibitive activity of invasion and migration at non-toxic doses on both skin cancer cell lines tested. The anti-metastatic activity of α-mangostin was associated with downregulation of mRNA expression of MMP-2 and MMP-9 through inhibiting NFκB and Akt pathways.

This study provides important scientific evidence of the potential antioxidant and antiproliferative activity of extracts and xanthone compounds from the pericarp of mangosteen, and increases understanding of their underlying mechanisms. These findings can contribute to the development of novel plant-derived antioxidant strategies in the treatment of skin cancers.

Keywords: skin cancer; mangosteen; xanthones; cytotoxicity; apoptosis; survival pathway; metastasis

Acknowledgements and Dedication

First and foremost, I would like to pay principal acknowledgement to my supervisors, Prof. Wei Zhang and Dr. Barbara Sanderson, for their very great help in supervision of the project, my PhD candidature and the laboratory.

Thank you, Wei, your concern for my project, career, and professional development provided the perfect role model for an all-round mentor and advisor, and for your encouragement of critical thinking and your high expectations of me.

Thank you, Barbara, for your continuous support, assistance, advice and perspective, especially your help with improving my scientific writing, at various points throughout my candidature. I am very grateful that I could always count on you whenever I needed your help.

Thank you goes to all past and present members of the Department of Medical Biotechnology for assistance with experiments, for advice, and for their companionship. In particular, I would like to thank Professor Chris Franco, for his care and concern, in helping me to get through a difficult time. I wish to directly thank Mrs. Angela Binns and Mrs. Barbara Kupke. Without their continuous and generous help, I could not have completed my project so quickly and smoothly. Thank you, Niki Sperou, for your interest in my project and your help with my slides; Julian Adams, for your help with everything and your sense of humour; Jeff Barrett, for spending time with me to refine my presentation slides. I further thank Onuma Kaewkla, Tanya Bernardo, Vicki Edwards, Hao Jiang, Peng Su, Fitri Widi, Liufei Tan, Shuang Peng, Mahnaz Ramezanpour, Xuelian Zhao, and Shan He for

List of Abbreviations

%	Percentage
AAPH	2, 2'-Azobis (2-amidinopropane) dihydrochloride
Akt	Protein kinase B
ANOVA	Analysis of Variance
ATCC	American type culture collection
AU	Arbitrary unit
BRAF	Serine/threonine-protein kinase *B-Raf*
BSA	Bovine serum albumin
℃	Degree celcius
CDK	Cyclin-dependent kinases
CKI	Cyclin-dependent kinases inhibitors
COX-2	Cyclooxygenase-2
Ct	Threshold of cycle
DAPI	4′, 6-Diamidino-2-phenylindole dihydrochloride
DMBA	7,12-dimethyl[a]benzanthracene
DMEM	Dulbecco's Modified Eagle's Medium
DMSO	Dimethyl sulfoxide
DPPH	2, 2-Diphenyl-1-picrylhydrazyl
%DRSA	Percentage DPPH radical scavenging activity
DTIC	Dacarbazine
DW	Dry weight
EMEA	European agency for the evaluation of medicinal products
ECM	Extracellular matrix
EDTA	Ethylenediaminetetraacetic acid
ERK	Extracellular signal-regulated kinase
EtOH	Ethanol
FAK	Focal adhesion kinase
FBS	Foetal bovine serum
FDA	Food and drug administration
FRAP	Ferric reducing antioxidant power
5-FU	5-Fluorouracil
µg	Microgram
GAE	Gallic acid equivalents
GOI	Gene of interest
h	hour
HCl	Hydrochloric acid
HPLC	High performance liquid chromatography
HO$^-$	Hydroxide ion
IC$_{50}$	50% inhibitory concentration
IκB	Inhibitor of kappaB
IKK	IκB kinase
IL-8	Interleukin-8
IMDM	Iscoves Modified Dulbecco's Medium
IU	International units
JNK	c-Jun NH$_2$-terminal kinase
l	litre
LDL	Low density lipoprotein
µl	microlitre

μM	micromolar
ml	millilitre
MAPK	Mitogen-activated protein kinase
MMP	Matrix metalloproteinase
MPEE	Mangosteen pericarp ethanol extract
MPWE	Mangosteen pericarp water extract
MQ	Milli Q
mRNA	Messenger ribonucleic acid
MTT	3-(4,5-dimethylthiazol-2-yl)-2,5-diphenyl tetrazolium bromide
NFκB	Nuclear factor kappa B
NSAIDS	Nonsteroidal antiinflammatory drugs
OD	Optical density
ORAC	Oxygen radical absorbance capacity
PBS	Phosphate-buffered saline
ONOO⁻	Peroxynitrite
PCR	Polymerase chain reaction
PI	Propidium iodide
PI3K	Phosphoinositide 3-kinase
qRT-PCR	Quantitative real-time reverse transcription PCR
ROS	Reactive oxygen species
RPMI	Roswell Park Memorial Institute
R^2	R square
RT	Room temperature
s	second
SD	Standard deviation
SDS	Sodium Dodecyl Sulfate
SEM	Standard error of the mean
SPSS	Statistical Package for the Social Sciences
TE	Trolox equivalents
TF	Total flavonoids
TNF	Tumor necrosis factor
TP	Total phenolics
TPA	12-O-tetradecanoylphorbol-13-acetate
TRAP	Total radical trapping antioxidant parameter
UCA	Urocanic acid
uPA	Urokinase-type plasminogen activator
UV	Ultraviolet
VEGF	Vascular endothelial growth factor

Publications, Presentations and Awards

Publications

- Jing J. Wang, Barbara J.S. Sanderson, Wei Zhang, 2011. Cytotoxic effect of xanthones from pericarp of the tropical fruit mangosteen (*Garcinia mangostana* Linn.) on human melanoma cells. Food and Chemical Toxicology. 49: 2385–2391

- Jing J. Wang, Barbara J.S. Sanderson, Wei Zhang, 2012. Significant anti-invasive activities of α-mangostin on metastasis of human skin cancer cells. Anticancer Research (Article in press)

- Jing J. Wang, Qing H. Shi, Wei Zhang, Barbara J.S. Sanderson, 2012. Anti-skin cancer properties of phenolic-rich extract from the pericarp of mangosteen (*Garcinia mangostana* Linn.). Food and Chemical Toxicology. 50: 3004-3013.

Publications in Submission

- Jing J. Wang, Wei Zhang, Barbara J.S. Sanderson, 2012. Altered mRNA expression related to the apoptotic effect of three xanthones on human melanoma SK-MEL-28 cell line. Food and Chemical Toxicology (Under review; manuscript No. FCT-6676).

Publications in preparation

- Jing J. Wang, Barbara J.S. Sanderson, Wei Zhang. Anti-proliferative and apoptotic effect of 6 pure xanthone compounds on human squamous cell carcinoma A-431 cells.

- Jing J. Wang, Wei Zhang, Barbara J.S. Sanderson. Xanthones isolated from mangosteen pericarp induce apoptosis in human melanoma SK-MEL-28 cells.

- Jing J. Wang, Barbara J.S. Sanderson, Wei Zhang. Potential synergistic skin cancer suppression by combination of xanthones.

Presentations

- ASMR SA Scientific Meeting 6th June 2012. Adelaide, Australia. Oral Presentation "Inhibitory effect of α-mangostin on proliferation and metastasis of human melanoma SK-MEL-28 cell line"

- Cancer Research Day. 25th November 2011. Adelaide, Australia. Oral Presentation. "Xanthones from mangosteen pericarp: anti-skin cancer properties"

- AusBiotech 2011 National Conference. 16th -19th October 2011. Adelaide, Australia. Oral and Poster Presentation "*In vitro* anti-skin cancer properties and mechanisms of action of α-mangostin from the mangosteen pericarp"

- Asian Congress on Biotechnology. 11th-15th May 2011. Shanghai, China.

Poster Presentation. "Anti-skin cancer activity of crude extract of mangosteen (*Garcinia mangostana* Linn.)"

- Three Minute Thesis Competition 2011. 6th May 2011. Adelaide, Australia. Oral Presentation "Mangosteen combats skin cancer"

- Chemeca 2010. 26th -29th Septemper 2010. Adelaide, Australia. Oral Presentation "Compounds from pericarp of mangosteen (*Garcinia Mangostana* Linn.) induce cell cycle arrest and apoptosis in human melanoma cells"

- 13th World Congress on Cancers of the Skin. 7th -10th April 2010. Madrid, Spain. Oral Presentation "Evaluation of antiproliferation properties of xanthones from pericarp of mangosteen (*Garcinia mangsotana* L.) on human melanoma cells"

Awards
- 2012   Ross Wishart Memorial Award finalist

- 2011   AusBiotech-GSK Student Excellence Award – State Winner

- 2011   Chinese Government Award for Outstanding Self-financed Students Abroad

- 2010   "Top Ten Cited Author in 2007 & 2008" from Mutation Research

- 2010   AusBiotech-GSK Student Excellence Award – State Finalist

- 2008   AusBiotech-GSK Student Excellence Award – State Finalist

- 2008 – 2012 EPRIS Scholarship, Flinders University, Australia

Professional Membership

- 2010- current AusBiotech (Australia's Biotechnology Organisation)

- 2012 – 2013   Australian Society for Medical Research

- 2012-2013   Bioprocessing Network

Table of Content

List of Tables

List of Figures

CHAPTER 1
INTRODUCTION AND LITERATURE REVIEW

1.1 Skin cancer

1.1.1 The skin

The skin is the largest and most versatile organ in our body (Nouri 2008). It serves many distinct functions, including being a protective barrier to infections, ultraviolet radiation (UV), toxins, and temperature extremes, and providing sensory perception, immunologic surveillance, and control of fluid loss (Murphy *et al.* 2005).

The skin consists of three layers (Figure 1-1). The most superficial layer is called the epidermis, the underlying layer is the dermis, and the fatty subcutaneous layer is called the hypodermis. The epidermis contains the keratinocyte, melanocytes, Langerhans cells, while the dermis houses collagen, elastic fibres, blood vessels, and fibroblasts (Murphy *et al.* 2005).
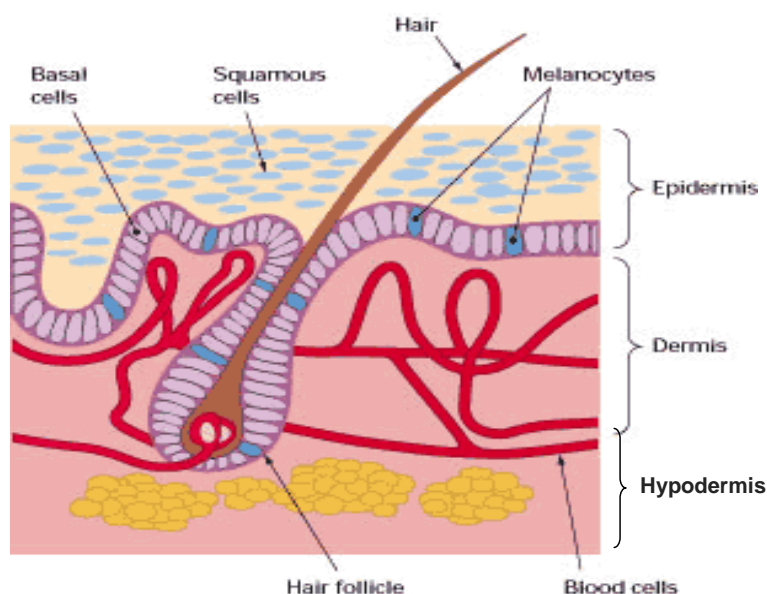
Figure 1-1
The layers of the skin: epidermis, dermis, and hypodermis. The image is adapted from http://drmargaretmann.com/TypesofSkinCancer.aspx.

1.1.2 Major types of skin cancers

Skin cancers are named after the cells from which they originate. There are three major types of skin cancers. Basal cell carcinoma (BCC) and squamous cell

carcinoma (SCC) originat from keratinocyte and melanomas are derived from melanocyte. BCC (70-85% of skin cancers) and SCC (15-20% of skin cancers) are the two most common types of skin cancer (Gupta & Mukhtar 2001). They are often referred to together as "nonmelanoma" skin cancers (NMSC) (Gonzales *et al.* 2008). SCC is invasive and more than 10% will metastasise, while BCC can be locally invasive and destructive (Kwa *et al.* 1992; Miller 1991). Cutaneous malignant melanoma (CMM; 5% of skin cancers) is the third most common type of skin cancer but the most aggressive, being responsible for 80% of total skin cancer deaths (Autier 2004; Mohapatra *et al.* 2007). The appearance of these types of skin cancer is presented in Figure 1-2.
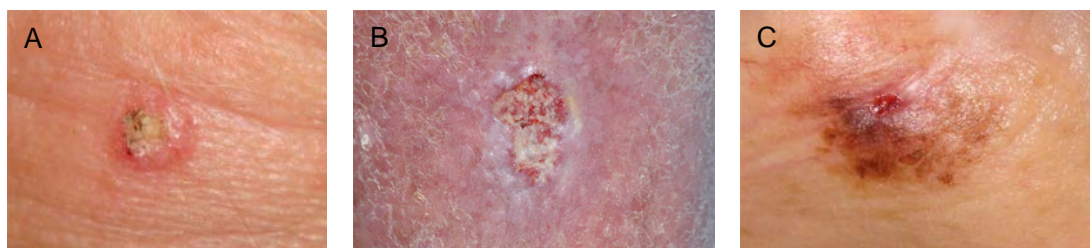
Figure 1-2
The typical appearance of three types of skin cancer: A. Basal cell carcinoma; B: Squamous cell carcinoma; and C: Melanoma. The images are taken from http://drmargaretmann.com/TypesofSkinCancer.aspx.

1.1.3 Epidemiology of skin cancer

Skin cancer is a growing public health problem worldwide because the incidence of both CMM and NMSC has increased dramatically, especially in the population of fair-skinned Caucasians (Carsin *et al.* 2011; Gupta & Mukhtar 2001; Hollestein *et al.* 2012; Nouri 2008). There are one million new cases of skin cancer in the United States per year, and this accounts for 40% of all new cancer cases diagnosed in that country (Jemal *et al.* 2006). It has been estimated that every year 2.75 million new cases of NMSC will be diagnosed worldwide (Armstrong & Kricker 1995). As for melanoma, from 1979 until 1997, a 3.6-fold increase in melanoma incidence was

observed in Caucasian Americans (Autier 2004). In Australia, skin cancer is the most common form of cancer, and Australians have the highest incidence in the world, with at least two in three Australians diagnosed with skin cancer before the age of 70 (AIHW 2008; Parkin *et al.* 2005; Sinclair & Foley 2009; Staples *et al.* 2006). Most skin cancers at early stage can be removed in clinics without being registered for cancer. Therefore, these numbers might be underestimated (Baliga & Katiyar 2006). Furthermore, the increase in the incidence of skin cancer is expected to be sustained due to the ageing of the population and the increased amounts of UV exposure (one causative agent for skin cancer) reaching the earth surface (Johnson *et al.* 1998; Miller & Weinstock 1994; Urbach 1991). Therefore, it is of importance to develop effective chemotherapeutic agents that can prevent or treat skin cancer in order to solve this public health problem.

1.1.4 Ultraviolet (UV) radiation, antioxidants, and skin cancers

1.1.4.1 UV and skin cancers

Skin cancers can be induced by many factors, such as UV radiation from sun exposure, lowered immunity, radiotherapy treatment, and exposure to chemicals and genetic conditions (Nouri 2008). Among these, extensive exposure to UV radiation is a well-recognized causative factor for both melanoma and non-melanoma skin cancers (Armstrong & Kricker 2001).

The relationship between UV radiation and skin cancers has been comprehensively reviewed by de Gruijl *et al.* (2005) and Sander *et al.* (2004). The mechanism involved in the development of UV-induced skin cancer is complex (Figure 1-3). UV exposure of skin induces reactive oxygen species (ROS) that react with proteins, lipids and DNA (Berton *et al.* 1997; Li *et al.* 1996; Peak *et al.* 1988). The increased

generation of ROS results in oxidative stress that overwhelms the antioxidant defence ability of the target system (Sies 1991). The induction of oxidative stress and imbalance of the antioxidant defence system can lead to inflammation, photoageing, systemic immunosuppression, and eventually skin cancer (Cole *et al.* 1986; de Gruijl *et al.* 1993; Mukhtar & Elmets 1996). It has been suggested that oxidative stress may play different roles in the pathogenesis of melanoma and nonmelanoma skin cancers (Sander *et al.* 2004). It is likely that in nonmelanoma skin cancers, a diminished antioxidant defence caused by chronic UV-exposure contributes to multistep carcinogenesis. Melanoma cells might use their ability to generate ROS to damage surrounding tissue and thus support the progression of metastasis (Sander *et al.* 2004).
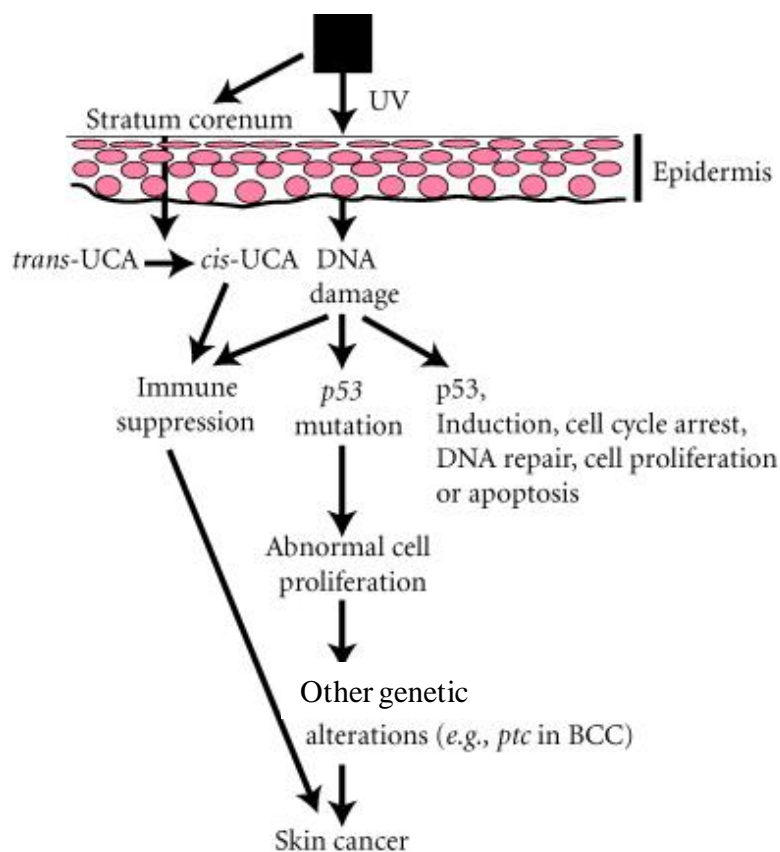
Figure 1-3
The cellular and molecular pathways involved in the development of UV-induced skin cancer is a complex process involving at least two distinct pathways that interact or converge to cause skin cancer (Ouhtit & Ananthaswamy 2001). Abbreviations: UCA, urocanic acid; Ptc, patched (a tumor suppressor gene, which has been indicated in the development of basal cell carcinoma (BCC)) (Ouhtit & Ananthaswamy 2001).

Between 1970 and 1987, substantial damage to the protective ozone layer resulted in greater amount of UV radiation reaching the earth's surface (Duthie *et al.* 1999). UV radiation is divided into three categories dependent on wavelength: long wave UVA (320-400 nm), medium wave UVB (280-320 nm), and short wave UVC (200-280 nm) (Afaq *et al.* 2002; Clydesdale *et al.* 2001; Duthie *et al.* 1999).

UVA, the ageing ray, accounts for 90-95% of solar UV radiation. UVA has the ability to penetrate into the epidermis and dermis and generate ROS (e.g. singlet oxygen and hydroxyl free radicals), resulting in damage to DNA, protein and lipids

(Burney *et al.* 1999; DiGiovanni 1992). UVA has been linked to 67% of malignant melanomas (Afaq & Mukhtar 2001, 2002; Clydesdale *et al.* 2001; Trautinger 2001).

UVB, the burning ray, makes up approximately 5% of total UV light. It acts mainly in the epidermal basal cell layer of the skin and induces direct and indirect adverse biological effects. These effects include the isomerisation of trans- to cis-urocanic acid (UCA), induction of ornithine decarboxylase activity, stimulation of DNA synthesis, production of free radical in the skin, photoageing, and eventually photocarcinogenesis (Filip *et al.* 2009). The effect of UVB significantly decreases antioxidants in the skin, impairing the skin's ability to protect itself against the free radicals generated by exposure to UV light. It is considered responsible for inducing skin cancer (squamous and basal cell carcinoma) by inducing DNA damage (Afaq *et al.* 2002). It is also suggested to suppress the skin's immune defence system (Afaq & Mukhtar 2002; Clydesdale *et al.* 2001; De Gruijl 2002; Trautinger 2001).

UVC from the sun is absorbed by molecular oxygen and ozone in the earth's atmosphere and no solar radiation below 290 nm reaches the surface of the earth (Clydesdale *et al.* 2001; De Gruijl 2002). UVC is therefore not of physiological significance even though it has potential mutagenic nature. However, it remains unclear to what extent UVC could induce skin cancer in humans, even though the incidence of skin cancer would increase if ozone dismantling continues increase levels of UVC. (Rass & Reichrath 2008).

1.1.4.2 Antioxidants and UV-induced skin cancers

Antioxidants are compounds that can delay or inhibit the oxidation of lipids and other molecules by inhibiting the initiation or propagation of oxidative chain

reactions, and they can therefore prevent or repair oxygen damage done to the body's cells (Javanmardi *et al.* 2003). ROS, in the form of superoxide anion, hydrogen peroxide and hydroxyl radical, are natural by-products of the human organism's metabolism (Manda *et al.* 2009). Mammalian preventive and defensive systems combat and reduce the oxidative damage. However, the system cannot completely eliminate the harmful activities of ROS, particularly when the productions are increased in some metabolic, physiologic, pathologic, and other situations, such as UV exposure (Sies 1991). Therefore, antioxidants play a beneficial role in protection against oxidative stress induced damage, such as ageing and cancer (Aramwit *et al.* 2010; Nakamura *et al.* 2008; Tsao & Deng 2004).

In recent years, naturally occurring compounds, such as curcumin, silymarin, green tea, and proanthocyanidins (Baliga & Katiyar 2006), have gained considerable attention as protective antioxidant agents. The mechanism of efficacy of antioxidants in protecting against UV damage probably results from their effect in quenching and scavenging free radicals induced by UV exposure (Krinsky 1989; Sies 1993). The mechanisms may also involve blocking the activation of carcinogens and inducing detoxification pathways (Bertram *et al.* 1987; Wattenberg 1985), and in modulating mitogenic and survival signalling cascades leading to cell cycle arrest and apoptosis induction (Singh *et al.* 2002; Sun *et al.* 2004). A summary of the chemopreventive effect, including UV-protective effects, of natural antioxidants is discussed in Section 1.2.1.

1.1.5 Skin cancer development

UV radiation-induced skin cancer is complex, involving multiple steps mediated via various cellular, biochemical, and molecular changes. The development of UV-

induced skin cancer has been demonstrated to consist of three stages (Sander *et al.* 2004). They are listed as follows: (1) tumour initiation consisting of genotoxic effects in normal cells, (2) tumour promotion consisting of clonal expansion of initiated cells (This stage is considered to be reversible), and (3) tumour progression consisting of malignant transformation of papillomas to carcinomas (This stage requires further genotoxic stimulus). The frequency of progression to a malignant status appears to be promoter independent (Hennings *et al.* 1985). Multiple UV irradiations are required for tumour promotion and progression. A schematic representation of these stages is shown in Figure 1-4 (adapted from the review by Baliga & Katiyar (2006)). Chemopreventive agents (e.g. Curcumin, green tea and resveratrol) have been shown to block, reverse or slow down the process of multi-stage carcinogenesis at one or more stages depending on their efficacy and/or anticarcinogenicity (Baliga & Katiyar 2006).
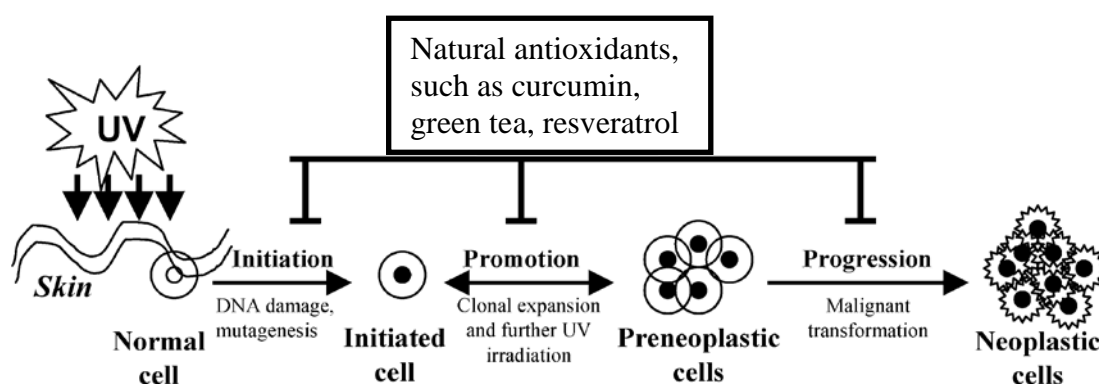
Figure 1-4
Schematic representation of UV radiation-induced multi-stage (initiation, promotion and progression) skin carcinogenesis. This figure is adapted from (Baliga & Katiyar 2006).

1.1.6 Current strategies for skin cancer prevention and therapies and their limitations

1.1.6.1 Skin cancer prevention

The strategies for skin cancer prevention can be categorised into three types

(summarised in Table 1-1) (Wasserman & Gilchrest 2008). The strategy for primary prevention is to prevent *de novo* malignancies in healthy populations to avoid initiation (Wasserman & Gilchrest 2008). As the majority of skin cancers are attributable to UV radiation, primary prevention is to protect from UV-induced skin damage and this involves the use of protective garments and sunscreens. Sunscreens are widely used as a protection from UV exposure. Regular sunscreen use is shown to reduce the risk of melanoma (Green *et al.* 2011). However, when activated by UV radiation, sunscreen ingredients may become free radicals themselves (Xu *et al.* 2001). Sunscreen chemicals may be absorbed into skin to potentially cause harm (Cross *et al.* 2001). Therefore, the use of sunscreen by itself is not sufficient for skin cancer prevention and may even be damaging. Secondary prevention strategies target the tumour progression stage, preventing the malignant transformation of existing premalignant lesions (Wasserman & Gilchrest 2008). Tertiary prevention strategies aim to prevent or reduce new independent malignancies in those with a prior history of cancer (Wasserman & Gilchrest 2008).

Table 1-1
Cancer prevention strategies used for skin cancers (adapted from (Wasserman & Gilchrest 2008)).

Type	Definition	Targeted carcinogenesis stage	Agents used for skin cancer
Primary	Prevent cancer from occurring in healthy individuals	Initiation	Sunscreens, DNA repair enhancers
Secondary	Prevent premalignant lesions from becoming cancers	Promotion	Sunscreens, NSAIDs, retinoid, PDT, Immunomodulators
Tertiary	Prevent new cancers in individuals with prior cancer history	N/A	N/A

Normally, cancer chemoprevention trials are time-consuming and expensive to employ any of the three prevention strategies (Wasserman & Gilchrest 2008). To permit cancer prevention trials, skin cancer, in comparison with other malignancies, has the advantage of occurring on a readily accessible and easily monitored organ with a sufficiently high incidence (Wasserman & Gilchrest 2008). Current chemopreventive agents include retinoid (topical or systemic), fluorouracil (5-FU), and nonsteroidal anti-inflammatory drugs (NSAIDs). These agents present some side effects. The advantages and disadvantages of these agents are summarised by Wasserman and Gilchrest (2008).

1.1.6.2 Skin cancer therapies

Current therapies for treatment of skin cancers include surgical excision, Mohs' micrographic surgery, cryotherapy, electrodesiccation and curettage, radiation therapy, chemotherapy, and photodynamic therapeutic agents in primary or adjuvant setting (Nouri 2008).

Surgical excision is the most effective treatment for limited or early skin cancers. However, it is expensive (Housman *et al.* 2003), is limited by the proximity of essential anatomical structures (Petit *et al.* 2000), and may not be a suitable treatment in cosmetically sensitive locations (Anthony 2000). Electrodessication, curettage, and cryotherapy are commonly used for certain BCCs. However, repeated treatment is required to remove the tumour completely. Additionally, hypopigmentation and delay in wound healing may occur (Anthony 2000; Hacker *et al.* 1993). Radiotherapy is a good option for the primary lesions that need extensive surgery. However, it may result in poor cosmetic results and wound healing problems

(Mazurkiewicz & Peszynski 1998; Petit *et al.* 2000).

Apart from the therapies mentioned as above, chemotherapy is another important approach to treat skin cancer. 5-FU is most widely used chemotherapy for NMSC. However, it has shown 5-year recurrence rates of 13.7% for BCCs and 20% for SCCs, respectively (Goette 1981). It is well known that melanoma with distant metastasis has a very poor prognosis, with a median survival of less than 1 year (Jemal *et al.* 2005). Advanced stages are currently not curable, because malignant melanoma has proven to be highly resistant to standard antineoplastic chemotherapy treatment. Dacarbazine (DTIC), an alkylating agent, is considered to be a standard agent for treating metastatic melanoma, and is the only drug for use in this disease approved by both the United States Food and Drug Administration (FDA) and the European Agency for the Evaluation of Medicinal Products (EMEA) (Garbe & Eigentler 2007; Tsao *et al.* 2004). However, it only has a response rate < 20%, with complete response observed in only <5% of cases (Lev *et al.* 2003).

Despite the recent advances (e.g. BRAF inhibitors) in skin cancer treatment, current therapeutic strategies have shown limitations and they are not satisfactory due to chemoresistance. Therefore, the identification of novel treatment for skin cancer, particularly for advanced resistant melanoma, remains a high priority in this research area.

1.1.7 Therapeutic strategies for skin cancers

Cancer cell development is complex. The hallmarks of cancer cells have been recently reviewed and are shown in Figure 1-5 (Hanahan & Weinberg 2011). This Chapter focussed on four of them, as they are relevant to the current study. They are

1) deregulating the cell cycle; 2) resisting cell death; 3) activating survival pathways; and 4) activating invasion and metastasis. They are briefly discussed in the following section.
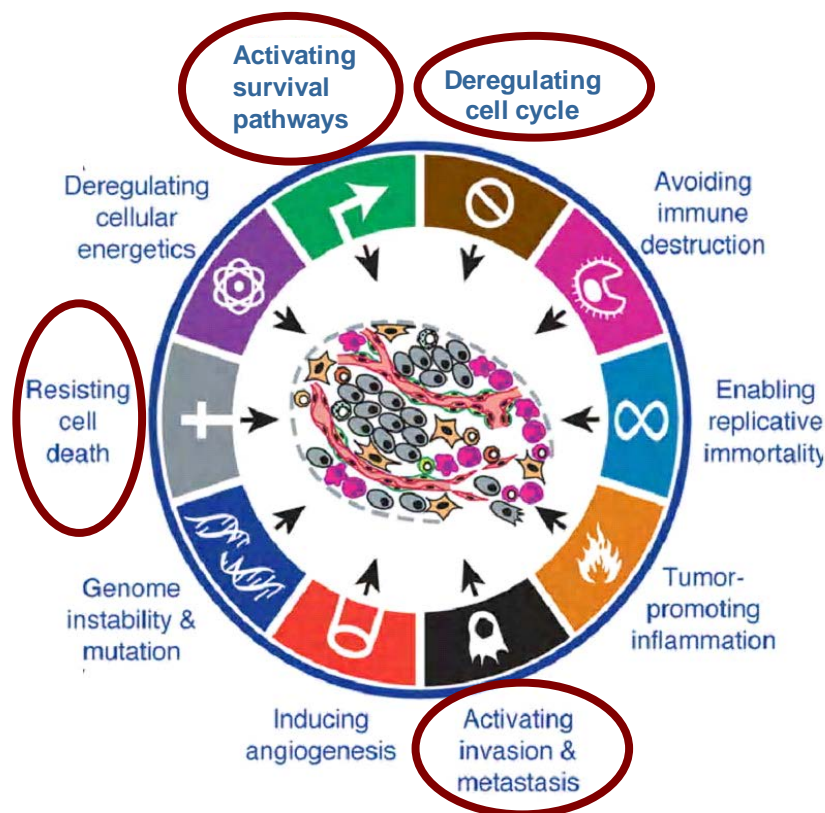
Figure 1-5
Ten hallmarks of cancer as summarised by Hanahan & Weinberg (2011). The new therapeutic strategies can target each of the enabling characteristics and hallmarks. The circled ones are the hallmarks that this review focused on.

1.1.7.1 Targeting deregulation of cell cycle

Cell division consists of two stages: mitosis (M) which is the process of nuclear division and interphase which is the interlude between two M phases (Figure 1-6). Mitosis includes prophase, metaphase, anaphase, and telophase. Interphase includes G_1 (a gap during which cells prepare for DNA synthesis), S (replication of DNA) and G_2 (a gap during which cells prepare for mitosis) (Norbury & Nurse 1992) (Figure 1-6). Additionally, before DNA replication, cells in G_1 phase can enter a resting

phase that is called G_0 (Vermeulen *et al.* 2003).

The cell division cycle is highly controlled to ensure correct progression through the cell cycle and a balance between cell death and cell division. It is mainly controlled by two groups of proteins: the cyclin-dependent kinases (CDK) and the CDK inhibitors (CKI). CDK are the key regulatory proteins and they are activated at specific points of the cell division cycle. The current identified Cyclin-CDK complexes are shown in Table 1-2 (Vermeulen *et al.* 2003). Upon activation, CDK phosphorylate specific proteins and subsequently induce downstream processes (Morgan 1995; Pines 1995). CKI can counteract the CDK activities by binding to CDK alone or to the CDK-cyclin complex and regulate CDK activity. To date, the INK4 family and Cip/Kip family are the two key CKIs that have been discovered, as presented in Table 1-3 (Vermeulen *et al.* 2003). For detailed information on controlling the cell cycle refer to the review by Vermeulen *et al.* (2003).
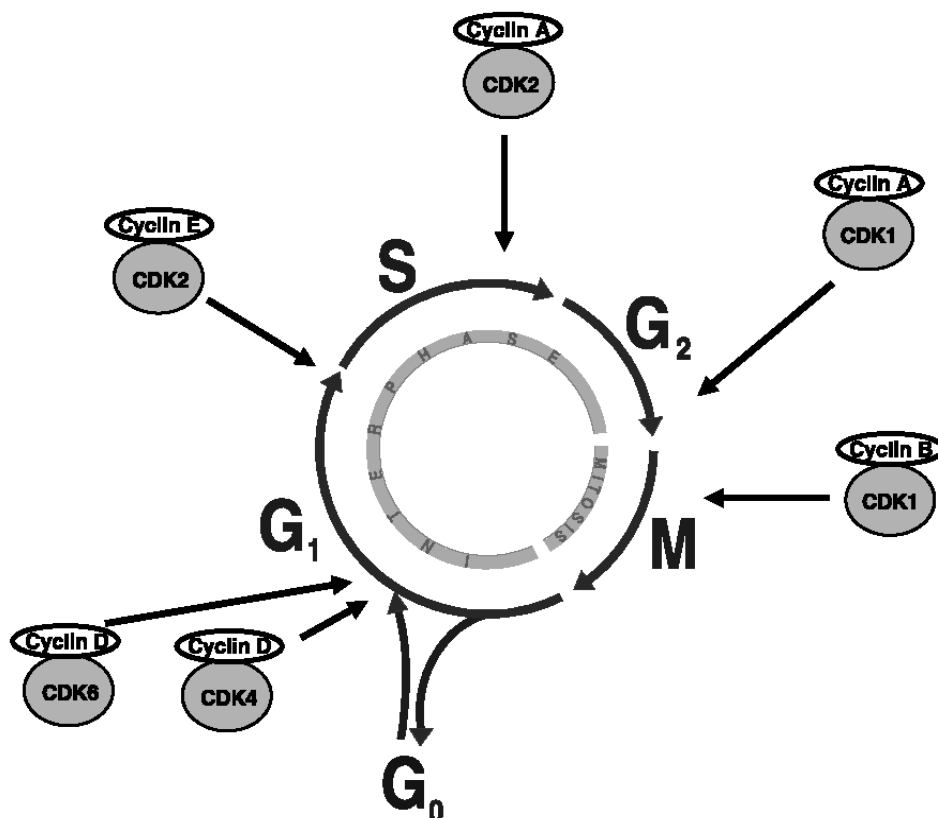
Figure 1-6
The stages of cell cycle and the site of activity of regulatory CDK/cyclin complexes
are indicated (Vermeulen *et al.* 2003).

Table 1-2
Cyclin-CDK complexes are activated at specific points of the cell cycle (Vermeulen
et al. 2003).

CDK	Cyclin	Cell cycle phase activity
CDK4	Cyclin D1, D2, D3	G_1 phase
CDK6	Cyclin D1, D2, D3	G_1 phase
CDK2	Cyclin E	G_1/S phase transition
CDK2	Cyclin A	S phase
CDK1	Cyclin A	G_2/M phase transition
CDK1	Cyclin B	Mitosis
CDK7	Cyclin H	CDK activating kinase, all cell cycle phases

Table 1-3
Cyclin dependent kinases inhibitors (CKI) bind to CDK alone or to the CDK-cyclin complex and regulate CDK activity (Vermeulen *et al.* 2003).

CKI family	Function	Family members	
INK4 family	Inactivation of G_1 CDK (CDK4, CDK6)	p15 p16 p18 p19	(INK4b) (INK4a) (INK4c) (INK4d)
Cip/Kip family	Inactivation of G_1 cyclin-CDK complexes and cyclin B-CDK1	p21 p27 p57	(Waf1, Cip1) (Cip2) (kip2)

In cancer cells, the alterations in the genetic control of the cell cycle lead to uncontrolled proliferation. There are two major types of mutated genes: proto-oncogenes and tumour suppressor genes. Mutation of proto-oncogenes promotes cancer cell growth, whereas inactivation of tumour suppressor genes (e.g. *pRb* and *p53*) results in the failure of normal inhibition of cell cycle progression (Vermeulen *et al.* 2003). The mutations related to cell cycle deregulation in cancer cells have been found in genes for CDK, cyclins, CDK-activating enzymes, CDK substrates, CKI, and checkpoint proteins (Malumbres & Carnero 2003; McDonald & El-Deiry 2000; Sherr 1996; Vermeulen *et al.* 2003). For example, overexpression of CDK4 has been found in melanoma, sarcoma, and glioma cell lines (Wölfel *et al.* 1995), overexpression of cyclin D1 has been found in breast, bladder, lung and squamous cell carcinomas cells (Hall & Peters 1996), and abnormalities of the pRb pathway (the most important CDK substrate during G_1 phase) has been observed in approximately 90% of human cancers (Hall & Peters 1996).

Therefore, targeting these alterations to halt uncontrolled cell division of cancer cells is an important therapeutic strategy against cancer development.

1.1.7.2 Targeting resistance to apoptotic cell death

<u>General background of apoptotic pathways</u>

There are two principal types of cell death: necrosis and apoptosis. Necrosis is a kind of accidental cell death. In contrast, apoptosis is a programmed cell death, acting as a natural barrier to cancer development involving the removal of mutant clones and the prevention of uncontrolled rapid cell proliferation (Lowe *et al.* 2004).

The mechanisms of apoptosis are highly complex, involving multiple molecular events (Figure 1-7). There are two major apoptotic pathways: the intrinsic, or mitochondrial pathway and the extrinsic, or death receptor pathway (Elmore 2007; Fulda & Debatin 2006). These two pathways are outlined below.

1) Intrinsic apoptotic pathway

Mitochondria play a critical role in the intrinsic apoptotic pathway (Green & Reed 1998) and the outer membrane permeabilisation is an essential event for initiating the release of the molecules (e.g. cytochrome c and apoptosis inducing factor) into the cytoplasm. It is well known that the release of cytochrome c promotes the formation of the apoptosome and activation of caspase-9 (initiator caspase) and consequently activation of downstream caspase 3 and 7 (executioner caspases) (Rodriguez & Lazebnik 1999; Zou *et al.* 1997).

The Bcl-2 family of proteins regulates the integrity of the mitochondrial membrane and the efflux of pro-apoptotic proteins from the mitochondria and contains three groups (Figure 1-8). The first group is anti-apoptotic, including Bcl-2 and Bcl-Xl, and acts to preserve mitochondrial integrity and prevent cells from apoptosis (Adams & Cory 1998). The second group is pro-apoptotic, including Bax and Bak, and acts

to disrupt mitochondrial membrane and promote cell apoptosis (Antonsson & Martinou 2000). The third group is a large family, including Bim, Bad, Bid, Noxa, and Puma, which interacts with other Bcl-2 family members (Huang & Strasser 2000). Therefore, if there are more anti-apoptotic members than pro-apoptotic ones, the integrity of mitochondrial membrane will be protected and the cells will resist cell death and promote survival. In contrast, if there are more pro-apoptotic ones than anti-apoptotic, the loss of mitochondrial membrane potential will be induced and a cascade of events, as mentioned above, will be activated, and therefore the cells will undergo apoptosis (Adams & Cory 2001).

2) Extrinsic apoptotic pathway

Extrinsic apoptosis can be activated by ligands binding to cell surface receptors (Wang & El-Deiry 2003). Currently, the well-characterised ligands and corresponding death receptors include FasL/FasR, TNF-α/TNFR1, Apo3L/DR3, Apo2L/DR4 and Apo2L/DR5 (Ashkenazi & Dixit 1998; Chicheportiche *et al.* 1997; Peter & Krammer 1998; Rubio-Moscardo *et al.* 2005; Suliman *et al.* 2001). The binding of a ligand to the corresponding receptor leads to the binding of the corresponding adapter protein, for example, the binding of Fas ligand to Fas receptor leads to the binding of the adapter protein FADD (Hsu *et al.* 1995; Wajant 2002). Consequently, the adapter protein associates with procaspase-8. Meanwhile, formation of the death-inducing signaling complex induces the autocatalytic activation of procaspase-8 (Kischkel *et al.* 1995). Subsequently, caspase-8 can cleave and activate effector caspase 3 and hence trigger apoptosis induction.
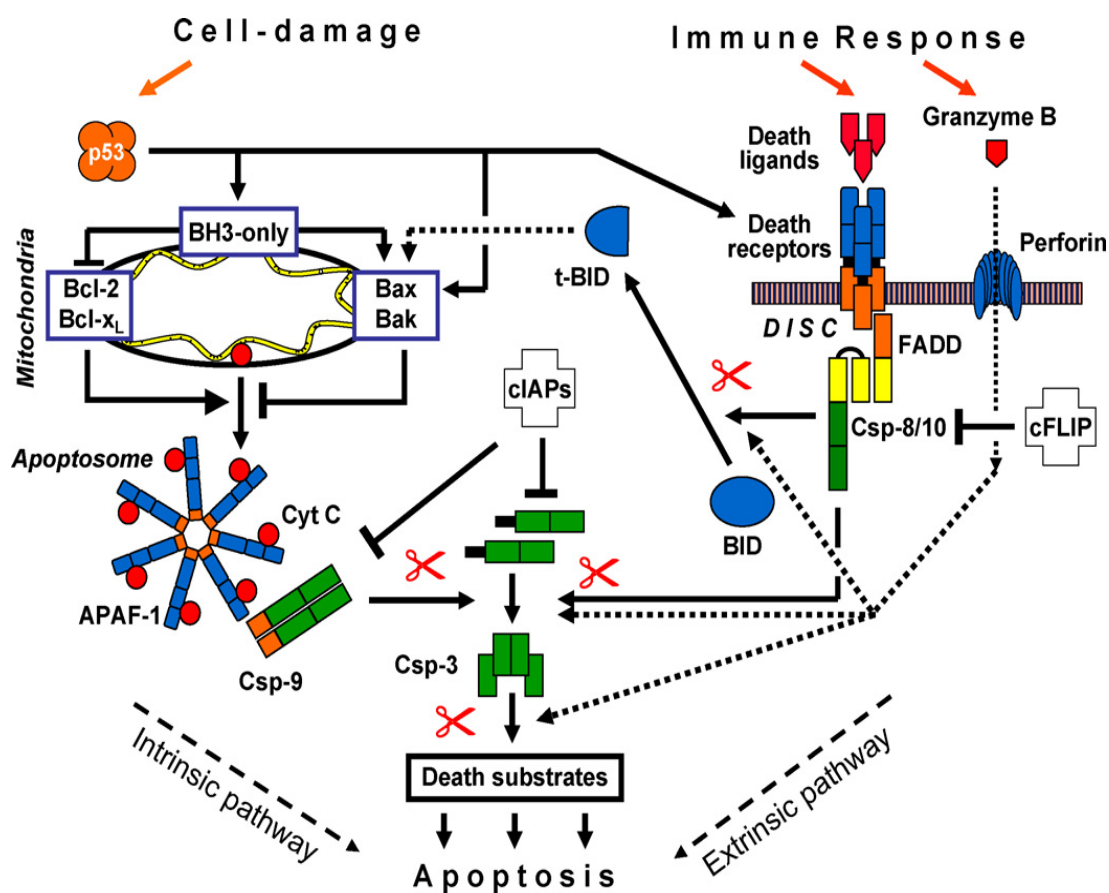
Figure 1-7

The intrinsic and extrinsic apoptotic pathways in response to cellular damage or immune challenge. Abbreviations: Cyt C, cytochrome C; Apaf-1, apoptosis-activating factor; TNF, tumor necrosis factor; TRAIL, TNF-related apoptosis-inducing ligand; NK, natural killer; DISC, death-inducing signaling complex; FADD, Fas-associated death domain; Csp, caspase; tBid, truncated Bid; cFLIP, cellular FLICE-inhibitory protein; IAPs, inhibitors of apoptosis proteins; BH3-only, BH3-only proteins. Scissors indicate protease activities. This figure is taken from the review by Eberle *et al.* (2007b).
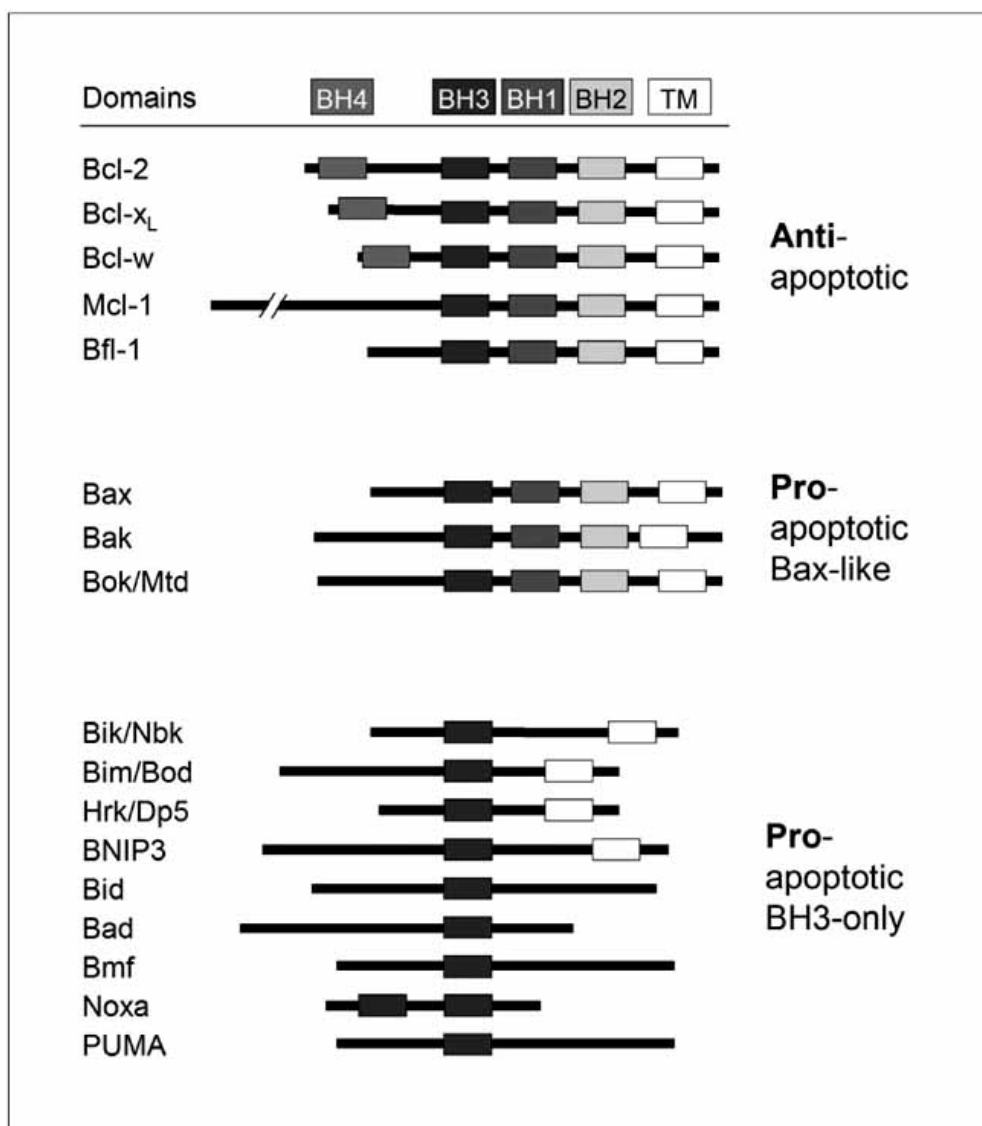
Figure 1-8
The superfamily of Bcl-2 proteins encloses antiapoptotic factors, proapoptotic Bax-like factors and BH3-only proteins. The presense of up to four Bcl-2 homology domains (BH 1-4) as well as in some proteins the transmembrane domain (TM) is indicated. This figure and figure legend are taken from the review by Eberle & Hossini (2008).

Apoptosis resistance in skin cancer

Apoptosis plays a critical role in the prevention of cancer. However, most cancer cells show resistance to cell death, and skin cancer cells are no exception. It seems that the resistance to apoptosis is required for tumour growth, and it also contributes to chemoresistance (Eberle *et al.* 2007b). The resistance of skin cancer cells,

especially melanoma, to apoptosis may be due to inactivation of pro-apoptotic effectors (e.g. p53 pathway) (Müller *et al.* 2006; Yu 2006); activation of anti-apoptotic factors (e.g. Bcl-2, Bcl-x_L, and Mcl-1 are highly expressed in melanoma cells) (Hossini *et al.* 2003; Selzer *et al.* 1998; Wolter *et al.* 2007); or from reinforcement of survival pathways (e.g. NFκB and Akt). Furthermore, melanoma shows resistance to death receptor-mediated apoptosis (extrinsic pathway), possibly due to resistance to CD95 (also known as FasR) stimulation (Raisova *et al.* 2000) and resistance to TNF-α-mediated apoptosis (Ivanov *et al.* 2003). For detailed information on the apoptosis deficiency of melanoma refer to the review by Eberle *et al.* (2007b).

Therefore, an efficient strategy against skin cancer is to induce apoptosis by activating the intrinsic and/or extrinsic pathways.

1.1.7.3 Targeting activation of survival pathways

Activation of survival pathways contributes to the resistance of cancer cells to chemotherapy. Three major survival pathways are highly active in skin cancer cells, especially in melanoma (Eberle *et al.* 2007b). They are mitogen activated protein kinases (MAPKs), phosphatidylinositol 3-kinase (PI3K)/Akt (protein kinase B) and nuclear factor kappa B (NFκB) pathways, which regulate apoptosis at multiple levels. The details are shown in Figure 1-9.
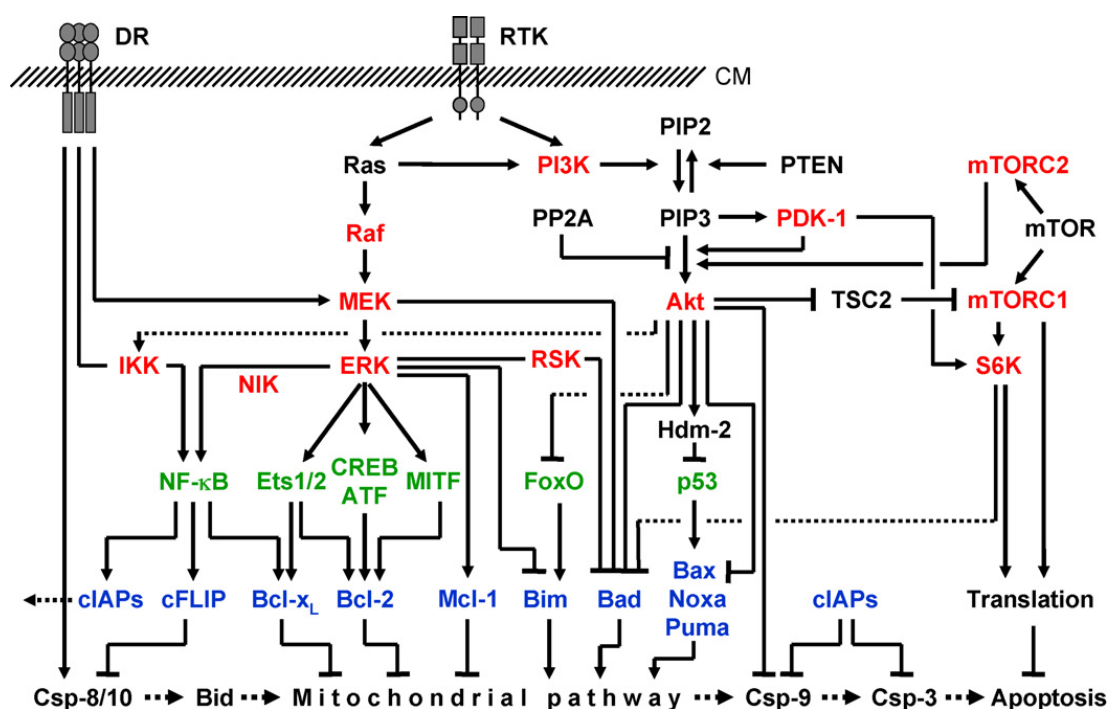
Figure 1-9
Survival pathways and their relations to apoptosis. Three main survival pathways downstream of receptor tyrosine kinases (RTK) are indicated namely the MAPK, PI3K-Akt and NFκB pathway. In addition, signaling from death receptors (DR) is outlined, which results in caspase activation as well as in triggering of MAPKs and NFκB. The level of kinases is shown in red, transcription factors in green and apoptosis regulators in blue. The pathways show multiple links to apoptosis regulators, as in particular pro- and anti-apoptotic Bcl-2 proteins, thus resulting in a suppression of apoptosis. Several transcription factors are employed as NFκB, Ets1/2, CREB/ATF family, MITF and FoxO. Further abbreviations: CM, cytoplasma membrane; Csp, caspase; PP2A, protein phosphatase 2a. This figure and figure legend are taken from the review by Eberle *et al.* (2007b).

1) MAPK pathway

There are five groups of MAPKs characterised currently. They are extracellular signal-regulated kinases (ERKs) 1 and 2, c-Jun amino-terminal kinases (JNKs) 1, 2, and 3, p38 isoforms α, β, γ and δ, ERKs 3 and 4, and ERK5 (Chen *et al.* 2001b; Kyriakis & Avruch 2001). MAPK activation has been found to be associated with survival and chemoresistance of skin cancer cells (Smalley & Eisen 2003), through downregulation of pro-apoptotic Bcl-2 proteins (Bad, Bim, and PUMA) and upregulation of anti-apoptotic Mcl-1 (Eisenmann *et al.* 2003; Panka *et al.* 2006;

Wang *et al.* 2007). In melanoma, the frequency of mutation of BRAF and NRAS is reported to be up to 60% and 30% (Davies *et al.* 2002; Edlundh-Rose *et al.* 2006; Hatzivassiliou *et al.* 2010; Vultur *et al.* 2010). These mutations constitutively activate RAS-RAF-MEK-ERK pathway in melanoma cells (Cohen *et al.* 2002; Mirmohammadsadegh *et al.* 2007). Therefore, this signaling pathway is an important target for anti-skin cancer therapy.

2) PI3K/Akt pathway

Akt, a protein serine/threonine kinase, consists of three isoforms of Akt1 (PKBα), Akt2 (PKBβ), and Akt3 (PKBγ) (Brazil *et al.* 2002; Nicholson & Anderson 2002). Akt is a downstream effector of PI3K and mainly regulated by phosphorylation of Threonine 308 and Serine 473 via activation of PI3K (Hanada *et al.* 2004; Scheid & Woodgett 2003). Akt is constitutively activated in many human cancers (Testa & Bellacosa 2001), including melanoma and squamous cell carcinoma of the oral cavity (Li *et al.* 2003; Nakayama *et al.* 2001). Particularly, activated Akt3 has been reported to express in 60-70% of sporadic melanoma, indicating its essential role in the progress of melanoma (Dhawan *et al.* 2002; Stahl *et al.* 2004). Activated Akt can phosphorylate many downstream targets (e.g. Bad, Bax, and caspase-9) and suppress pro-apoptotic transcription factors (e.g. FoxO and p53) (Cardone *et al.* 1998; Datta *et al.* 1997; Gardai *et al.* 2004; Manning & Cantley 2007). Consequently, activation of this signalling pathway can block apoptosis, thus supporting cancer cell growth (Easton & Houghton 2006; Guertin & Sabatini 2007).

3) NFκB pathway

NFκB family consists of five subunits: NFκB1 (p50/p105), NFκB2 (p52/p100), RelA

(p65), RelB and c-Rel. NFκB is maintained in the cytoplasm by binding to the inhibitors of NFκB (IκBs) (Eberle *et al.* 2007b). Activation of IκB kinase complex (IKK) can result in IκBs phosphorylation and degradation, leading to dissociation of NFκB and IκB (Ravi & Bedi 2004). Consequently, NFκB translocates into the nucleus and becomes activated (Fan *et al.* 2002). Activation of NFκB can result in anti-apoptotic activities by transactivation of IAP proteins (e.g. Bcl-xL) (Demarchi & Brancolini 2005), and inhibition of death ligand-induced apoptosis (Ivanov *et al.* 2003). Activation of NFκB and IKK has been observed in melanoma (Ravi & Bedi 2004), associated with resistance to radio and chemotherapy (Heon Seo *et al.* 2006; Munshi *et al.* 2004; Romano *et al.* 2004). Hence, targeting the NFκB pathway can be an important strategy for anti-skin cancer therapy.

1.1.7.4 Targeting activation of invasion and metastasis

During the development of most types of human cancer, cells from the primary tumour will migrate, invade nearby tissues, and then spread to distant sites where they may form new colonies. This process is known as metastasis, which is responsible for 90% of human cancer deaths (Weigelt *et al.* 2005). Melanoma is an aggressive skin cancer that is notorious for its tendency to metastasise to the lung, liver and brain (Tarhini & Agarwala 2006; Tsao & Sober 2005). Nonmelanoma skin cancers are also invasive and metastatic to fatty tissues beneath the skin and nearby lymph nodes, however the metastasis rate is much lower than that of melanoma (Kwa *et al.* 1992; Miller 1991).

The process of metastasis is controlled by the balance of promoters and suppressors (Table 1-4) in each step (Furuta *et al.* 2006). Hence, either suppressing the promoters or activating the suppressors can be a strategy to develop anti-metastatic therapy

(Figure 1-10) (Iiizumi *et al.* 2008).

Table 1-4
The promoters and suppressors of metastasis (extracted from the review by Iiizumi *et al.* (2008)).

Metastasis promoters	Metastasis suppressors
AMF (Autocrine motility factor)	NM23
HGF (Hepatocyte growth factor)	KiSS-1
TGFβ (Transforming growth factor-β)	MKK4 (Mitogen-activated protein kinase kinase 4)
MMP (Matrix metalloproteinase)	E-cadherin
uPA (Urinary-type plasminogen activator)	Ndrg1 (N-myc downstream regulated gene 1)
β-catenin	

(a) Metastasis Promoters
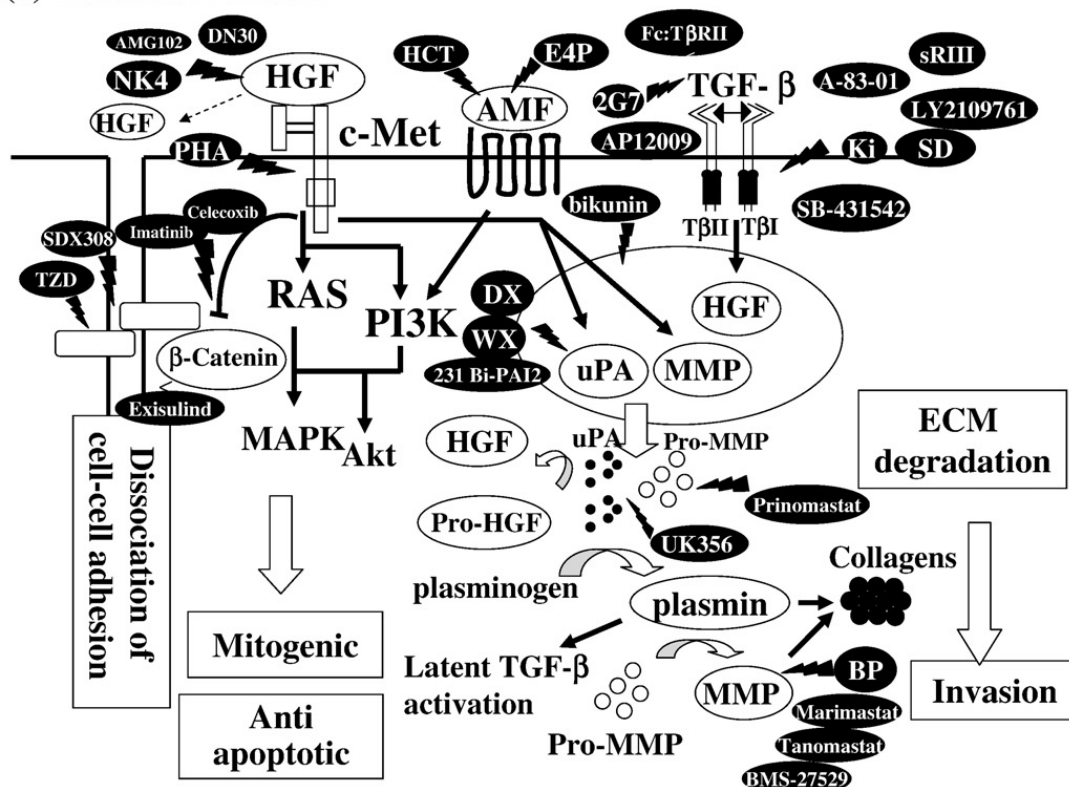
(b) Metastasis suppressors
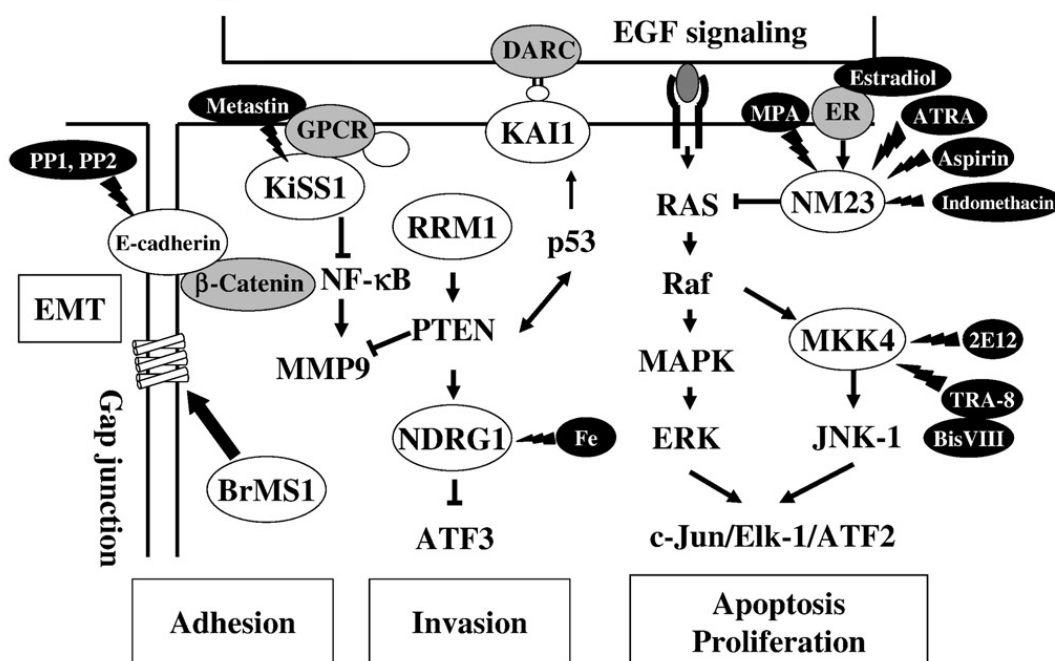
Figure 1-10
Signal pathway of tumour metastasis. Tumour metastasis is a result of complex interplay of both positive (a) and negative (b) factors. These pathways and their factors are potential targets for anti-metastatic therapy. The drugs currently under development are shown as black oval shapes. This figure and figure legend are taken from the review by Iiizumi *et al.* (2008).

1.2 The role of plant-derived natural products in skin cancer treatment and prevention

More than 65% of anti-cancer drugs currently in clinical trials are derived from, or inspired by, natural products, especially terrestrial plants (Nuijen *et al.* 2000). Therefore, plant-derived natural products have attracted great attention for anti-cancer drug development (Balunas & Kinghorn 2005; Gordaliza 2007; Newman *et al.* 2003; Tan *et al.* 2006).

The term "plant-derived natural products" usually refers to plant secondary metabolites. They are a group of naturally occurring substances, variously distributed in the plant kingdom, and they have specific functions in the plants in which they are found. They include phenolics, terpenoids, nitrogen-containing alkaloids and sulfur-containing compounds (Crozier *et al.* 2006).

A number of plant secondary metabolites exhibit significant anti-cancer activities. Some of them have already been commercialised into anti-cancer drugs and some are at present in clinical trials, for example, taxol, 3-ingenyl angelate, and curcumin (Nirmala *et al.* 2011).

In Sections 1.2.1-1.2.3, the anti-skin cancer activities of plant secondary metabolites are summarised in three areas based on the developmental stages of skin cancer (Section 1.1.5). These are chemopreventive activity (for the initiation stage), cytotoxcity (for the promotion stage), and inhibition of metastasis (for the progression stage).

1.2.1 Chemopreventive activity of plant secondary metabolites in skin cancers

There are comprehensive reviews of the effect of plant natural products on UV or DMBA-induced skin damage by Baliga and Katiya. (2006), Svobodova *et al.* (2003), and Filip *et al.* (2009). A summary of the chemopreventive effect of plant secondary metabolites and the underlying mechanisms is shown in Table 1-5. These studies have been carried out using *in vitro* (e.g. human keratinocyte HaCaT cell line) or *in vivo* (e.g. SKH-1 hairless transgenic mouse) models. UV radiation, DMBA (7,12-dimethyl[a]benzanthracene), or TPA (12-O-tetradecanoylphorbol-13-acetate) are used to induce skin damage. The chemopreventive activity of the plant secondary metabolites in skin cancer are mainly due to their antioxidant and antiinflammatory properties (Baliga & Katiyar 2006) and the potential mechanisms are as discussed in Section 1.1.4.2.

For example, topical application of resveratrol, a phenolic compound from grapes, to SKH-1 hairless mouse skin significantly inhibited UVB-induced increase in bi-fold skin thickness (a marker of oedema), hyperplastic response, generation of hydrogen peroxide, lipid peroxidation and activities of COX-2 and ornithine decarboxylase (Afaq *et al.* 2003; Aziz *et al.* 2005b). At the molecular level, treatment with resveratrol inhibited UV-mediated increase in proliferating cell nuclear antigen, CDK (cdk2, 4 and 6), cyclins (D1 and D2), the MAPK kinase (MAPKK) and MAPK in SKH-1 hairless mice (Reagan-Shaw *et al.* 2004). In *in vitro* studies, the treatment of HaCaT cells with resveratrol has been shown to inhibit UVB-induced activation of NFκB in a dose and time dependent manner (Adhami *et al.* 2003). Cimino *et al.* (2007) have reported that red orange extract is able to effectively counteract UVB-induced responses, and particularly some events associated with inflammation and apoptosis, such as NFκB and AP-1 translocation and procaspase-3 cleavage,

probably due to the blocking of cellular oxidative stress-related events. Additionally, Tomaino *et al.* (2006) demonstrated that pre-treatment with Jacquez grape wine extract reduced the release of IL-1α and PGE2 and inhibited oxidative damage (e.g. decreasing MDA/HNE content) after exposure of reconstituted human epidermis to UVB.

Taken together, these findings indicate that natural antioxidants have potential uses for preventing the initiation of skin cancer. This encourages researchers to identify more novel natural antioxidant compounds, which have potential chemopreventive effect to protect skin from UV-induced damage or cancer.

Table 1-5
Chemopreventive effect of selected plant natural products in skin cancers *in vitro* and *in vivo* systems (adapted from (Baliga & Katiyar 2006; Filip *et al.* 2009)).

Extract / Compound	Plant source	Experimental model	Mechanism of action	Reference
Leaf extract	*Ocimum sanctum*	DMBA-induced skin papillomagenesis in Swiss albino mice	Antioxidant and detoxification mechanisms	(Prashar *et al.* 1994)
Root extract	*Withania somnifera*	DMBA-induced papillomas in mice	Antioxidant	(Prakash *et al.* 2002)
Clocimum oil	*Ocimum gratissimum*	DMBA-induced skin papillomas	Antioxidant, elevation in hepatic and skin GST, sulfhydryl (-SH), cytochrome b5 activity	(Singh *et al.* 1999)
Lantadene A	*Lantana camara* L.	DMBA-TPA-induced skin tumours in Swiss albino mice (LACCA)	Suppression of AP-1, NFκB and p53	(Kaur *et al.* 2010)
Silymarin	*Silybum marianum* L.	UVB-induced DNA lesions in mouse epidermis	Antioxidant (inhibition of H_2O_2, LPO, NO, iNOS, MPO)	(Chatterjee *et al.* 1996)
Curcumin	Rhizome (*Curcuma longa* L.)	DMBA-TPA-induced mouse skin papillomas	Suppression of extracellular signal regulated kinase activity and NFκB	(Chun *et al.* 2003)
	Rhizome (*Curcuma longa* L.)	DMBA-induced skin papillomas	Antioxidant	(Soudamini & Kuttan 1989)
	Rhizome (*Curcuma longa* L.)	UV-induced oxidative stress in human squamous cell carcinoma A-431 cells	Antioxidant (Inhibition of superoxide anions and H_2O_2)	(Chan *et al.* 2003)
Proanthocyanidins	Grape seeds (*Vitis vinifera*)	DMBA-TPA-induced skin tumorigenesis in mice	Suppression of ornithine decarboxylase, myeloperoxidase and protein kinase c	(Bomser *et al.* 2000)

Table 1-5 (Continued)

Extract / Compound	Plant source	Experimental model	Mechanism of action	Reference
Polyphenols	Grape seeds (*Vitis vinifera*)	DMBA-TPA-induced skin carcinogenesis	Antioxidant	(Zhao *et al.* 1999)
	Camellia sinensis	UV irradiated SKH-1 hairless mice	Antioxidant (inhibition of H_2O_2, NO, iNOS)	(Vayalil *et al.* 2003)
	Camellia sinensis	Photocarcinogenesis in C3H/HeN mice	Induction of IL-12 and prevention of UV-induced immune-suppression	(Ahmad *et al.* 2000)
Resveratrol	Grape seeds (*Vitis vinifera*)	UVB-induced skin cancer in SKH-1 hairless mice	Antioxidant (inhibition H_2O_2); inhibition of Survivin-phosphorylation and up-regulation of Smac/DIABLO in skin tumors; inhibition of MAPK proteins	(Afaq *et al.* 2003; Aziz *et al.* 2005a; Aziz *et al.* 2005b)

1.2.2 Cytotoxicity of plant secondary metabolites in skin cancers

A number of studies have been carried out to investigate the cytotoxic effect of plant natural products on human skin cancer cell lines (summarised in Table 1-6). These natural products exert their cytotoxic effect mostly via cell cycle arrest and induction of apoptotic and necrotic cell death through various mechanisms (Table 1-6).

In particular, the anti-skin cancer activities of resveratrol have been well studied. Madan *et al.* (2008) revealed that inhibition of proliferation of human epidermoid carcinoma A-431 cells by resveratrol was associated with regulation of the JAK/STAT survival pathway, where resveratrol prevented phosphorylation of JAK,

thereby inhibiting STAT1 phosphorylation. Furthermore, resveratrol treatment actively stimulated ROS and mitochondrial membrane depolarisation. Meanwhile, an imbalance in the Bax/Bcl-2 ratio triggered the caspase cascade and subsequent cleavage of PARP, thus shifting the balance in favour of apoptosis. A similar study by Kim *et al.* (2006) demonstrated that resveratrol inhibited the proliferation in A-431 cells accompanied by G_1 cell cycle arrest. It was suggested that this was associated with a marked inhibition of G_1 cell cycle regulatory proteins, including cyclins A and CDK 6 and p53-independent induction of $p21^{WAF1}$, and the accumulation of hypophosphorylated Rb and $p27^{KIP1}$. Another study has been performed using human SK-MEL-28 melanoma cells (Larrosa *et al.* 2003). This study demonstrated that resveratrol inhibited cell growth and upregulated the expression of cyclins A, E, and B1 with subsequent irreversible arrest in the S phase.

Cytotoxicity of compounds from other natural plants has also been reported in skin cancer cells. 3-Ingenyl angelate has been found to induce necrosis of skin cancer cells through disruption of mitochondrial membrane potential (Ogbourne *et al.* 2004) and is under clinical trials for treating actinic keratosis and basal cell carcinoma (Siller *et al.* 2009). 4-Nerolidylcatedchol exerted cytotoxicity on melanoma cell lines (SK-MEL-28, SK-MEL-103 and SK-MEL-147) by inducing cell cycle arrest in G_1 phase and apoptosis. This compound showed selectivity against melanoma cell lines with less cytotoxicity towards normal human fibroblasts, as evidenced by the IC_{50} values (50% inhibitory concentration) obtained (IC_{50}= 20-40 µM for cancer cell lines and IC_{50}= 50 µM for fibroblast cell line) (Brohem *et al.* 2009). A study by Chang *et al.* (2009) showed that γ-tocotrienol induced apoptosis as evidenced by activation of procaspases and the accumulation of sub-G_1 cell population in melanoma cells. This

was associated with the suppression of NFκB, EGFR, and Id family proteins. In addition, treatment with γ-tocotrienol resulted in the induction of the JNK signalling pathway. Furthermore, synergistic effect was found when cells were cotreated with γ-tocotrienol and chemotherapy drugs, such as docetaxel and DTIC. The synergistic effect was found to be via enhancing cell apoptosis by activation of proapoptotic proteins (e.g. caspase 3, 7) and suppression of prosurvival proteins (e.g. EGFR and phosphorated-IκB) (Chang *et al.* 2009).

In summary, these studies have demonstrated that plant secondary metabolites can kill cancer cells via cell cycle arrest (e.g. inhibition of cyclins and activation of CDK inhibitors), induction of apoptosis (e.g. activation of caspase and disruption of mitochondrial membrane potential), and inhibition of survival pathways (e.g. JAK/STAT and NFκB). Some natural plant secondary metabolites exhibit selectivity (e.g. 4-nerolidylcatedchol) against cancer cells, or synergistic effect when combined with chemotherapeutic drugs (e.g. γ-tocotrienol plus DTIC). These findings provide a solid basis for the development of these plant secondary metabolites as anti-skin cancer agents; however, further experiments are required to understand the precise underlying molecular mechanisms for the observed effects.

Table 1-6

Cytotoxic effects of selected plant secondary metabolites on skin cancer cells / models.

Extract / Compound	Plant source	Activities	Reference
Resveratrol	Grape skins and seeds, peanuts, red wine, mulberries	Induction of apoptosis via increasing expression and accumulation of COX-2 by activation of ERK1/2 on human head and neck squamous cancer UMSCC-22B cells	(Lin *et al.* 2008)
		Inhibition of human squamous cell carcinoma A-431 cell proliferation through suppression of the JAK/STAT pathway; induction of apoptosis by increasing the ratio of Bax/Bcl-2 and activating caspase cascade and subsequent PARP cleavage	(Madan *et al.* 2008)
		Inhibition of A-431 cell proliferation by inducing cell cycle arrest in G_1 phase, associated with inhibition of G_1 cell cycle regulatory proteins, including cyclin A, CDK6 and p53-independent induction of p21^{WAF1}, and the accumulation of hypophosphorylated Rb and p27^{KIP1}	(Kim *et al.* 2006)
		Inhibition of human melanoma SK-MEL-28 cell growth by inducing cell cycle arrest in S phase via upregulating the expression of cyclins A, E, and B1	(Larrosa *et al.* 2003)
3-Ingenyl angelate	Sap of *Euphorbia peplus*	Induction of necrosis of skin cancer cells through disruption of mitochondrial membrane potential	(Ogbourne *et al.* 2004)

Table 1-6 (Continued)

Extract / Compound	Plant source	Activities	Reference
γ-Tocotrienol	Palm oil	Induction of apoptosis by the activation of caspases and the accumulation of sub-G_1 phase; suppression of NFκB, EGFR, and Id family proteins	(Chang *et al.* 2009)
4-Nerolidylcatechol	*Pothomorphe umbellata*	Induction of cytotoxicity of melanoma cell lines (SK-MEL-28, SK-MEL-103 and SK-MEL-147), but less cytotoxicity towards normal human fibroblasts. Antiproliferative effect was via cell cycle arrest in G_1 phase and apoptosis	(Brohem *et al.* 2009)
Proanthocyanidin	Grape seeds (*Vitis vinifera*)	Inhibition of A-431 cell proliferation by increasing G_1-phase arrest through the inhibition of Cdk2, Cdk4, Cdk6 and cyclins D1, D2 and E and simultaneous increase in Cdki, Cip1/p21 and Kip1/p27; and inducing apoptosis by increasing Bax, decreasing Bcl-2 and Bcl-x_L, disrupting mitochondrial membrane potential, cleavaging caspase-9, caspase-3 and PARP	(Meeran & Katiyar 2007)
α-Santalol	Sandalwood oil	Induction of apoptosis on A-431 cells by the activation of caspase-3, -8 and -9, and disruption of the mitochondrial membrane potential with cytochrome c release into the cytosol	(Kaur *et al.* 2005)

Table 1-6 (Continued)

Extract / Compound	Plant source	Activities	Reference
Berberine	An isoquinoline alkaloid in the roots, rhizome and stem bark of *Berberis aquifolium, Berberis vulgaris, Berberis aristata* and *Tinospora cordifolia*	Decrease in cell viability and increase in cell death on A-431 cells; increase in G_1 arrest through the increased expression of Cip1/p21 and Kip1/p27, a simultaneous decrease in Cdk2, Cdk4, Cdk6 and cyclins D1, D2 and E; increasing in apoptosis via increasing the expression of Bax, decreasing the expression of Bcl-2 and Bcl-xl, decreasing the mitochondrial membrane potential, activating caspases 9, 3 and poly (ADP-ribose) polymerase	(Mantena *et al.* 2006)

1.2.3 Anti-metastatic effect of plant secondary metabolites in skin cancers

Metastasis is a major cause of human cancer deaths and involves multiple steps, as discussed in Section 1.1.7.4. A number of natural compounds from various plant sources have been reported to possess the capacity to inhibit metastasis of melanoma (summarised in Table 1-7).

Curcumin, for example, inhibited the invasion of B16F-10 melanoma cells by inhibition of MMP-2 and MMP-9, which are associated with melanoma progression (Banerji *et al.* 2004; Hofmann *et al.* 2005; Lin *et al.* 1998). Likewise, 4-nerolidylcatechol inhibited MMP-2 activity on human melanoma SK-MEL-147 cells (Brohem *et al.* 2009). This compound also inhibited MMP-2 and MMP-9 activity in a skin photoageing model (Ropke *et al.* 2006). Chang *et al.* (2009) showed that γ-tocotderienol inhibited melanoma cell invasion via suppression of mesenchymal markers and restoration of e-cadherin and γ-catenin expression. Downregulation of e-cadherin expression is an important feature of metastatic cancers, and therefore restoration of e-cadherin can suppress cancer cell metastasis (Chu *et al.* 2006).

Convincing evidence of anti-metastatic activity has been provided by studies using animal models. As shown in Table 1-7, metastasis of melanoma can be inhibited in different animal models through a number of mechanisms. In the study by Lee *et al.* (2006), aqueous extract of the root of *Platycodon grandiflorum* inhibited the lung metastasis of B16-F10 melanoma cells by inhibiting the adhesion of tumour cells to the basement membrane and activating natural killer cells. Likewise, methanol extract from the leaf of *Jatropha curcas* inhibited metastatic melanoma colony formation in lungs (Balaji *et al.* 2009). Genistein was reported to inhibit melanoma-

induced angiogenesis in a murine melanoma B16 mouse model (Farina *et al.* 2006).

In summary, these findings show that plant secondary metabolites have the potential to inhibit melanoma metastasis *in vitro* and *in vivo* via inhibiting motility, adhesion, invasion, MMP-2 and MMP-9 activities, or angiogenesis.

Even though squamous cell carcinoma is generally less aggressive than melanoma and it is usually cured with surgical excision at an early stage, it has the potential to invade deeper structures and to metastasise (Cherpelis *et al.* 2002). There is limited information available regarding the anti-metastatic activity of plant secondary metabolites on squamous cell carcinoma in the current literature. Further investigation is warranted.

Table 1-7
Anti-metastatic activity of selected plant secondary metabolites in melanoma skin cancers using *in vitro* and *in vivo* models.

Extract / compound	Experimental model	Activities	Reference
Curcumin (*Curcuma longa*)	Murine melanoma B16-F10 cells	Inhibition of MMP-2 and downregulation of FAK	(Banerji *et al.* 2004)
4-Nerolidylcatechol (*Pothomorphe umbellata*)	Human melanoma SK-MEL-147 cells	Inhibition of MMP-2	(Brohem *et al.* 2009)
γ-Tocotrienol (Palm oil)	Human melanoma C32 and G361 cells	Inhibition of mesenchymal markers and activation of E-cadherin and γ-catenin	(Chang *et al.* 2009)

Table 1-7 (Continued)

Extract / compound	Experimental model	Activities	Reference
Resveratrol (Grape)	Murine melanoma B16M cells in C57BL/c mice	Inhibition of hepatic metastasis of B16M cells by suppression of interleukin-18	(Salado *et al.* 2011)
Genistein (Soybean)	Murine melanoma B16 and mammary carcinoma F3II in mice	Reduction of motility and uPA secretion but no effect on MMP-2 and -9 *in vitro*; reduction of tumour-induced angiogenesis after administration of genistein *in vivo*	(Farina *et al.* 2006)
Aqueous extract of the root of *Platycodon grandiflorum*	Murine melanoma B16-F10 cell line and an experimental induced lung cancer in C57BL/6 mice	Inhibition of invasion, and adhesion to Matrigel, fibronectin, and laminin; reduction of the extent of lung metastasis of B16-F10 melanoma cells by activating natural killer cells.	(Lee *et al.* 2006)
Methanol extract of the leaf of *Jatropha curcas*	Murine melanoma B16-F10 cells in C57BL/c mice	Inhibition of metastatic colony formation of the melanoma in lungs; reduction of hexosamine and uronic acid content; reduction of serum sialic acids and γ-glutamyltranspeptidase	(Balaji *et al.* 2009)
Ethyl acetate extract of *Dioscorea nipponica* Makino	Murine melanoma B16-F10 cells in C57BL/c mice; murin melanoma B16F10 cells and human melanoma A2058 cells	Reduction of lung metastases formation by about 99.5% as compared to untreated control animals; inhibition of invasion, motility, secretion of MMPs, and u-PA on B16-F10 and A2058 cells by inhibiting phosphorylation of Akt, inhibiting NFκB and activating IκB.	(Ho *et al.* 2011)

1.3 *Garcinia mangostana* Linn.

1.3.1 Botanical description

The genus Garcinia (Clusiaceae) includes 50-300 species of evergreen trees and shrubs native to Asia, Australia, tropical and southern Africa and Polynesia. Many of the species bear edible fruits. *Garcinia mangostana* is one of them (Ji *et al.* 2007).

A.

B.
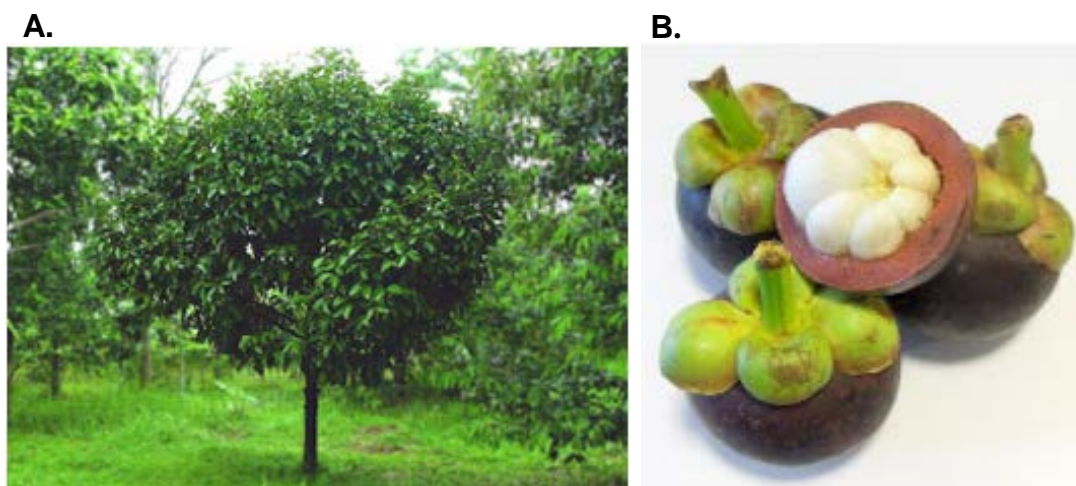
Figure 1-11
The images of the *Garcinia mangostana* Linn tree (A) and the mangosteen fruit (B) (Akao *et al.* 2008).

The mangosteen (*Garcinia mangostana* Linn.) is native to Malaysia and has been introduced to Northern Australia, Brazil, Central America, Hawaii, Southern India, Indonesia, Thailand and other tropical areas (Ji *et al.* 2007). This tropical tree is 6-25 m in height, has leathery leaves and is slow growing (Figure 1-11A) (Morton 1987). The mangosteen fruit, shown in Figure 1-11B, is dark purple or reddish in colour, with white, soft and juicy edible pulp that has a slightly acid and sweet flavour and a pleasant aroma (Jung *et al.* 2006). It is known as "the queen of fruits" because of its delicious pulp. Xanthones, anthocyanins, flavonoids, and benzophenones are found in the mangosteen, with xanthones being the major bioactive compounds (Govindachari & Muthukumaraswamy 1971; Jung *et al.* 2006; Peres *et al.* 2000;

Sultanbawa 1980; Yamakuni *et al.* 2006).

1.3.2 Traditional medical properties

Various plant parts of the mangosteen (e.g. pericarp, bark, and roots) have been used

for centuries as a medicine by Southeast Asians and South Americans for a great

variety of medical conditions, as summarised in Table 1-8 (Obolskiy *et al.* 2009;

Pedraza-Chaverri *et al.* 2008a). The pericarp, for example, has been used to treat skin

infections and wounds in Southeast Asia for hundreds of years (Mahabusarakam *et

al.* 1987; Pierce 2003).

Table 1-8
Traditional medicinal uses of *Garcinia mangostana* (adapted from the review by
Pedraza-Chaverri *et al.* (2008a)).

Medical conditions	References
Dysentery	(Morton 1987; Yates & Stout 1958)
Diarrhoea and chronic diarrhoea	(Morton 1987)
Haemorrhoids	(Pierce 2003)
Food allergies	(Pierce 2003)
Arthritis	(Pierce 2003)
Wounds	(Mahabusarakam *et al.* 1987; Pierce 2003)
Skin infections	(Jinsart *et al.* 1992; Mahabusarakam *et al.* 1987; Pierce 2003)
Tuberculosis	(Suksamrarn *et al.* 2006)
Inflammation	(Chairungsrilerd *et al.* 1996; Harbone *et al.* 1999)
Ulcers	(Harbone *et al.* 1999)
Micosis	(Harbone *et al.* 1999; Saralamp *et al.* 1996)
Gonorrhoea, cystitis and urethra suppuration	(Moongkarndi *et al.* 2004; Morton 1987)
Mouth aphthae	(Caius 2003)
Fever	(Caius 2003; Morton 1987; Yates & Stout 1958)
Amoebic dysentery	(Caius 2003; Morton 1987)
Eczema	(Morton 1987)
Acne	(Chomnawang *et al.* 2005; Saralamp *et al.* 1996)
Thrush	(Morton 1987)
Abdominal pain	(Moongkarndi *et al.* 2004)
Leucorrhoea	(Moongkarndi *et al.* 2004)

1.3.3 Xanthones in the mangosteen and their chemical structures

Xanthones are a class of polyphenolic compounds. They have a skeleton of a

xanthene-9-one, which is symmetrical and carbons are counted based on a

biosynthetic convention (see Figure 1-12) (Obolskiy *et al.* 2009).

Xanthones occur commonly in only a few higher plant families, including fungi and lichens (Jung *et al.* 2006; Peres *et al.* 2000). To date, approximately 200 xanthones have been found in nature (Akao *et al.* 2008) and they can be subdivided, based on the nature of substituent, into simple oxygenated xanthones, glycosylated xanthones, prenylated xanthones and their derivatives, xanthone dimers, xanthonolignoids and miscellaneous xanthones (Pinto *et al.* 2005)

In the mangosteen, approximately 50 xanthones are found in different parts of the plant (summarised in Table 1-9) (Akao *et al.* 2008). They are the major bioactive compounds in the mangosteen (Jung *et al.* 2006; Peres *et al.* 2000). The majority of xanthones present in mangosteen have a ring system that is substituted with a variety of isoprene, phenolic and methoxy groups that give a large variety of possible structures. The chemical structures of eight major xanthones contained in pericarps are shown in Figure 1-12.

The majority of investigations on mangosteen that have been performed to date are focused on extraction and structure elucidation of xanthones from the pericarp of the fruit (Asai *et al.* 1995; Puripattanavong *et al.* 2006; Suksamrarn *et al.* 2002). Recently, the presence of these compounds in the heartwood, stem and seed has also been reported (Table 1-9) (Ee *et al.* 2006; Harrison 2002; Sakagami *et al.* 2005; Suksamrarn *et al.* 2003). The profiles and structures of all currently known secondary metabolites of mangosteen were reviewed by Obolskiy *et al.*(2009) and Pedraza-Chaverri *et al.*(2008a).

As shown in Table 1-9, over 50% of known mangosteen xanthones are isolated from the pericarp of mangosteen. α-Mangostin appears to be the most abundant xanthone compound in the mangosteen because it exists in various parts of the plant, including pericarp, whole fruit, stem, arils, and seed.
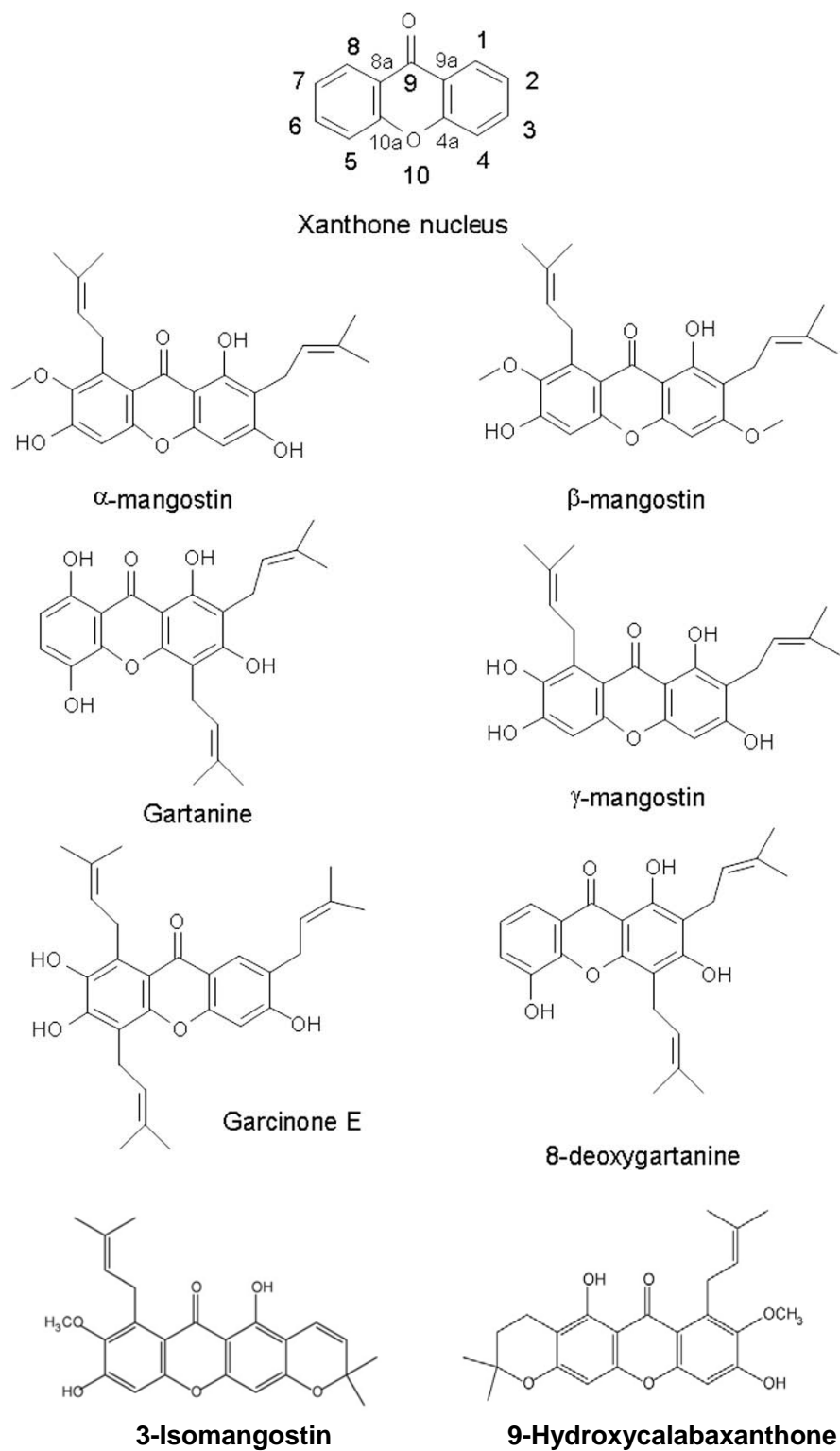
Figure 1-12
Xanthone nucleus with IUPAC numbers of carbons and chemical structures of the most studied xanthones (Obolskiy *et al.* 2009; Pedraza-Chaverri *et al.* 2008a).

Table 1-9
Xanthones isolated from *Garcinia mangostana* (mangosteen) (adapted from (Obolskiy *et al.* (2009)).

Compound name	Plant parts used	References
α-Mangostin	Pericarp, whole fruit, stem, arils, seeds	(Asai *et al.* 1995; Chen *et al.* 2008; Chin *et al.* 2008; Ee *et al.* 2006; Jung *et al.* 2006; Mahabusarakam *et al.* 1987; Matsumoto *et al.* 2003; Puripattanavong *et al.* 2006; Sakagami *et al.* 2005; Suksamrarn *et al.* 2006; Suksamrarn *et al.* 2003; Suksamrarn *et al.* 2002; Vieira & Kijjoa 2005)
β-Mangostin	Pericarp, Whole fruit, Stem	(Ee *et al.* 2006; Mahabusarakam *et al.* 1987; Matsumoto *et al.* 2003; Sakagami *et al.* 2005; Suksamrarn *et al.* 2006; Suksamrarn *et al.* 2002; Vieira & Kijjoa 2005)
γ-Mangostin	Pericarp, Whole fruit	(Asai *et al.* 1995; Gopalakrishnan *et al.* 1997; Jung *et al.* 2006; Mahabusarakam *et al.* 1987; Matsumoto *et al.* 2003; Peres *et al.* 2000; Suksamrarn *et al.* 2006; Suksamrarn *et al.* 2003)
(16E)-1,6-Dihydroxy-8-(3-hydroxy-3-methylbut-1-enyl)-3,7-dimethoxy-2-(3-methylbut-2-enyl)-xanthone	Heartwood	(Harrison 2002; Vieira & Kijjoa 2005)
Mangostinone	Pericarp, Whole fruit	(Asai *et al.* 1995; Jung *et al.* 2006; Matsumoto *et al.* 2003; Suksamrarn *et al.* 2006; Vieira & Kijjoa 2005)
Trapezifolixanthone	Pericarp	(Suksamrarn *et al.* 2002; Vieira & Kijjoa 2005)

Table 1-9 (Continued)

Compound name	Plant parts used	References
1,2-Dihydro-1,8,10-trihydroxy-2-(2-hydroxypropan-2-yl)-9-(3-methylbut-2-enyl)furo[3,2-a]xanthen-11-one	Whole fruit	(Chin *et al.* 2008)
1,3,6,7-Tetrahydroxy xanthone	Heart wood	(Farnsworth & Bunyapraphatsara 1992)
1,3,6,7-Tetrahydroxy-2,8-(3-methyl-2-butenyl) xanthone P1	Pericarp	(Yu *et al.* 2007)
1,3,6-Trihydroxy-7-methoxy-2,8-(3-methyl-2-butenyl) xanthone P2	Pericarp	(Yu *et al.* 2007)
1,3,8-Trihydroxy-4-methyl-2,7-diisoprenylxanthone	*Not stated*	(Vieira & Kijjoa 2005)
1,3,7-Trihydroxy-2,8-di-(3-methylbut-2-enyl)-xanthone	Whole fruit	(Chin *et al.* 2008)
1,3-Dihydroxy-2-(2-hydroxy-3-methylbut-3-enyl)-6,7-dimethoxy-8-(3-methylbut-2-enyl)-xanthone	Heartwood	(Harrison 2002; Vieira & Kijjoa 2005)
1,5-Dihydroxy-2-(3-methylbut-2-enyl)-3-methoxy-xanthone	Pericarp	(Asai *et al.* 1995)
1,5-dihydroxy-2-isopentyl-3-methoxy xanthone	Pericarp	(Farnsworth & Bunyapraphatsara 1992)
1,5,8-Trihydroxy-3-methoxy-2-(3-methylbut-2-enyl) xanthone	Leaves	(Farnsworth & Bunyapraphatsara 1992; Peres *et al.* 2000)
1,6-Dihydroxy-2-(2-hydroxy-3-methylbut-3-enyl)-3,7-dimethoxy-8-(3-methylbut-2-enyl)-xanthone	Heartwood	(Harrison 2002; Vieira & Kijjoa 2005)
1,6-Dihydroxy-3-methoxy-2-(3-methyl-2-buthenyl)-xanthone	Leaves	(Farnsworth & Bunyapraphatsara 1992)
(16E)-1-Hydroxy-8-(3-hydroxy-3-methylbut-1-enyl)-3,6,7-trimethoxy-2-(3-methylbut-2-enyl)-xanthone	Heartwood	(Harrison 2002; Vieira & Kijjoa 2005)

Table 1-9 (Continued)

Compound name	Plant parts used	References
1,6-Dihydroxy-3,7-dimethoxy-2-(3-methylbut-2-enyl)-8-(2-oxo-3-methylbut-3-enyl)-xanthone	Heartwood	(Harrison 2002; Vieira & Kijjoa 2005)
1,6-Dihydroxy-3,7-dimethoxy-2-(3-methylbut-2-enyl)-xanthone	Heartwood, Stem	(Ee *et al.* 2006; Harrison 2002; Vieira & Kijjoa 2005)
1,6-Dihydroxy-8-(2-hydroxy-3-methylbut-3-enyl)-3,7-dimethoxy-2-(3-methylbut-2-enyl)-xanthone	Heartwood	(Harrison 2002; Vieira & Kijjoa 2005)
1,7-Dihydroxy-2-(3-methylbut-2-enyl)-3-methoxy-xanthone	Pericarp	(Asai *et al.* 1995; Matsumoto *et al.* 2003; Suksamrarn *et al.* 2003; Vieira & Kijjoa 2005)
1,7-dihydroxy-2-isopentyl-3-methoxy xanthone	Pericarp	(Farnsworth & Bunyapraphatsara 1992)
11-Hydroxy-1-isomangostin	Whole fruit	(Suksamrarn *et al.* 2006)
1-Hydroxy-2-(2-hydroxy-3-methylbut-3-enyl)-3,6,7-trimethoxy-8-(3-methylbut-2-enyl)-xanthone	Heartwood	(Harrison 2002; Vieira & Kijjoa 2005)
1-Hydroxy-8-(2-hydroxy-3-methylbut-3-enyl)-3,6,7-trimethoxy-2-(3-methylbut-2-enyl)-xanthone	Heartwood	(Harrison 2002; Vieira & Kijjoa 2005)
1-Isomangostin	Pericarp	(Farnsworth & Bunyapraphatsara 1992; Jung *et al.* 2006; Mahabusarakam *et al.* 1987; Peres *et al.* 2000; Vieira & Kijjoa 2005)
1-Isomangostin hydrate	Pericarp	(Mahabusarakam *et al.* 1987; Peres *et al.* 2000)
2-(γ,γ-Dimethylallyl)-1,7-dihydroxy-3-methoxyxanthone	Pericarp, Arils	(Farnsworth & Bunyapraphatsara 1992; Mahabusarakam *et al.* 1987)
2,3,6,8-Tetrahydroxy-1-isoprenylxanthone	*Not stated*	(Vieira & Kijjoa 2005)

Table 1-9 (Continued)

Compound name	Plant parts used	References
2,8-bis-(γ,γ-Dimethyallyl)-1,3,7-trihydroxyxanthone	Arils	(Farnsworth & Bunyapraphatsara 1992; Mahabusarakam *et al.* 1987)
3-Isomangostin	Pericarp	(Farnsworth & Bunyapraphatsara 1992; Mahabusarakam *et al.* 1987; Vieira & Kijjoa 2005)
3-Isomangostin hydrate	Pericarp	(Farnsworth & Bunyapraphatsara 1992; Mahabusarakam *et al.* 1987)
5,9-Dihydroxy-8-methoxy-2,2-dimethyl-7-(3-methylbut-2-enyl)-2H,6Hpyrano-[3,2,6]-xanthene-6-one	Pericarp	(Ee *et al.* 2006)
6-Deoxy-7-demethylmangostanin	Whole fruit	(Chin *et al.* 2008)
6-O-Methylmangostanin	*Not stated*	(Vieira & Kijjoa 2005)
8-Deoxygartanine	Pericarp, Whole fruit	(Farnsworth & Bunyapraphatsara 1992; Gopalakrishnan *et al.* 1997; Suksamrarn *et al.* 2006; Vieira & Kijjoa 2005)
8-Hydroxycudraxanthone	Pericarp	(Jung *et al.* 2006)
BR-Xanthone	Pericarp	(Gopalakrishnan *et al.* 1997; Peres *et al.* 2000)
Calabaxanthone	Arils	(Farnsworth & Bunyapraphatsara 1992; Mahabusarakam *et al.* 1987)
Cudraxanthone G	Pericarp	(Jung *et al.* 2006)
Demethylcalabaxanthone	Whole fruit, Arils, Seed	(Mahabusarakam *et al.* 1987; Suksamrarn *et al.* 2003)
Garcimangosone A	Pericarp	(Huang *et al.* 2001; Vieira & Kijjoa 2005)
Garcimangosone B	Pericarp	(Huang *et al.* 2001; Jung *et al.* 2006; Vieira & Kijjoa 2005)
Garcimangosone C	Pericarp	(Huang *et al.* 2001; Vieira & Kijjoa 2005)
Garciniafuran	Heartwood	(Harrison 2002)

Table 1-9 (Continued)

Compound name	Plant parts used	References
Garcinone B	Pericarp, Whole fruit	(Farnsworth & Bunyapraphatsara 1992; Suksamrarn *et al.* 2006; Suksamrarn *et al.* 2002)
Garcinone C	Whole fruit	(Farnsworth & Bunyapraphatsara 1992; Peres *et al.* 2000; Suksamrarn *et al.* 2006)
Garcinone D	Pericarp, Whole fruit, Stem	(Farnsworth & Bunyapraphatsara 1992; Jung *et al.* 2006; Suksamrarn *et al.* 2006; Suksamrarn *et al.* 2003; Vieira & Kijjoa 2005)
Garcinone E	Pericarp, Whole fruit	(Asai *et al.* 1995; Jung *et al.* 2006; Matsumoto *et al.* 2003; Peres *et al.* 2000; Suksamrarn *et al.* 2006; Vieira & Kijjoa 2005)
Gartanine	Pericarp, Whole fruit	(Asai *et al.* 1995; Gopalakrishnan *et al.* 1997; Jung *et al.* 2006; Mahabusarakam *et al.* 1987; Peres *et al.* 2000; Suksamrarn *et al.* 2006; Vieira & Kijjoa 2005)
Mangosharin	Stem	(Ee *et al.* 2006)
Mangostanin	Pericarp	(Harrison 2002; Suksamrarn *et al.* 2003; Vieira & Kijjoa 2005)
Mangostanol	Whole fruit, Stem	(Peres *et al.* 2000; Suksamrarn *et al.* 2006; Suksamrarn *et al.* 2002; Vieira & Kijjoa 2005)
Mangostenol	Pericarp	(Suksamrarn *et al.* 2002; Vieira & Kijjoa 2005)
Mangostenone A	Pericarp	(Suksamrarn *et al.* 2002; Vieira & Kijjoa 2005)
Mangostenone B	Pericarp	(Suksamrarn *et al.* 2002; Vieira & Kijjoa 2005)
Mangostenone C	Whole fruit	(Suksamrarn *et al.* 2006)
Mangostenone D	Whole fruit	(Suksamrarn *et al.* 2006)
Mangostenone E	Whole fruit	(Suksamrarn *et al.* 2006)
Smeathxanthone A	Pericarp	(Jung *et al.* 2006)
Thwaitesixanthone	Whole fruit	(Suksamrarn *et al.* 2006)
Tovophyllin A	Pericarp	(Jung *et al.* 2006)
Tovophyllin B	Pericarp	(Suksamrarn *et al.* 2002; Vieira & Kijjoa 2005)

1.3.4 Biological activities of extracts and pure compounds derived from mangosteen

Extracts and pure compounds derived from mangosteen, mainly individual xanthones, have been reported to have a great variety of biological activities. These include antioxidant, antifungal, antibacterial, antitumoral, anti-inflammatory, antihistamine, anti-HIV and others. These activities have been reviewed in detail (Obolskiy *et al.* 2009; Pedraza-Chaverri *et al.* 2008a; Shan *et al.* 2011) and are summarised below.

1.3.4.1 Antioxidant effect of mangosteen

Mangosteen extracts and xanthone compounds have exhibited antioxidant activity as summarised in Table 1-10.

The antioxidant activity was detected using various chemical-based assays (e.g. DPPH (2, 2-diphenyl-1-picrylhydrazyl) radical scavenging assay, the ferric thiocyanate method, and ABTS (2, 20-azino-bis-(3-ethylbenzthiazoline-6-sulfonic acid) assays). Mangosteen extracts and compounds exert their antioxidant activity by scavenging free radicals (e.g. DPPH free radicals, hydroxyl radical (HO^-) and peroxynitrite ($ONOO^-$)), and/or inhibiting oxidation (e.g. lipid peroxidation, limoleic acid oxidation, and low-density lipoprotein (LDL) oxidation).

Mangosteen displays a high level of antioxidant activities, compared with other fruit and vegetables. For example, among 19 Thai medicinal plant extracts, mangosteen exhibited the highest level of antioxidant activity, as evidenced by the lowest IC_{50} value (the concentration scavenging 50% of DPPH radicals) for DPPH assay (6.1 µg/ml for mangosteen extract; 32.5 ─ >150 µg/ml for the other plants extracts tested) and the highest superoxide radical inhibition rate (77.8% for mangosteen; 8.0─

62.6% for the other plants extracts tested) (Chomnawang *et al.* 2007). Similar results were reported by Leong & Shui (2002) when the antioxidant activity was detected by the DPPH and ABTS assays among 27 different fruit pulps.

The level of antioxidant activity of mangosteen extract varies depending on the extraction methods used. For example, as detected by DPPH assay, different IC_{50} values were obtained from different mangosteen pericarp extracts: 6.1 µg/ml for 100% ethanol extract (Chomnawang *et al.* 2007), 30.8, 58.5, 77.8 and 35.0 µg/ml for 50% ethanol, 95% ethanol, ethyl acetate and water extract, respectively (Weecharangsan *et al.* 2006). Therefore, in the future, the extraction method could be optimised to achieve higher antioxidant activity.

The antioxidant capacity of mangosteen xanthones was also tested on cell-based assays. The antioxidant capacity of ethanol and water extracts of mangosteen pericarp was tested by Weecharangsan *et al.* (2006) on a neuroblastoma cell line (NG108-15) exposed to hydrogen peroxide; both extracts exhibited neuroprotective activity at a concentration of 50 µg/ml. The 50% ethanolic extract had higher neuroprotective activity than the water extract (Weecharangsan *et al.* 2006). Chin *et al.* (2008) have also demonstrated the antioxidant activities of selected xanthones. 1,2-dihydro-1,8,10-trihydroxy- 2 -(2-hydroxypropan- 2 -yl)- 9 -(3-methylbut- 2 -enyl) furo [3, 2-a] xanthen-11-one, 6-deoxy-7-demethylmangostanin, 1,3,7-trihydroxy-2,8-di-(3-mehylbut-2-enyl)-xanthone and mangostanin all induced quinone reductase in the Hepa 1c1c7 cell line in an *in vitro* screening assay (IC_{50}, 0.68-2.2 µg/ml), whereas γ-mangostin exhibited hydroxyl radical-scavenging activity (IC_{50}, 0.2 µg/ml).

Mahabusarakam *et al.* (2000) found that the antioxidant activity of α-mangostin can be affected by its structural modifications. For example, substitution of C-3 and C-6 with aminoethyl derivatives enhanced the activity, whereas substitution with methyl, acetate, propanediol or nitrile reduced the antioxidant activity. This shows that the structure of xanthone compounds can be modified to improve their antioxidant activity.

Antioxidants are important for preventing cancer development by inhibiting oxidative damage through mechanisms such as scavenging free radicals and inhibiting oxidation (Weisburger 1999), as discussed in Sections 1.1.4.2 and 1.2.1. Therefore, due to their antioxidant activity, mangosteen extracts and compounds may have the potential to prevent UV-induced skin damage and subsequent cancer.

Table 1-10

Antioxidant properties of extracts and xanthones isolated from mangosteen, including information from the review by Obolskiy *et al.* (2009) and Pedraza-Chaverri *et al.* (2008a).

Extract / Compound	Activities	Reference
Methanol extract of pericarp	DPPH free radical scavenging activity	(Yaoshikawa *et al.* 1994)
Methanol extract of pericarp	Amelioration of the intracellular production of ROS in SKBR3 cells	(Moongkarndi *et al.* 2004)
Methanol extract of pericarp	Scavenging of HO⁻ and effective inhibition of lipid peroxidation	(Garcia *et al.* 2005)
Ethanol extract of pericarp	DPPH free radical scavenging and ROS reduction	(Chomnawang *et al.* 2007)
Aqueous and ethanol extract of pericarp	DPPH radical scavenging activity and protection of neuroblastoma cell line NF108-15 from H_2O_2 cytotoxicity	(Weecharangsan *et al.* 2006)
Chloroform extract of pericarp	DPPH free radical scavenging activity	(Puripattanavong *et al.* 2006)
Methanol extract of pulp	DPPH radical scavenging activity and prevention of decrease in antioxidant activity induced by a cholesterol supplemented diet in rats	(Haruenkit *et al.* 2007)
Methanol extract of pulp	Antioxidant activity using DPPH and ABTS assays	(Leong & Shui 2002)
α-Mangostin	Scavenging of singlet oxygen, superoxide anion and peroxynitrite anion	(Pedraza-Chaverri *et al.* 2008b)
α-Mangostin	Inhibition of copper-induced LDL oxidation *in vitro*	(Williams *et al.* 1995)
α-Mangostin	Protection against isoproterenol-induced oxidative damage and myocardial injury in rats	(Devi Sampath & Vijayaraghavan 2007)
α-Mangostin and its derivatives	Inhibition of copper-induced LDL oxidation *in vitro*	(Mahabusarakam *et al.* 2000)
α-Mangostin and γ-mangostin	Antioxidant activity as detected by the ferric thiocyanate method	(Fan & Su 1997)
γ-Mangostin	HO⁻-scavenging activity	(Chin *et al.* 2008)

Table 1-10 (Continued)

Extract / Compound	Activities	Reference
α-Mangostin γ-Mangostin Gartanine Smeathxanthone 8-Hydroxycubraxanthone	$ONOO^-$-scavenging activity *in vitro*	(Jung et al. 2006)
P1(1,3,6,7-tetrahydroxy-2,8-(3-methyl-2-butenyl)xanthone) P2(1,3,6-trihydroxy-7-methoxy-2,8-(3-methyl-2-butenyl)xanthone) Epicatechin	DPPH radical scavenging activity Hydroxy radical scavenging activity Superoxide anion radical scavenging activity Inhibition of linoleic acid oxidation	(Yu *et al.* 2007)

1.3.4.2 Cytotoxicity of mangosteen towards cancer cells

The significant cytotoxicity of xanthones has been demonstrated on a range of cancer cell lines (summarised in Table 1-11). It can be mediated by several modes of action, including the following three major aspects:

1) Significant cell cycle arrest of cancer cells at various phases (Figure 1-13). For example, α-mangostin induced G_1/S cell cycle arrest and γ-mangostin induced S phase arrest on colon cancer DLD-1 cells by modulation of the expression of cyclin A, B1, D1, E1, or p27 (Matsumoto *et al.* 2005);

2) Significant apoptosis induction via different pathways (Figure 1-14). Xanthones can exert the apoptotic effect through intrinsic (Matsumoto *et al.* 2004; Nakagawa *et al.* 2007) and / or extrinsic pathways (Krajarng *et al.* 2011; Watanapokasin *et al.* 2011). Additionally, treatment with xanthone compounds in different cell lines can mediate apoptosis in different pathways. For example, α-mangostin induced apoptosis in human leukaemia HL-60 cells by activation of caspase-3 and caspase-9 (Matsumoto *et al.* 2004), while

in human colon DLD-1 cells it was by a caspase-independent pathway (Nakagawa *et al.* 2007);

3) Modulation of different survival pathways (Figure 1-14). For example, treatment with α-mangostin downregulated MAPK and Akt pathways on human colon DLD-1 cells (Nakagawa *et al.* 2007), and human Chondrosarcoma SW1353 cells (Krajarng *et al.* 2011).

After treatment with a xanthone compound, different sensitivities were observed in different types of cancer cells, as evidenced by the IC_{50} values (summarised in Table 1-12). For example, after treatment with γ-mangostin, IC_{50} values ranging from 6.1 to 74.1 µg/ml were observed in different cancer cell lines. Therefore, treatment with the same xanthone compound can induce different cytotoxic responses in different cancer cell lines, possibly due to the different mechanisms as discussed above.

A correlation between the structures and cytotoxicity of xanthones has been reported. For a high anticancer activity, the xanthones should contain tetraoxygen functional groups with two C5 isoprenyl units in rings A and B. In contrast, cyclisation of the C5 group results in a significant decrease of activity (Suksamrarn *et al.* 2006). The prenyl group of xanthones is implied to be involved in internalization into the cell, resulting in interaction with the signal transduction molecules and the proteins involved in mitochondria permeability transition (Bae *et al.* 2006; Watjen *et al.* 2007).

The studies on cytotoxicity using *in vivo* models have also been reported (Table 1-11). Administration of α-mangostin significantly inhibited the occurrence of

biomarkers (e.g. aberrant crypt foci, dysplastic foci, and β-catenin accumulated crypt) in a rat colon cancer model (Nabandith *et al.* 2004). Likewise, α-mangostin was found to inhibit DMBA-induced preneoplastic lesions in a mouse mammary organ culture assay (Jung *et al.* 2006). However, a lack of activity was also reported when α-mangostin (20 µg/ml) was tested in an *in vivo* hollow fibre assay, using HT-29, LNCaP, and MCF-7 cells (Han *et al.* 2009). This discrepancy may be explained by the different origins of cancer, the different routes of administration, and the different concentrations tested (Shan *et al.* 2011).

In summary, xanthones have been shown to induce cytotoxicity *in vitro* and in some studies also *in vivo*. The mechanisms have been found to be through various modes of action, which are cell-type dependent and xanthone structure related.

.

Table 1-11

Cytotoxicity of xanthones isolated from mangosteen, including information from the review by Obolskiy *et al.* (2009) and Pedraza-Chaverri *et al.* (2008a).

Extract / Compound	Activities	Reference
Ethanol extract of pericarp	Antiproliferative activity against SKBR3 human breast adenocarcinoma cell line	(Moongkarndi *et al.* 2004)
Ethyl acetate extract of pericarp	Cytotoxicity against colon cancer both *in vitro* (COLO 205) and in a mouse subcutaneous tumour model by induction of apoptosis	(Watanapokasin *et al.* 2010)
Methanol extract of pericarp	Antiproliferation, antioxidation and induction of apoptosis of SKBR3 human breast cancer cell line	(Moongkarndi *et al.* 2004)
Aqueous extract of pericarp	Cytotoxic effect against K562 and Raji leukaemia cells	(Chiang *et al.* 2004)
α-Mangostin	Cytotoxic effect against murine BJMC3879luc2 mammary adenocarcinoma cells and human mammary carcinoma MDA-MB231 cells by inducing cell1 cycle arrest in G_1 phase and inducing apoptosis via activation of caspase 3 and 9 and suppression of phospho-Akt-threonine 308 (Thr308), but not serine 473 (Ser473)	(Shibata *et al.* 2011)
α-Mangostin	Induction of apoptosis by a caspase-indepent pathway via mitochondria with the release of Endonuclease-G in human colon cancer DLD-1 cells.	(Nakagawa *et al.* 2007)
α-Mangostin	Induction of Ca^{2+}-ATPase-dependent apoptosis via mitochondrial pathway through induction of cytochrome c release in PC12 pheochromocytoma (cancer) cells	(Sato *et al.* 2004)

Table 1-11 (Continued)

Extract / Compound	Activities	Reference
α-Mangostin	Inhibition of DMBA-induced preneoplastic lesions in a mouse mammary organ culture	(Jung *et al.* 2006)
α-Mangostin	Dietary administration of α-mangostin significantly inhibited the occurrence of biomarkers for short-term colon carcinogenesis (aberrant crypt foci, dysplastic foci and β-catenin accumulated crypt) induced by DMH in rat. It can be suggested that longer exposure might result in suppression of tumour development	(Nabandith *et al.* 2004)
α-Mangostin γ-Mangostin	α-mangostin induced G_1/S cell cycle arrest and subsequent apoptosis via the intrinsic pathway in human colon cancer DLD-1 cells, while a cell cycle arrest by γ-mangostin was S-phase	(Matsumoto *et al.* 2005)
α-Mangostin	Targeting mitochondria pathway, resulting in indication of apoptosis in human leukaemia cell line HL60	(Matsumoto *et al.* 2004)
α-Mangostin; β-Mangostin γ-Mangostin; Mangstinone Garcinone E 2-Isoprenyl-1,7-dihydroxy-3methoxy xanthone	Significant human leukaemia HL60 cell growth inhibition, α-mangostin, β-mangostin and γ-mangostin were particularly effective. In addition, α-mangostin induced caspase 3-dependent apoptosis in HL60	(Matsumoto *et al.* 2003)
α-Mangostin; β-Mangostin γ-Mangostin; Gartanine Garcinone C, D, E; Mangostenone C, D; Demethylcalabaxanthone	Cytotoxicity on epidermoid carcinoma of the mouth (KB), breast cancer (BC-1), and small cell lung cancer (NCI-H187) cells	(Suksamrarn *et al.* 2006)

Table 1-11 (Continued)

Extract / Compound	Activities	Reference
γ-Mangostin	Induction of apoptosis by intracellular ROS accumulation on human malignant glioblastomas U87 MG and GBM 8401 cells	(Chang *et al.* 2010)
Garcinone E	Cytotoxic effect on all hepatocellular carcinoma cell lines as well as on the other gastric and lung cancer cell lines	(Ho *et al.* 2002)
11-hydroxy-3-O-methyl-1-isomangostin (1), 11-hydroxy-1-isomangostin(2), 11 α-mangostin(3), 3-isomangostin (4), α-mangostin (5), β-mangostin (6), garcinone D (7), 9-hydroxycalabaxanthone (8), 8-deoxygartanin (9), gartanin (10) and cratoxyxanthone (11)	Compounds 4-8 exhibited cytotoxcity against the colon cancer HT-29 cell line with ED50 values of 4.9, 1.7, 1.7, 2.3 and 9.1 µM, respectively. In an ELISA NFκB assay, compounds 5-7, 9, and 10 inhibited p65 activation with IC_{50} values of 15.9, 12.1, 3.2, 11.3 and 19.0 µM, respectively, and 6 showed p50 inhibitory activity with and IC_{50} value of 7.5 µM. α-mangostin was further tested in an *in vivo* hollow fibre assay, using HT-29, LNCaP, and MCF-7 cells, but it was found to be inactive at the highest dose tested (20 µg/ml).	(Han *et al.* 2009)
1,3,7-Trihydroxy-2,8-di-(3-methylbut-2-enyl)-xanthone 1,2-Tihydro-1,8,10-trihydroxy-2-(2-hydroxypropan-2-yl)-9-(3-methylbut-2-enyl)furo[3,2-*a*] xanthen-11-one-6-Deoxy-7-demethylmangostanin	Quinone reductase inductive activity using Hepa1c1c 7 cells of murine hepatoma	(Chin *et al.* 2008)

Table 1-11 (Continued)

Extract / Compound	Activities	Reference
Twelve xanthone constituents of a botanical dietary supplement from the mangosteen pericarp, including α-mangostin, γ-mangostin, garcinone D and E.	These xanthones were screened using a noncellular enzyme-based microsomal aromatase inhibition assay and followed by a cell-based assay using SKBR3 breast cancer cells. The results of both assays showed that certain xanthones from mangosteen fruits act as potent aromatase inhibitors, especially γ-mangostin, and might thus have a potential role in cancer chemoprevention for postmenopausal women with hormone-dependent breast cancer	(Balunas *et al.* 2008)

Table 1-12

IC_{50} values of mangosteen extracts and xanthone compounds *in vitro,* including information from the review by Shan *et al.* (2011).

Extract / xanthone compound	Cancer cell line	IC_{50} value (µg/ml)	Reference
Aqueous extract of pericarp	Leukaemia K562	61.0	(Chiang *et al.* 2004)
	Leukaemia Raji	159.2	(Chiang *et al.* 2004)
Ethyl acetate extract of pericarp	Colon cancer COLO 205	7.5	(Watanapokasin *et al.* 2010)
	Colon cancer CX-1	17.7	(Watanapokasin *et al.* 2010)
	Colon cancer MIP-101	10.0	(Watanapokasin *et al.* 2010)
	Colon cancer SW620	16.1	(Watanapokasin *et al.* 2010)
Ethanol extract of pericarp	Breast cancer SKBR3	15.5	(Moongkarndi *et al.* 2004)
Methanol extract of pericarp	Breast cancer SKBR3	9.3	(Moongkarndi *et al.* 2004)
α-Mangostin	Leukaemia HL-60	2.8	(Matsumoto *et al.* 2003)
	Lung cancer A549	5.1-6.2	(Shih *et al.* 2010)
	T-lymphoblastic leukaemia CEM-SS	5.3	(Ee *et al.* 2008)
	Leukaemia K562	< 4.1	(Matsumoto *et al.* 2003)
	Leukaemia NB4	< 4.1	(Matsumoto *et al.* 2003)
	Leukaemia U937	< 4.1	(Matsumoto *et al.* 2003)
	Mouth epidermoid carcinoma KB	2.1	(Suksamrarn *et al.* 2006)
	Pheochromocytoma PC12	1.6	(Sato *et al.* 2004)
	Colon cancer DLD-1	3.1	(Matsumoto *et al.* 2004)
	Colon cancer HT-29	0.7	(Laphookhieo *et al.* 2006)
	Colon cancer COLO 205	9.7	(Watanapokasin *et al.* 2011)
	MIP-101	11.35	(Watanapokasin *et al.* 2011)
	SW620	19.6	(Watanapokasin *et al.* 2011)
	Breast cancer BC-1	0.9	(Suksamrarn *et al.* 2006)
	Chondrosarcoma SW1353	10	(Krajarng *et al.* 2011)

Table 1-12 (Continued)

Extract / xanthone compound	Cancer cell line	IC$_{50}$ value (µg/ml)	Reference
β-Mangostin	Leukaemia HL-60	3.2	(Matsumoto *et al.* 2003)
	Colon cancer DLD-1	3.4	(Matsumoto *et al.* 2004)
	Colon cancer HT-29	0.7	(Laphookhieo *et al.* 2006)
γ-Mangostin	Leukaemia HL-60	2.4	(Matsumoto *et al.* 2003)
	T-lymphoblastic leukaemia CEM-SS	4.5	(Ee *et al.* 2008)
	Colon cancer DLD-1	2.8	(Matsumoto *et al.* 2004)
	Rat glioma C6 cells	>11.9	(Nabandith *et al.* 2004)
	Human glioblastoma U87 MG	28.3	(Chang *et al.* 2010)
	Human glioblastoma GBM 8401	25.7	(Chang *et al.* 2010)
Gartanine	Lung cancer NCI-H187	1.0	(Suksamrarn *et al.* 2006)
9-Hydroxycalabaxanthone	Colon cancer HT-29	3.7	(Laphookhieo *et al.* 2006)
Mangostinone	Leukaemia HL-60	7.2	(Matsumoto *et al.* 2003)
Garcinone E	Leukaemia HL-60	7.8	(Matsumoto *et al.* 2003)
Garcinone D	T-lymphoblastic leukaemia CEM-SS	3.3	(Ee *et al.* 2008)
	Colon cancer HT-29	0.99	(Laphookhieo *et al.* 2006)
Mangostenone C	Lung cancer NCI-H187	3.72	(Suksamrarn *et al.* 2006)
	Breast cancer BC-1	3.53	(Suksamrarn *et al.* 2006)
	Mouth epidermoid carcinoma KB	2.8	(Suksamrarn *et al.* 2006)
Mangostenone D	Lung cancer NCI-H187	9.1	(Suksamrarn *et al.* 2006)
	Breast cancer BC-1	3.9	(Suksamrarn *et al.* 2006)
	Mouth epidermoid carcinoma KB	9.8	(Suksamrarn *et al.* 2006)
3-Isomangostin	Colon cancer HT-29	2.0	(Laphookhieo *et al.* 2006)
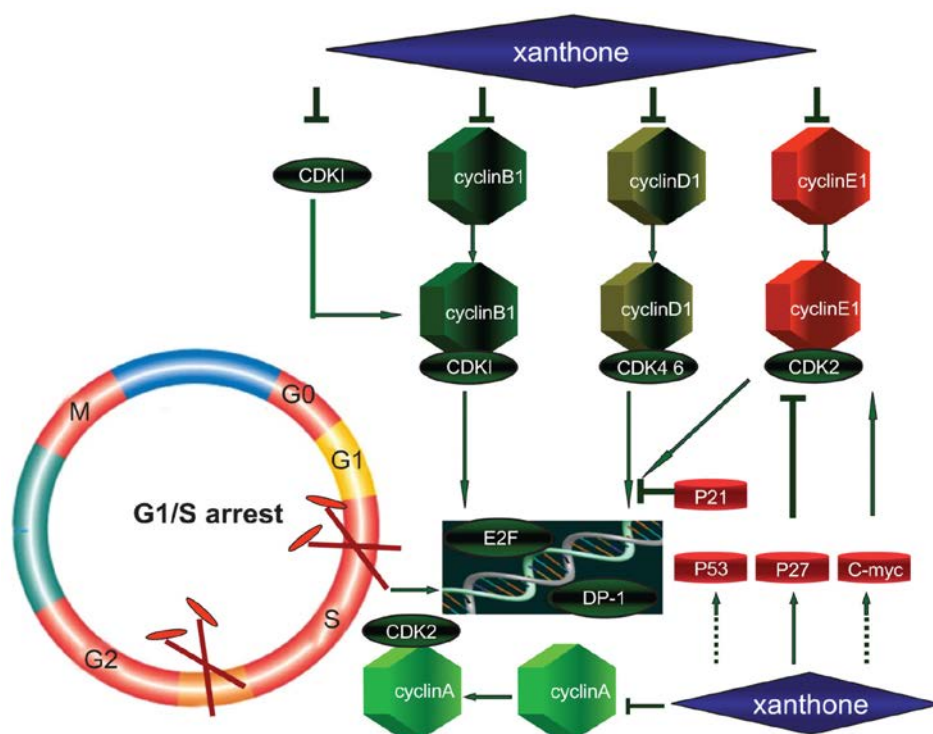
Figure 1-13
An overview of how xanthones induce cell-cycle arrest. Xanthones block the cell cycle by activation or inhibition of cyclins, cdks, inhibitor of cdks, transcription factors or oncoproteins in cancer cells (Taken from (Shan *et al.* 2011)).
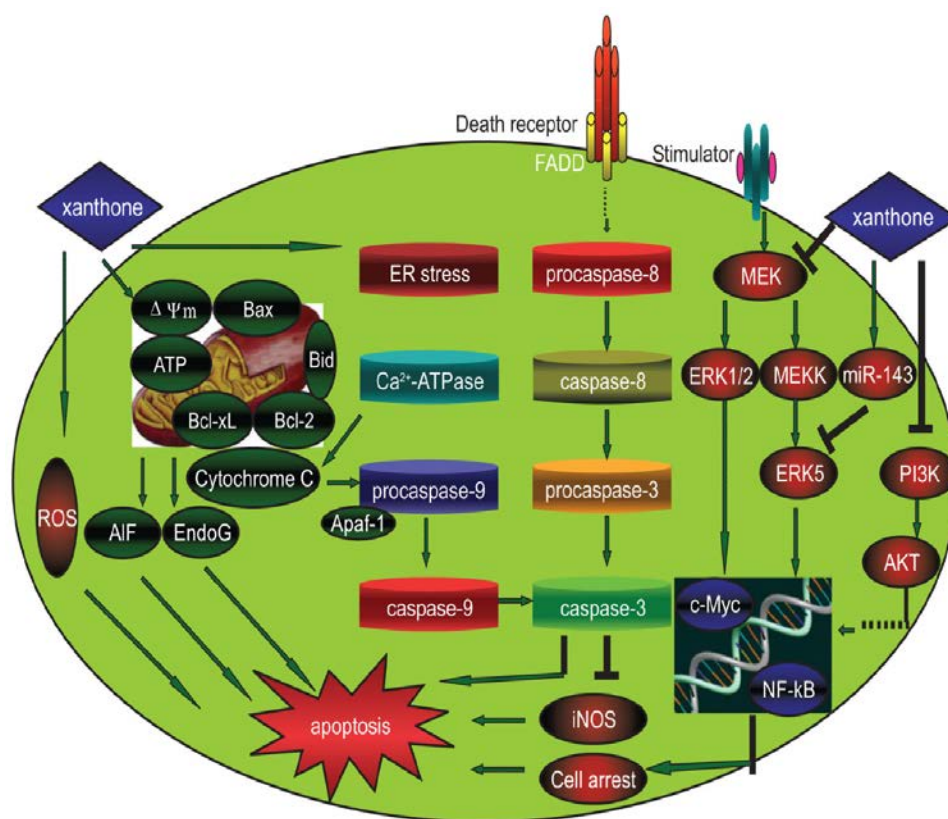
Figure 1-14
Schematic diagram shows the possible effect of xanthones on the apoptosis pathways. Xanthones induce apoptosis occurrence, preferentially activate the mitochondrial pathway, support intracellular ATP decrease, cytochrome c/AIF release, caspase-9 and caspase-3 activation, endonuclease-G release. Furthermore, xanthones also influence cancer cell apoptosis *via* miR-143/ERK5/c-Myc pathway, NO inhibition, cell-cycle arrest, sarcoendoplasmic reticulum Ca^{2+}-ATPase inhibition, and intracellular ROS accumulation (Taken from (Shan *et al.* 2011)).

1.3.4.3 Inhibition of metastasis

A number of studies have been carried out to investigate the anti-metastatic activity

of α-mangostin on different cancer cell lines (summarised in Table 1-13).

α-Mangostin inhibited the expression of MMP-2 and MMP-9 as well as NFκB

pathway via inhibition of degradation of IκBα in prostate PC3 (Hung *et al.* 2009),

lung A549 (Shih *et al.* 2010), and breast cancer MCF-7 (Lee *et al.* 2010) cell lines.

However, different mechanisms were found after treatment with α-mangostin in

these three different cell lines. Treatment with α-mangostin inhibited the JNK1/2

pathway but not the ERK1/2 pathway in PC3 cells (Hung *et al.* 2009). In contrast, treatment with α-mangostin inhibited the ERK1/2 pathway but not the JNK1/2 pathway in A549 (Shih *et al.* 2010) and MCF-7 cells (Lee *et al.* 2010). Additionally, the Akt pathway was not involved after treatment with α-mangostin in these three cancer cell lines (Hung *et al.* 2009; Lee *et al.* 2010; Shih *et al.* 2010). In contrast, study by Shibata *et al.* (2011) showed phospho-Akt-threonine 308 (Thr308) was inhibited after treatment with α-mangostin in human mammary carcinoma MDA-MB231 cells. Furthermore, the extent of these activities was found to be cell-type dependent. For example, α-mangostin at 2.1 µg/ml in A-549 cells reduced the invasion to 20% and migration to 40%, at 5 µg/ml in PC-3 cells reduced the invasion to 60% and migration to 40%, and at approximately 2.5 µg/ml in MCF-7 cells reduced the invasion to 55% and migration to 61% compared with the untreated control (Hung *et al.* 2009; Lee *et al.* 2010; Shih *et al.* 2010). These results suggest that α-mangostin exerts its anti-metastatic activity through different pathways in different types of cancer cells.

Promising results of anti-metastatic activity of xanthones were also indicated by the data obtained using *in vivo* models. Doi *et al.* (2009) reported that panaxanthone (a mixture of α- and γ-mangostin) exhibited anti-tumour and anti-metastatic activity in a mouse metastatic mammary cancer model. These effects were associated with induction of apoptosis, antiproliferation, and antiangiogenesis via inhibition of microvessel density. Likewise, in a xenograft model of metastatic mammary cancer in mice, administration of α-mangostin significantly reduced the tumour growth by inducing apoptosis via caspase 3 and 9 activation and reducing phospho-Akt-threonine 308 (Thr308), and reduced lymph node metastasis via decreasing

microvessel density (Shibata *et al.* 2011).

In summary, xanthones (e.g. α-mangostin, panaxanthone) have been found be effective to inhibit cancer cell metastasis both *in vitro* and *in vivo*. The effect has been shown to be associated with inhibition of cancer cell motility, migration, invasion, and angiogenesis. The underlying molecular mechanisms have been demonstrated to be via inhibition of expression of MMP-2 and MMP-9, NFκB, JNK1/2, ERK1/2, or Akt (Figure 1-15). The magnitude of the activity and the underlying molecular mechanisms are cell type dependent.

Table 1-13
Anti-metastatic activity of xanthones from mangosteen.

Xanthone	Experimental model	Activities	Reference
α-Mangostin	Human prostate carcinoma PC3 cell line	Reduction of MMP-2, MMP-9, and uPA expression through the suppression of the JNK1/2 signalling pathway and inhibition of NFκB and AP-1 binding activity	(Hung et al. 2009)
α-Mangostin	Human lung adenocarcinoma A549 cell line	Inhibition of the adhesion, invasion, and migration; inhibition of the activation of avb3 integrin, FAK, and ERK1/2 involved in the downregulation MMP-2 and MMP-9; inhibition of degradation of IκBα and the nuclear levels of NFκB.	(Shih *et al.* 2010)
α-Mangostin	Human breast adenocarcinoma MCF-7 cell line	Inhibition of the adhesion, invasion, and migration; inhibition of the activation of ERK1/2 involved in the downregulation the enzyme activities, protein, and messenger RNA levels of MMP-2 and MMP-9; inhibition of degradation of IκBα and the nuclear levels of NF-κB, c-Fos, and c-Jun	(Lee *et al.* 2010)

Table 1-13 (Continued)

Xanthone	Experimental model	Activities	Reference
α-Mangostin	Immunocompet-ent xenograft model of metastatic mammary cancer carrying a p53 mutation	Reduction of tumour growth and lymph node metastasis by inducing apoptosis via activation of caspase 3 and 9 and suppression of phospho-Akt-threonine 308 (Thr308), but not serine 473 (Ser473) and reducing microvessel density and numbers of dilated lymphatic vessels in mammary carcinoma tissues	(Shibata *et al.* 2011)
Panaxanthone (approximately 75% to 85% α-mangostin and 5% to 15% γ-mangostin)	Mouse model of mammary cancer	The antitumour growth and antimetastatic activity of panaxanthone were found in a mouse metastatic mammary cancer model. The antitumor effects were associated with elevation of apoptotic cell death, antiproliferation (inhibition of PCNA) and antiangiogenesis (inhibition of microvessel density)	(Doi *et al.* 2009)
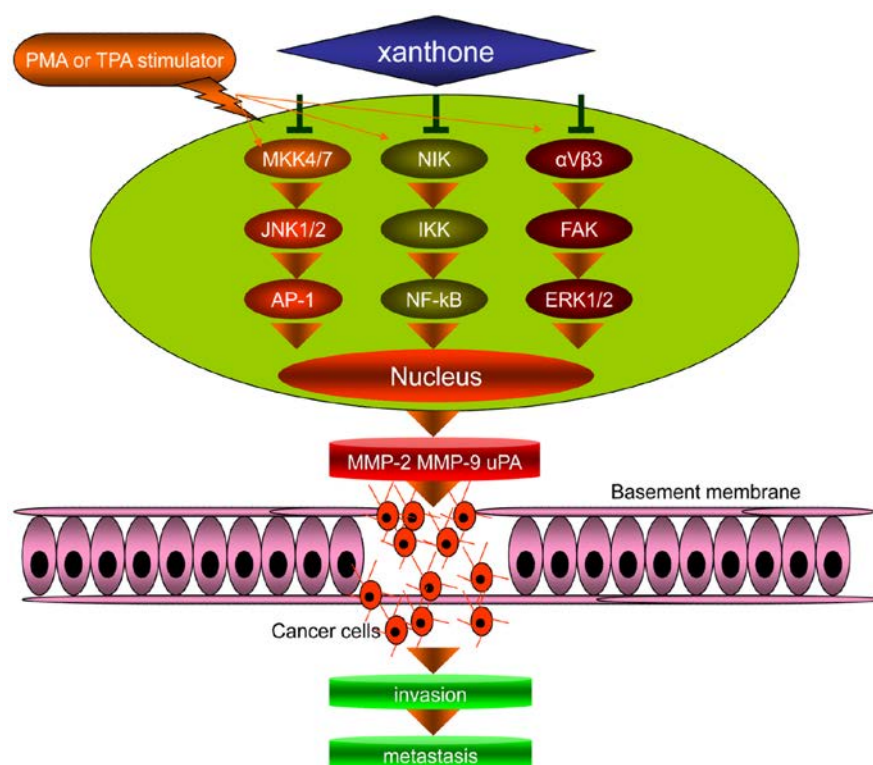
Figure 1-15
Simplified model showing potential contributions of xanthones to cancer invasion and metastasis. Some external stimulator (PMA, TPA) induces the cell-matrix adhesion, invasion, and migration of cancer cells by upregulating MAPK kinases such as JNK or ERK1/2. Xanthones diminish this induced effect, prevent NF-κB and AP-1 binding activity, and block their DNA binding site. Consequently, the expression of downstream genes (MMP-2, MMP-9, and u-PA) is downregulated (Taken from (Shan *et al.* 2011)).

1.3.4.4 Other effects

Apart from the activities summarised above (Sections 1.3.4.1-3), xanthones also exhibit many other activities, including anti-inflammatory, anti-allergy, anti-bacterial, antifungal, and antiviral properties as extensively reviewed by Pedraza-Chaverri *et al.* (2008a) and Obolskiy *et al.* (2009).

1.4 Hypotheses

The hypotheses to be tested in this thesis are:

1) The mangosteen pericarp possesses bioactive compounds with antioxidant activities.

2) Mangosteen pericarp compounds can inhibit skin cancer cell proliferation, induce skin cancer cell apoptosis, inhibit skin cancer cell survival pathways, and/or inhibit skin cancer cell invasion and metastasis.

The rationales for the above hypotheses

As discussed in Section 1.2, many natural compounds from plants exhibit significant anti-skin cancer activity. Additionally, as summarised in Section 1.3, the extracts and xanthone pure compounds from mangosteen exhibit antioxidant activity, and anti-cancer activity against a range of cancer cell types. However, there has been no study on the anti-skin cancer activity of xanthones on human skin cancer cells.

Therefore, the rationales, on which the above hypotheses are based, are:

1) A number of studies have demonstrated anti-skin cancer properties of plant extracts and their derived compounds.

2) The mangosteen pericarp has a long history as a remedy for various skin ailments.

3) A growing body of evidence has demonstrated the biological activities of extracts and compounds from the mangosteen pericarp, especially antioxidant and anti-proliferative activities.

4) There is evidence showing that some xanthones (e.g. α-mangostin and γ-mangostin) can inhibit metastasis of some human cancer cell lines, such as prostate cancer PC3, lung cancer A549, and breast cancer MCF-7 cell lines.

1.5 Thesis scope and aims

To understand the anti-skin cancer activity of mangosteen xanthones, this study used two different types of skin cancer cells as *in vitro* models: human squamous cell

carcinoma A-431 and melanoma SK-MEL-28 cell lines. Two non-cancerous cell lines were used as toxicity controls: human skin fibroblast CCD-1064Sk and keratinocyte HaCaT cell lines. In the current study, two different crude extracts (polar and non-polar) and six major xanthone compounds from the mangosteen pericarp were studied. The two different crude extracts were water and ethanol extract, respectively. The following six major xanthone compounds were selected because of the abundance and commercial availability: α-mangostin, β-mangostin, γ-mangostin, 8-deoxygartanine, gartanine, and 9-hydroxycalabaxanthone.

The outline of the scope of this study is presented in Figure 1-16. The potential cytotoxicity of xanthones or xanthone combinations was determined by the Crystal Violet assay. The underlying cellular and molecular mechanisms of cytotoxicity were studied by the following methods. Firstly, the modulatory effect of mangosteen xanthones on cell cycle was measured by the propidium iodide (PI) staining and detected by flow cytometry. The expression of genes involved in cell cycle regulation (p21^{WAF1} and cyclin D1) was studied using quantitative real-time reverse transcription PCR (qRT-PCR). Secondly, the apoptotic effect of mangosteen xanthones was measured by PI and Annexin V-FITC staining and detected by flow cytometry. Two distinct apoptotic pathways (extrinsic and intrinsic) were investigated by examining caspase 3/7, 8, 9 enzyme activities and mitochondrial membrane potential. The expression of apoptosis-related genes (Bcl-2, Bax, and cytochrome c) was determined using qRT-PCR. Thirdly, the modulatary effect of mangosteen xanthones on survival pathways was determined. As discussed in Section 1.1.7.3, MAPK, NFκB, and Akt pathway are highly active in skin cancers. Therefore, the expression of key genes involved in these three major survival

pathways was studied: BRAF V600E, NFκB and IκB, and Akt. The potential anti-metastatic activities of mangosteen xanthones were investigated by assessing the effect of xanthones on the cancer cell mobility, adhesion, migration and invasion as detected by wound healing assay, Boyden chamber assay, and cell-matrix adhesion assay. The expression of key metastasis-related genes (MMP-2, MMP-9, BRAF V600E, NFκB and IκB, and Akt) was studied by qRT-PCR.
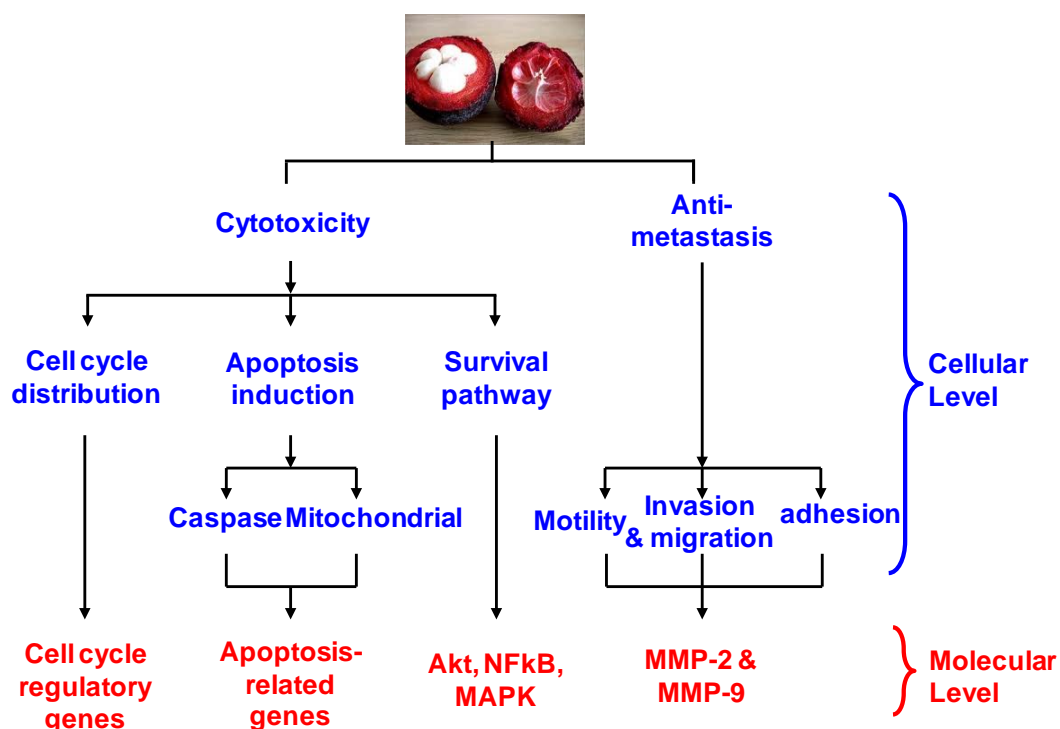
Figure 1-16
Brief outline of the scope of the thesis for the mechanisms to be studied for the potential cytotoxicity and anti-metastatic activity of xanthones.

The specific aims of this project are:

1) To develop and standardise extraction methods for crude extracts from the mangosteen pericarp. The protocol developed is based on the most efficient extraction method found to obtain phenolic-rich extracts.

2) To investigate the potential anti-skin cancer properties of the extracts and

individual xanthone compounds on human skin cancer cell lines. The cytotoxicity induced by the extracts and xanthones is also tested on skin cell lines of a non-malignant origin, to examine if there is any selectivity towards cancer cell lines.

3) To investigate the potential anti-metastatic activity of the extracts and individual xanthone compounds on human skin cancer cell lines

4) To investigate the potential synergistic effects between xanthone compounds and commercial drugs or between individual xanthone compounds.

5) To investigate the underlying cellular and molecular mechanisms of the effects observed in specific aims 2-4.

1.6 Significance

This is the first investigation on the activity of mangosteen extract and xanthones for anti-skin cancer potential. This study provides important scientific evidence to reveal the potential cytotoxic and anti-metastatic activities of extracts and xanthone compounds from pericarp of mangosteen on human skin cancer cells. It also contributes to a fundamental understanding of the underlying cellular and molecular mechanisms for these activities. These findings can contribute to the development of novel plant-derived antioxidant strategies in the prevention and treatment of skin cancer, which is the most prevalent cancer in Australia.

CHAPTER 2
OPTIMISATION OF THE EXTRACTION METHODS AND CHARACTERISATION OF THE ANTIOXIDANT PROPERTIES OF MANGOSTEEN PERICARP EXTRACTS

2.1 Introduction

In vegetables and fruits, the external and other lignocellulosic parts (e.g. skins, hulls, and seeds) usually present higher levels of phenolic compounds than their corresponding inner parts (Cruz *et al.* 2004). Research involving these becomes highly appealing because the cost of materials is low and their use offers the potential to solve environmental problems involved in the disposal of these normally discarded parts of the plants (Laroze *et al.* 2010). The pericarp of mangosteen is a case in point. Despite the abundant literature about the presence of phenolic antioxidants (e.g. xanthones; Chapter 1) in the pericarp of mangosteen, standardised procedures for the extraction of these compounds from the pericarp need to be developed to ensure the consistency and reproducibility of the extract for both research and commercialisation. Previous studies have described the crude extraction of compounds from mangosteen using various procedures. The variations in these procedures involving extraction time, temperature, and ratios of solvent volume are summarised in Table 2-1.

One single plant may contain thousands of secondary metabolites; therefore it is necessary to develop high performance and rapid extraction methods (Hemalatha *et al.* 2007). There are a number of extraction methods available currently: solid-liquid extraction (Fellows 2000), supercritical fluid extraction (Hedrick *et al.* 1992), accelerated solvent extraction (Gan *et al.* 1999), ultrasound-assisted extraction (Herrera & de Castro 2005), and microwave-assisted extraction (Hemalatha *et al.* 2007). A review of all these methods is beyond the scope of this study. We will focus on the conventional solid-liquid extraction method, which is used in the current study for experimental scale extraction.

Table 2-1

Summary of methods used in previous studies for extracting antioxidants from mangosteen.

Plant part	Extraction parameters					References
	Solvent (%, v/v)	Ratio of solid/solvent (g/ml)	Temperature (°C)	Time	Yield% (w/w)	
Whole fruit	Methanol	1:2.5	Room temperature (RT)	Up to 1 day	18.3	(Chin *et al.* 2008)
Whole fruit	50% acetone	1:12.5	RT	1 hour (h)	–	(Patthamakanokporn *et al.* 2008)
Whole fruit	40% ethanol	1:12.5	RT	1 h	–	(Patthamakanokporn *et al.* 2008)
Pericarp	Aqueous	1:10	100	1 h	5.6~18.5	(Chiang *et al.* 2004)
Pericarp	Ethyl acetate	–	50	–	–	(Watanapokasin *et al.* 2010)
Pericarp	Distilled water	1:4	RT	7 days	22.3	(Weecharangsan *et al.* 2006)
Pericarp	50% ethanol	1:4	RT	7 days	2.0	(Weecharangsan *et al.* 2006)
Pericarp	95% ethanol	1:4	RT	7 days	6.1	(Weecharangsan *et al.* 2006)
Pericarp	Ethyl acetate	1:4	RT	7 days	6.2	(Weecharangsan *et al.* 2006)
Pericarp	Ethanol	–	–	–	23.8	(Moongkarndi *et al.* 2004)
Pericarp	Methanol	–	–	–	9.7	(Suksamrarn *et al.* 2002)
Pericarp	Methanol	1:1	RT	1 week	20	(Moongkarndi *et al.* 2004)
Pericarp	Methanol	1:5	RT	3 days	32.4	(Jung *et al.* 2006)
Stem bark	Ethanol	–	–	–	4.4	(Ee *et al.* 2008)
Stem bark	Methanol	1:2.5	RT	Overnight	18.8	(Han *et al.* 2009)
Root bark	n-Hexane	–	–	–	0.8	(Ee *et al.* 2008)
Root bark	Chloroform	–	–	–	2.3	(Ee *et al.* 2008)
Root bark	Acetone	–	–	–	4.3	(Ee *et al.* 2008)

Solid-liquid extraction is one of the oldest extraction methods for the extraction of a range of compounds (including phenolic antioxidants) from various sources (Fellows 2000). It is efficient but relies on several factors during the extraction, such as raw material composition, conditioning, solvent polarity, extraction time, temperature and solid/solvent ratio (Laroze *et al.* 2010). These factors need to be optimised to obtain a high level of recovery of antioxidants.

A number of chemical assays are available currently to measure the antioxidant activity of a large variety of compounds. They can be divided into two major types according to the type of reaction involved: assays based on hydrogen atom transfer and assays based on electron transfer (Huang *et al.* 2005). The first type of assay determines a competitive reaction scheme in which the antioxidant and substrate compete for peroxyl radicals (Huang *et al.* 2005), including oxygen radical absorbance capacity (ORAC) assay and total radical trapping antioxidant parameter (TRAP). The second type assay detects the ability of antioxidant to reduce an oxidant. The degree of decoloration of the solution indicates the scavenging efficiency of the added sample. Folin-Ciocalteu total phenols assay, ferric ion reducing antioxidant power (FRAP), and DPPH assay belong to the second type of assay (Ballard 2008).

Mangosteen compounds exhibit antioxidant activity as detected by different assays, as shown in Section 1.3.4.1 in Chapter 1. Due to the complex nature of phytochemicals, their antioxidant activity cannot be fully evaluated using one single method. Therefore, at least two assays are recommended to be performed to evaluate the various mechanisms of antioxidant action (Schlesier *et al.* 2002).

The aims of this chapter are therefore to describe the preparation and characterisation of mangosteen pericarp crude extracts to subsequently investigate their anti-skin cancer activities (see Chapters 3 – 5). The first part of this chapter describes the development and optimisation of extraction methods to produce standardised extracts; and the second part describes the characterisation of the chemical constituents and the antioxidant properties of the extracts as obtained using the optimal extraction method in the first part of this chapter.

Pure xanthone compounds from the pericarp of mangosteen are commercially available. Therefore, isolation, identification and purification of the pure compounds were not carried out in this study.

2.2 Materials and methods

2.2.1 Materials

All reagents and chemicals used in this study were of analytical grade from Merck (Australia) or tissue culture tested grade from Sigma-Aldrich (St. Louis, USA) unless otherwise noted within this chapter. High purity MilliQ (MQ) grade water was prepared using MQ® Academic system with Quantum® EX Ultrapure Organex cartridge filter (Millipore, Billerica, USA).

2.2.2 Preparation of mangosteen pericarp

Fresh mangosteen fruits were purchased from the local market in Adelaide, South Australia. The mangosteen fruit was cleaned with MQ water. The pericarp was peeled from the fruit, ground into a fine powder in a juice blender with a cross blade, and dried at 35 ºC in an oven. The dry powder was stored at –20 ºC until required. The percentage of pericarp weight over the whole fruit weight was calculated by the following formula:

[1]Pericarp% (w/w)

= weight of pericarp / weight of whole fruit $\times$ 100 %

The water content in the pericarp was calculated by the following formula:

[2]Water content % (w/w)

= (Initial wet weight-final dry weight) / initial wet weight $\times$ 100 %

[1] The result was averaged across 6 batches of fruit with 10 fruit in each batch and expressed as mean $\pm$ SEM.

[2] The result was averaged across 6 separate batches of mangosteen pericarp powder samples and expressed as mean $\pm$ SEM.

2.2.3 Mangosteen pericarp extraction methods

Ethanol (EtOH) and MQ water were selected as extraction solvents because of their broad and safe uses in preparation of extracts from diverse plant material (Chirinos *et al.* 2007; Kalia *et al.* 2008). After extraction under different conditions (Table 2-2), the mixtures were centrifuged at 10,000 $\times$ g for 10 min at 4 ℃. Each sample was prepared in duplicate and each experiment was repeated three times. The supernatant was collected, filtered through a 0.22 µm filter (Minisart, Sartorius Stedim Biotech, Germany), and stored at –20 ℃ until required. The filtered supernatant was used for the analytical procedures as described subsequently.

Table 2-2
Extraction was carried out under various extraction conditions to identify optimal extraction condition.

Extraction condition	Water extraction	EtOH extraction
Pericarp/solvent ratio (w/v)	1:5; 1:10; 1:20	1:10; 1:20
Temperature (℃)	25 (RT); 100	50; 75
Extraction duration (h)	0.5; 1; 2; 24	1; 2
Solvent concentration (%, v/v)	100%	50%; 100%

2.2.4 Preparation of green tea extract

A green tea (*Camellia sinensis*) sample branded as "Chinatea" was purchased as ground dried plant leaves from a local store and used as an antioxidant comparison standard. The green tea extraction method was established in our laboratory (Vuong 2009). Briefly, the extraction was carried out by mixing green tea powder with MQ water at 100 ºC for 1h with a weight-to-volume ratio of 1:10. The remaining steps were the same as for the mangosteen pericarp extraction.

2.2.5 Chemical profile characterisation of mangosteen pericarp extracts

The chemical profile characterisation of mangosteen pericarp ethanol extract (MPEE) and water extract (MPWE) was carried out using the following methods. The green tea extract was used as a comparison standard and measured using the same method.

2.2.5.1 Total Phenolics (TP) analysis

Total phenolics (TP) content of the extract was determined by the method described previously (Singleton & Rossi 1965) with minor modification. Briefly, 1 ml MQ water was added into the 200 µl of the extract followed by adding 50 µl Folin-Ciocalteu reagent. The mixture was vortexed and incubated for 7 min at RT. Then 290 µl of sodium carbonate (20%; w/v) was added and mixed evenly. The absorbance was measured at 760 nm by UV-Vis spectrophotometer (UV mini 1240, Shimadzu Corporation, Kyoto, Japan) after 1 h incubation. Quantitation of TP content was based on the standard curve of gallic acid. Results were expressed in terms of gallic acid equivalence (GAE) in mg per dry pericarp weight (DW) in g. The following formulas were used to calculate the TP content in the dry mangosteen pericarp:

TP concentration (mg GAE/ ml extract)

$$= \text{(Absorbance at 760 nm/slope)} \times \text{dilution factor}$$

TP content (mg GAE/g DW)

$$= \text{(Concentration of TP} \times \text{volume of supernatant (ml))/equivalent DW (g)}$$

2.2.5.2 Total flavonoid (TF) analysis

Total flavonoid (TF) content in the extract was measured by UV spectrophotometry based on a colorimetric oxidation/reduction reaction (Chen *et al.* 2002). Briefly, 75 µl 5% (w/v) $NaNO_2$ was added to 450 µl of extract supernatant in amicrofuge tube. The mixture was incubated for 6 min. Then 75 µl 10% (w/v) $Al(NO_3)_3$ was added and incubated for 6 min, and 375 µl 5% (w/v) NaOH was added and incubated for 15 min at RT. Finally, 525 µl of MQ water was added and the absorbance was measured immediately at 506 nm by UV-Vis spectrophotometer (UV mini 1240, Shimadzu Corporation, Japan). Quantitation of flavonoid content was based on the standard curve of catechin. Results were expressed in terms of catechin equivalents (CE) in mg per dry pericarp weight (DW) in g. The following formulas were used to calculate the flavonoid content in the dry mangosteen pericarp.

TF concentration (mg CE/ ml extract)

$$= \text{(Absorbance at 506 nm/slope)} \times \text{dilution factor}$$

TF content (mg CE/g DW)

$$= \text{(Concentration of flavonoids} \times \text{volume of supernatant (ml))/equivalent DW}$$

(g)

2.2.5.3 High performance liquid chromatography (HPLC) profile of mangosteen pericarp extracts

The TP profile of MPEE and MPWE was analysed using a Shimadzu LC-10ADvp (Shimadzu Corporation, Kyoto, Japan) with a diode array detector (Shimadzu Corporation, Kyoto, Japan), using an Eclipse XDB C-18 reversed phase column (150 mm× 4.6 mm, 5 µm; Agilent Technologies, St. Clara, USA). The mobile phase was

composed of two solvents, liquid phase A (1% (v/v) acetic acid in water/methanol (9:1; v/v) and liquid phase B (100% (v/v) methanol).

Mangosteen pericarp extract with TP concentration of 1 mg/ml was prepared for the HPLC analysis. An injection volume of 10 µl was used and the temperature was set at 25 ºC. A gradient elution started from 100% liquid phase A at 0 min. The solvent gradient increased gradually to 100% liquid phase B at 15 min following an isocratic elution of liquid phase B for 10 min. 100% liquid phase A was introduced after 25 min and the run was stopped at 40 min of run time. The flow rate was set at 1 ml /min, and the UV spectra were collected between 200 and 400 nm and the signals at 320 nm were selected as the chromatograms. Shimadzu CLASS-VP software was used for data collection, instrument control and data processing.

2.2.6 Antioxidant assays

The three antioxidant assays in this section were carried out in collaboration with Dr. Qinghong Shi (Department of Medical Biotechnology, Faculty of Health Sciences, Flinders University, Adelaide, Australia). MPWE, MPEE, and the green tea extract were tested for their antioxidant activities using these three assays.

2.2.6.1 DPPH radical scavenging activity

Each extract sample was tested for its ability to scavenge DPPH· radicals by DPPH radical scavenging assay as described previously by Blois (1958). Three ml of 0.1 mM DPPH· in EtOH was added to 0.5 ml of the extract and incubated for 30 min in the dark at RT. Absorbance was read at 517 nm using a UV-Vis spectrophotometer. Percentage DPPH radical scavenging activity (% DRSA) was calculated using the formula

$$\%DRSA = [(A_c - A)/A_c] \times 100$$

where A_c is the absorbance of the control and A is the absorbance of the extract.

The antioxidant activity of the extract was expressed as IC_{50} (the concentration of the extract required to inhibit DPPH radicals by 50%) using the exponential curve.

2.2.6.2 Ferric reducing antioxidant power (FRAP) assay

The FRAP assay was performed as previously described by Benzie and Strain (1996) to test the reducing activity of the extract. Briefly, the extract was centrifuged for 10 min at 2,830 ×g prior to use and the supernatant was saved. The FRAP reagent consisted of 25 ml of 300 mM acetate buffer at pH 3.6, 2.5 ml of 10 mM 2, 4, 6-tripyridyl-s- triazine and 2.5 ml of 20 mM $FeCl_3$. The FRAP reagent (900 µl) was heated at 37 ℃ for 10 min, then 90 µl of MQ water and 30 µl of extract sample were added to it and mixed well. The absorbance of the reaction mixture was measured at 593 nm spectrophotometrically after incubation at 37 ℃ for 4 min. $FeSO_4.7H_2O$ of 1 mM was used as the standard solution (standard solution ranged from 0 to 1 mM). The antioxidant activity of the tested extract sample was expressed as FRAP value/g dry pericarp weight (DW) as shown in the following equation:

FRAP value (µmol/L $FeSO_4$ equivalent (FE)/g DW)

= [(Absorbance at 593 nm/slope) × dilution factor] × volume of supernatant (ml)/ equivalent DW (g)/1000

2.2.6.3 Oxygen radical absorbance capacity (ORAC) assay

The assay was carried out as described previously by Huang *et al.* (2005) with minor modification. The ORAC assay was carried out on a microplate reader (DTX 880, Beckman Coulter, Atlanta, USA). Trolox, a water-soluble analogue of vitamin E, was used as a control standard. Firstly, the extract and trolox were diluted in a 96-well microplate. Trolox was prepared in concentrations of 100, 75, 50, 25, 12.5 and 0 µM while the dilution factors of 20, 200, 400, 800, 1600 and 3200 × were applied for

the extract. In the analysis, 180 µl of fluorescein working solution, 30 µl of phosphate working buffer and 30 µl of diluted sample/trolox were loaded into each well. The reaction was carried out at 37 ºC and the plate was incubated for 10 min before adding 2, 2'-azobis (2-amidinopropane) dihydrochloride (AAPH). After adding AAPH, the plate was shaken to mix the reagents in each well before recording the initial fluorescence (f0). Fluorescence readings were taken at 0 second (s) (f0) and then every 90 s thereafter (f1, f2, f3…) for 50 cycles. The final ORAC values were calculated by using a regression equation between trolox concentration and the net area under the curve by MATLAB program and were expressed as micromole trolox equivalents (TE) per gram of dry pericarp weight (µmol TE/g DW). All the reaction mixtures were prepared in duplicate, and at least three independent assays were performed for each sample.

2.2.7 Preparation of extracts for biological assays

After optimising the extraction conditions (Section 2.3.2.5), mangosteen pericarp was extracted in large-scale under optimal conditions for the subsequent biological assays. The extraction was conducted by mixing mangosteen pericarp dry powder with either absolute EtOH at 75 ºC or water at 100 ºC for 1h with a pericarp/solvent ratio of 1:10 (w/v). After extraction, the mixture was centrifuged at 10,000× g for 10 min and the supernatant was filtered through 0.22 µm and then vacuum dried to yield MPEE or freeze dried to yield MPWE. The MPEE and MPWE were stored at –20 ºC until required.

For the bioassay experiment, dry MPEE or MPWE of 250 mg was dissolved in 5 ml of absolute EtOH or MQ water, respectively, to give a concentration of 50 mg/ml. The extract solution was sterilised using a 0.22 µm filter and diluted with the

respective cell culture medium to the desired treatment concentrations (Section 3.2.2.3). Vehicle volume was consistently kept as 1% (v/v) for each treatment.

2.2.8 Statistical analysis

Data are expressed as mean (± standard error of mean (SEM)). The experiments were repeated at least three independent times. Statistical analysis of the data was carried out using one-way Analysis of Variance (ANOVA) followed by Tukey's HSD *post hoc* test, or independent sample t test. These tests were performed using SPSS version 17.0 for Windows (SPSS Inc., Chicago, Ill.). Although the sample sizes (≥ 3) are small in this study, ANOVA is valid to be used to analyse the data because the experimental design was balanced and well controlled (Kitchen 2009; Moongkarndi *et al.* 2004; Skovlund & Fenstad 2001). Additionally, many works in similar field with small sample sizes using ANOVA analysis have been published (Chen *et al.* 2011; Chu *et al.* 2009; Dia & Gonzalez de Mejia 2011). Difference was considered statistically significant when the *P*-value was less than or equal to 0.05. MATLAB version 7.0 and Microsoft Excel 2003 were also used for statistical analysis and graphical evaluation.

2.3 Results

2.3.1 The mangosteen pericarp

The mangosteen pericarp was collected and prepared as described in Section 2.2.2. The pericarp of mangosteen made up $68.6 \pm 1.0\%$ (w/w) of weight of the whole fruit and contained $65.3 \pm 0.2\%$ (w/w) water.

2.3.2 Optimisation of extraction method

The extraction procedure was optimised by maximising the TP content of the extracts under various extraction conditions.

2.3.2.1 Effect of the extraction temperature

The results show that the TP content increased with increasing temperature. For water extraction, the TP content was approximately two times higher when the extraction was carried out at 100 ℃ compared to RT (Figure 2-1). Similar results were found for EtOH extraction (Figure 2-2).

2.3.2.2 Effect of the pericarp/solvent ratio

Three different pericarp/solvent ratios (1:5, 1:10 and 1:20) (w/v) were evaluated for water extraction. As shown in Figure 2-1, the TP content of extract increased with the decreasing ratio (1:20 > 1:10 > 1:5) for water extraction. For the EtOH extraction, there was no significant difference between ratios of 1:10 and 1:20 ($P >$ 0.05).

2.3.2.3 Effect of the extraction duration

The effect of the extraction duration was evaluated in water extraction at different ratios at 100 ℃ (Figure 2-1). The results show that the highest TP yield was obtained at 1 h extraction duration.

2.3.2.4 Effect of solvent concentration for MPEE

Two different EtOH concentrations (50% and 100%) (v/v) were used for EtOH extraction. Absolute EtOH yielded higher TP content compared with 50% EtOH at each pericarp/solvent ratio and temperature (Figure 2-2).
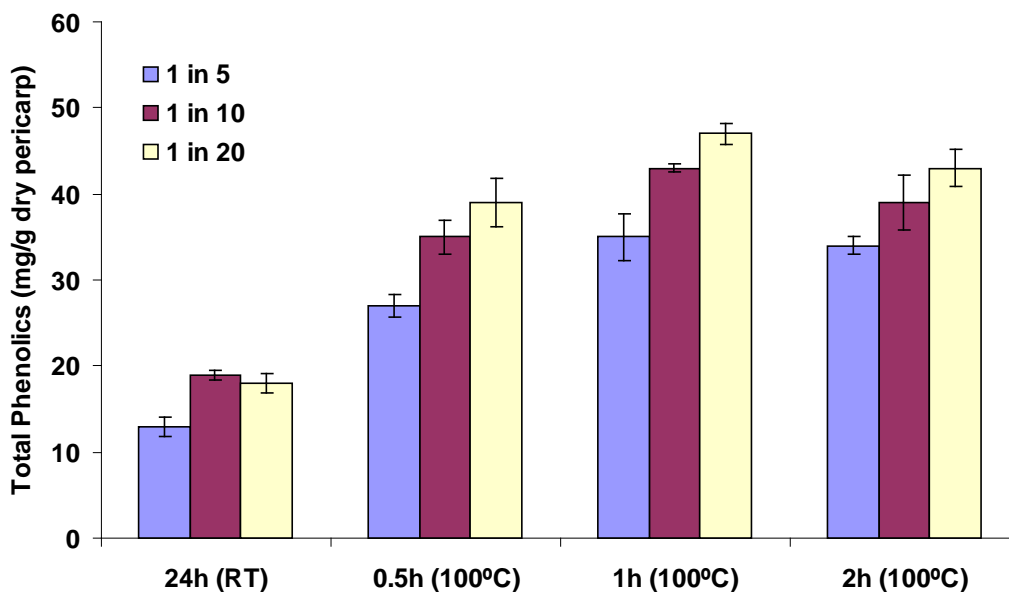
Figure 2-1

Total phenolics content of crude mangosteen pericarp water extract at different pericarp/solvent ratios (1:5; 1:10 and 1:20) (w/v), different temperatures (room temperature (RT) and 100ºC), and different extraction times (0.5, 1, 2, and 24 h). The values are shown as the mean ± SEM of three independent experiments.
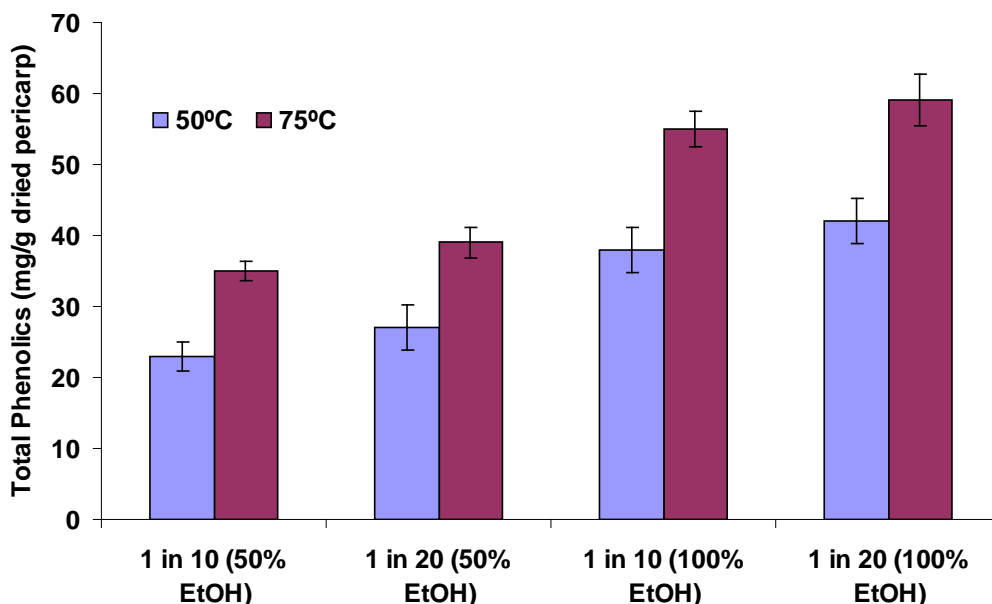
Figure 2-2

Total phenolics content of crude mangosteen pericarp ethanol (EtOH) extract at 2 different pericarp/solvent ratios (1:10 and 1:20) (w/v), 2 different temperatures (50 ºC and 75 ºC), and 2 different EtOH concentrations (50% and 100%) (v/v) for 1 h. The values are shown as the mean ± SEM of three independent experiments.

2.3.2.5 Optimal extraction conditions

According to the results as above, a temperature of 100 ºC (for water extraction) and 75 ºC (for 100% EtOH extraction), an extraction time of 1 h, and a pericarp/solvent ratio of 1:10 (w/v) were selected as the optimal extraction conditions.

2.3.3 Yield of extracts

Using the optimal extraction method (Section 2.3.2.5), 100 g of mangosteen pericarp powder yielded 24.3 g of MPWE dried by freeze drier and 23.2 g of MPEE dried by vacuum drier. The dry extract is a yellowish powder (for MPWE) or a yellowish paste (for MPEE).

2.3.4 Chemical profile characterisation of mangosteen pericarp extract

Phenolic compounds contained in the mangosteen pericarp extracts were analysed using chemical-based assays and HPLC as described in the method (see section 2.2.5).

2.3.4.1 TP and TF contents

MPWE and MPEE were analysed for their polyphenolic profiles which included TP and TF contents. The results are summarised in Table 2-3.

The TP content was similar in the MPWE and MPEE, but lower than the control antioxidant green tea extract ($P < 0.01$; Table 2-3).

Flavonoids are one of the major polyphenolic groups of the TP. The flavonoid content was 14.3 and 16.8 mg CE/g DW in the MPWE and MPEE, respectively, which was lower than the green tea ($P < 0.01$; Table 2-3).

Table 2-3

Total phenolics (TP) and total flavonoid (TF) content analysis of the MPWE, MPEE and green tea.

Extracts	TP content (mg GAE/g DW)	TF content (mg CE/g DW)
MPWE	58.2 ± 4.1	14.3 ± 2.1
MPEE	64.3 ± 3.2	16.8 ± 1.7
Green tea extract	72.5 ± 5.4	20.3 ± 2.2

Total phenolics (TP), expressed as mg gallic acid equivalents (GAE) per gram of dry pericarp weight (DW).

Total flavonoids (TF), expressed as mg catechin equivalents (CE) per gram of dry pericarp weight (DW).

The values are shown as the mean ± SEM of three independent experiments.

2.3.4.2 *HPLC profile of mangosteen pericarp extracts*

The TP profile of MPWE and MPEE was analysed by the HPLC. Chromatograms

that are used as "fingerprints" can provide the information for differentiating and

identification of the compounds in the extracts.
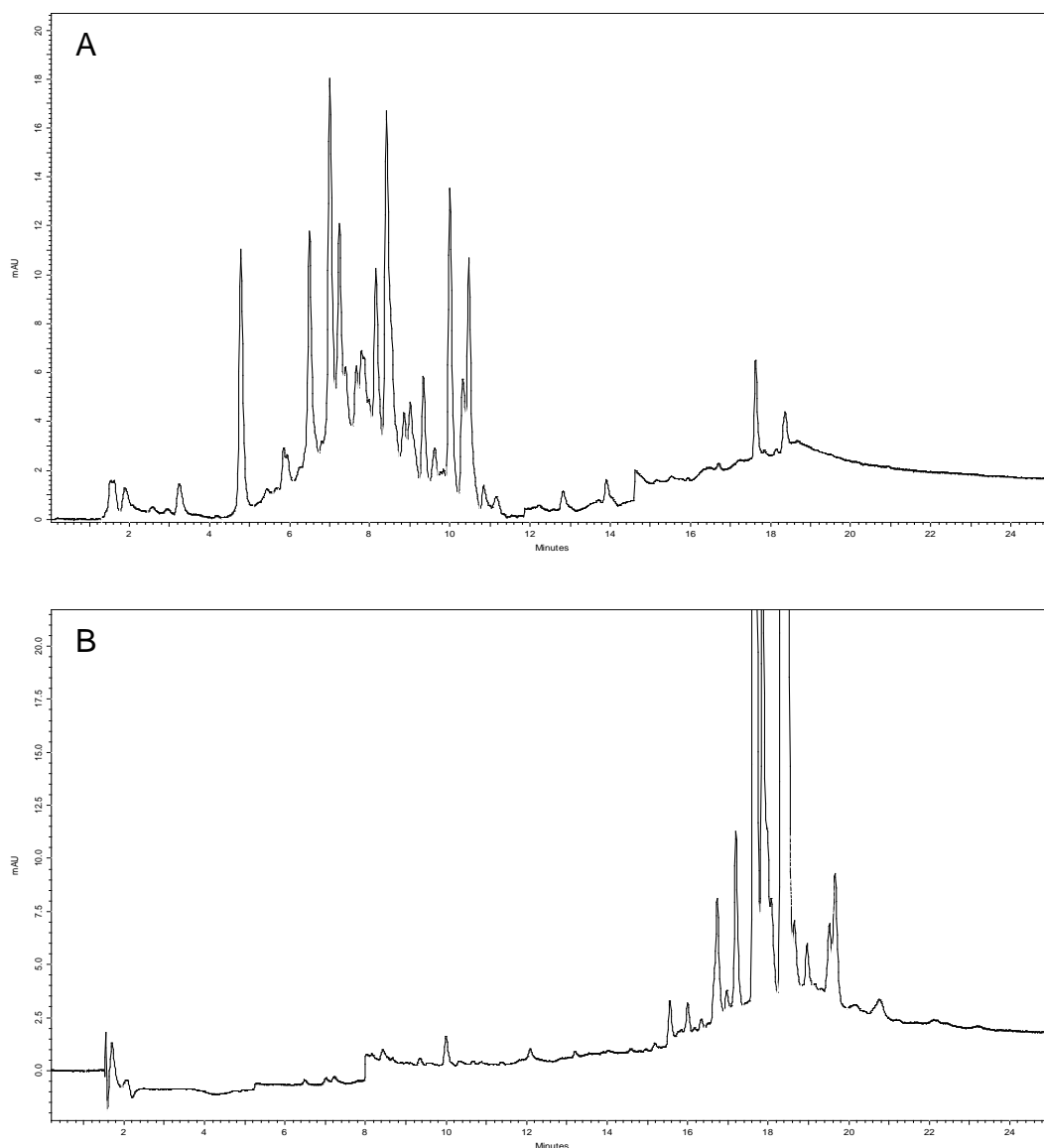
Figure 2-3

Total phenolic (TP) profile of (A) mangosteen pericarp water extract (MPWE) and (B) mangosteen pericarp ethanol extract (MPEE) was analysed by the HPLC as described in the method (see section 2.2.5.3). Prior to HPLC analysis, the TP concentration of extract samples was adjusted to 1 mg/ml.

Figure 2-3 shows the HPLC chromatogram in the TP analysis of the MPWE and

MPEE. A gradient of increasing hydrophobicity was used to provide good resolution

of different compounds in the extracts and a wavelength of 320 nm was used to

detect the TP compounds. As seen in the Figure 2-3, the compounds from MPWE

were eluted more quickly in a range of early retention times whereas the compounds

from MPEE were eluted at retention times later than 15 minutes, implying that MPEE contain more hydrophobic compounds. The chromatograms also indicated that different compounds were extracted by the use of different solvents as demonstrated by different patterns of HPLC peaks in each chromatogram.

The identification and quantification of xanthones in the MPEE was carried out by Dr. Yichu Shan in our laboratory (Appendix A2) (Shan & Zhang 2010).

2.3.5 Antioxidant properties of the mangosteen pericarp extract

The results on the antioxidant activities of the mangosteen pericarp extract are shown in Table 2-4 as evaluated using the FRAP, ORAC, and DPPH assays. The samples with higher TP content (Table 2-3) exhibited higher antioxidant activity in the FRAP assay, and higher ability to scavenge DPPH free radicals as evidenced by lower IC_{50} values (Table 2-4). However, a poor correlation between the TP and ORAC values were observed. MPEE showed the lowest ORAC value and MPWE the highest.

Table 2-4
Antioxidant properties of MPWE, MPEE and green tea extract were detected by three different chemical-based assays.

Samples	FRAP value (mM FE/g DW)	ORAC value (mmol TE/g DW)	DPPH IC_{50} value (µg/ml)
MPWE	0.4 ± 0.02	3.8 ± 0.07	8.9 ± 0.6
MPEE	0.5 ± 0.03	0.6 ± 0.05	7.3 ± 0.4
Green tea extract	1.8 ± 0.1	1.2 ± 0.08	6.41 ± 0.2

Ferric reducing antioxidant power (FRAP), expressed as mM of $FeSO_4$ equivalents (FE) per gram of dry weight (DW).
Oxygen radical absorbance capacity (ORAC), expressed as mmol of Trolox equivalents (TE) per gram of dry weight (DW).
DPPH IC_{50} value is the concentration scavenging 50% of DPPH radicals.
Values represent the mean ± SEM of three independent experiments.

2.4 Discussion

2.4.1 Optimisation of the extraction methods

Investigations of phenolic compounds from plants have attracted special interest due

to their health-promoting attributes (Konczak & Zhang 2004). However, these active compounds in plants usually are present at low concentrations and they are usually very complex. Therefore, the isolation of natural compounds with functional properties from natural sources has become a very important research area (Ramírez *et al.* 2005). Extraction is the main step for the recovery of these bioactive phytochemicals and the ultimate goal is the preparation of a standardised extract uniformly enriched with all components of interest and free from interfering matrix components (Pyrzynska & Biesaga 2009). The aim of the current study was to develop an effective and standardised extraction method for the maximum recovery of active compounds from the mangosteen pericarp for subsequent screening and biological assays.

The first step in the extraction is to select a solvent. In previous studies, various solvents (e.g. EtOH, methanol, acetone, hexane, water, and their mixtures) were applied (Cvek *et al.* 2007; Kalia *et al.* 2008; Padda & Picha 2007; Trabelsi *et al.* 2010) to the plant tissues. Although methanol is considered to be the best solvent to improve phenolic molecule extraction, ethanol may be a better choice due to its lower toxicity and therefore could be better suited for possible future application in food, cosmetic and pharmaceutical products (Adil *et al.* 2007; Padda & Picha 2007). MQ water was also selected as a solvent because of its non-toxicity and low cost.

Temperature, extraction time and the percentage of solvent are considered as the most important factors as they play a critical role in the extraction yields, phenolic concentration and antiradical activity of extracts obtained. For most phenolic compounds, a good recovery rate can be achieved by changing these parameters

(Tsao & Deng 2004).

As shown in Figures 2-1 and 2-2, higher TP recovery was obtained when extraction was carried out at a higher temperature in the same solvent system (100 ºC in the form of liquid for water extraction and 75 ºC for EtOH extraction). This is because the increase in temperature accelerates mass transfer and improves the extraction yield (Wang *et al.* 2008). The current result for both the water and EtOH extraction was in agreement with a previous study (Le Floch *et al.* 1998) which reported that increased TP amount and extraction efficiency with increasing temperature (80, 100 and 120°C) was observed in extraction from olive leaves. In the future, 120 ºC in the form of steam can be applied to improve the extraction efficiency. However, high temperature may enhance degradation of phytochemicals. To determine if the compounds obtained at 75 °C or 100 °C are identical with these present in the pericarp, or are they their degradation products, or mixture of both, the profiles of compounds obtained at different temperatures can be analysed using HPLC.

The extraction time is one of the important variables which can influence the solvent contact with sample material (Pourmortazavi & Hajimirsadeghi 2007). The current results demonstrated that the accumulative amount of phenolics extracted increased from 0.5 h to 1 h and then decreased from 1 h to 2 h of extraction time. This indicates that the first 1 h was the constant extraction rate period, where the solute was easily transferred from solid to fluid phase due to the significant difference of concentration between solvent and pericarp solid; after that, the extraction tended gradually to decrease due to a diminishing difference in concentrations. Le Floch *et al.* (1998) reported that increased dynamic extraction time enhanced the phenolic compounds

extraction; however, the authors stated that the time should be minimised due to economic aspects.

The effect of the percentage of co-solvent on extraction of phenolics compounds was investigated. The results showed that more phenolics compounds were obtained when extraction was carried out using 100% (v/v) EtOH compared with 50% (v/v) EtOH. The HPLC profiles of MPWE and MPEE suggest that MPEE contains more compounds than MPWE in terms of the total amount (Figure 2-3).

The TP recovery increased with the decreasing pericarp/solvent ratio when comparing ratio of 1:5 and 1:20. However, the difference between the ratio of 1:10 and 1:20 was not significant, especially for EtOH extraction. Additionally, a lower pericarp/solvent ratio involved longer times for freeze drying or vacuum drying during scale up extractions. Hence, due to energy-saving and cost-efficiency considerations, a 1:10 ratio was selected as the optimal pericarp/solvent ratio for both water and EtOH extraction.

In summary, the optimal extraction method of 100 ºC (for water extraction), and 75 ºC (for 100% EtOH extraction) for 1 h at the pericarp/solvent ratio of 1:10 was used for the scale-up extraction to obtain standardized MPWE and MPEE for the study of their antioxidant and anti-skin cancer activities.

2.4.2 Antioxidant properties of the mangosteen pericarp extract

Antioxidants play an important role in protection against ROS to maintain human health, including the prevention of cancer progression (Fridovich 1998; Rajkumar *et al.* 2011). Phenolics have been reported to possess multiple biological effects and a

capacity to scavenge free radicals (Hsu *et al.* 2007). They exhibit antioxidant activity mainly due to their properties which allow them to act as reducing agents, hydrogen donors and singlet oxygen quenchers (Javanmardi *et al.* 2003). There are strong correlations between total phenolic compounds and antioxidant activity in many different kinds of fruits (e.g. blackberry, grapefruit, and orange) (Gorinstein *et al.* 2004; Sellappan *et al.* 2002). Therefore, the TP content could indicate the level of antioxidant properties of the plant material extract.

Under the extraction conditions in this study, the TP content was 64.3 and 58.2 mg GAE/g dry pericarp weight in MPEE and MPWE, respectively, comparable with the standard antioxidant green tea extract (72.5 mg GAE/g dry green tea). The TP content in the green tea was similar with a previous study which reported the TP content of 62.1 mg GAE/g DW for green tea water extract (Vinokur *et al.* 2006). Patthamakanokporn *et al.* (2008) reported phenolic content for mangosteen fruit extract at only 4.2 mg GAE/g dry fruit weight. This difference may be explained firstly, by the fact that the mangosteen extract was from the whole fruit (including flesh and pericarp) in the Patthamakanokporn study, while the mangosteen extract in our study was from the pericarp. The TP level in the fruit flesh might be lower than in the pericarp (Cruz *et al.* 2004). We found that the TP level in the fruit flesh was 29.2 mg GAE/g dry flesh weight (data not shown). Also, in the Patthamakanokporn study, the extraction was carried out with 40% ethanol for 1 h at RT, compared to the optimal extraction temperature in our study of 75 ºC. Our study showed the TP level was 16.4 (± 2.1) mg GAE/g DW when the extraction was carried out with 50% ethanol for 24 h at RT. Additionally, this current study showed that the yield of MPEE and MPWE was 23.2% and 24.3% (w/w), respectively. A previous study

reported that the yield of extracts from the mangosteen pericarp was 2.0, 6.1, 6.2 and 22.3% (w/w) when extraction was carried out at RT for 7 days with 50% EtOH, 95% EtOH, ethyl acetate and water, respectively (Weecharangsan *et al.* 2006). Therefore, higher TP recovery was obtained when extraction was carried out at higher temperature in the same solvent system. This may be because the increase in temperature accelerates transfer of compounds from plant tissue to the solvent and improves the extraction yield (Wang *et al.* 2008). The current result was in agreement with the study from Le Floch *et al.* (1998) who reported that increased TP amount and extraction efficiency with increasing temperature was observed from the extraction of olive leaves.

Mangosteen displays a high level of antioxidant activities, compared with other fruit and vegetables (Chomnawang *et al.* 2007; Leong & Shui 2002). The antioxidant activities of mangosteen extracts and their major compounds have been reviewed (Akao *et al.* 2008; Obolskiy *et al.* 2009; Pedraza-Chaverri *et al.* 2008a). In the current study, the antioxidant potential of MPWE and MPEE was determined by three different assays (DPPH, FRAP and ORAC assays). Different antioxidant levels can be expected from these three methods because of the different principles involved. FRAP assay measures the total antioxidant concentration based on the total reducing capacity of electron-donating antioxidants (Benzie & Strain 1996). ORAC assay measures the effectiveness of antioxidant in a sample which reflects the antioxidant activity of a particular sample against peroxyl radicals (Huang *et al.* 2002). DPPH assay measures the ability of scavenging of DPPH free radicals (Blois *et at.* 1958). MPWE and MPEE had similar scavenging activity of DPPH radicals with the green tea extract, but lower activity than green tea by the FRAP assay.

MPWE had a 3-fold higher ORAC value than the green tea, while MPEE had a lower value. The lower ORAC value exhibited by MPEE might be due to its low solubility in the phosphate buffer used in the assay, since MPEE was extracted using absolute EtOH. It is likely that not all DPPH-scavenging antioxidants in MPEE are reducing agents and peroxyl radicals-scavenging agents as detected by the FRAP and ORAC assays. Consistent with this, Chomnawang et al. (2007) reported that mangosteen extract could inhibit 50% of free radicals at 6.1μg/ml as determined by the DPPH assay. The previous study (Patthamakanokporn *et al.* 2008) reported values for mangosteen extract of ORAC and FRAP values at 122.7 and 31.8 µM TE/g DW. The DPPH IC_{50} values were reported to be 30.8, 58.5, 77.8 and 35.0 µg/ml using 50% EtOH, 95% EtOH, ethyl acetate and water, respectively (Weecharangsan *et al.* 2006).

Compared to these previous studies, MPWE and MPEE from our study displayed higher yields (24.3 and 23.2%) and possessed higher antioxidant potential (see Table 2-3), indicating that the current extraction method was more efficient and more TP were recovered under the current methods. This may be due to the use of different solvents and different temperatures resulting in extraction of different amounts and proportions of active compounds (Rajkumar *et al.* 2011; Wang *et al.* 2008).

2.5 Summary

Conclusive results have been achieved to test the first hypothesis of this study "The mangosteen pericarp possesses bioactive compounds with antioxidant activities". In the first part of this chapter, the standardised extraction method was established for subsequent cell-based studies. As a result, the dried pericarp extracted with 100% EtOH or water at a pericarp/solvent ratio of 1:10 (w/v) at 75ºC (for EtOH extract) or

100 ℃ (for water extract) for 1 h was determined as the optimal extraction method. The second part of this chapter describes the chemical constituents of MPEE and MPWE as characterised using chemical assays and HPLC, and the antioxidant activities as evaluated by three different assays. MPEE and MPWE presented similar TP levels but with different chemical profiles. Both crude extracts showed comparable or higher antioxidant activities than the crude mangosteen extracts from previous studies using different procedures. In summary, the extraction method in our study was efficient in extracting and recovering the antioxidants from the pericarp of mangosteen.

CHAPTER 3
CYTOTOXIC EFFECT OF CRUDE MANGOSTEEN PERICARP EXTRACTS AND PURE XANTHONES ON HUMAN SKIN CELL LINES

3.1 Introduction

As discussed in the Chapter 1, a large variety of biological activities of xanthones have been reported extensively (Akao *et al.* 2008; Obolskiy *et al.* 2009; Pedraza-Chaverri *et al.* 2008a), especially their cytotoxicity on a variety of cancer cells, e.g. human breast cancer, colorectal cancer, hepatoma, leukaemia, and small cell lung cancer (Ho *et al.* 2002; Matsumoto *et al.* 2003; Moongkarndi *et al.* 2004; Nakagawa *et al.* 2007; Suksamrarn *et al.* 2006). These cytotoxicities were found to be associated with antiproliferative and apoptotic effects. As for skin cancer, there is only one study that has reported the anti-proliferative effect of synthetic oxygenated xanthones on one melanoma cell line (UACC-62), but without elucidating the underlying mechanisms (Pedro *et al.* 2002). Furthermore, there has been no study on the anti-skin cancer effects of any natural prenylated xanthones from mangosteen.

The main aim of this chapter is to evaluate the cytotoxic effect of crude extracts and six major prenylated xanthone compounds derived from the pericarp of mangosteen on human squamous cell carcinoma A-431 and melanoma SK-MEL-28 cells. As shown in Table A-1, the six major compounds are α-mangostin, β-mangostin, γ-mangostin and 8-deoxygartanine, gartanine, and 9-hydroxycalabaxanthone.

In orderto evaluate the cytotoxicity of xanthone compounds, the cell viability assays need to be selected based on rapidity, reproducibility, high throughput and sensitivity (Siddiqui *et al.* 2006). The proliferation of cells *in vitro* could be measured by different assays. Assays with different principles could result in different determinations of viability. Therefore, two methods with distinct mechanisms are recommended to assess the cytotoxic effects of substances (Fotakis & Timbrell 2006;

Hansen *et al.* 1989). In this study, the two most commonly used methods were applied: the Crystal Violet assay (Gillies *et al.* 1986; Ishiyama *et al.* 1996), which is a dye staining the cell membrane structures; and the MTT (3-(4,5-dimethylthiazol-2-yl)-2,5-diphenyl tetrazolium bromide) assay, which measures the metabolic activity of cells with conversion of the tetrazolium salts (Gillies *et al.* 1986; Ishiyama *et al.* 1996; Mosmann 1983). These two methods were well established in our laboratory. However, the assay conditions needed to be optimised based on the individual cell lines used in this study.

The aims of this chapter are to:

1. Optimise the MTT and the Crystal Violet assay conditions, including cell adherence time and cell density per well for four human skin cell lines

2. Compare between the MTT and the Crystal Violet assays based on rapidity, sensitivity and reproducibility

3. Evaluate the cytotoxicity of the crude extracts and pure xanthone compounds using the selected cell viability assay under the optimal conditions as determined in Aims 1 and 2.

3.2 Materials and methods

3.2.1 Materials

α-Mangostin, β-mangostin, 8-deoxygartanine, 9-hydroxycalabaxanthone, and gartanine were purchased from Phenomenex Australia Pty Ltd. (Sydney, NSW, Australia) and γ-mangostin was purchased from Biopurity Phytochemicals (Chengdu, China). All the other reagents and chemicals used in this chapter were of analytical grade from Merck (Australia) or tissue culture tested grade from Sigma-Aldrich (USA) unless otherwise noted.

3.2.2 Cell lines and cell culture

3.2.2.1 Cell lines

A-431, SK-MEL-28, and CCD-1064Sk cell lines were purchased from the American

Type Culture Collection (ATCC). Human normal keratinocytes (HaCaT) cell line

was firstly isolated by Boukamp *et al.* (1988). In this study, HaCaT cell line was

kindly provided by the Department of Haematology, Flinders University, Adelaide,

Australia. The details of the cell lines are listed in Table 3-1.

Table 3-1
Summary of the cell lines used in this study.

Cell line	ATCC number	Origin and cell type	Species	Age / gender of donor
A-431	CRL-1555	Skin epithelial squamous carcinoma	Homo sapiens	85 /F
SK-MEL-28	HTB-72	Skin malignant melanoma	Homo sapiens	51/M
HaCaT	N/A	Normal skin keratinocyte	Homo sapiens	62/M
CCD-1064Sk	CRL-2076	Normal skin fibroblast	Homo sapiens	Newborn/M

3.2.2.2 Cell morphology

The morphology of cells was observed under the microscope and recorded by the

Olympus 1X71 phase contrast inverted fluorescence microscope and analySIS image

capture software (magnification 100×). Figure 3-1 shows that the four cell lines are

adherent cells with different morphologies.

A-431

SK-MEL-28

CCD-1064Sk

HaCaT

100 µm
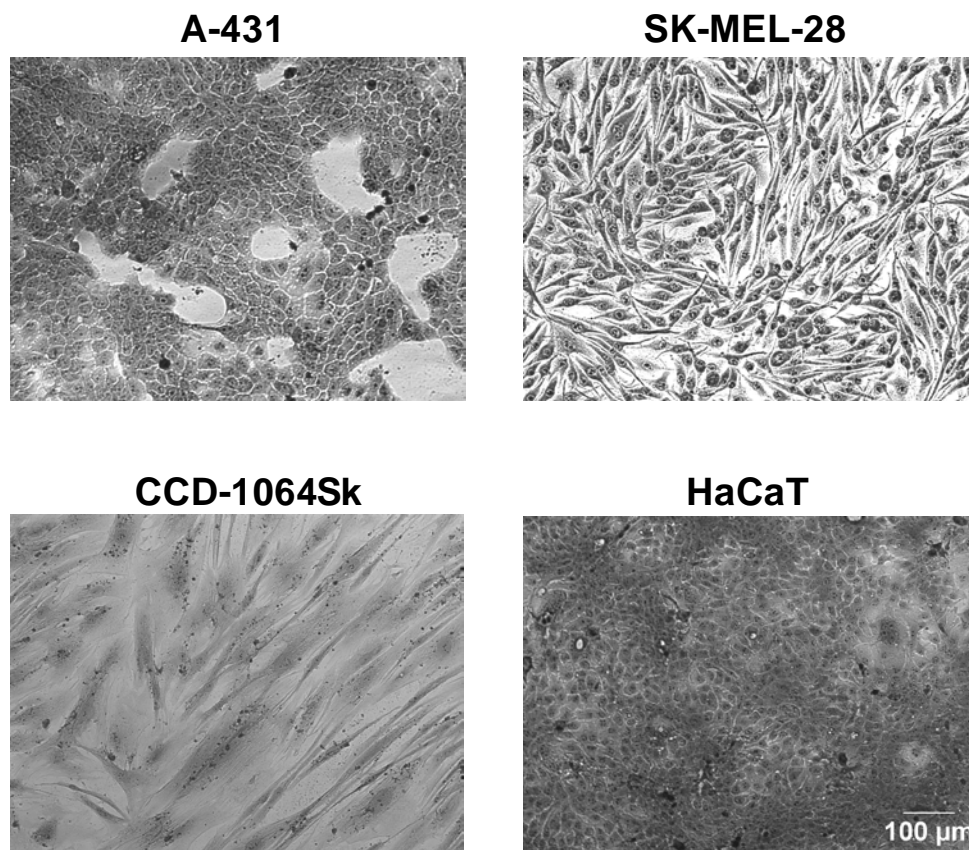
Figure 3-1

Morphology of A-431, SK-MEL-28, CCD-1064Sk and HaCaT cells. Each type of cells were grown to reach approximately 90% confluence in the incubator at 37ºC. Cells were fixed with 50% methanol (v/v) and stained with 0.5% (w/v) crystal violet. The morphology of four types of cells was observed and recorded by phase contrast inverted microscope (magnification 100×). The scale bar was set at 100 µm and same for the four images.

3.2.2.3 Cell culture

1) Cell culture media and preparation

SK-MEL-28 and A-431 cells were cultured in DMEM, supplemented with 10% (v/v)

heat inactivated foetal bovine serum (FBS; Invitrogen Corporation, Australia), 100

U/ml penicillin and 0.1 mg/ml streptomycin (Thermo Scientific, Melbourne,

Australia), 0.592 g/l L-glutamine, and 1.5 g/l sodium bicarbonate. HaCaT and CCD-

1064Sk were grown in RPMI 1640 and Iscoves Modified Dulbecco's Medium

(IMDM), respectively. The media supplement for these was the same as for SK-

MEL-28 and A-431. The FBS was heat inactivated at 56 ºC for 30 min in a waterbath

with occasional shaking. The heat inactivated FBS was stored in 50 ml aliquots at –20ºC.

All media were initially prepared in five litre batches (without FBS and sodium bicarbonate), adjusted to pH 7, and sterilised by 0.22 µm filter before storage at –20 ºC. Prior to use, media were prepared in 500 ml batches with the addition of FBS and sodium bicarbonate (1.5 g/l) followed by filtration then storage at 4 ºC. The temperature and pH of media were equilibrated for 30 min in a 37 ºC incubator immediately before use.

2) Cell subculture

Cell lines were grown to 80-90% confluence in a T75cm^2 cell culture flask (Nunc, Roskilde, Denmark) in a fully humidified incubator with 5% CO_2 at 37 ºC. Cells were washed with phosphate-buffered saline (PBS; see Appendix A1) and detached with 1 ml 0.25% trypsin-EDTA (Thermo Scientific, Melbourne, Australia). Fresh culture medium (5 ml) was added and the cell suspension was centrifuged at 312 $\times$g for 5 min. The medium was removed and the cell pellet was resuspended with fresh medium. Then cells with a total cell number of 2×10^6 (for SK-MEL-28 and A-431), 1×10^6 (for HaCaT), or 0.8×10^6 (for CCD-1064Sk) were seeded to the T75cm^2 cell culture flask containing 20 ml of the respective culture medium. All cell manipulations were done using autoclaved sterile tips and pipettes. Cells used in experiments were under the passage number of 20. Cell lines received from ATCC were designated as being passage 1.

3) Cell line storage

Cell lines were stored in liquid nitrogen in the respective medium containing 10% (v/v) FBS and 5% (v/v) dimethyl sulfoxide (DMSO) at a cell concentration of 4×10^6 cells/ml.

4) Mycoplasma test using polymerase chain reaction (PCR)

Mycoplasmas are a group of bacteria that lack a cell wall. They induce alterations in cell metabolism, growth rate and morphology (Roulland-Dussoix *et al.* 1994). Experimental results generated from the cell culture may be unreliable if there is contamination with mycoplasmas. Frequencies of such contaminations generally are between 5 and 87% (Garner *et al.* 2000; Rawadi & Dussurget 1995). However, mycoplasmas are not so easy to detect as other bacteria, mould or yeast, they can exist in cell cultures for a long time without being noticed. Therefore, regular detection of mycolplasmas in cell culture is important for cell-based assays.

Due to its sensitivity and rapidity, the PCR method is widely used to detect mycoplasma contamination in cell cultures (Rawadi & Dussurget 1995; van Kuppeveld *et al.* 1992). The four different cell lines used in this study were tested for mycoplasma contamination using the PCR method obtained from the Department of Haematology, Flinders University, Adelaide, Australia. Briefly, 1 ml sterile saline was added to 200 µl of cell suspension and the mixture was centrifuged at 3800 ×g for 5 min. The supernatant was aspirated and the cell pellet was lysed with 90 µl 0.05 M NaOH and heated at 98ºC for 10 min. After cooling, 10 µl of 1 M Tris (pH7.5) was added to the lysis solution to neutralize it. PCR amplification was carried out in 25 µl of PCR mixture consisting of 2 µl DNA sample and 23 µl mastermix

(Appendix A3.1) on a thermal cycler (Axygen MaxyGene, Perth, Australia). An internal control gene (human RAG1) was included to ensure that the DNA was amplifiable (Hayakawa *et al.* 1996). One positive control cells with mycoplasma contamination and one negative control cells were kindly provided by the Department of Haematology. The PCR profile was as follows:

94ºC	10 min
94ºC	30 sec
53ºC	1 min
72ºC	1 min
72ºC	5 min

50 cycles

The PCR products (10 µl) were analysed by gel electrophoresis using 1.5% (w/v) agarose gel and visualised by gel red staining (0.01%, v/v). As shown in the gel image (Figure A-2 in Appendix A3.2), all of four cell cultures tested were free from mycoplasma contamination, as only human RAG1 gene was amplified (size 600 bp) and the expected band for mycoplasma (size 715bp) was only observed in the positive control.

3.2.2.4 Cell doubling time

The cells for each cell line with a total number of 5×10^5 were seeded in a volume of 5 ml into wells of a 6-well flat bottom plate (Nunc, Denmark) and incubated for 24, 48, 72, 96, 120 and 144 h, respectively. After each time point, the cells were detached and counted by the Trypan Blue assay (see Section 3.2.4). Cell number per well was plotted against the incubation time for each cell line. The growth curve of HaCaT reached a plateau after 72 h, whereas those of A-431, SK-MEL-28 and CCD-

1064Sk reached a plateau after 96 h, due to cells reaching confluence in the well. The doubling time was calculated from the cell growth curve (Figure A-3 in Appendix A4) and analysed using the algorithm available at http://www.doubling-time.com. Cell doubling time was 40.24, 41.12, 41.31, and 29.98 h for A-431, SK-MEL-28, CCD-1064Sk, and HaCaT cell line, respectively.

3.2.3 Treatment preparation

Test compounds were solubilised in absolute ethanol and diluted with respective medium to the desired treatment concentration. The method for the treatment preparation of MPWE and MPEE refers to Section 2.2.7 in Chapter 2. Two commercial drugs of 5-FU and DTIC were used as positive controls for A431 and SK-MEL-28, respectively. 5-FU was dissolved in DMSO and DTIC was dissolved in 0.02 M acetic acid. Vehicle (EtOH, DMSO, and 0.02 M acetic acid) volume was consistently kept as 1% (v/v) for each treatment.

3.2.4 Trypan Blue exclusion assay

The Trypan Blue exclusion assay can differentiate between live and dead cells. Trypan Blue cannot penetrate the cell membrane of live cells and thus they remain yellow in colour, whereas in dying or dead cells membrane integrity is lost and hence the Trypan Blue can no longer be excluded by the cell and cells appear blue (Petty *et al.* 1995). In this study, the Trypan Blue assay was used for cell counting to calculate the cell concentration. Briefly, a solution of Trypan Blue (0.2%) (w/v) in sodium chloride (0.9%) (w/v) was filtered through Whatman grade I filter paper (Appendix A1). Fifty μl aliquots of cell suspension were each diluted 1:1(v/v) with Trypan Blue. Twenty μl aliquots were loaded onto a haemocytometer for counting. The viable cell concentration and the viability% were calculated by the following formulas.

Viable cell concentration (Cells/ml)

$$= \text{viable cell number} \times 2 \times 10^4 / \text{the number of squares}$$

Viability %

$$= \text{viable cell number} / (\text{viable cell number} + \text{dead cell number}) \times 100\%$$

The cells with a viability above 90% were used in the experiments.

3.2.5 Cell proliferation assays

3.2.5.1 MTT Assay

The MTT assay was based on the reduction of the water-soluble MTT dye to the purple formazan crystalline product (Mosmann 1983; Plumb *et al.* 1989). MTT was dissolved in sterile PBS at 5 mg/ml, and 5 ml aliquots stored at –20ºC (Appendix A1). The MTT assay was carried out as described previously (Mosmann 1983). Briefly, 1×10^4 cells were seeded in a volume of 100 μl into the wells of a 96-well flat bottom plate (Nunc, Denmark) and incubated for 24 h. The 100 μl culture media were aspirated. Cells were then treated with 100 µl media (used as untreated control), 100 µl 1% (v/v) ethanol in media (used as vehicle control) or 100 µl of varying concentrations of treatment for the desired exposure duration. After treatment, treatment media were aspirated and MTT was added to each well at a final concentration of 0.5 mg/ml. Plates were then incubated at 37ºC for 18 h, after which 80 µl of 20% (w/v) sodium dodecyl sulfate (SDS) in 0.02 M HCl was added to each well and mixed thoroughly. The plates were kept in the dark at room temperature for 1.5 h. Optical density (OD) was read at 570 nm with 630 nm as a reference wavelength on a µQuant automatic spectrophotometer (Bio-TEK instruments, NSW, Australia) with KC Junior software (Bio-Tek, Vermont, USA). The OD values were converted to cells/well using a standard curve run (Section 3.2.5.3) with each experiment (Young *et al.* 2005). The results were expressed as relative viability (%)

compared to the untreated control.

3.2.5.2 Crystal Violet assay

Loss of membrane integrity and the detachment of cells are the important indicators of loss of cell viability (Gillies *et al.* 1986; Ishiyama *et al.* 1996). Crystal Violet (N-hexamethylpararosaniline), a metachromophoric basic dye, stains the membrane of cells (Gillies *et al.* 1986; Ishiyama *et al.* 1996). Similar to the MTT assay, an experimental treatment plate was set up accompanied by a standard curve plate (Section 3.2.5.3). After treatment, the treatment media were aspirated and cells were stained with 50 µl/well of 0.5% (w/v) crystal violet in 50% (v/v) methanol for 10 min at RT to allow cells to be stained by the crystal violet and fixed by the methanol. Plates were gently rinsed with water and air dried in a fumehood. Fifty µl of 33% (v/v) acetic acid was added to each of the wells and incubated for 10 min at RT. The OD was read on a microplate reader at 570 nm and the values were converted to cells/well using a standard curve run with each experiment. The effect of the compounds on cell proliferation was determined by converting cells/well to the relative cell number and the results were expressed as relative viability (%) compared to the untreated control.

3.2.5.3 Standard curves for the MTT assay and Crystal Violet assay

Viable cell suspensions were serially diluted in a 96 well plate using a multi-channel pipette (625 – 40,000 cells per well in six replicates) in 100 µl of their respective media. The plate was incubated for 24 h to allow cell attachment. Cell numbers were measured using the MTT or Crystal Violet assay as described (Sections 3.2.5.1 & 3.2.5.2). The average OD of the six replicates was related to the initial cell number in each well using a linear regression function in Microsoft Excel 2003. The equation was used to convert OD to cell number after the MTT or Crystal Violet assay.

3.2.6 Statistical analysis

Data are presented as mean (±SEM). Each assay was repeated in at least three independent experiments with six technical replicates for each condition. The intra- and inter-run coefficients of variation (CV) were calculated using Microsoft Excel 2003. CV was calculated as the fractional percentage of standard deviation divided by the mean (Hendricks & Robey 1936). Statistical analysis between comparison of the MTT and the Crystal Violet was performed using independent sample t test.

To assess the effect of xanthones on the cell viability, statistical analysis of the data was carried out using ANOVA, followed by Tukey's HSD *post hoc* test / Dunnett's T3 *post hoc* test for equal and unequal variances as appropriate. These tests were performed using SPSS software (Version 17). Differences were considered statistically significant when the *P*-value was less than 0.05 (significant) and 0.01 (highly significant). IC_{50} values were calculated using GraphPad Prism 5 software (San Diego, CA, USA).

3.3 Results

3.3.1 Optimisation of cell adherence time and cell density per well

The conditions for both of the MTT and the Crystal Violet assays have been optimised and validated in our laboratory. They include the optimal concentrations and exposure periods for MTT, SDS, crystal violet, and acetic acid. However, A-431 and SK-MEL-28 were newly introduced into our laboratory. Prior to the cytotoxicity studies, two key parameters need to be optimised for both assays: cell adherence time and cell density per well.

3.3.1.1 Cell adherence time

In orderto determine the optimal adherence time required for A-431 and SK-MEL-28

cells, a series of adherence standard curves were carried out. Three adherence times were investigated: 2, 4 and 24 h. The adherence plate was set up identically to a standard curve plate (Section 3.2.5.3). The Crystal Violet assay (Section 3.2.5.2) was carried out and a linear regression analysis was undertaken to assess the relationship of OD with cell number for each attachment time.

A strong linear relationship was observed at the three adherence times for each cell line as evidenced by high R-square (R^2) value (> 0.99). For each cell line, the average of OD increased with the increasing adherence time at each cell concentration (Figure 3-2). Therefore, an adherence time of 24 h was selected for all subsequent experiments.
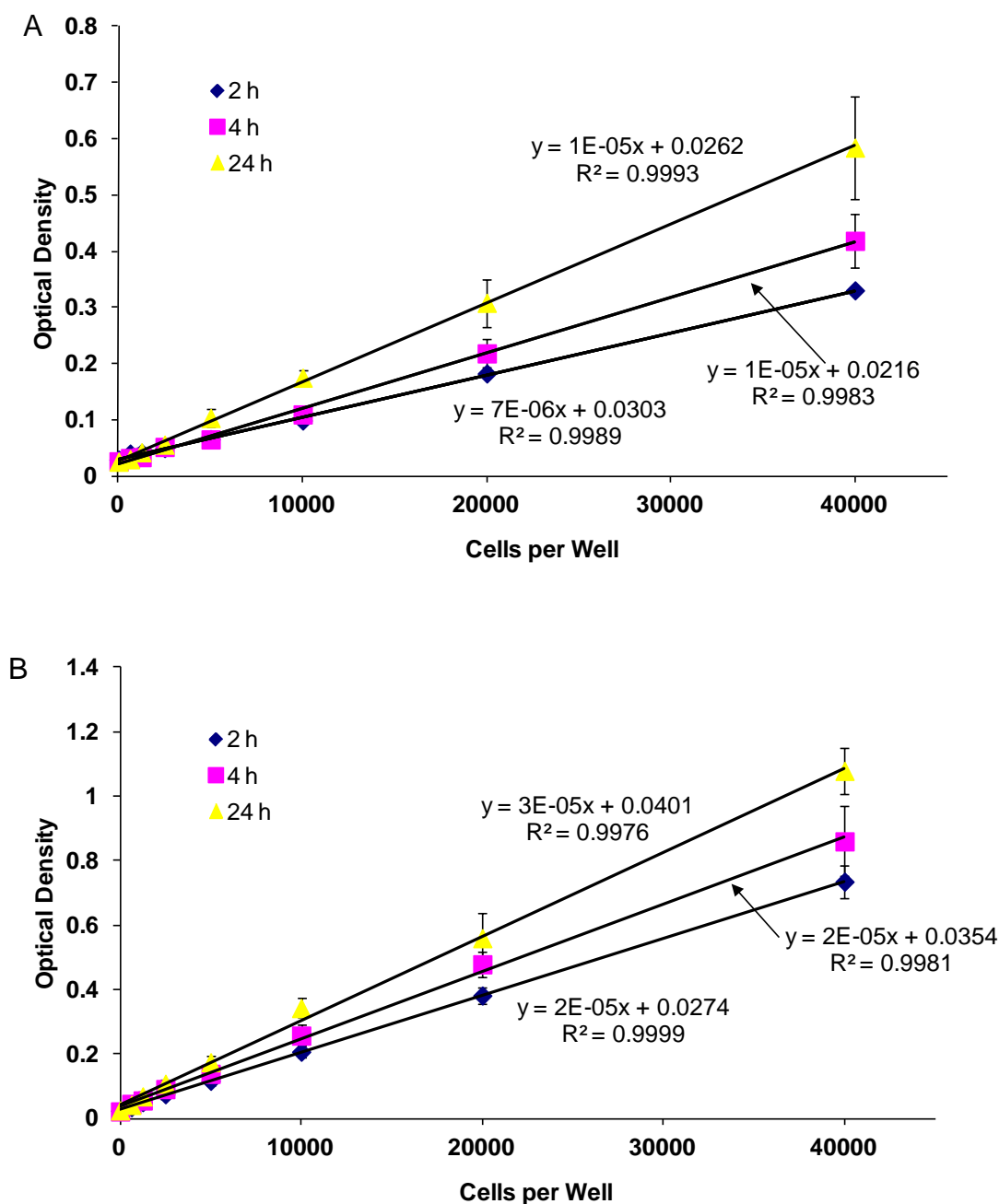
Figure 3-2

A comparison of attachment of each cell line after 2, 4, and 24 h. A-431 (A) and SK-MEL-28 (B) cells seeded at concentrations from 0 to 4×10^4 cells/well were allowed to adhere for 2, 4, or 24 h in complete DMEM culture media. After each adherence time, the Crystal Violet assay was carried out and the optical density was measured at 570 nm. Each line is derived from one adherence time with respective R-square value determined by linear regression analysis. The experiment was repeated three times and the data are represented as mean ± SEM.

3.3.1.2 Cell density seeded per well

As shown in Section 3.2.2.4, A-431, SK-MEL-28, and CCD-1064Sk have similar

cell doubling time of approximately 43 h, while HaCaT cell line has relatively shorter cell doubling time of approximately 32 h. Therefore, SK-MEL-28 and HaCaT were selected to optimise the cell density seeded per well in a 96-well plate. Three identical standard curves with cell numbers ranging from 0 to 4×10^4 were set up for each cell line. After the cells were seeded, the standard curves were incubated for 24, 48, and 72 h, respectively. At the end of each time point, the Crystal Violet assay was performed and the OD values were read and recorded. The results are presented in Figure 3-3. In SK-MEL-28 cells, with increasing incubation time, the ODs were not increased proportionally when the initial seeding cell number was higher than 2×10^4. Likewise, a similar pattern was observed in HaCaT cells. The ODs were not increased proportionally when the initial seeding cell number was higher than 1×10^4. It might be because of nutrient depletion and cells reaching confluence in the well. Therefore, the suitable range of initial seeding cell number should be no more than 1×10^4. Additionally, the standard curve was not sensitive in determining the number of viable cells ranging of 625 to 2,500 initial cells seeded per well. The sensitivity of the cell number of 5000 was acceptable. However, this study was to investigate the cytotoxicity of xanthones and cell killing to different extents was expected. Therefore, after treatment with xanthones at 5000 cell per well, the OD would be out of sensitivity range of this assay. Taken together, 1×10^4 cells/well was selected as the optimal cell density for all the four cell lines in the subsequent experiments.
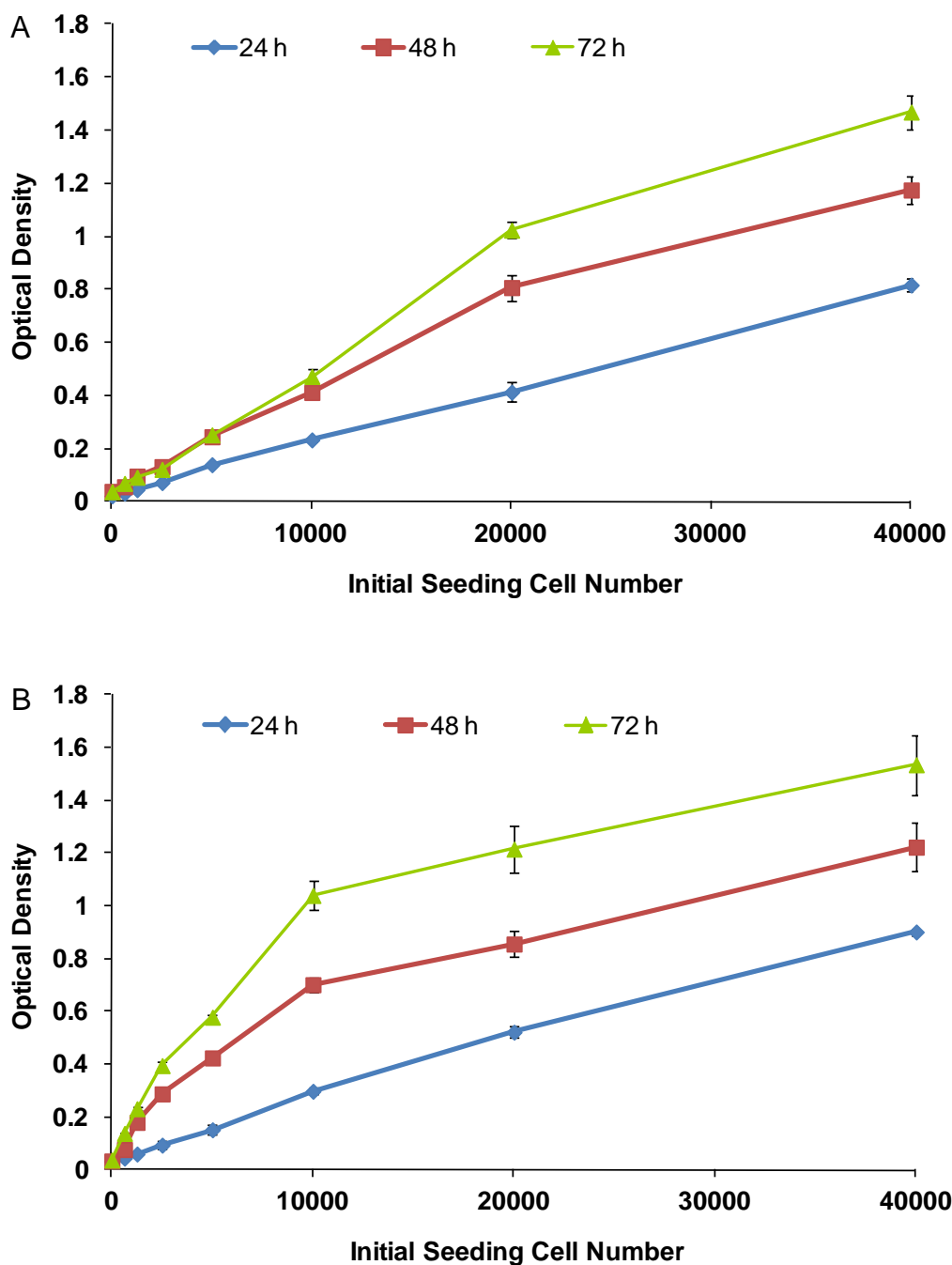
Figure 3-3
Cell density per well for each cell line was optimised using the Crystal Violet assay. Cells (A: SK-MEL-28 and B: HaCaT) were seeded at densities in the range of 0 to 2 × 10⁴ cells/well in respective culture media. After seeding cells, the plates were incubated for 24, 48, and 96 h, respectively. After incubation, the Crystal Violet assay was carried out and the optical density was recorded. The experiment was repeated three times and the data are represented as mean ± SEM.

3.3.2 Comparison of MTT assay and the Crystal Violet assay

These two assays are based on different principles: the MTT assay is dependent on metabolic production of formazan, while the Crystal Violet assay stains adhered cells. The accuracy, sensitivity, and reproducibility of these two assays were compared in the following three aspects.

3.3.2.1 Standard curves

To determine the sensitivity, the standard curves were set up for each cell line using the MTT and Crystal Violet assays. There was a strong linear correlation between the OD after 24 h adherence and the number of cells initially seeded in both the MTT assay and the Crystal Violet assay ($R^2 > 0.99$, Figure 3-4). The incremental increases in OD (slope) obtained for the Crystal Violet assay were higher than with the MTT assay in the A-431, SK-MEL-28, and CCD-1064Sk cells. The slopes were similar in HaCaT cells as detected by both the MTT and the Crystal Violet assay (Figure 3-4).
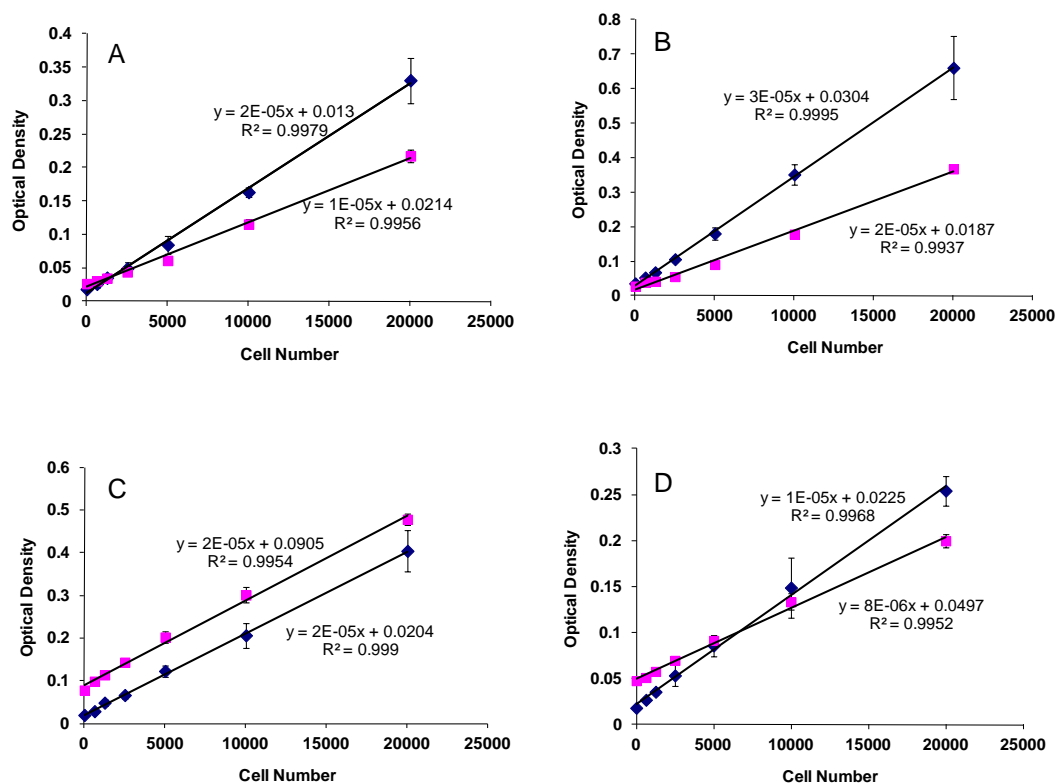
Figure 3-4
A comparison of MTT and Crystal Violet standard curves for each cell line. Cells (A: A-431; B: SK-MEL-28; C: HaCaT; and D: CCD-1064Sk) seeded at densities in the range of 0 to 2×10^4 cells/well in respective culture media. The MTT (■) and Crystal Violet (♦) assay were carried out and the absorbance was read as described previously (3.2.5 & 3.2.6). The experiment was repeated three times and the data are represented as mean ± SEM.

3.3.2.2 Cell viability

A comparison between the cell viability calculated from the MTT and Crystal Violet assays was carried out after 48 h treatment with MPEE at an initial density of 1×10^4 cells/well (Figure 3-5). At some concentrations, the cell viability calculated by the Crystal Violet assay was significantly lower than that calculated by the MTT assay. In A-431 cell line, the significant differences were found after treatment with MPEE at both 5 and 10 µg/ml of TP (Figure 3-5 A; $P < 0.01$). In SK-MEL-28, the significant differences were observed after treatment with MPEE at ≥1.25 µg/ml of TP (Figure 3-5 B; $P < 0.01$).

The viable cell numbers calculated from the MTT and Crystal Violet assays are presented in Figure A-4 in Appendix A5. In A-431 cell line, the viable cell number of the untreated control was 1.8 and 1.4×10^4 as detected by the Crystal Violet and MTT assay, respectively. In SK-MEL-28 cell line, similar results were observed with 2.0 and 1.4×10^4 as detected by the Crystal Violet and MTT assay, respectively. According to the results from cell doubling time (Appendix A4), the cell number after 48 h was expected to be approximately 2×10^4 as the initial seeded cell number of 1×10^4. Therefore, the results suggest that the Crystal Violet assay reflect the true cell number more accurately than the MTT assay.
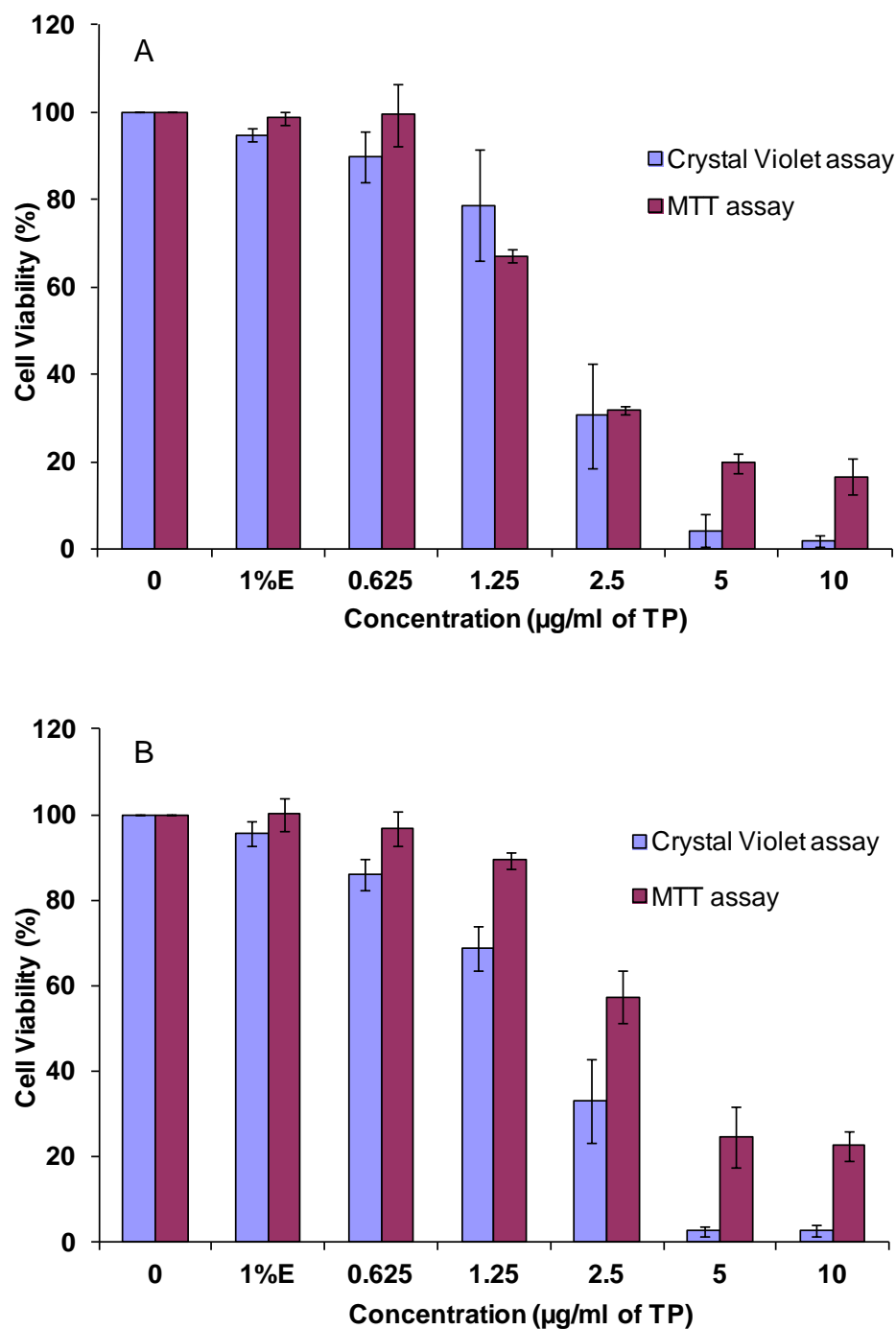
Figure 3-5

A comparison between the cell viability calculated from the Crystal Violet and MTT assays. A-431 (A) and SK-MEL-28 (B) cells were cultured at 1×10^4 cells/well in DMEM media. Cells were treated with mangosteen pericarp ethanol extract (MPEE) (0-10 µg/ml of total phenolics (TP)). Ethanol (1%E; v/v) was used as vehicle control. After 48 h treatment, the MTT and Crystal Violet assay were carried out and the absorbance was read as described in the method (Section 3.2.5). The absorbance was used to calculate the number of viable cells from the 24 h adherence linear regression equation. The experiment was repeated three times and the data are represented as mean ± SEM.

3.3.2.3 Intra- and inter-assay coefficients of variance (CV)

To determine the reproducibility of the MTT and Crystal Violet assays, A-431 and SK-MEL-28 cells (at the cell density of 10^4 cells per well) were seeded in 96-well plates. After 24 h incubation, the MTT and Crystal Violet assay were performed and the OD was measured as described in the Sections 3.2.5.1 & 3.2.5.2. The experiments were repeated on five separate occasions, with six replicates for each condition. The intra- and inter-assay coefficient of variances (CV) of OD values between replicate wells and runs were calculated (Section 3.2.6) and the results are shown in Table 3-2. As for the intra-assay CV, the two assays displayed similar levels of CV on A-431 and SK-MEL-28 cells, except that the CV value was slightly higher when detected by the Crystal violet assay on SK-MEL-28 cells. For the inter-assay CV, the two assays displayed similar levels of CV on A-431 and SK-MEL-28 cells. The low CVs suggest that both assays have good reproducibility.

Table 3-2
Intra- and inter-assay coefficients of variance (CV) of the MTT and Crystal Violet assay.

Assays	Cell lines	Intra-assay CV (%)	Inter-assay CV (%)
MTT	A-431	5.2	9.0
	SK-MEL-28	6.5	15.6
Crystal Violet	A-431	6.8	15.3
	SK-MEL-28	10.7	9.9

3.3.2.4 Summary of comparison of the MTT and Crystal Violet assays

The MTT and Crystal Violet assays displayed similar reproducibility and high throughput. However, the Crystal Violet assay showed higher sensitivity than the MTT assay as evidenced by higher standard curve slopes (Figure 3-4). Additionally, MTT assay requires extra steps of incubation with MTT for 18 h, and addition and incubation with SDS for 1.5 h after cell treatment, while the Crystal Violet assay

only need 10 min incubation with crystal violet staining and 10 min incubation with acetic acid. Hence, in terms of rapidity, the Crystal Violet assay was better than MTT assay. Therefore, the Crystal Violet assay was selected as the method to measure the cytotoxicity induced by xanthones in the subsequent experiments.

3.3.3 Cytotoxicity of crude extracts and pure xanthone compounds from the mangosteen pericarp on human skin cells

The cytotoxicity of crude extracts and pure xanthone compounds was investigated using the Crystal Violet assay on human skin cancer cells and normal skin cells. A 1% (v/v) ethanol vehicle control was included in each experiment and did not significantly alter cell viability of each cell line compared to the medium control: 95.9 (± 2.4) %, 98.7 (± 3.6) %, 93.1 (± 1.5) %, and 94.5 (± 1.7) % for A-431, SK-MEL-28, HaCaT, CCD1064Sk, respectively.

3.3.3.1 Cellular morphological changes with or without treatment with xanthones

After treatment with all xanthones tested, morphological alterations in the two types of skin cancer cells were observed compared with the untreated cells. Figure 3-6 shows an example of cell morphological changes after 48 h treatment with MPEE on the A-431 and SK-MEL-28 cell lines. Untreated cells were polygonal in ordinary shape, while treated cells were shown to be retracted and rounding in shape with some cells detached from the surface and floating in the media.
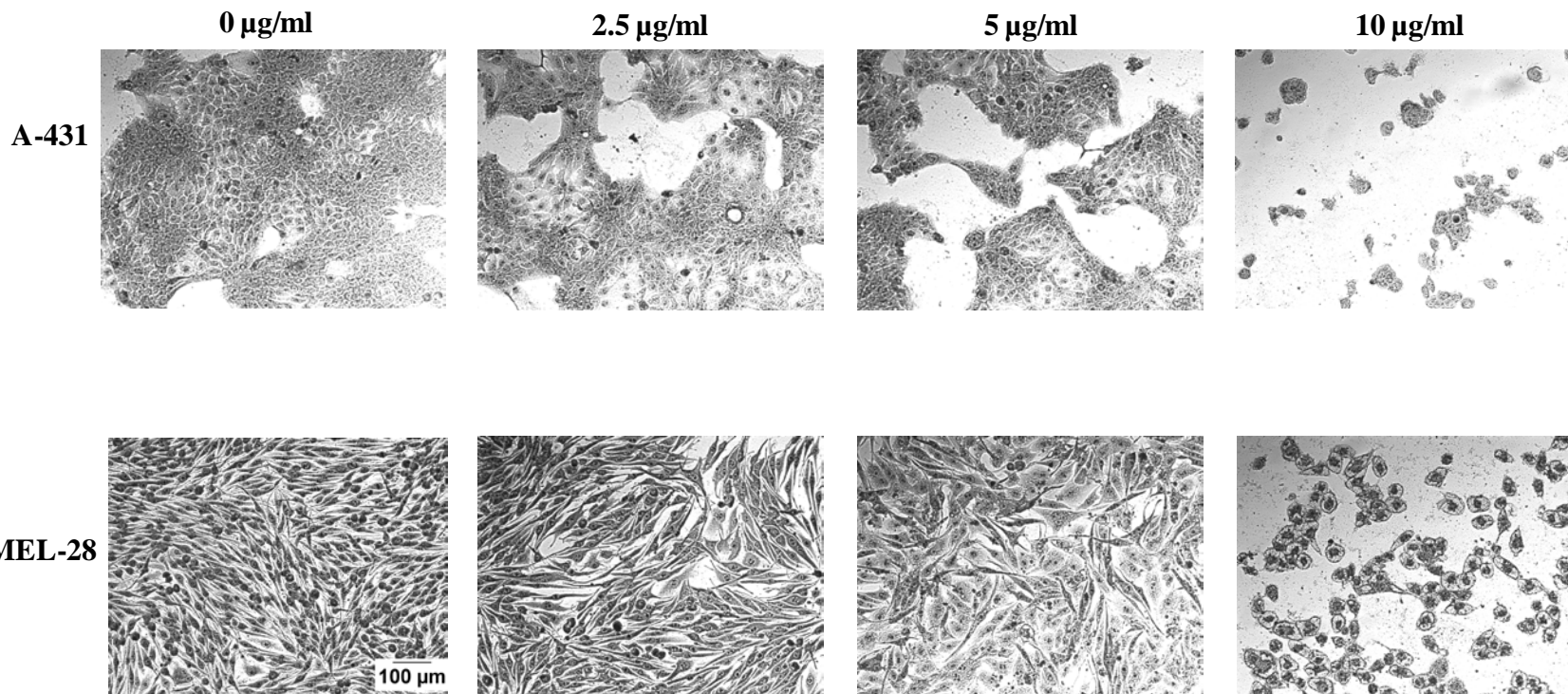
Figure 3-6
One example of morphological changes: after 48 h treatment with MPEE (0-10 µg/ml) on human squamous cell carcinoma A-431 and melanoma SK-MEL-28 cells. All theimages were taken by Olympus IX70 phase contrast inverted fluorescence microscope and analysis image capture software at $100 \times$ magnification (Scale bar was set at 100 µm and same for all the images)

3.3.3.2 Cytotoxicity of MPEE and MPWE on human skin cancer cell lines

MPEE significantly inhibited the proliferation of A-431 and SK-MEL-28 cells in a dose-dependent manner. A time-dependent influence was only observed at higher concentrations (Figure 3-7 A & B). However, the difference between 48 h and 72 h was not significant for the A-431 cells ($P > 0.05$). Therefore, further investigation was carried out using MPEE at the 48 h treatment time. The IC_{50} (50% of inhibition concentration) values were 5.0-6.7 µg/ml on A-431 cell line and 5.8-6.9 µg/ml on SK-MEL-28 cell line after treatment with MPEE for 24, 48 and 72 h.

In contrast, MPWE only showed significant cytotoxic effect at ≥ 200 µg/ml on these two types of skin cancer cells (Figure 3-7 C & D), therefore, no further studies were carried out with this extract.
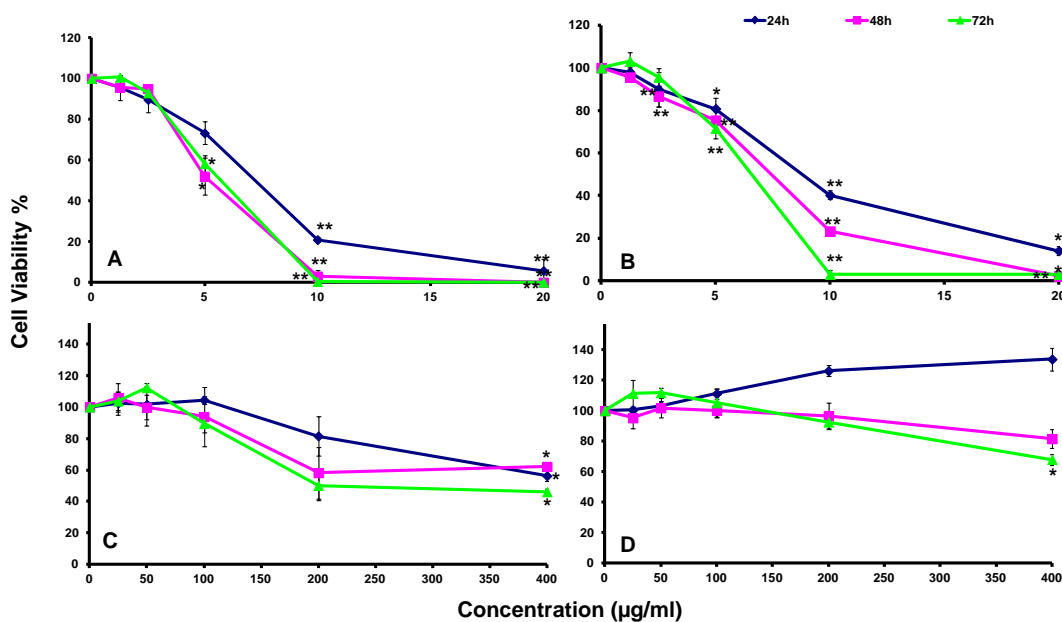
Figure 3-7
Cell viability measured by the Crystal Violet assay after 24, 48, and 72 h treatment with mangosteen pericarp ethanol extract on (A) A-431 cell line and (B) SK-MEL-28 cell line, or with mangosteen pericarp water extract on (C) A-431 and (D) SK-MEL-28 cell line. Data are shown as percentage viability compared to the untreated control and presented as the mean ± SEM of 3 independent experiments. Treatments significantly different from the untreated control at $P < 0.05$ are presented as * and $P < 0.01$ as **.

3.3.3.3 Cytotoxicity of MPEE on human normal skin cell lines

Although MPEE showed dose-dependent cell killing on HaCaT and CCD-1064Sk cells lines, it was less cytotoxic on the human normal skin cell lines than human skin cancer cells (Figure 3-8). This was evident from higher IC_{50} values of 12.62 µg/ml on CCD-1064Sk and 8.32 µg/ml on HaCaT compared to 5.07 µg/ml on A-431 and 6.89 µg/ml on SK-MEL-28 after 48-h treatment with MPEE (Table 3-3).
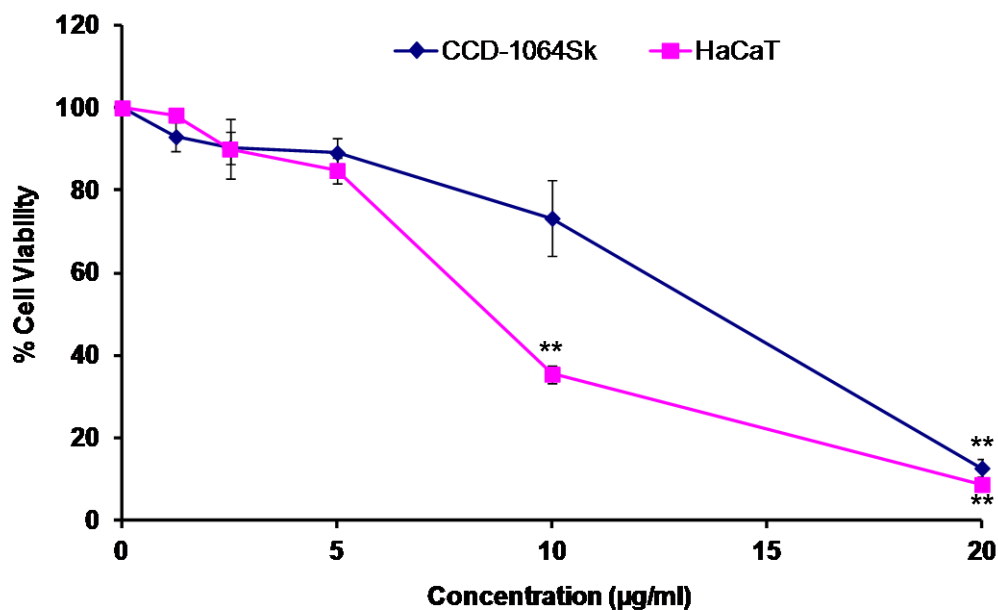
Figure 3-8

Cell viability measured by the Crystal Violet assay after 48 h treatment with mangosteen pericarp ethanol extract on human normal skin fibroblast CCD-1064Sk cell line and keratinocyte HaCaT cell line. Data are shown as percentage viability compared to the untreated control and are presented as the mean ± SEM of three independent experiments. Treatments significantly different from the untreated control at $P < 0.05$ are presented as * and $P < 0.01$ as **.

3.3.3.4 Cytotoxicity of pure xanthone compounds on human skin cancer and normal cell lines

The six xanthones tested were found to significantly inhibit the growth of A-431 and SK-MEL-28 cells in a dose-dependent manner (Figure 3-9 A&B). Among these, α-mangostin and γ-mangostin show the most marked cytotoxicity on A-431 cells, and gartanine on SK-MEL-28 cells, with an IC$_{50}$ value of 2.5 µg/ml.

In contrast, xanthones, especially γ-mangostin and gartanine, caused less cytotoxicity on normal CCD-1064Sk and / or HaCaT cell line (Figure 3-9 C&D), as evidenced by higher IC$_{50}$ values on normal cell lines compared to the values on cancer cell lines (Table 3-3).

3.3.3.5 *Cytotoxicity of commercial drugs on human skin cell lines*

Significant decreases in cell viability were observed after treatment with the positive

controls of 5-FU and DTIC (Figures A-5 and A-6 in Appendix A6). The IC_{50} values

are summarised in Table 3-3. 5-FU and DTIC showed similar toxicity on both cancer

and normal cells as evidenced by similar IC_{50} values on normal cell lines and cancer

cell lines.
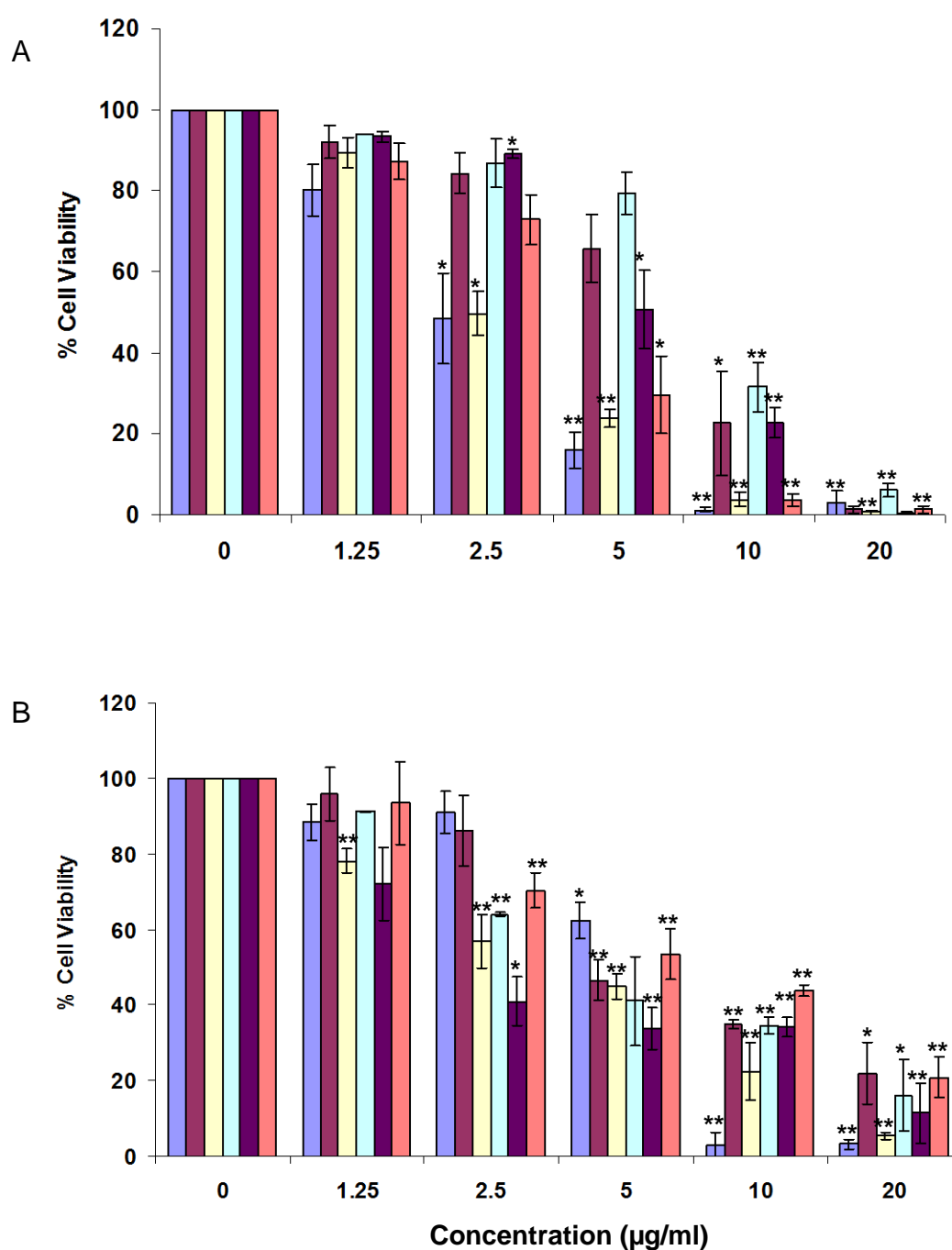
Figure 3-9

(Continued)
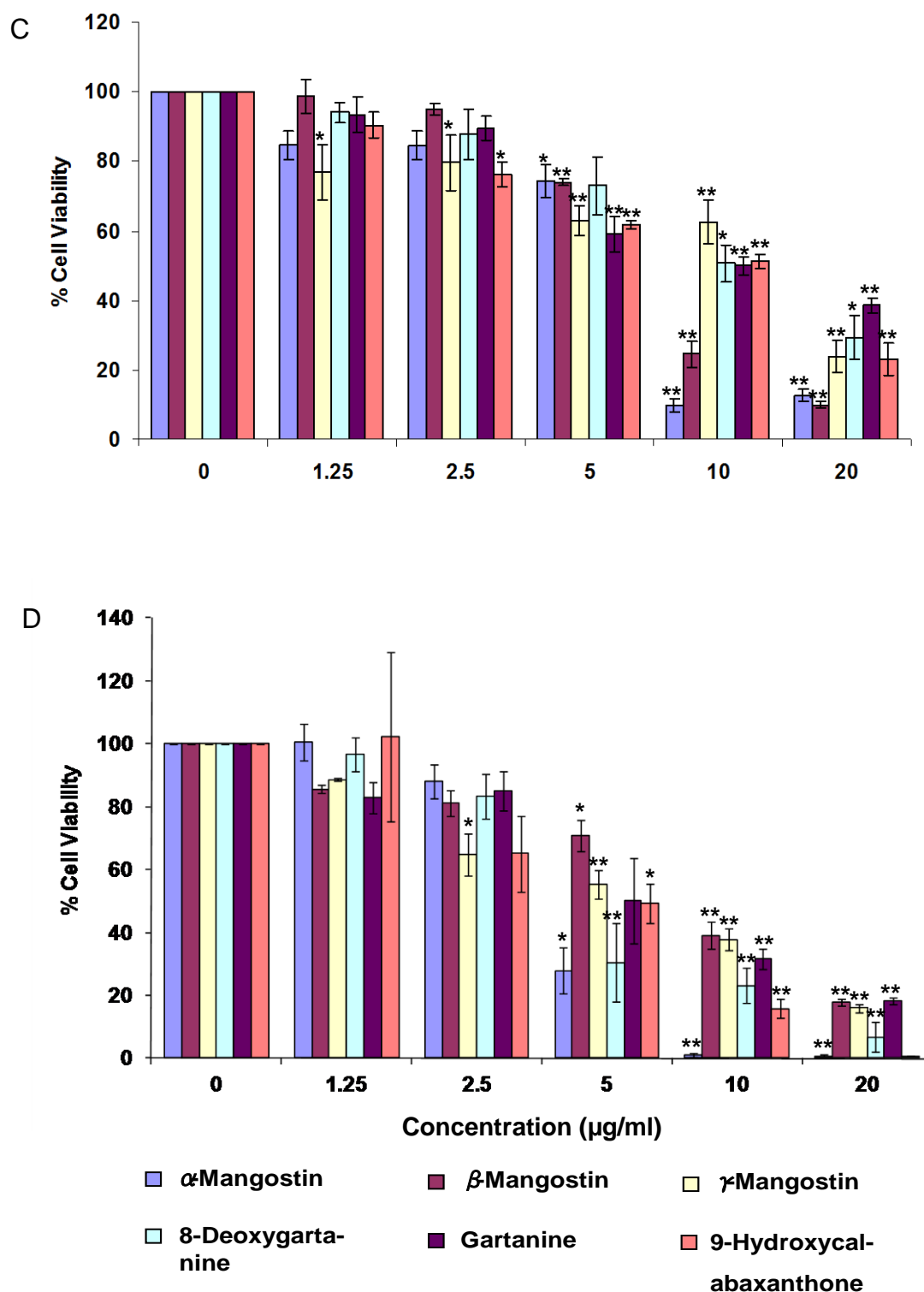
Figure 3-9
Cell viability measured by the Crystal Violet assay after 48 h treatment of A-431 (A), SK-MEL-28 (B), CCD-1064Sk (C), and HaCaT (D) with α-mangostin, β-mangostin, γ-mangostin, 8-deoxygartanine, gartanine, 9-hydroxycalabaxanthone. Data are shown as percentage viability compared to the untreated control and are presented as the mean ± SEM (n=4 for A-431, SK-MEL-28 and HaCaT; n=7 for CCD-1064Sk). Treatments significantly different from the untreated control at $P < 0.05$ are presented as * and $P < 0.01$ as **.

Table 3-3
IC_{50} values (µg/ml) based on the results (Figure 3-9) obtained using the Crystal Violet assay (as per the methods section 3.2.5).

Xanthones / Commercial drugs	A-431	SK-MEL-28	CCD-1064Sk	HaCaT
MPEE	5.07	6.84	12.62	8.32
α-Mangostin	2.39	5.92	7.27	3.91
β-Mangostin	6.09	6.22	7.3	7.62
γ-Mangostin	2.7	3.55	11.33	5.62
8-Deoxygartanine	7.61	3.83	10.35	4.26
Gartanine	5.35	2.59	10.59	5.83
9-Hydroxy-Calabaxanthone	3.52	6.58	8.27	4.39
5-FU	1.28	—	1.22	0.31
DTIC	—	> 100	> 100	50

3.4 Discussion

3.4.1 Cytotoxicity of crude extracts

Although MPWE and MPEE presented similar levels of total phenolics, as discussed in Chapter 2, MPWE showed much lower cytotoxic effect than MPEE on two skin cancer cell lines (A-431 and SK-MEL-28) as evidenced by more than 40-fold higher IC_{50} values. This might be explained by two factors: firstly, different total phenolics were extracted by different solvents as evidenced by the different HPLC profiles (Chapter 2); secondly, the major secondary metabolites in the perciarp of mangosteen are xanthone compounds, which are insoluble in water (Shan & Zhang 2010). Therefore, antioxidant activity and cytotoxic activity are not always necessary correlated, depending on the constituents of the antioxidants.

MPEE, in addition to high antioxidant activity as discussed in Chapter 2, exhibited significant cytotoxic effects when tested on the two skin cancer cell lines (A-431 and SK-MEL-28) in the present study. The results are consistent with a previous study in which a crude methanol extract from the mangosteen pericarp exhibited an anti-

proliferative effect on a human breast cancer (SKBR3) cell line with an IC_{50} of 9.25 µg/ml (Moongkarndi *et al.* 2004). According to the American National Cancer Institute, the IC_{50} value of a crude extract should be less than 30 µg/ml to be considered as promising for further purification and investigation (Stuffness & Pezzuto 1990). It is noteworthy that the current IC_{50} values obtained for MPEE were within this threshold on both tested cell lines, and hence it could be considered as a potential anti-skin cancer drug candidate.

3.4.2 Cytotoxicity of tested xanthone pure compounds

This study is the first demonstration of the cytotoxicity induced by these six xanthones on human skin cancer cell lines. The xanthones tested exerted strong growth inhibition with IC_{50} values of 2.39-7.61 µg/ml for human squamous cell carcinoma A-431 cell line, and 2.59-6.58 µg/ml for human melanoma SK-MEL-28 cell line. The IC_{50} values of mangosteen compounds are summarised in Table 1-12. The current results are consistent with a previous study in which α-mangostin exhibited antiproliferative effect in the T-lymphoblastic leukaemia CEM-SS cell line with IC_{50} of 5.5 µg/ml (Ee *et al.* 2008). Additionally, IC_{50} values of 6.8, 7.6, 6.1 µg/ml were reported after treatment of human leukaemia HL-60 cells with α-mangostin, β-mangostin, and γ-mangostin, respectively (Matsumoto *et al.* 2003). IC_{50} values of 9.1, >10, >10 µg/ml were reported after treatment of human colon cancer HT-29 cells with 9-hydroxycalabaxanthone, 8-deoxygartanine, and gartanine, respectively (Han *et al.* 2009). In addition, lower IC_{50} values were reported previously in other cancer cell lines. α-Mangostin showed IC_{50} of 3.1 µg/ml in human colon cancer DLD-1 cell line (Nakagawa *et al.* 2007) and 1.7 µg/ml in HT29 human colon cancer cell line (Han *et al.* 2009), and β-mangostin showed IC_{50} of 1.7 µg/ml in HT29 human colon cancer cell line(Han *et al.* 2009). IC_{50} values of some of

these xanthones were also reported against KB, BC-1 and NCI-H187 cancer cell lines as 2.08, 0.92, and 2.87 µg/ml of α-mangostin; 4.69, 1.6, and 2.55 µg/ml of γ-mangostin; ≥ 20, ≥ 20, and 16.88 µg/ml of 8-deoxygartanine; 2.5, 2.04, and 2.88 µg/ml of β-mangostin; 15.63, 15.54, and 1.08 µg/ml of gartanine (Suksamrarn *et al.* 2006). The IC_{50} values of different synthetic oxygenated xanthones were reported on a melanoma UACC-62 cell line, ranging from 14 to >200 µM (Pedro *et al.* 2002). Hence, it is apparent that different cancer cell lines exhibit different sensitivity to each specific xanthone compound. This study provides important information on the anti-skin cancer activity of xanthones that cannot be predicted from any existing studies.

3.4.3 Cytotoxicity against cancer cells induced by MPEE and xanthones

It is noteworthy that the MPEE and six natural xanthones tested in the current study displayed selective activity to different extents against cancer cells as evidenced by higher IC_{50} values on normal cells (Table 3-3). Our results indicate that some of the xanthones tested would have less toxicity on normal cells under the conditions tested. This is an important finding, because one reason why current anti-cancer drugs have side effects is due to their strong toxicity toward normal cells (Li *et al.* 2009). Chiang *et al.* (2004) have similarly reported that aqueous extract of mangosteen pericarp showed selectivity against leukaemia cells with IC_{50} values of 61.0 µg/ml for leukaemia K562 cells, 159.2 µg/ml for leukaemia Raji cells, and 4780.8 µg/ml for normal human lung fibroblast HEL299 cells. Another study demonstrated that α-mangostin showed no cytotoxicity on human epithelial fibroblast WI-38 cells at the concentration of 17.5 µM that killed 50% of human lung cancer A549 cells (Shih *et al.* 2010). In the future, the selectivity of xanthones against the non-tumorous counterpart of the cell lines (e.g. primary melanocyte and keratinocyte cells) need

further verification, and the underlying mechanisms of the selectivity need further investigation.

3.4.4 Competitive advantage over the tested commercial drugs

Two commercial drugs, 5-FU and DTIC, were used as positive controls in this study. The IC_{50} value of 5-FU was found to be 1.28 µg/ml for A-431 cells. The value is similar to that of a previous study that showed the IC_{50} value of this drug at 0.59 µg/ml for DLD-1 cells (Nakagawa *et al.* 2007). The IC_{50} value for DTIC treatment could not be obtained for SK-MEL-28 cell line due to having to go to such a high dose that there were potential solvent effects (DTIC was dissolved in 0.02 M acetic acid). The maximum concentration possible to use without significantly altering the cell culture medium pH was 100 µg/ml. At this concentration of DTIC, 25% cell killing was observed on SK-MEL-28 cell lines, which was consistent with a previous study (Lillehammer *et al.* 2007).

To compare the two commercial drugs for the skin cancer treatment with the xanthone compounds: the IC_{50} values of MPEE and six xanthone compounds to A-431 cell line were similar to that of 5-FU (1.28 µg/ml) but they were much lower than that of DTIC (IC_{25} 100 µg/ml) for SK-MEL-28 cell line (Table 3-3). This is an important finding because melanoma is the most aggressive skin cancer and shows high frequency of chemoresistance (Autier 2004; Mohapatra *et al.* 2007). Therefore, these results indicate that xanthones could be more potent than DTIC for the treatment of melanoma, and could offer a real promise for new treatment of resistant melanoma. Additionally, as evidenced by the IC_{50} values summarised in Table 3-3, and in contrast to the xanthones, the toxicity of 5-FU and DTIC on human normal skin cells was equal to, or greater than, that to skin cancer cells. These results clearly

demonstrate that xanthones could be excellent candidates for skin cancer chemotherapy.

3.4.5 Potential synergistic effect among individual xanthones

The concentration of xanthone compounds in the MPEE was determined to be approximately 440 mg/g extract in total (Appendix A2.2). It was found to contain α-mangostin, β-mangostin, γ-mangostin, 8-deoxygartanine, gartanine, and 9-hydroxycalabaxanthone (321, 3.9, 81.3, 10.7, 18.7, 4.8 mg/g extract, respectively) (Shan & Zhang 2010). The IC_{50} value of MPEE for SK-MEL-28 was 6.84 µg/ml (Table 3-3). MPEE of 6.84 µg contains 3.00 µg of a total of the six xanthones. Therefore, MPEE at 6.84 µg/ml can be considered equivalent to 3.00 µg/ml of mixture of six xanthones. The IC_{50} values of these compounds individually for SK-MEL-28 cells were 5.92, 6.22, 3.55, 3.83, 2.59, and 6.58 µg/ml, respectively (Table 3-3). These IC_{50} values are higher than that calculated for the mixture of six xanthones (3.00 µg/ml), except for gartanine. These results indicate that there might be synergistic effects when individual xanthone compounds are used together in a mixture. Similar results were obtained in A-431 cell line. The potential synergistic effects were thus investigated and discussed in Chapter 5.

3.4.6 Structure-related cytotoxicity

The anticancer potency of xanthones may correlate with the ring substituent and their position (Na 2009; Suksamrarn *et al.* 2006). In the study conducted by Suksamrarn *et al.* (2006), the anti-cancer activity was compared among 19 prenylated xanthones including α-mangostin, β-mangostin, γ-mangostin, 8-deoxygartanine and gartanine. Among these, α-mangostin exhibited the most potent effects against the oral (KB) and breast cancer (BC-1) cell lines. They also reported that the activity was enhanced when xanthones contained tetraoxygen functions with two C_5 units in rings A and C

(as in α-mangostin, β-mangostin, and γ-mangostin) and hydroxyl group at C-1 in the xanthone nucleus (as in the α-mangostin and γ-mangostin). However, activity was reduced with the increase in the number of hydroxyl groups in the C_5 side chain (as in 8-deoxygartanin) (Suksamrarn *et al.* 2006). The current results were partially consistent with this correlation. α-Mangostin and γ-mangostin showed the most potent effects against A-431 but not SK-MEK-28. Additionally, in our study, 8-deoxygartanin treatment displayed similar toxicity as γ-mangostin and higher toxicity than α-mangostin in SK-MEL-28 cells. This indicates that the anti-skin cancer potency of xanthones can be affected by the compound structures and also the type of cell line screened.

3.5 Summary

MPEE and six pure xanthone compounds demonstrated significant cytotoxicity on human squamous cell carcinoma A-431 and melanoma SK-MEL-28 cell lines. These xanthones (especially MPEE, γ-mangostin, and gartanine) showed significant toxicity against cancer cells, with less toxicity on normal cells. Importantly, the cytotoxicity of xanthones was found to be competitive with two commercial drugs. Furthermore, the results of this study suggest that the anti-cancer activity of xanthones was linked with their structures and the type of cancer cell line screened.

CHAPTER 4
UNDERLYING MECHANISMS OF CYTOTOXIC EFFECTS OF CRUDE EXTRACT AND PURE XANTHONE COMPOUNDS

4.1 Introduction

One of the main aims of this thesis was to identify the modes of action of cell killing activity induced by xanthones on skin cancer cells. As discussed in Chapter 1, xanthone compounds can induce cytotoxicity on some cancer cell types via cell cycle arrest and apoptosis induction (Ho *et al.* 2002; Matsumoto *et al.* 2003; Moongkarndi *et al.* 2004; Nakagawa *et al.* 2007; Suksamrarn *et al.* 2006). However, the precise effect and underlying cellular and molecular mechanisms of xanthones on skin cancer cells were not known.

In Chapter 3, MPEE and six pure xanthone compounds were demonstrated to have significant cytotoxicity on human squamous cell carcinoma A-431 and melanoma SK-MEL-28 cell lines. The purpose of the work for this next chapter is therefore to investigate the further underlying mechanisms at the cellular and molecular level of the cytotoxicity in the following three areas (summarised in Figure 4-1):

1) Inhibition of cell proliferation. The potential anti-proliferative effect of xanthones was investigated by cell cycle analysis using PI staining as detected by flow cytometry, and the modulatory effect of xanthones on the genes involved in cell cycle modulation ($p21^{WAF1}$ and cyclin D1) was investigated by quantitative real-time reverse transcription (qRT-PCR).

2) Induction of apoptosis. The apoptotic effect of xanthones was investigated using PI and Annexin V-FTIC staining as detected by flow cytometry. The underlying mechanism of apoptosis induced by xanthones was investigated using caspase 3/7, 8 and 9 assays and mitochondrial membrane potential assay. The modulatory effect of xanthones on apoptosis-related genes (Bcl-2, Bax, and cytochrome c) was investigated by qRT-PCR.

3) Inhibition of survival pathways. The modulatory effect of xanthones on the genes involved in the three survival pathways (Akt, NFκB and IκB) was investigated by qRT-PCR. BRAF V600E, a mutation presented in most melanoma cells, was also investigated.
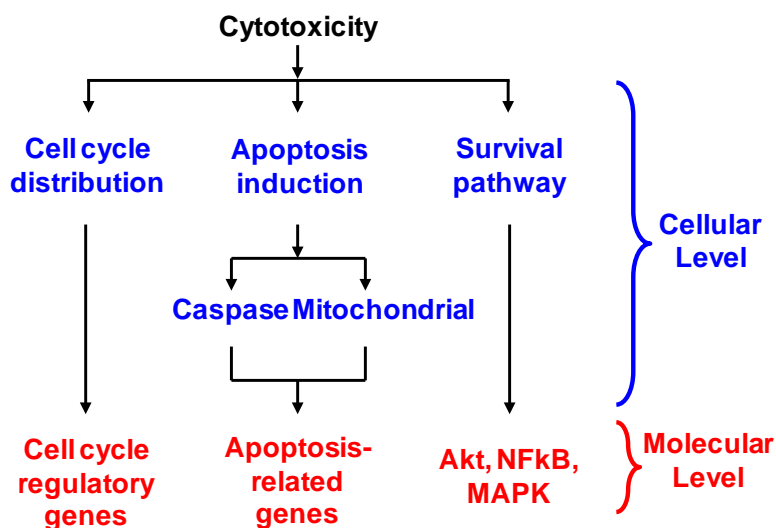
Figure 4-1
Schematic overview of the experimental design in this chapter.

4.2 Materials and methods

4.2.1 Materials

All the reagents and chemicals used in this chapter were of analytical grade from Merck or tissue culture tested grade from Sigma-Aldrich unless otherwise noted.

4.2.2 Cell lines and cell culture

Human squamous cell carcinoma A-431 and melanoma SK-MEL-28 cell lines were used as *in vitro* models in this Chapter. For description of the cell lines and cell culture refer to Section 3.2.2.

4.2.3 Cell cycle analysis

Cell cycle distribution was evaluated by flow cytometry using PI staining as described by Nicoletti *et al.* (1991) with minor modifications. A-431 and SK-MEL-28 cells were treated with varying concentrations of compounds in complete culture

medium for 48 h. After treatment, the cells were washed, harvested, fixed in 70% (v/v) cold ethanol at -20°C overnight, and then processed for cell cycle analysis. Briefly, the cells were suspended with 1ml of PI mixture (20 µg/ml of PI and 200 µg/ml of RNase in 0.1% (v/v) Triton X-100 in PBS) and incubated at RT in the dark for 30 min. The samples were then analysed by Fluorescence Activated Cell Sorting (FACScan) flow cytometry (Becton & Dickson, San Jose, CA) for the relative DNA content in each cell cycle phase according to an increased red fluorescence. Fluorescence emitted from PI-DNA complexes was quantified after argon laser excitation of the fluorescent dye at 488 nm and emission at 610 nm (red). Data acquisition and analysis were performed using Cell Quest software. A total of 20,000 cells was analysed for each treatment.

For each sample, the forward versus right side scatter (FSC and SSC) dot-plot was used to eliminate debris, small particles and aggregates in conditional acquisitions, while G_1 doublets were excluded from analysis using the area versus width fluorescence dot-plot. Cell cycle phase distribution, percentage of stained nuclei was analysed by gating the cells count histogram (cell counts versus intensity of PI stain) with markers. The width of the gates was dependent on the mean fluorescence intensity of the G_0/G_1 and G_2/M population. The mean fluorescence intensity of the G_2/M population was twice as much of the population in G_0/G_1 phase. Finally, extend of DNA fragmentation was determined by measuring the percentage of gated of the cells below the G_0/G_1 peak as indicated as sub-G_1 peak. One example of histogram is shown in Figure A-7 in Appendix A7.

4.2.4 Apoptosis analysis

Apoptotic cells were measured using an Annexin V-FITC Apoptosis Detection kit

(BD Biosciences, USA) according to the manufacturer's protocol. Briefly, treated cells were washed in cold 1% (w/v) sodium azide in PBS and then the cell pellets were resuspended in binding buffer at 10^6 cells/ml. A sample (100 µl) of the solution was transferred to a culture tube and double-stained with 5 µl of annexin V-FITC and 5 µl of PI for 15 min at RT in the dark. 400 µl of $1 \times$ binding buffer was added to the mixture before analysis using FACScan flow cytometry equipped with CellQuest software. A total of 20,000 cells was analysed for each sample.

The viable cells are negative in both Annexin V-FITC and PI; the early apoptotic cells are Annexin V-FITC positive and PI negative; and the late apoptotic or necrotic cells are both Annexin V-FITC and PI positive (Koopman *et al.* 1994; Vermes *et al.* 1995) (Shown in Appendix A8.2 is an example of dot plot for apoptosis analysis).

4.2.5 Caspase 3/7, 8 and 9 assays

Caspase activity was measured in microplates using Caspase-Glo® 3/7, 8 and 9 assay kit (Promega Corporation, Melbourne, Australia). The principle of the assays is shown in Figure A-10 in Appendix A9. For the assays, SK-MEL-28 and A-431 cells (1×10^4 cells/well) were seeded in a luminometer plate and incubated for 24 h at 37ºC. Cells were then treated with different concentrations of individual compounds for 48 h. To each well, 50 µl of caspase 3/7, 8 or 9 reagents were added and the luminescence was recorded every 15 min for 1 h at 28 °C in a microplate reader (Synergy 4, Bioteck, Millennium Science). Prior to the caspase assay, the cell number in the each well after treatment was measured by the Cell Titer Blue assay (Promega Corporation, Australia) to normalise the result. Briefly, 10 µl of the Cell Titer Blue staining was added to each well and incubated for 1 h at 37 ºC. The fluorescence was recorded at 560(excitation) / 590(emission) in a microplate reader.

The results of caspase activity were presented as relative luminescence unit (RLU)/cell/min.

4.2.6 Mitochondrial membrane potential ($\triangle \Psi$m) detection

Change in $\triangle \Psi$m was quantitatively determined by staining the cells with the cationic dye, JC-1, following the manufacturer's instructions (Sigma, St Louis, USA). Briefly, after 48 h treatment, cells were washed with PBS and incubated with medium containing 2.5 µg/ml of JC-1 staining reagent at 37ºC for 20 min followed by a wash with ice-cold 1×JC-1 staining buffer. The stained cells were analysed by FACScan flow cytometry equipped with CellQuest software. A total of 20,000 cells was analysed for each treatment (Shown in Appendix A10 is an example of dot plot for mitochondrial membrane potential analysis).

4.2.7 General methods for quantitative Real-time reverse transcription PCR (qRT-PCR)

4.2.7.1 Primer preparation for qRT-PCR

qRT-PCR primers are required to conform to the rules of generic primer design , including random distribution of bases within the primer, 50-60% G/C content, balanced melting temperatures (Tm) for the primer pair, and non-complementary bases at 3′ end of primers (Kohler 1995). Details of each primer set used in the project are shown in Table 4-1. β-Actin primer sequences were provided by Dr. George Mayne (Department of Surgery, Flinders University, Adelaide, Australia). The other primers used in this study were based on those in the literature (Hahnvajanawong *et al.* 2010; Jarry *et al.* 2004; Jenkins *et al.* 2004; Kim *et al.* 2006; Li *et al.* 2010; Prasad *et al.* 2009; Shan *et al.* 2005). They were selected according to the guidelines above and to amplify products 100-200 base pairs in length. Potential primer pairs were evaluated using the Oligo Analyzer tool (http://www.idtdna.com/analyzer/Applications/OligoAnalyzer/) and Primer

Designing tool (http://www.ncbi.nlm.nih.gov/tools/primer-blast/), and selected based on low self-and cross-complementary potential, balanced Tm, and the software ranking.

All primers were manufactured by Geneworks (Adelaide, Australia), suspended in sterile Nuclease-free water at 100 µM, and stored at –80ºC until required.

Table 4-1

List of primers used in qRT-PCR gene expression studies.

Name	Primer sequence (5′-3′)	Accession Number	Product size (bps)
Bax	F:AACCATCATGGGCTGGA	L22473.1	133
	R:CGCCACAAAGATGGTCA		
Bcl-2	F:TGGATGACTGAGTACCTGA	M14745.1	139
	R:TGAGCAGAGTCTTCAGAGA		
Cytochrome C	F: CCAGTGCCACACCGTTGAA	NM018947.5	136
	R:TCCCCAGATGATGCCTTTGTT		
Cyclin D1	F: CGTGGCCTCTAAGATGAAGG	NM053056.2	215
	R: TGCGGATGATCTGTTTGTTC		
P21^{WAF1}	F:GACACCACTGGAGGGTGACT	NM001220778.1	172
	R: CAGGTCCACATGGTCTTCCT		
Akt1	F: TCTATGGCGCTGAGATTGTG	NM005163.2	113
	R: CTTAATGTGCCCGTCCTTGT		
NFκB	F: CCACAAGACAGAAGCTGAAG	NM001165412.1	149
	R: AGATACTATCTGTAAGTGAACC		
IκBα	F: ACACTAGAAAACCTTCAGATGC	NM020529.2	110
	R: ACACAGTCATCATAGGGCAG		
MMP-2	F: AGTCTGAAGAGCGTGAAG	NM004530.4	192
	R: CCAGGTAGGAGTGAGAATG		
MMP-9	F: TGACAGCGACAAGAAGTG	NM004994.2	143
	R: CAGTGAAGCGGTACATAGG		
BRAF V600E	F: AGGTGATTTTGGTCTAGCTACAGA	HM459603.1	149
	R: TAGTAACTCAGCAGCATCTCAGGGC		
β-actin	F: TTGCCGACAGGATGCAGAAG	NM001101.3	101
(House-keeping gene)	R: GCCGATCCACACGGAGTACT		

4.2.7.2 Total RNA extraction

Total cellular RNA was isolated using TRIzol® (Invitrogen Life Technologies, New York, USA) according to the manufacturer's instructions. Briefly, RNA was isolated using TRIzol solution from untreated and treated cells in a T25 cm^2 flask. The treatment media was aspirated. TRIzol (2.5 ml) was dispensed onto the monolayer and cells were homogenised in the solution by repeat pipetting. The cell mix was transferred to a microfuge tube. The aqueous and organic phases were separated, after the addition of chloroform (200 µl / ml TRIzol) and centrifugation (12,000 × g for 15 min). RNA remained exclusively in the upper aqueous phase and was purified with subsequent precipitation and washing in isopropylalcohol (500 µl / ml TRIzol) and 75% ethanol (1 ml / ml TRIzol). Total RNA was air dried to a pellet in a microfuge tube (Sartedt, Numbrecht, Germany). The pellet was dissolved in 100 µl nuclease free water and the solution was incubated for 10 min at 55 to 60 ºC using a heating block. The RNA sample was immediately stored at –80 ºC until required.

4.2.7.3 Quantification of RNA concentration

One µl of RNA sample was diluted 1/80 in TE buffer (10 mM Tris-Cl, 1 mM EDTA, pH 7.4) for quantification of total RNA with Genequant Pro (Amersham Biosciences, Uppsala, Sweden). The quantification was carried out in triplicate per sample. The quality of RNA was indicated by the ratio of 260/230 and 260/280. These two ratios should be above 1.8 indicating good quality of RNA.

4.2.7.4 Verification of RNA integrity

The integrity of each RNA sample or the presence of genomic DNA contamination was determined using 1.2% formaldehyde–agarose gel electrophoresis. Each sample (500 ng of RNA) was diluted in 6 × RNA loading dye. The mixture was incubated at 65 ºC for 2 min using a heating block and then cooled on ice for 10 min. The sample

was then loaded in a gel and resolved for 40 min at 100 volts in $0.5 \times$ TBE buffer (45 mM Tris-Cl, 45 mM boric acid, 1 mM EDTA, pH 8.0), containing 0.01% (v/v) gel red staining. The gel was visualised and recorded using a LAS-4000 imager (FujiFilm Global, Tokyo, Japan). Quality of the preparation was determined by visualisation of distinct 28S and 18S rRNA species. An example of a gel is shown in Appendix A11.1.

4.2.7.5 Removal of DNA contamination

The DNA contamination from each RNA preparation was removed by using Ambion TURBO DNA-free DNase treatment reagent (Applied Biosystems, Australia) according to the manufacturer's instructions. Briefly, 10 µg RNA, 5 µl $10 \times$ TURBO DNase buffer and 1 µl TURBO DNase in a total 50 µl reaction were incubated at 37 ºC for 30 min. DNase Inactivation Reagent of 5 µl was added, mixed and incubated at RT for 5 min, followed by centrifugation ($12,000 \times$ g for 1.5 min) to remove the inactivation complex.

After removal of DNA contamination, the RNA was quantified in triplicate using a Genequant Pro (Section 4.2.7.3).

4.2.7.6 Reverse transcription of total RNA to cDNA

Reverse transcription was carried out using a High Capacity cDNA Reverse Transcription kit (Applied Biosystems, Australia) following the manufacturer's instructions. Briefly, one µg of total RNA was mixed with the reverse transcription reagents in a reaction volume of 20 µl as shown in Table 4-2. The solution was mixed and centrifuged briefly at low speed to collect residual liquid from tube walls. The reaction was carried out by running the program as described in Table 4-3 using a thermal cycler (Axygen MaxyGene, Australia). The cDNA template was diluted 4×

in nuclease-free water for use in all reactions.

Table 4-2

Preparation of reverse transcription.

Component	Volume/Reaction	Final concentration
Master Mix		
10× RT buffer	2 µl	1×
25× dNTP Mix (100 mM)	0.8 µl	4 mM
Random Primers	2 µl	
Multiscribe Reverse Transcriptase	1 µl	
RNase Inhibitor (10 U/µl)	1 µl	10 U (per 20 µl reaction)
Template RNA	Variable	1 µg (per 20 µl reaction)
RNase free water	Variable to give final volume 20 µl	
Total volume: 20 µl		

Table 4-3

The program for the reverse transcription reaction, carried out in a thermal cycler.

Conditions	Step 1	Step 2	Step 3	Step 4
Temperature (ºC)	25	37	85	4
Time (min)	10	120	5	∞

4.2.7.7 Validation of qRT-PCR

Efficacy of DNase treatment

Total RNA and DNase-treated RNA were run on a 1.2% (w/v) agarose gel. After DNase treatment, disappearance of the genomic DNA band was observed (Appendix A11.1). The results were confirmed by running qRT-PCR. Selected total RNA samples and their accompanying DNase-treated portions were subjected to qRT-PCR with primers for β-actin. Reactions were carried out as in the Section 4.2.7.8, and the PCR products were analysed on a 1% agarose TBE gel (Appendix A11.2).

qRT-PCR using different SYBR-green master mixes

In order to select an efficient SYBR-green master mix with lower cost, three commercial SYBR-green master mixes were compared by running the standard

curves using the primers for housekeeping gene of β-actin. Triplicate reactions with a final volume of 20 µl consisted of different SYBR-green master mix, forward and reverse primers, and 2 µl of cDNA. Amplification was carried out on a Rotorgene 3000 Thermocycler (Corbett Life Science, Sydney, NSW, Australia) by the following protocol: 95ºC for 2 min, 40 cycles (95 ºC for 5 sec, 60 ºC for 30 sec). Following amplification, products were gradually melted from 55 ºC to 99 ºC over 5 min for detection of primer-dimer or other incorrect amplification products. Data were acquired on the FAM channel with gain set at 5.

Similar results were obtained when using these three commercial master mixes, in terms of the linearship of the standard curve, the amplification efficiency, and the reproducibility of results (Table A-2 in Appendix A11.3). Due to the similar performance of these three master mixes, the one with lowest cost (GoTaq® qPCR Master Mix) was selected for the subsequent experiments.

Primer set amplification efficiency

Prior to use in qRT-PCR, primers were initially qualified for their amplification efficiency (AE). A-431 and SK-MEL-28 cDNAs were pooled and serially diluted (1:10) (v/v) including a water control. Reactions were carried out in triplicate on three separate occasions with 10 µl 2 × GoTaq® qPCR Master Mix and 10 µl of primers and cDNA sample on a Rotorgene 3000 Thermocycler and the following protocol: 95ºC for 2 min, 40 cycles (95ºC for 5 s, 60 ºC for 30 s) . Data were analysed using an Excel macro working sheet designed by George Mayne (Department of Surgery, Flinders University, Adelaide, Australia). The standard curve was derived by creating a graph which had an X-axis representing template

dilution (arbitrary unit) in a log scale and a Y-axis representing cycle threshold values. A linear regression value of R square (R^2) and slope were calculated from the standard curve. R^2 value was accepted if ≥ 0.98. One example of standard curve derived from qRT-PCR for β-actin is presented in Figure A-16 in Appendix A11.8, and one example of raw data for the standard curve is shown in Figure A-17 in Appendix 11.9. AE was calculated by the formula of EXP(-1/slope of standard curve). AE value of 2 indicates 100% efficiency. The results of AE for each gene are presented in Table A-3 in Appendix A11.4.

Optimisation of annealing temperature using Gradient PCR

According to the manufacturer's instruction for the SYBR master mix, an annealing temperature of 60 ºC can be adapted by most primer sets. Therefore, this temperature was used for the initial PCR reaction for each primer set. If the AE obtained was too low or too high, a gradient annealing temperature of 52-66 ºC was used in PCR reactions to determine the optimal primer annealing temperature using the thermal cycler. PCR product was visualized on 1% (w/v) agarose gel containing 0.01% (v/v) gel red staining using a LAS-4000 imager (FujiFilm Global, Tokyo, Japan). A 100-3000 bp molecular weight marker (Thermo Scientific, Australia) was used to determine amplicon sizes. By inspection of the gel, optimal annealing temperatures were chosen based on the most abundant amplicon without the formation of primer dimmers. The results are presented in Table A-3 in Appendix A11.4.

Optimisation of the ratio of forward and reverse primers

The following ratios of forward (nM) and reverse primers (nM) were tested to select the most efficient one: 50/50, 50/100, 50/150, 100/50, 100/100, 100/150, 150/50,

150/100, 150/150, 500/500. For each ratio, a negative template control using nuclease-free water was included for minimal primer dimer formation. Primer optimisation conditions were selected by an earliest threshold of cycle (Ct) and no primer dimer formation. The results are presented in Table A-3 in Appendix 11.4.

Verification of qRT-PCR amplicon

Agarose gel (1%; w/v) containing 0.01% (v/v) gel red staining was run to verify the PCR amplicon size and identify any primer dimer formation. The gel image of qRT-PCR amplicon is shown in Figure A-14 in Appendix A11.5. A single sharp band with specific size (refer to Table 4-1) was observed for each individual gene. Additionally, no primer dimer formation was found. No band was found when using nuclease water as template (data not shown). The specificity was confirmed by the single narrow peak as observed in the melting curve (Figure A-18 in Appendix A11.10).

Stability of housekeeping gene (β-actin) expression

β-Actin is a commonly used housekeeping gene for normalisation in qRT-PCR (Suzuki *et al.* 2000). Stability of β-actin gene expression was evaluated among samples under different treatments. Transcript levels (relative concentrations) were normalised against the untreated control. The values were compared across the different treated samples (Figure A-15 in Appendix A11.6). At each data point, the error bar represented variability in transcript levels that resulted from the treatment conditions, variation of RNA quantitation, RNA loading, and reverse transcription efficiency. Furthermore, the variability of the β-actin qRT-PCR assay alone (see Table A-4 in Appendix 11.7) also contributed to the variation seen in Figure A-15 in

Appendix 11.6.

The relative gene expression of β-actin was from 1 (untreated control) to 1.91 (treatment with gartanine) in SK-MEL-28 cells and from 0.81 (treatment with 8-deoxygartanine) to 1.47 (treatment with gartanine) in A-431 cells. The difference of relative gene expression across the untreated and treated samples was not statistically significant as analysed by One-way ANOVA. Additionally, 2-fold differences in gene expression between samples are generally not considered as significant (Ross *et al.* 2000).

The results suggested that the gene expression of β-actin was comparatively constant and was not significantly regulated by the different treatments, and therefore it was stable to be used as a housekeeping gene for normalisation.

Reproducibility of qRT-PCR

A pool sample of A-431 and SK-MEL-28 cDNAs was used to validate the qRT-PCR. Each gene was run in duplicate on three independent occasions. The intra- and inter-run CVs were calculated as described in Section 3.2.6.

CVs reported based on the raw Ct values could be misleading due to the low variations (Pfaffl *et al.* 2002). Therefore, to reflect the true quantitative capacity, the CVs in this study were derived from the relative concentrations as calculated using Q-gene software instead of the raw Ct values. The results for the intra- and inter-run CV% are shown in Table A-4 in Appendix A11.7.

4.2.7.8 qRT-PCR reactions

qRT-PCR was carried out in 20 µl of PCR mixture consisting of 10 µl of 2 × GoTaq® qPCR Master Mix (Promega Corporation, Australia) and 10 µl of primers and cDNA sample on a Rotorgene 3000 Thermocycler (Corbett Life Science, Sydney, NSW, Australia). Each sample was amplified in triplicate. The mRNA level of the β-actin housekeeping gene was also determined by qRT-PCR in each cDNA sample to provide data to normalise the expression of genes of interest (GOI). The primers used are listed in Table 4-1. The PCR condition for each particular amplicon was optimised (see Table A-3 in Appendix A11.4) to establish a linear relationship between Ct values and the input amount of cDNA (a correlation coefficient >95%) and to achieve PCR efficiency around 100% (± 10%). Cycling was followed by Melt Curve Analysis to confirm the specificity of the PCR product. The melt curve for each gene is presented in Appendix A11.10. Quantitative analysis was performed using Q-Gene software (Simon 2003). The expression of levels of GOI was normalised to the expression levels of β-actin, which exhibited comparable expression across different groups (Figure A-15 in Appendix A11.6). The ratio of GOI/ β-actin was compared among samples, and the fold change of GOI expression was obtained by setting the values from the untreated cells to one.

4.2.8 Statistical analysis

Data are presented as mean (±SEM). Each assay was repeated in at least three independent experiments. Statistical analysis of the data was carried out using ANOVA, followed by Tukey's HSD *post hoc* test (equal variances) or Dunnett's T3 *post hoc* test (unequal variances). These tests were performed using SPSS software (version 17.0). Differences were considered statistically significant when the *P*-value was less than 0.05 (significant) and 0.01 (highly significant).

4.3 Results

4.3.1 Effect of xanthones on cell cycle in human skin cancer cells

Treatment with xanthones induced increases in $subG_1$ peak in human squamous carcinoma A-431 cells, indicating apoptosis induction. Significant increases were found after treatment with MPEE, α-mangostin, 8-deoxygartanine and 9-hydroxycalabaxanthone (Figure 4-2 A; $P< 0.05$). Supplementary data are shown in Table 4-4.

Treatment with xanthones induced significant increases in cell cycle arrest in G_1 phase compared with untreated human melanoma SK-MEL-28 cells (Figure 4-2 B1; $P< 0.01$), except for α-mangostin and β-mangostin. Treatment with α-mangostin at 7.5 µg/ml did not induce cell cycle arrest in G_1 phase, but did significantly increase the sub G_1 peak (29%; $P < 0.01$) compared to the untreated control (2%) (Figure 4-2 B2). A significant increase in sub G_1 peak was also observed after treatment with γ-mangostin (Figure 4-2 B2; $P< 0.01$). Supplementary data are shown in Table 4-5.

A

% Cell Distribution in Sub G1 phase

Concentration (µg/ml)

■ Control   ■ γ-Mangostin

■ MPEE   ■ 8-Deoxygartanine

□ α-Mangostin   □ Gartanine

□ β-Mangostin   □ 9-Hydroxycalabaxanthone
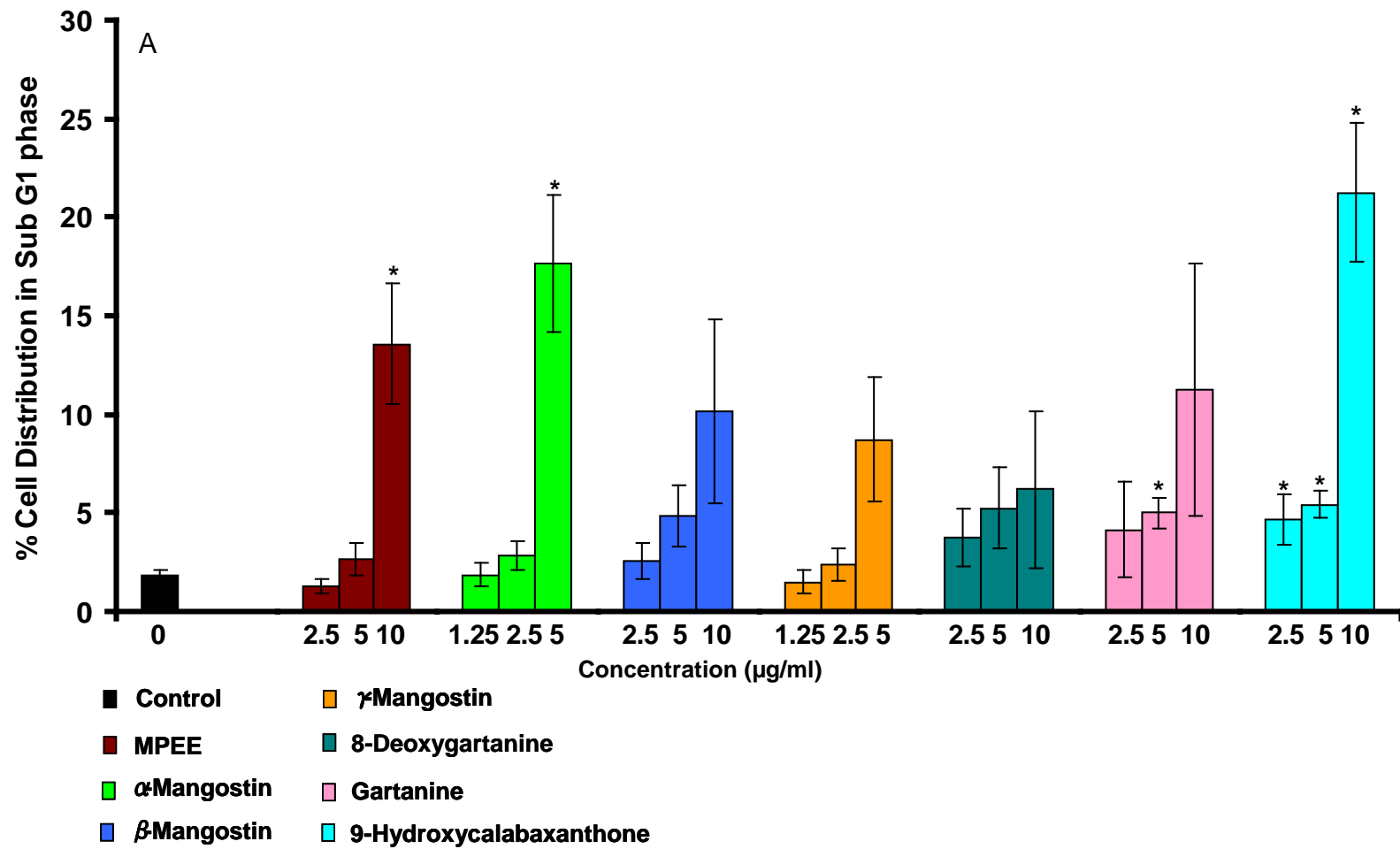
Figure 4-2

(Continued)
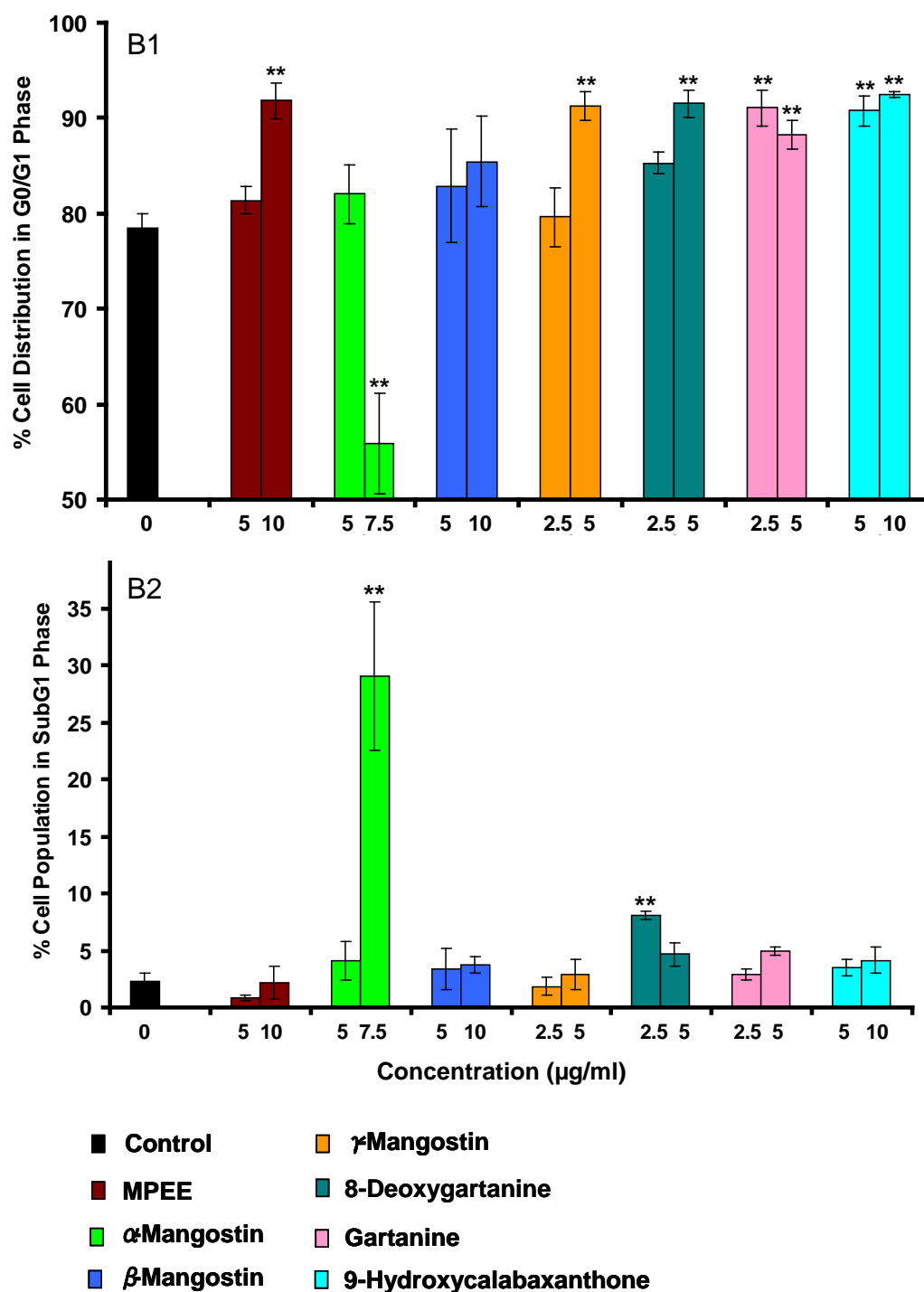
Figure 4-2

Effect of xanthones on cell cycle progression on A-431 (A) and SK-MEL-28(B1 and B2) was determined by PI staining and analysed for DNA content by flow cytometry. Data were obtained from 20,000 events and presented as the percentage of cells in the sub G_1, G_0/G_1, S and G_2/M phases. The values are shown as the mean ± SEM of 3 independent experiments. Treatments significantly different from the untreated control at $P < 0.05$ are presented as * and $P < 0.01$ as **.

Table 4-4
Cell cycle distribution in A-431 cell line after 48-h treatment with the tested xanthones. Data are shown as mean ± SEM of three independent experiments.

Extract / Compound	µg/ml	% Cell Distribution ± SEM			
		$SubG_1$	G_1/G_0	S	G_2/M
Control	0	1.8 ± 0.3	72.1 ± 0.8	12.8 ± 0.8	12.6 ± 0.5
MPEE	2.5	1.3 ± 0.4	75.6 ± 2.1	11.4 ± 1.1	12.5 ± 1.1
	5	2.7 ± 0.8	76.3 ± 0.9	11.5 ± 0.7	10.3 ± 0.6
	10	13.6 ± 3.0	68.1 ± 3.7	10.8 ± 2.1	9.2 ± 1.0
α-Mangostin	1.25	1.9 ± 0.6	73.2 ± 1.1	12.5 ± 0.5	13.5 ± 0.7
	2.5	2.8 ± 0.8	72.9 ± 1.1	13.2 ± 1.4	12.0 ± 0.7
	5	17.7 ± 3.4	66.9 ± 3.1	10.6 ± 1	6.3 ± 1.3
β-Mangostin	2.5	2.6 ± 0.9	78.8 ± 2.8	9.8 ± 0.8	9.2 ± 1.9
	5	4.8 ± 1.5	75.4 ± 2.1	11 ± 0.8	9.2 ± 1.4
	10	10.1 ± 4.7	76.7 ± 5.6	8.5 ± 1.8	5.6 ± 1.3
γ-Mangostin	1.25	1.5 ± 0.6	75.3 ± 1.5	11.4 ± 0.8	12.7 ± 0.7
	2.5	2.4 ± 0.8	80 ± 1.6	9.3 ± 0.7	9.1 ± 0.8
	5	8.7 ± 3.2	75.3 ± 3.7	9 ± 0.9	8 ± 1.1
8-Deoxygartanine	2.5	3.8 ± 1.5	77.1 ± 2.5	11.6 ± 3.4	7.8 ± 0.9
	5	5.2 ± 2	76.7 ± 1.4	11.5 ± 1.4	6.8 ± 0.6
	10	6.2 ± 4	74.1 ± 5.1	10.6 ± 2.4	9.7 ± 1.2
Gartanine	2.5	4.2 ± 2.5	77.6 ± 2.4	10.6 ± 1	8 ± 0.4
	5	5 ± 0.8	73.1 ± 3.7	9.6 ± 1.1	12.9 ± 2.6
	10	11.2 ± 6.4	64.5 ± 5.4	16.2 ± 3.6	11.2 ± 2.3
9-Hydroxycalabax anthone	2.5	4.7 ± 1.2	77.5 ± 1.1	8.8 ± 0.3	8.9 ± 0.4
	5	5.4 ± 0.7	76.6 ± 0.5	11.2 ± 0.6	7.3 ± 0.4
	10	21.2 ± 3.5	69.5 ± 2.9	6.2 ± 1	4.1 ± 0.8

Table 4-5

Cell cycle distribution in SK-MEL-28 cell line after 48-h treatment with the tested xanthones. Data are shown as mean ± SEM of three independent experiments.

Extract / Compound	µg/ml	% Cell Distribution ± SEM			
		$SubG_1$	G_1/G_0	S	G_2/M
Control	0	2.3 ± 0.7	78.5 ± 1.5	7.0 ± 0.6	12.3 ± 0.8
MPEE	5	0.8 ± 0.2	81.4 ± 1.4	6.3 ± 0.5	12.0 ± 1.2
	10	2.2 ± 1.5	91.8 ± 1.9	2.9 ± 0.5	3.6 ± 0.7
α-Mangostin	5	4.1 ± 1.7	82.0 ± 3.1	5.4 ± 0.8	8.8 ± 2.0
	7.5	29.0 ± 6.5	55.9 ± 5.2	8.3 ± 0.3	7.1 ± 2.0
β-Mangostin	5	3.4 ± 1.8	82.8 ± 5.9	5.4 ± 1.9	8.5 ± 2.8
	10	3.8 ± 0.7	85.5 ± 4.7	3.7 ± 0.7	7.0 ± 4.3
γ-Mangostin	2.5	1.8 ± 0.8	79.6 ± 3.1	8.7 ± 1.9	10.6 ± 3.2
	5	2.9 ± 1.3	91.3 ± 1.5	3.3 ± 0.7	2.8 ± 0.8
8-Deoxygartanine	2.5	8.0 ± 0.4	85.3 ± 1.1	2.8 ± 0.8	3.6 ± 1.8
	5	4.7 ± 1.0	91.5 ± 1.5	2.2 ± 0.7	1.7 ± 1.1
Gartanine	2.5	2.9 ± 0.5	91.0 ± 1.9	3.4 ± 1.6	2.5 ± 0.9
	5	4.9 ± 0.4	88.2 ± 1.5	2.7 ± 0.7	3.8 ± 1.0
9-Hydroxycalaba-xanthone	5	3.5 ± 0.7	90.8 ± 1.6	1.5 ± 0.3	4.3 ± 0.8
	10	4.1 ± 1.1	92.4 ± 0.3	1.3 ± 0.2	2.2 ± 0.4

4.3.2 Effect of xanthones on apoptosis induction in human skin cancer cells

Treatment with all the tested xanthones induced significant increases in early apoptosis compared to untreated A-431 cells (Figure 4-3A) ($P < 0.01$), except for 8-deoxygartanine. The most significant increases were found after treatment with α-mangostin, β-mangostin, and 9-hydroxycalabaxanthone (40, 30, and 50% apoptotic population, respectively) compared with untreated control (2% apoptotic population).

Significant increases were also observed after treatment with xanthones in SK-MEL-28 cells (Figure 4-3B), except for γ-mangostin. The most significant increase was observed after treatment with α-mangostin, which induced approximately 30% early

apoptosis compared with 2% in untreated cells.

Late apoptosis and necrosis are not distinguishable using current method because cells at both stages are stained by PI and Annexin V-FITC. Significant increases in late apoptosis (or necrosis) were observed after treatment with MPEE, α-mangostin, β-mangostin, gartanine, and 9-hydroxycalabaxanthone in A-431 cell line, and treatment with α-mangostin in SK-MEL-28 cell line (see results in Figure A-8 in Appendix A8.1).
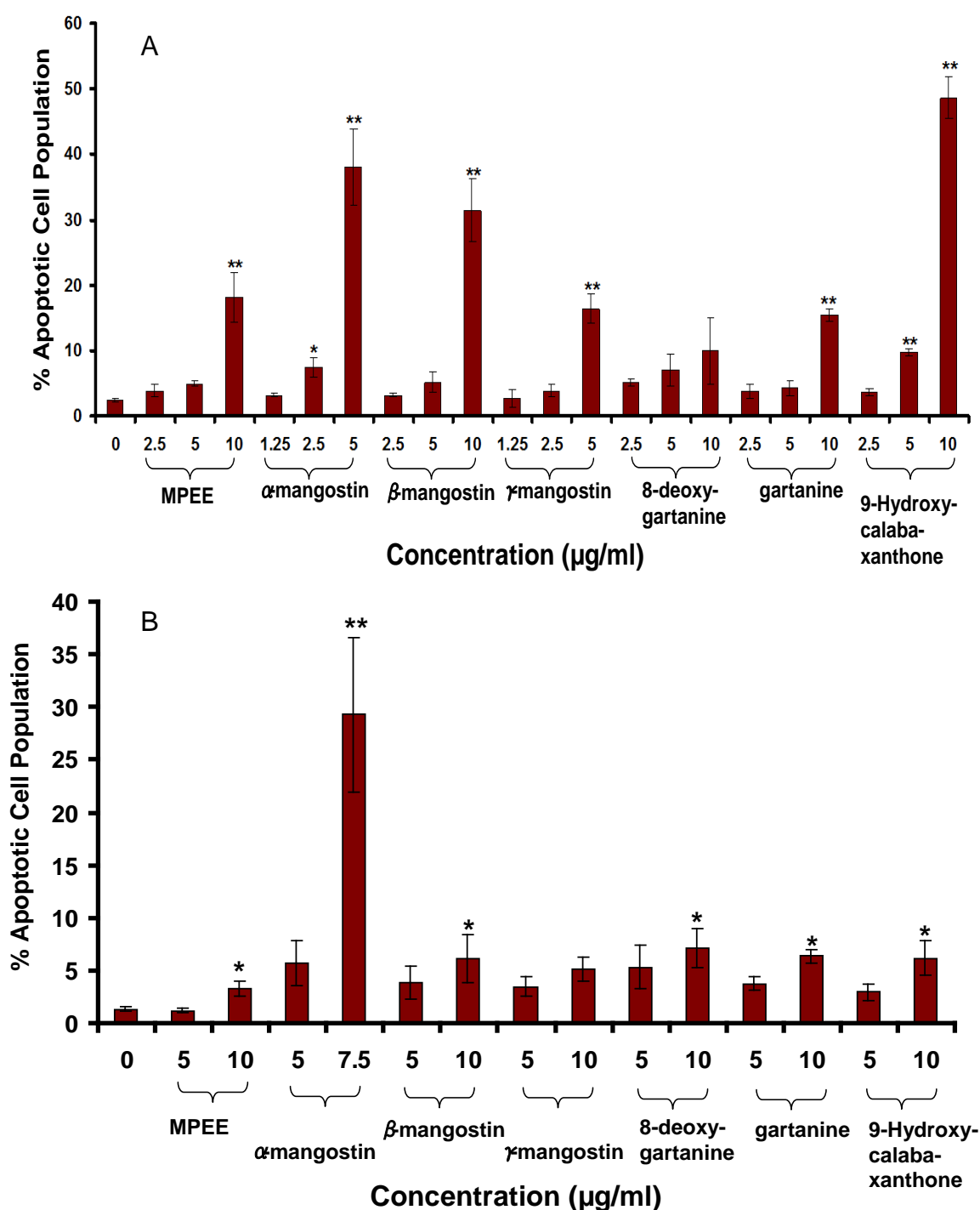
Figure 4-3

Apoptotic effect of xanthones on human squamous carcinoma A-431 (A) and human melanoma SK-MEK-28 cells (B) was determined by Annexin V-conjugated PI staining through flow cytometry. Data were obtained from 20,000 events and presented as the percentage of early apoptotic cells (Annexin positive and PI negative). The values are shown as the mean ± SEM of 3 independent experiments. Treatments significantly different from the untreated control at $P < 0.05$ are presented as * and $P < 0.01$ as **.

4.3.3 Effect of xanthones on caspase activities in human skin cancer cells

Caspase cascade activation plays a crucial role in apoptosis. To determine the involvement of caspases in xanthone-induced apoptosis, the activities of the executioner caspase 3/7 and initiator caspase 8 and 9 were examined.

4.3.3.1 Caspase 3/7 activities

Treatment of A-431 cells for 48 h with all the xanthones tested, except for 8-deoxygartanine, resulted in significant increases ($P < 0.01$ for gartanine and $P < 0.05$ for the others) in caspase 3 activity relative to untreated cells (Figure 4-4A). The most marked ones are MPEE (at 10 µg/ml) and α-mangostin (5 µg/ml), which induced an approximate 23- and 26-fold increase compared to untreated cells.

Treatment of SK-MEL-28 cells with α-mangostin at 7.5 µg/ml for 48 h resulted in an approximately 15-fold increase ($P < 0.05$) in caspase 3/7 activity relative to untreated cells (Figure 4-4B). Significant changes in caspase 3/7 activity were also observed after treatment with MPEE, 8-deoxygartanine, 9-hydroxycalabaxanthone, and gartanine ($P < 0.05$). Treatment with γ-mangostin (10 µg/ml) induced an approximately 5-fold increase, but this was not statistically significant ($P > 0.05$) due to the large error bar from the biological variation.

4.3.3.2 Caspase 8 activities

Treatment of A-431 cells with MPEE, α-mangostin, β-mangostin, γ-mangostin, and 9-hydroxycalabaxanthone for 48 h resulted in significant increase in caspase 8 activity relative to untreated cells (Figure 4-5A). The most marked one is α-mangostin (5 µg/ml) and 9-hydroxycalabaxanthone (10 µg/ml), which induced 8.3-fold and 6.6-fold increases, respectively, compared with untreated cells.

In SK-MEL-28 cells, significant increase in caspase 8 activity was only observed after 48 h treatment with α-mangostin. Treatment with α-mangostin at 5 µg/ml resulted in an approximate 1.6-fold increase ($P < 0.05$) and at 7.5 µg/ml resulted in an approximate 3-fold increase ($P < 0.01$) relative to untreated cells (Figure 4-5B).

4.3.3.3 Caspase 9 activities

Treatment of A-431 cells with MPEE, α-mangostin, 8-deoxygartanine, gartanine, and 9-hydroxycalabaxanthone for 48 h resulted in significant increase in caspase 9 activity relative to untreated cells (Figure 4-6A). The most marked one is α-mangostin (5 µg/ml), which induced a 13-fold increase compared with untreated cells. Treatment with γ-mangostin (5 µg/ml) induced an approximate 13-fold increase, but this was not statistically significant ($P > 0.05$) due to the large error bar from the biological variation.

In SK-MEL-28 cells, significant increase in caspase 9 was observed after 48 h treatment with α-mangostin only. Treatment with α-mangostin at 7.5 µg/ml resulted in an approximate 4-fold increase ($P < 0.05$) relative to untreated cells (Figure 4-6B).
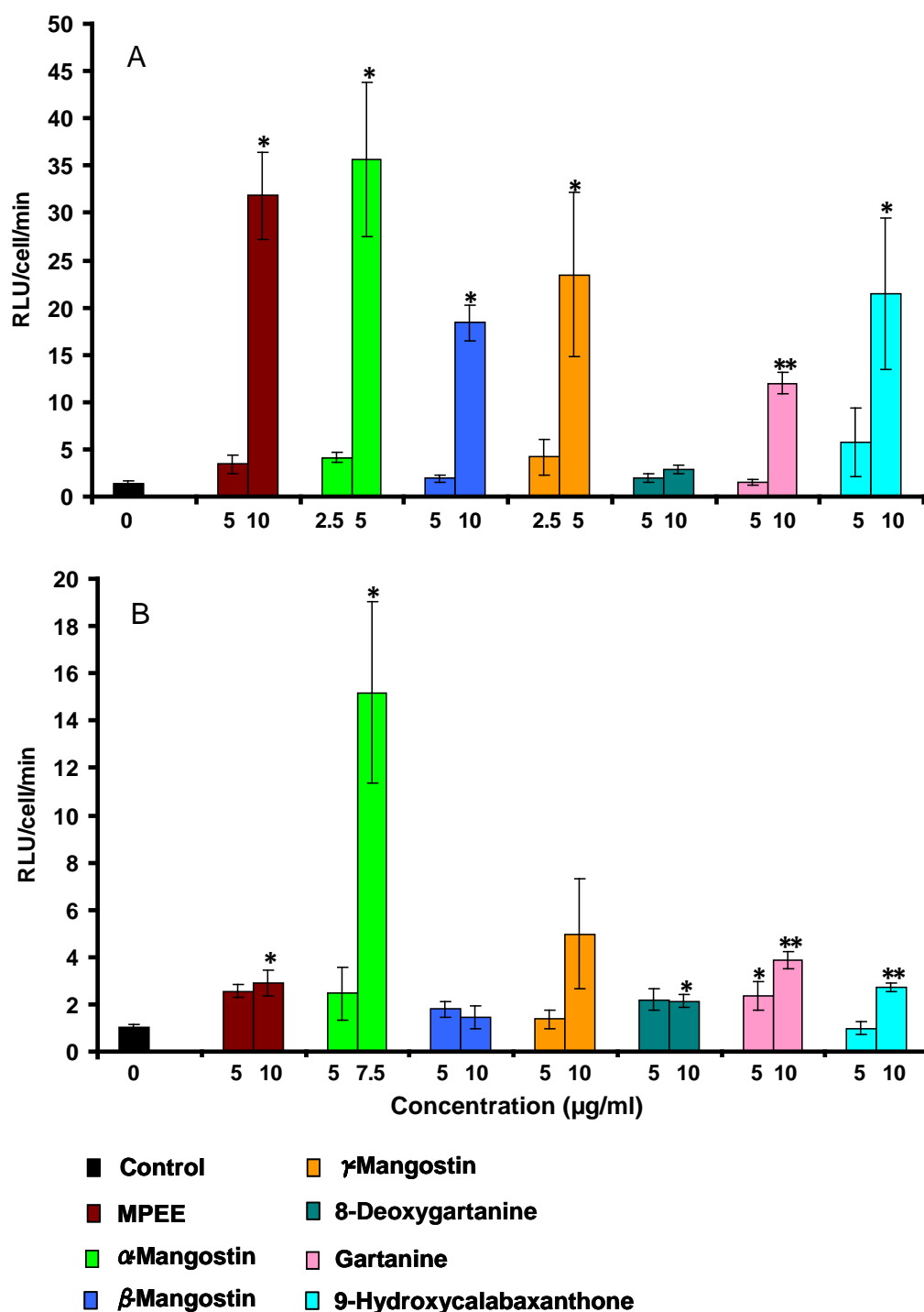
Figure 4-4

Caspase 3/7 was determined on (A) A-431and (B) SK-MEL-28 cells after 48 h treatment with xanthones using luminescent kits as described in the method (Section 4.2.5). The values are shown as the mean ± SEM of three independent experiments. Treatments significantly different from the untreated control at $P < 0.05$ are presented as * and at $P < 0.01$ as **.
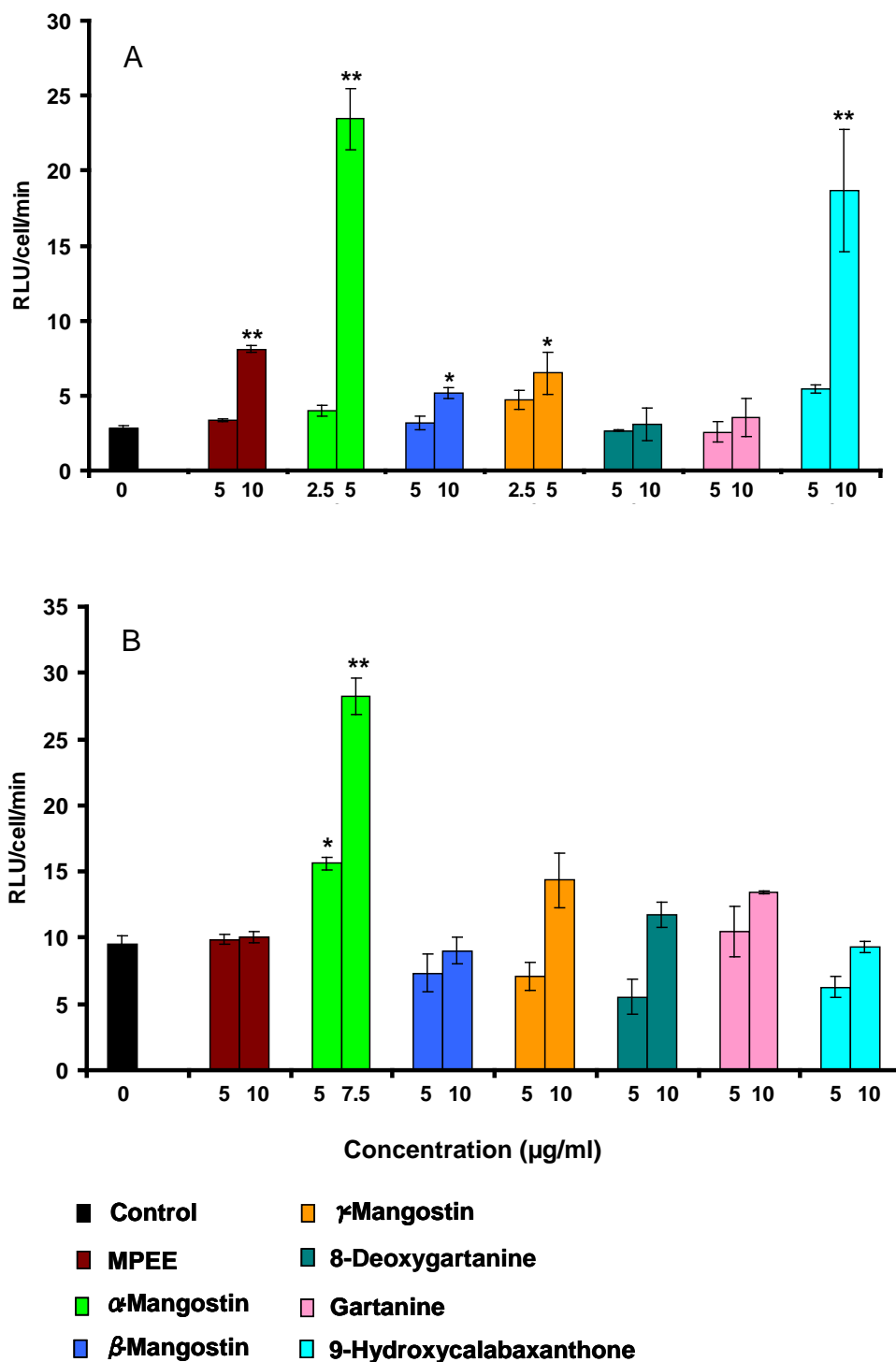
Figure 4-5

Caspase 8 activity was determined on (A) A-431and (B) SK-MEL-28 cells after 48 h treatment with xanthones using luminescent kits as described in the method (Section 4.2.5). The values are shown as the mean ± SEM of three independent experiments. Treatments significantly different from the untreated control at $P < 0.05$ are presented as * and at $P < 0.01$ as **.
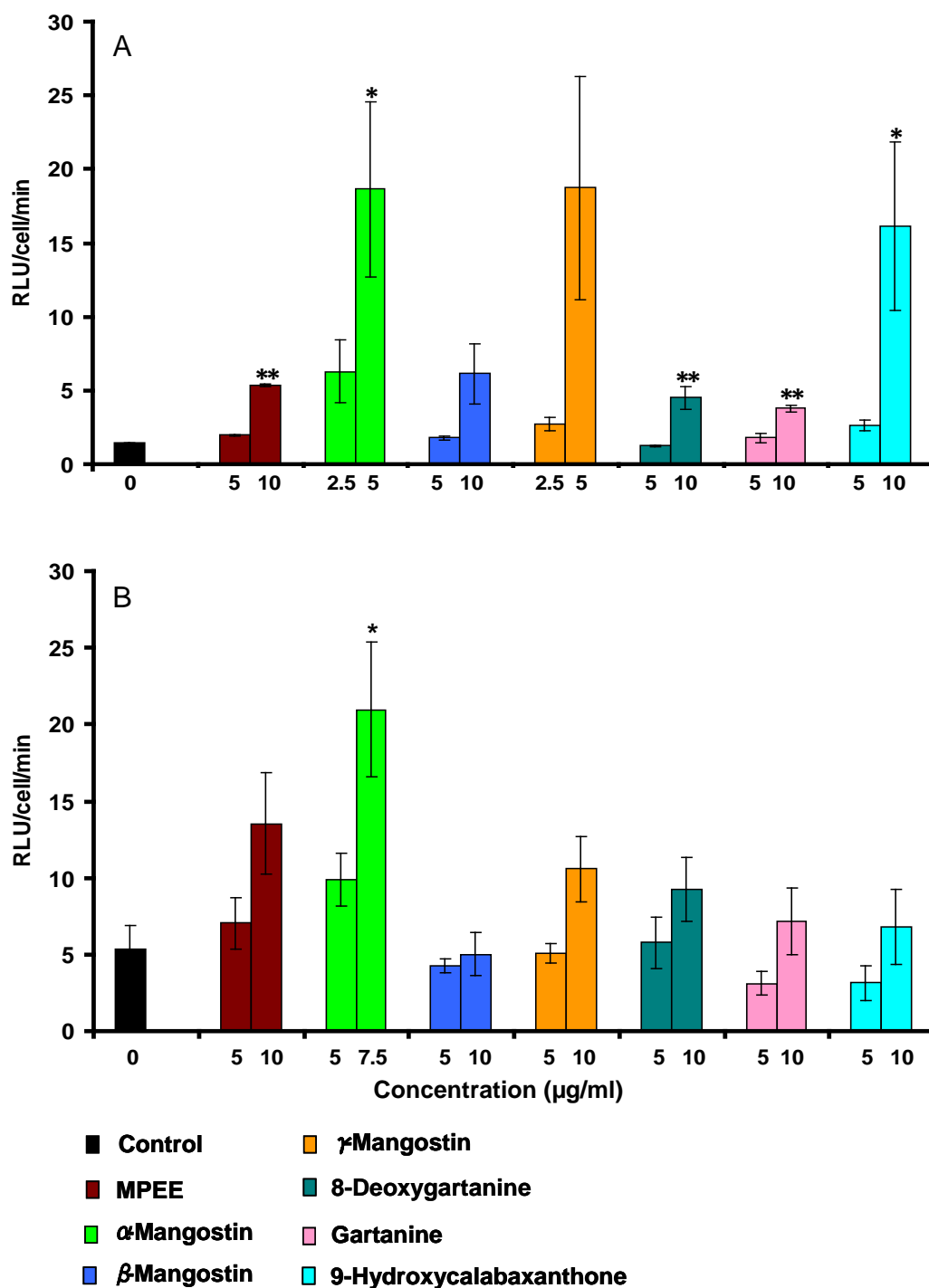
Figure 4-6

Caspase 9 activity was determined on (A) A-431and (B) SK-MEL-28 cells after 48 h treatment with xanthones using luminescent kits as described in the method (Section 4.2.5). The values are shown as the mean ± SEM of three independent experiments. Treatments significantly different from the untreated control at $P < 0.05$ are presented as * and at $P < 0.01$ as **.

4.3.4 Effect of xanthones on mitochondrial membrane potential ($\triangle\Psi$m) in human skin cancer cells

In A-431 cells, significant decreases in $\triangle\Psi$m were observed after treatment with MPEE, α-mangostin, γ-mangostin, and 9-hydroxycalabaxanthone (Figure 4-7A) as evidenced by the increased percentage of cells positive for JC-1 monomers. The most marked one is for α-mangostin, which increased the loss of mitochondrial membrane to 76.1% compared with untreated cells (8.2%). Treatment with β-mangostin (10 µg/ml) and γ-mangostin (5 µg/ml) induced the increase of loss of mitochondrial membrane to 49.8% and 62.5%, respectively, but this was not statistically significant ($P > 0.05$) due to the large error bar from the biological variation.

Similar results were found in SK-MEL-28 cells. Significant increases in the loss of $\triangle\Psi$m were found after treatment with MPEE, α-mangostin, β-mangostin, γ-mangostin, and 8-deoxygartanine (Figure 4-7B). The most marked one is for α-mangostin, which increased the loss of mitochondrial membrane to 80.3% compared with untreated cells (6.6%). Treatment with gartanine (10 µg/ml) induced the increase to 44.3%, but this was not statistically significant ($P > 0.05$) due to the large error bar from the biological variation.
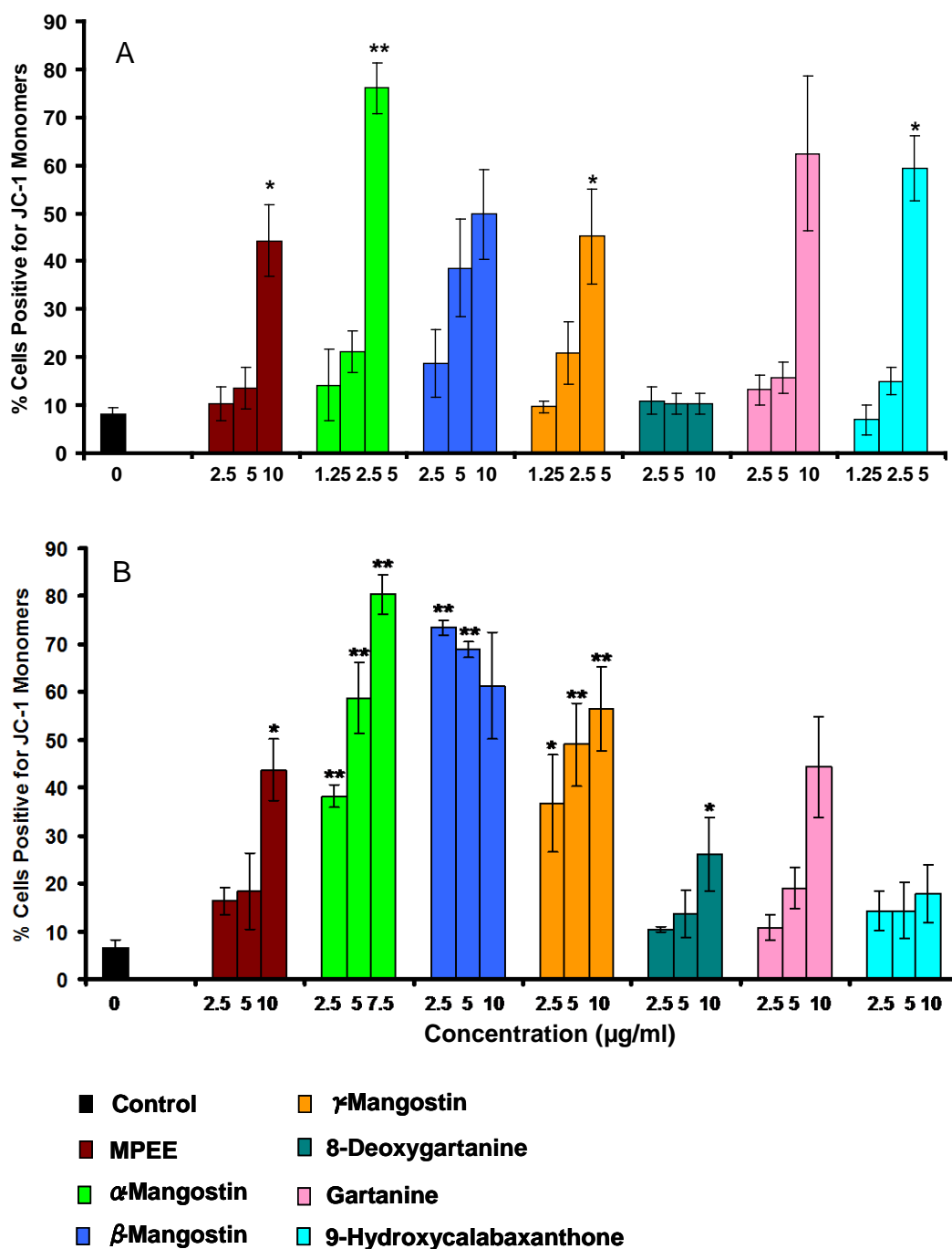
Figure 4-7

Loss of mitochondrial membrane potential was examined by JC-1 dye as detected by flow cytometry after 48 h treatment with xanthones on (A) A-431 and (B) SK-MEL-28 cell lines. Data were obtained from 20,000 events and presented as the percentage of cells positive for the JC-1 monomer. The values are shown as the mean $\pm$ SEM of 3 independent experiments. Treatments significantly different from the untreated control at $P < 0.05$ are presented as * and $P < 0.01$ as **.

4.3.5 Modulation of gene expressions involved in cytotoxicity induced by xanthones in human skin cancer cells

4.3.5.1 Modulation of cell cycle-related genes

As shown in Section 4.3.1, treatment with xanthones induced significant increases in cell cycle arrest in G_1 phase in SK-MEL-28 (Figure 4-2B). We next examined the effect of these xanthones on the modulation of the cell cycle-related gene expressions in SK-MEL-28.

Significant increases in mRNA level of p21^{WAF1} were observed after treatment with MPEE, α-mangostin, β-mangostin, 8-deoxygaratanine, and 9-hydroxycalabaxanthone (Figure 4-8A). The most marked one was 8-deoxygaratanine, which induced an 87.1-fold increase of the mRNA level of p21^{WAF1} compared with untreated control ($P < 0.01$). Treatment with γ-mangostin (10 µg/ml) and gartanine (10 µg/ml) induced 37.6- and 68.4-fold increases, respectively, but this was not statistically significant ($P > 0.05$).

Significant decreases in the mRNA level of cyclin D1 were observed after treatment with α-mangostin, β-mangostin, 8-deoxygaratanine, gartanine, and 9-hydroxycalabaxanthone, respectively (Figure 4-8B). The most marked ones were α-mangostin and gartanine. Both compounds caused a 10-fold decrease of the mRNA level of cyclin D1 compared with untreated control ($P < 0.01$).

In A-431 cells, treatment with xanthones increased subG$_1$ peak, indicating induction of apoptosis (Figure 4-2A). Therefore, the modulatory effect on cell-cycle related genes was not studied for this cell line; instead, apoptosis-related genes were investigated in the section 4.3.5.2.
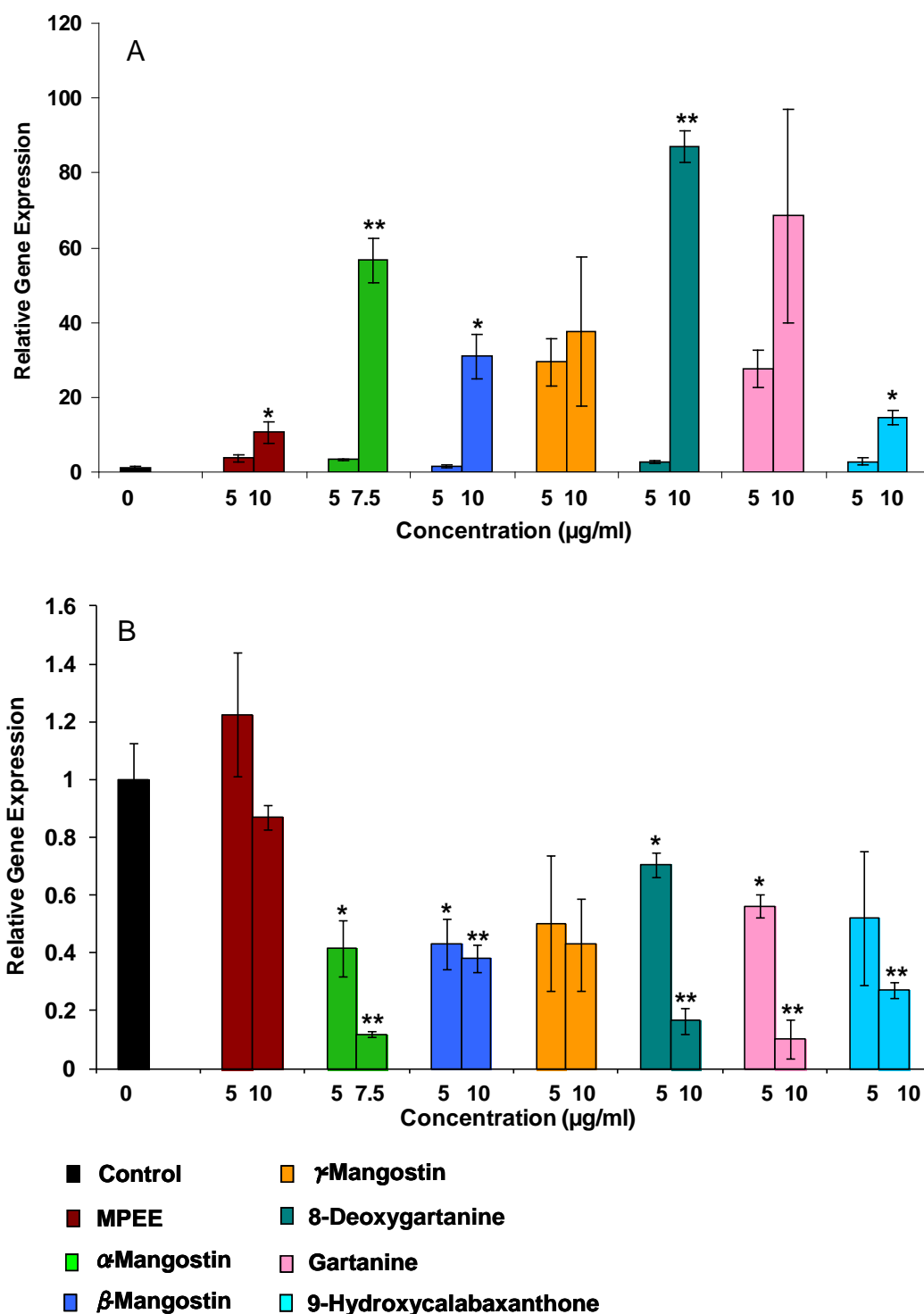
Figure 4-8
Effect of xanthones on the expression of (A) p21^{WAF1} and (B) cyclinD1 mRNA in SK-MEL-28 cell line was determined by qRT-PCR. The values shown are the mean ± SEM of three independent experiments. Treatments significantly different from the untreated control at $P < 0.05$ are presented as * and at $P < 0.01$ as **.

4.3.5.2 Modulation of apoptosis-related genes

In orderto understand the molecular mechanisms of apoptosis induced by xanthones, we firstly examined the effect of xanthones on the mRNA expression of cytochrome c, which is an important signalling event in the intrinsic apoptotic activation pathway. Significant increases in cytochrome c mRNA level were observed after 48 h treatment with MPEE, α-mangostin, gartanine, and 9-hydroxycalabaxanthone in A-431 cells (Figure 4-9A). The most marked one is MPEE, which induced a 12.5-fold increase of the cytochrome c mRNA level compared with untreated control ($P < 0.05$). In SK-MEL-28 cells, significant increases were also found after 48 h treatment with MPEE, α-mangostin, β-mangostin, and 9-hydroxycalabaxanthone (Figure 4-9B). Treatment with γ-mangostin (10 µg/ml) induced a 14.1-fold increase, but this was not statistically significant ($P > 0.05$).

We secondly examined the effect of xanthones on the Bax and Bcl-2 mRNA levels. Significant increases in the Bax/Bcl-2 ratio were observed after treatment with MPEE, α-mangostin, β-mangostin in A-431 cells (Figure 4-10). Compared with untreated control, although gartanine and 9-hydroxycalabaxanthone induced 15.3- and 13.2-fold increases, respectively, this effect was not statistically significant. In SK-MEL-28 cells, no significant alteration in the ratio of Bax/Bcl-2 was found after treatment with xanthones (data not shown).
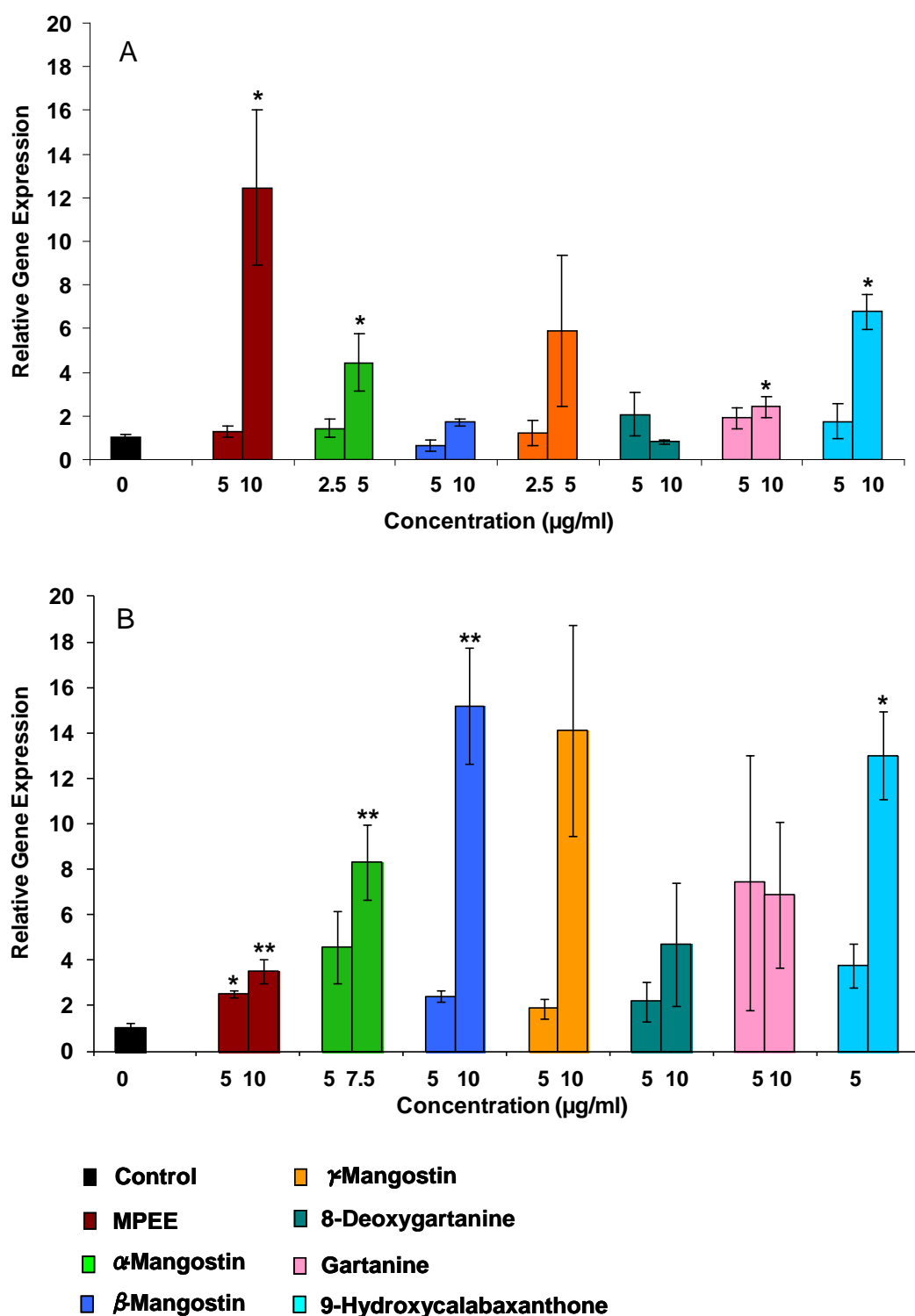
Figure 4-9
Effect of xanthones on the expression of cytochrome c mRNA in (A) A-431 and (B) SK-MEL-28 cell lines as determined by qRT-PCR. The values shown are the mean ± SEM of three independent experiments. Treatments significantly different from the untreated control at $P < 0.05$ are presented as * and at $P < 0.01$ as **.
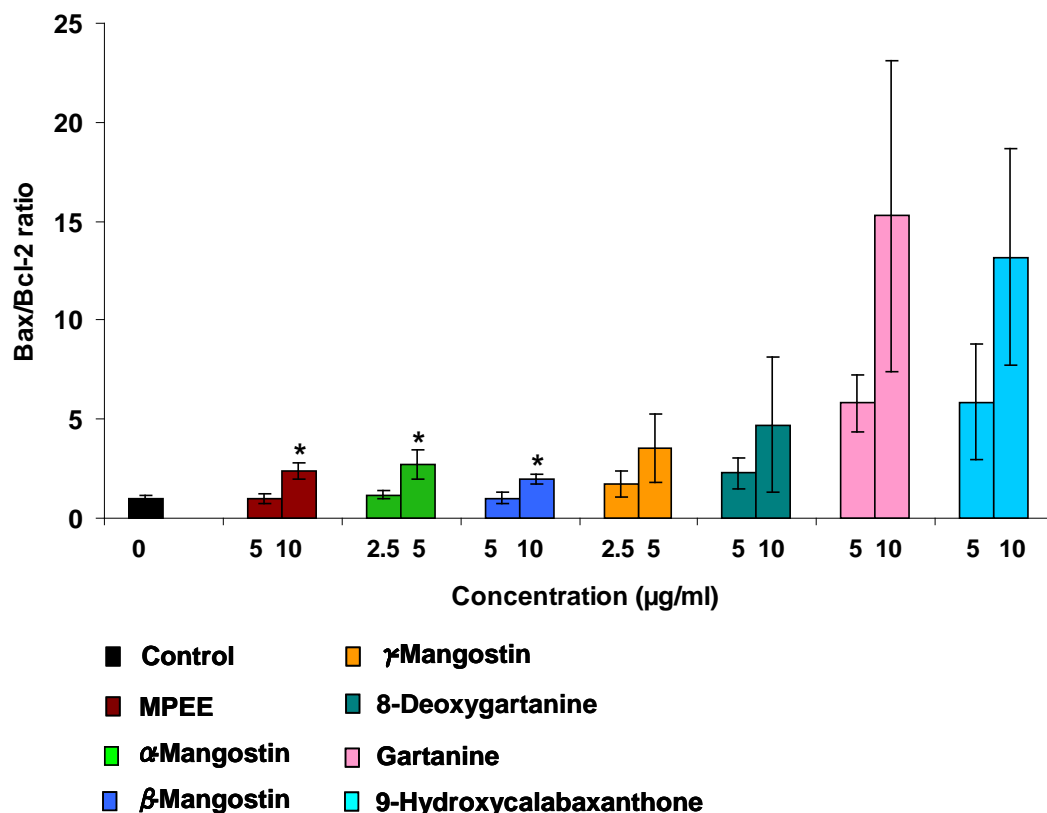
Figure 4-10
Effect of xanthones on the ratio of Bax and Bcl-2 mRNA expression in A-431 cells as determined by qRT-PCR. The values shown are the mean ± SEM of three independent experiments. Treatments significantly different from the untreated control at $P < 0.05$ are presented as * and at $P < 0.01$ as **.

4.3.5.3 Modulation of genes in survival pathways

In addition to apoptosis-related genes, we also examined the genes involved in several survival signalling pathways as discussed in Chapter 1. The key genes studied were Akt1, NFκB, IκBα, and BRAF V600E.

Significant decreases in mRNA level of Akt1 were observed after treatment with all tested xanthones, except for 8-deoxygartanine, in A-431 cells (Figure 4-11A). The most marked one was γ-mangostin, which induced a 6.6-fold decrease of the mRNA level of Akt1 compared with untreated control (P <0.01). In SK-MEL-28 cells, treatment with α-mangostin (7.5 µg/ml) and γ-mangostin (10 µg/ml) also induced

3.8- and 3.2-fold decreases, respectively ($P < 0.05$; Figure 4-11B).

Significant decreases in mRNA level of NFκB were observed after treatment with α-mangostin, γ-mangostin, 8-deoxygartanine, gartanine, and 9-hydroxycalabaxanthone in A-431 cells (Figure 4-12A). The most marked one was gartanine, which induced a 3.8-fold decrease of the mRNA level of NFκB compared with untreated control ($P < 0.01$). Significant decreases were also found in SK-MEL-28 cells after treatment with α-mangostin, β-mangostin, γ-mangostin, and 8-deoxygartanine (Figure 4-12B).

Significant increases in mRNA level of IκBα were observed after treatment with α-mangostin, β-mangostin, γ-mangostin, and 9-hydroxycalabaxanthone in A-431 cells (Figure 4-13A). The most marked one was 9-hydroxycalabaxanthone, which induced a 3.3-fold increase of the level of IκBα mRNA compared with untreated control ($P < 0.05$). However, in SK-MEL-28 cells, significant increase in the level of IκBα mRNA was found only after treatment with γ-mangostin (10 µg/ml) with a 4.1-fold increase compared with untreated control ($P < 0.05$; Figure 4-13B).

In SK-MEL-28 cells, significant decreases in mRNA level of BRAF V600E mutation were observed after treatment with α-mangostin, γ-mangostin, 8-deoxygartanine, gartanine, and 9-hydroxycalabaxanthone (Figure 4-14). The most marked one was γ-mangostin, which induced a 6.8-fold decrease of the mRNA level of BRAF V600E compared with untreated control ($P < 0.01$).

The BRAF V600E mutation had a very low expression in A-431 cells, which was not detectable by the current methods (data not shown).
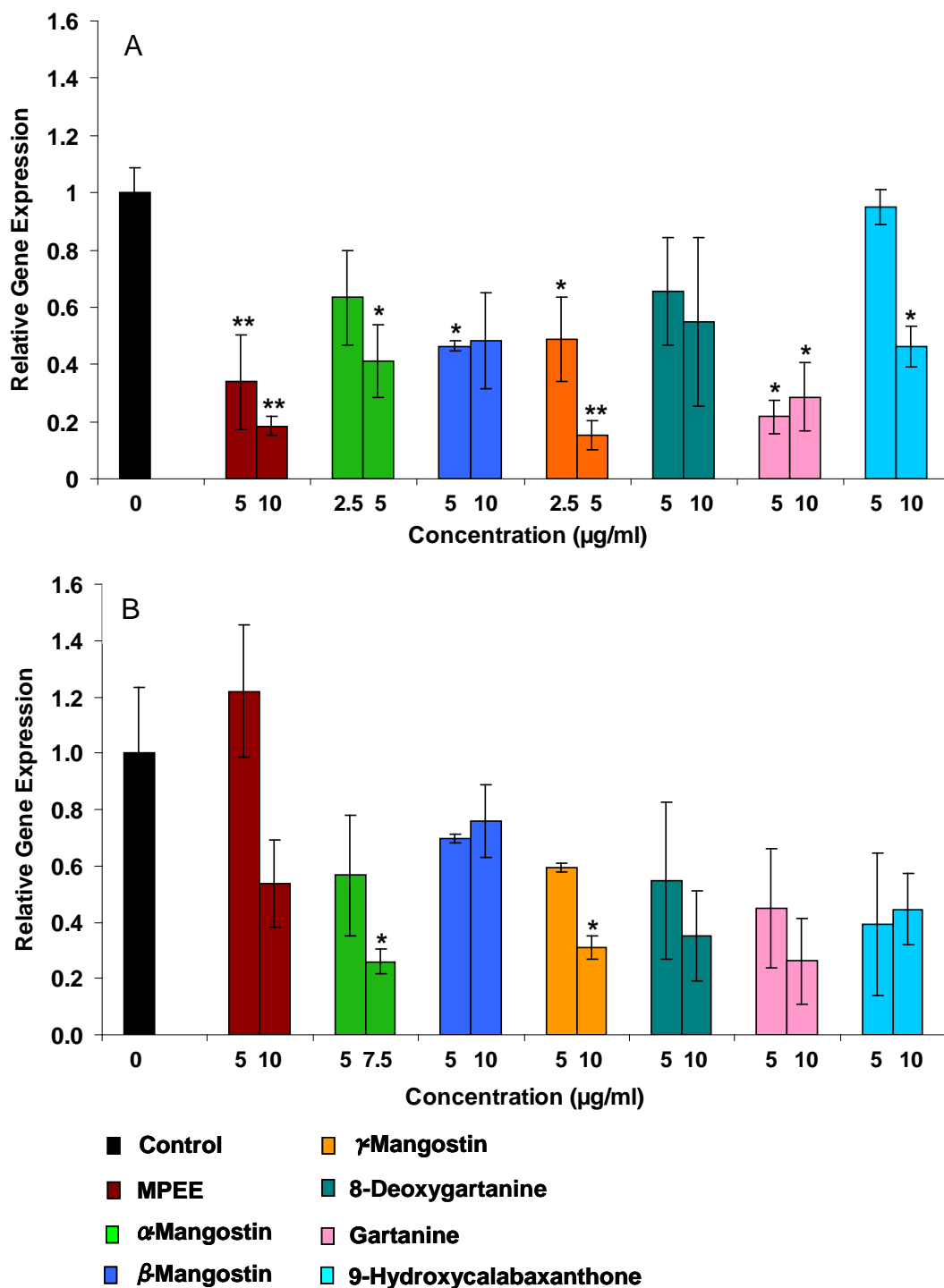
Figure 4-11
Effect of xanthones on Akt1 mRNA expression in (A) A-431 and (B) SK-MEL-28 cell line was determined by qRT-PCR. The values shown are the mean ± SEM of three independent experiments. Treatments significantly different from the untreated control at $P < 0.05$ are presented as * and at $P < 0.01$ as **.
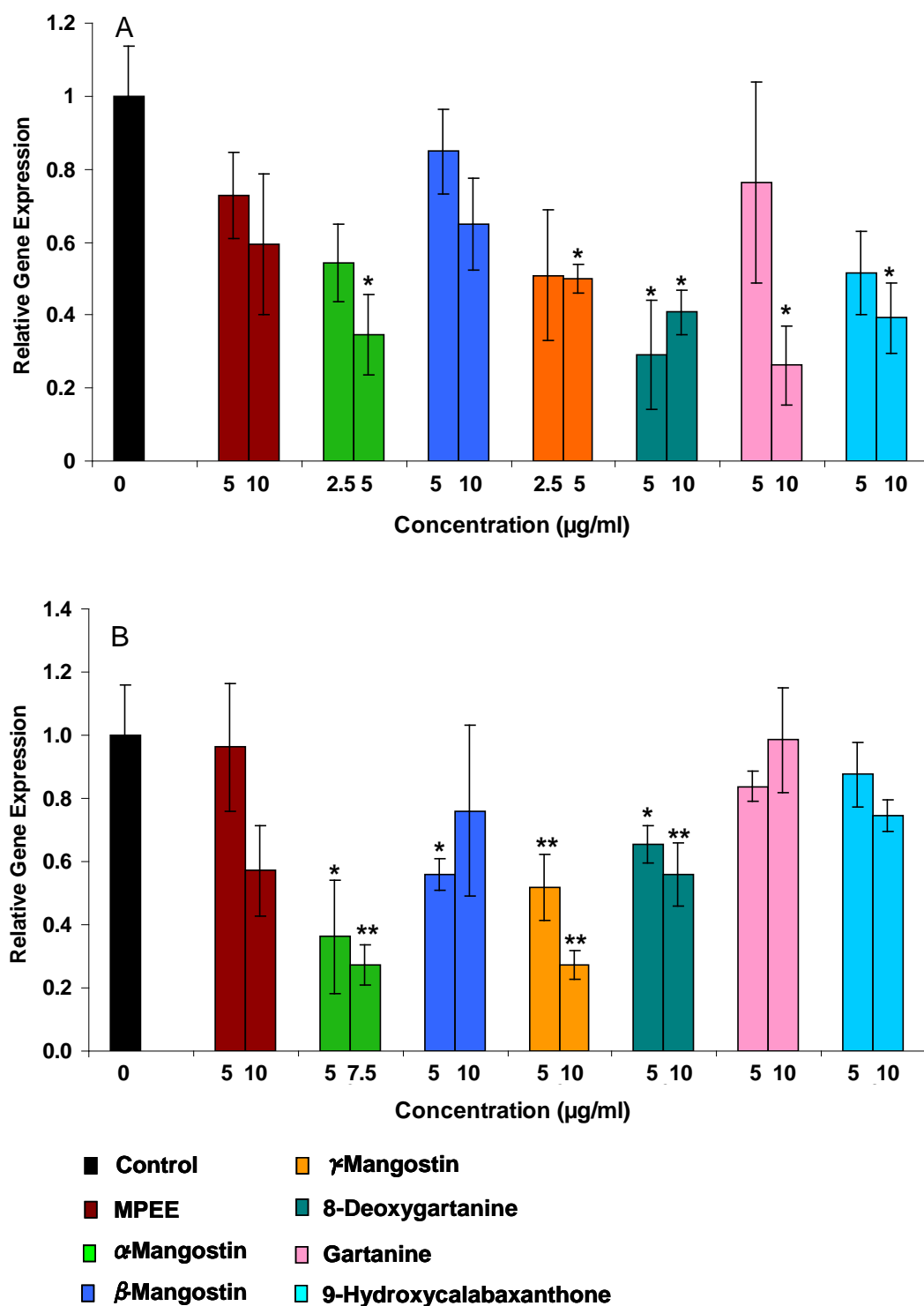
Figure 4-12

Effect of xanthones on NFκB mRNA expression in (A) A-431 and (B) SK-MEL-28 cell lines as determined by qRT-PCR. The values shown are the mean ± SEM of three independent experiments. Treatments significantly different from the untreated control at $P < 0.05$ are presented as * and at $P < 0.01$ as **.
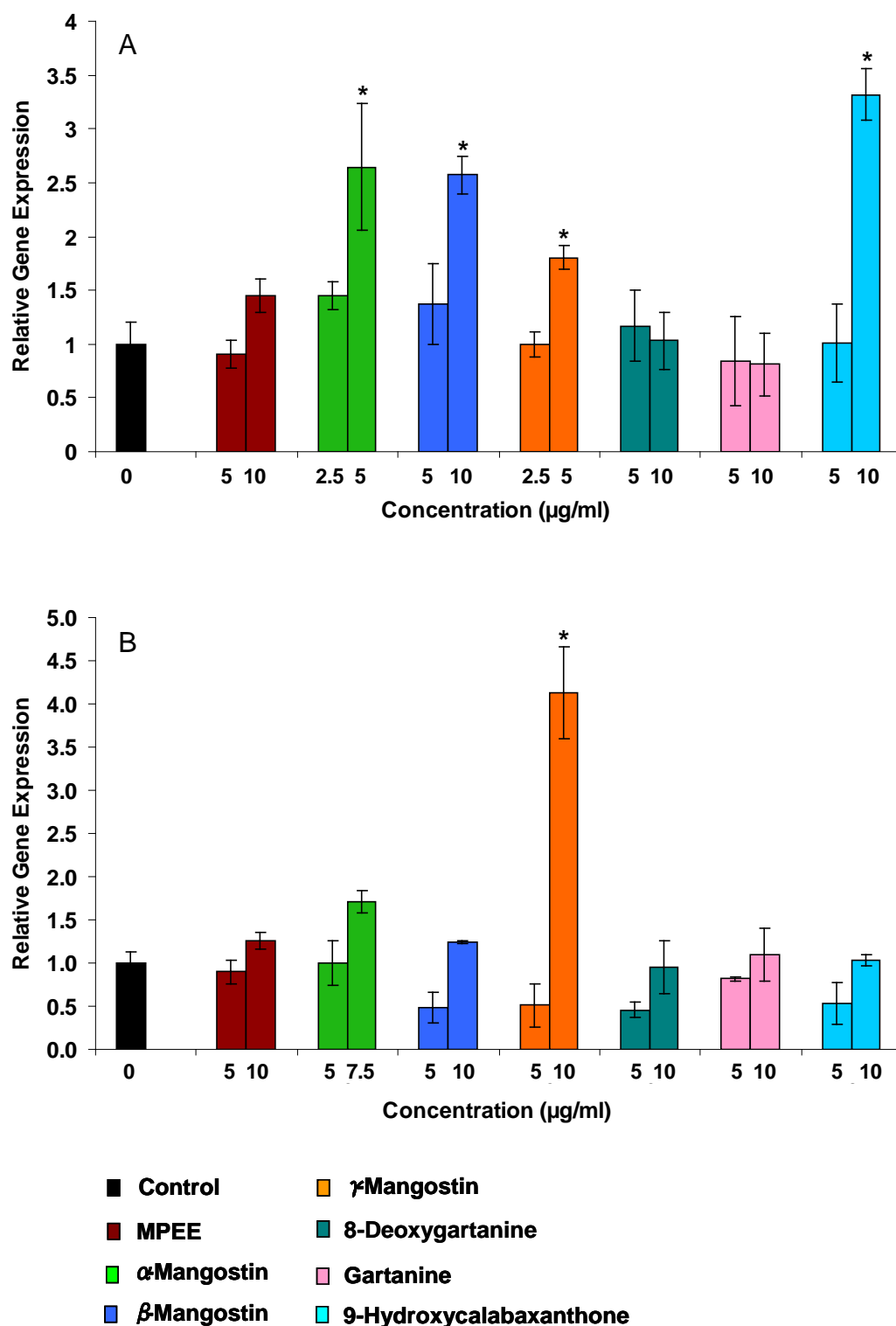
Figure 4-13

Effect of xanthones on IκBα mRNA expression in (A) A-431 and (B) SK-MEL-28 cell lines as determined by qRT-PCR. The values shown are the mean ± SEM of three independent experiments. Treatments significantly different from the untreated control at $P < 0.05$ are presented as * and at $P < 0.01$ as **.
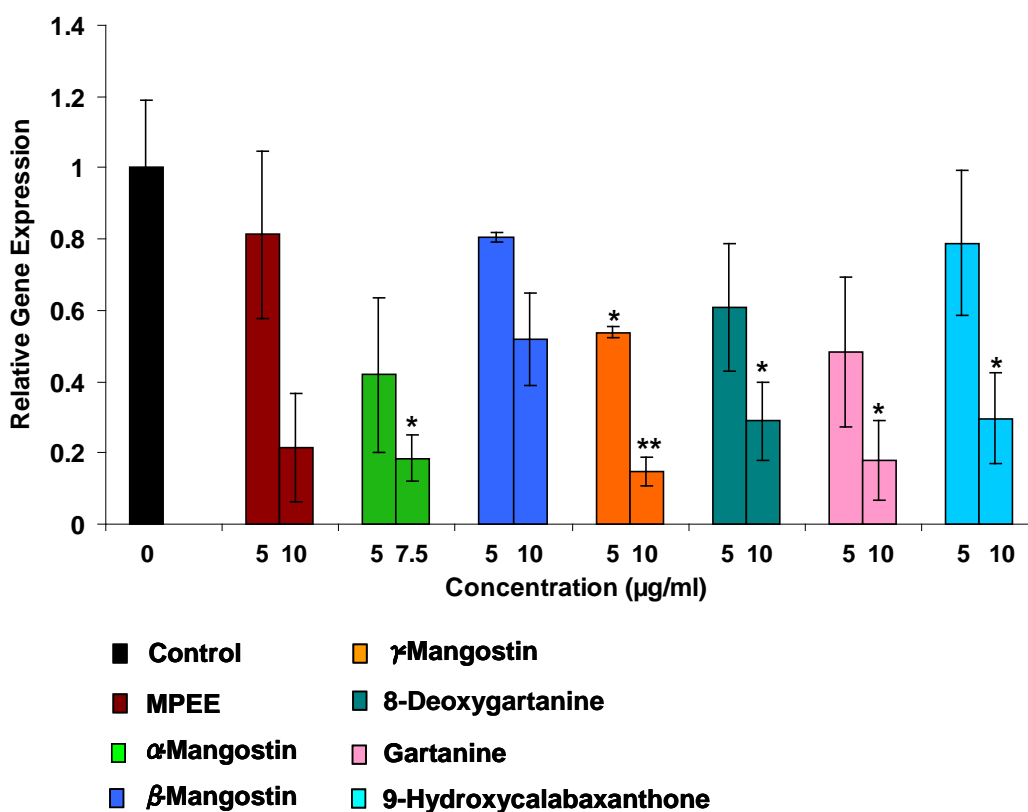
Figure 4-14
Effect of xanthones on BRAF V600E mRNA expression in SK-MEL-28 cell line as determined by qRT-PCR. The values shown are the mean ± SEM of three independent experiments. Treatments significantly different from the untreated control at $P < 0.05$ are presented as * and at $P < 0.01$ as **.

4.4 Discussion

4.4.1 Cell cycle modulatory effect of xanthones and the molecular mechanisms in human skin cancer cells

Control of cell cycle progression of cancer cells is an effective strategy for cancer therapy because cell cycle deregulation is one of the hallmarks of many common malignancies (Grana & Reddy 1995; Molinari 2000; Pavletich 1999; Senderowicz 2003). Cell cycle phase distribution of treated and untreated cells was analysed to determine if the proliferation inhibition by xanthones (described in Chapter 3) involved cell cycle arrest. Treatment of SK-MEL-28 cells with xanthones induced G_1 phase arrest. Treatment of A-431 cells with xanthones increased the sub G_1 peak

(hypodiploid debris), indicating induction of apoptosis. The current results are not in agreement with the study by Matsumoto *et al.* (2005), who reported that S phase cell cycle arrest was induced by γ-mangostin, and G_1 phase arrest by α-mangostin and β-mangostin in human colon cancer DLD-1 cells by affecting the expression of cyclins, cdc2 and p27. This discrepancy might be due to the difference in cell type analysed.
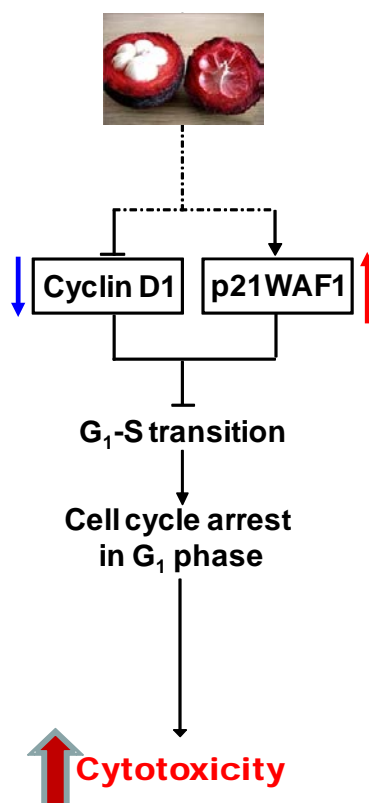
Figure 4-15
Proposed model of mechanisms of xanthone induced modulatory effect on cell cycle distribution on human squamous cell carcinoma A-431 and melanoma SK-MEL-28 cells. The arrow ↑ represents activation or increased expression, and ↓ represents inhibition or decreased expression.

The G_1 phase of cell cycle is controlled by cyclin dependent kinases, cyclin kinase inhibitors and cyclins (Mantena *et al.* 2006). In orderto determine the molecular mechanisms, the mRNA expression levels of cell cycle regulating genes at the G1/S boundary (Cyclin D1) and the universal CKI (p21^{WAF1}) were determined by qRT-PCR. The model of mechanisms of xanthone-induced modulatory effect on cell cycle

in SK-MEL-28 cells is presented in Figure 4-15. A significant increase in the expression of p21^{WAF1} was observed after treatment of SK-MEL-28 with MPEE, α-mangostin, β-mangostin, 8-deoxygartanine, and 9-hydroxycalabaxanthone. The xanthone-induced increase in p21^{WAF1} could be p53-independent, because SK-MEL-28 cells possess mutant p53 (Soengas *et al.* 2001). Additionally, significant decrease in the expression of cyclin D1 was observed after treatment with α-mangostin, β-mangostin, 8-deoxygartanine, gartanine, and 9-hydroxycalabaxanthone. The mRNA and protein expression of the other cyclins (e.g. A/E) and cyclin-dependent kinases (CDK) (e.g. CDK2/4/6) which regulate G_1/S transition can be studied in the future to further elucidate this mechanism.

4.4.2 Apoptotic effect of xanthones and the cellular and molecular pathways in human skin cancer cells

4.4.2.1 Apoptosis-inducing activity of xanthones in human skin cancer cells

Apoptosis is an important defence against cancer (Campbell *et al.* 2007). However, skin cancer, especially melanoma, is known to be resistant to the induction of apoptosis. This is probably due to down-regulation of Apaf-1, overexpression of Bcl-2 family members and increases in PI3 K/Akt/mTOR pathway signalling (Braun *et al.* 2007; Eberle *et al.* 2007b; Manning & Cantley 2007; Raisova *et al.* 2000). Therefore, apoptotic pathways are emerging as promising targets for skin cancer therapy (Eberle *et al.* 2007a; b). The apoptotic effect of xanthones was investigated in the current study. Significant induction of apoptosis was observed after 48 h treatment with the some xanthones tested, most markedly for α-mangostin treatment. Based on extensive literature searching, this is the first demonstration of the apoptotic effect on squamous cell carcinoma A-431 and melanoma SK-MEL-28 cells, although previous studies have shown the capability of xanthones to induce apoptosis in a number of cancer cell lines (Akao *et al.* 2008; Matsumoto *et al.* 2004;

Moongkarndi *et al.* 2004), other than skin cancer.

As shown in Figure 4-3 A, the apoptotic data for the A431 were very consistent in that the anti-proliferative data in Figure 3-9 A. However, SK-MEL-28 appeared to be mostly cell cycle arrested, which was not consistant with the cell viability data in Figure 3-9 B. Control of cell cycle might be one of the mechanisms of anti-proliferative effect induced by xanthones on SK-MEL-28 cells. During 48-h treatment, the melanoma cell proliferation was inhibited by the xanthones due to the effect of cell cycle arrest , thus the cell number in the treated wells was fewer than the untreated wells. However, apoptotic effect of xanthones also contributed to the anti-proliferative effect, although the apoptotic population induced by xanthones on SK-MEL-28 was not as significant as that on A-431 cells.

4.4.2.2 Mechanisms of xanthone-induced apoptosis

In orderto understand the mechanisms of xanthone-induced apoptosis, two distinct apoptotic pathways were studied: the extrinsic pathway involving the death receptor signalling and the intrinsic pathway involving the mitochondrial cascades (Henry-Mowatt *et al.* 2004). Activation of caspase 3/7 (effector caspases) is involved in both pathways, while caspases 8 and 9 (initiator caspases) are involved in extrinsic and intrinsic pathway respectively (Ashkenazi & Dixit 1998; Green & Amarante-Mendes 1998). The potential mechanisms of xanthone-induced apoptosis are presented in Figure 4-16, based on the current results.
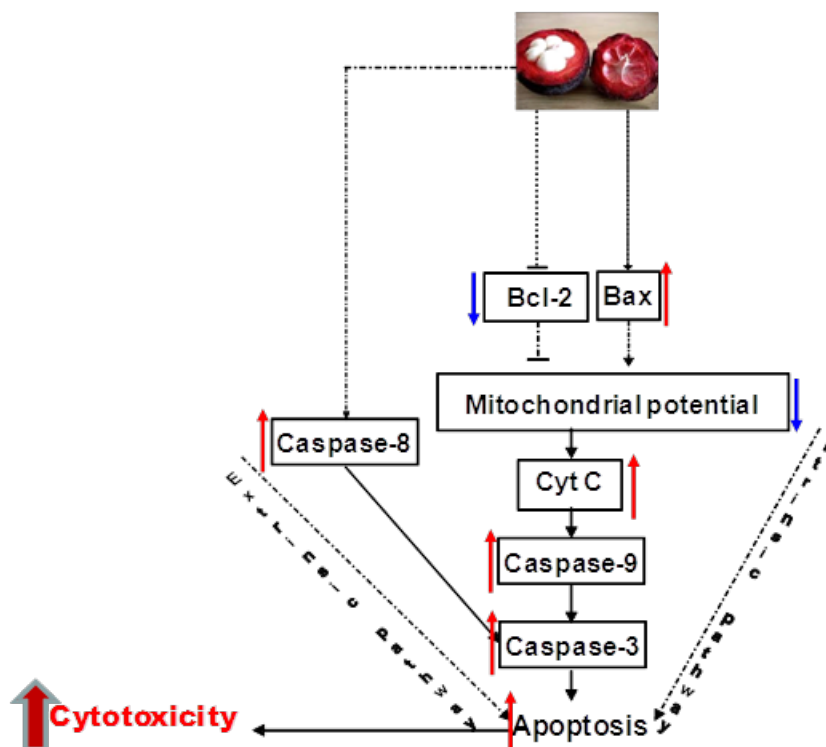
Figure 4-16
Proposed model of mechanisms involved in xanthone induced apoptosis on human squamous cell carcinoma A-431 and melanoma SK-MEL-28 cells. The arrow ↑ represents activation or increased expression, and ↓ represents inhibition or decreased expression.

Caspase activities

Caspase-3/7 is the most prevalent caspase within cells and responsible for most apoptotic effects (Zimmermann *et al.* 2001). Caspase 3/7 activation induces PARP cleavage, DNA breaks and finally leads to apoptosis (Rehm *et al.* 2002). Caspase 8 and 9 are important effectors. Caspase activation was investigated to identify the pathways involved in apoptosis in A-431 and SK-MEL-28 cells in response to the xanthones tested. α-Mangostin and 8-deoxygartanine exerted apoptotic effects by acting on caspase 3. α-Mangostin showed the most potent effect on the caspase activation on the two skin cancer cell lines, because it activated Caspase 3/7, 8, and 9 enzymes. In contrast, the other xanthones tested only activated one or two of the enzymes. The results show that α-mangostin induced apoptosis through both the

extrinsic and intrinsic pathways on both A-431 and SK-MEL-28 cells, but some of the xanthones or extract induced the apoptosis only through the intrinsic pathway (e.g. MPEE, 8-deoxygartanine, gartanine and 9-hydroxycalabaxanthone in SK-MEL-28 cells). Different responses to xanthones by different cell lines have been reported by Matsumoto *et al.*(2005), who found α-mangostin induced caspase-independent apoptosis via the mitochondrial pathway in colon cancer cells (Matsumoto *et al.* 2005). In contrast, in human leukaemia HL60 cells, α-mangostin induced apoptosis via caspase 3 and 9 activation and disruption of mitochondrial membrane potential (Matsumoto *et al.* 2004). This difference may be due to the cell type investigated. Further study is required to clarify this difference. In the current study, the caspase cascade was determined at 48 h when significant apoptosis was observed. Caspase activation usually occurs before apoptosis induction. Therefore, the caspase activity should be monitored over time, especially at earlier time points (e.g. 2, 6, 24 h).

Mitochondrial membrane potential

Mitochondrial dysfunction is another key event of apoptosis. An important parameter of mitochondrial dysfunction is the loss of mitochondrial membrane potential ($\Delta\Psi$m) (Kroemer 2003). Loss of $\Delta\Psi$m is lethal to cells because they become bioenergetically deficient (Crompton 2000). Breakdown of $\Delta\Psi$m in turn leads to the release of cytochrome c into the cytosol and activation of caspase cascades that result in cell death. The design of mitochondria-targeted therapeutic strategies for cancer has recently been reviewed (Fulda *et al.*2010). The present study demonstrated that the tested xanthones induced loss of $\Delta\Psi$m on the two skin cancer cell lines. These findings are consistent with previous studies. Matsumoto *et al.* (2004) reported that α-mangostin preferentially targeted mitochondria with loss of $\Delta\Psi$m, decrease in

ATP, ROS accumulation and cytochrome c/AIF release in human leukaemia HL60 cells. Nakagawa *et al.* (2007) showed that α-mangostin induced decreased $\Delta\Psi$m with release of endonuclease-G from mitochondria. Additionally, gaudichaudione A, a cytotoxic xanthone, induced mitochondrial destabilization (Wu *et al.* 2002). Therefore, although xanthones induced apoptosis via different pathways in different cancer cell types, current studies support that xanthones preferentially target the mitochondria for apoptosis induction.

However, inconsistency of results was found. The mitochondrial membrane alterations did not reflect the proliferative or cell death effects after treatment with β-mangostin. For example, the cell killing (%) was approximately 10-60% after treatment with 2.5-10 µg/ml of β-mangostin as detected by the Crystal Violet assay (Figure 3-9B). However, the mitochondrial membrane disruption (%) was approximately 70-60% after treatment with 2.5-10 µg/ml of β-mangostin (Figure 4-7B). To clarify these results, additional experiments (e.g. observation by Fluorescence microscopy using JC-1 dye and TUNEL assay) need to be carried out in the future.

Modulation of genes in apoptotic pathways

In order to understand the molecular mechanism of apoptosis induced by the xanthones tested, the genes involved in apoptosis were analysed by the qRT-PCR. Release of mitochondrial cytochrome c is an important signalling event in the intrinsic apoptotic activation pathway. A significant increase in the mRNA expression of cytochrome c was observed after treatment with MPEE, 9-hydroxycalabaxanthone, and α-mangostin for both skin cancer cell lines. The result

of the cytochrome c gene expression was partially consistent with the result of the mitochondrial membrane potential. For example, treatment with 8-deoxygartanine did not decrease the mitochondrial membrane potential in A-431. Consistently, the mRNA level of cytochrome c was not changed after the same treatment on the same cell line. In contrast, treatment with 9-hydroxycalabaxanthone significantly increased the loss of mitochondrial membrane potential in SK-MEL-28, however, no significant increase in the mRNA level of cytochrome c was observed. This may indicate that cytochrome c was not involved in the 9-hydroxycalabaxanthone induced intrinsic apoptotic pathway in SK-MEL-28 cell line. Transcriptional activation of cytochrome c can lead to increased protein expression in both the cytosol and mitochondria (Chandra *et al.* 2002). The levels of cytochrome c in the cytosol and mitochondria after treatment could be determined by western blotting analysis.

Bcl-2 family are key regulators of the intrinsic pathway, which either suppress or promote changes in mitochondrial membrane permeability required for release of cytochrome-c (Green & Reed 1998; Gross *et al.* 1999). Overexpression of anti-apoptotic Bcl-2 probably occurs in most cancers (Amundson *et al.* 2000) and a low ratio of pro-apoptotic Bax and anti-apoptotic Bcl-2 implies apoptosis resistance (Raisova *et al.* 2001). Treatment with MPEE, α-mangostin, and β-mangostin enhanced the ratio of Bax/Bcl-2 in A-431 cells (Figure 4-10). This supports that the release of cytochrome c from the mitochondria into the cytosol by these xanthones results from down-regulation of Bcl-2 and /or upregulation of Bax in A-431 cells. However, the Bax/Bcl-2 ratio was not affected by the xanthone tested in SK-MEL-28, indicating these two genes are not involved in xanthone-induced apoptosis in this cell line. This is in agreement with findings of Matsumoto *et al.* (2004). Additional

studies on other genes of Bcl-2 family (e.g. Puma, Bad, Mcl-1, etc) are required to understand further the mechanism involved.

4.4.3 Modulation of genes in survival pathways

Activation of survival pathways contributes to the resistance of cancer cells to chemotherapy by regulating apoptosis at multiple levels, as discussed in Chapter 1. In this study, the key genes in three major survival pathways in skin cancer cells were investigated and they are NFκB, IκBα, Akt and BRAF V600E. The alterations in expression of these genes after treatment with xanthones are shown in the model in Figure 4-17.
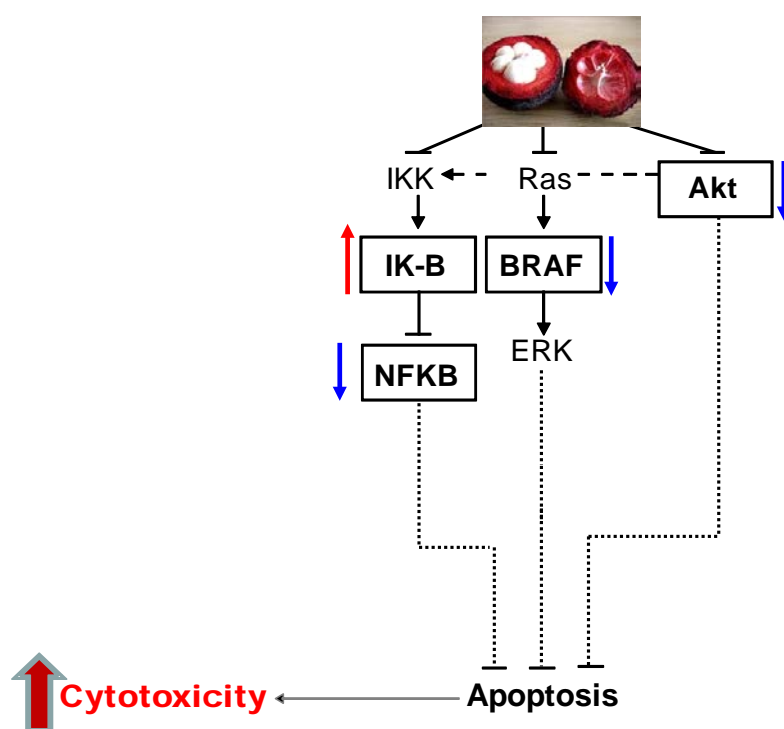
Figure 4-17
Proposed model of mechanisms of xanthone-induced modulatory effect on survival pathways on human squamous cell carcinoma A-431 and melanoma SK-MEL-28 cells. The arrow ↑ represents increased expression, and ↓ represents decreased expression.

1) NFκB pathway

NFκB activation is associated with chemoresistance by activation of anti-apoptotic proteins (Demarchi & Brancolini 2005) and inhibition of extrinsic apoptotic pathway (Ivanov *et al.* 2003), as discussed in Chapter 1. Therefore, inhibition of NFκB can result in apoptosis induction, thus blocking tumour development, although this apoptosis induction may also involve elevated proliferation rate (Crowley-Weber *et al.* 2002; Johnstone *et al.* 2002; Li *et al.* 1997; Rayet & Gelinas 1999). Down-regulation of NFκB was found after treatment with α-mangostin, γ-mangostin, 8-deoxygartanine, gartanine, and 9-hydroxycalabaxanthone on A-431 cells, and with α-mangostin, β-mangostin, γ-mangostin, and 8-deoxygartanine on SK-MEL-28 cells (Figure 4-12). Likewise, compounds of α-mangostin, β-mangostin, 8-deoxygartanine, and gartanine were reported to inhibit the activation of p65 (one of the subunits of NFκB) on colon cancer HT-29 cell line as detected by an ELISA assay (Han *et al.* 2009). Also, α-mangostin was reported to inhibit the activation of p50 (another subunits of NFκB) on lung cancer A549 cell line as tested by western blotting (Shih *et al.* 2010). The compounds showed similar activity on the colon cancer HT-29 cells as on the skin cancer cells tested in this study, as evidenced by the similar range of effective concentrations: 5.0-10.0 µg/ml from the current study and 4.3-7.5 µg/ml from the study by Han *et al.* (2009). However, the inhibitory effect of xanthone compounds on NFκB was found to be cell type dependent. For example, 9-hydroxycalabaxanthone was found to be only effective on A-431 cells, but not on SK-MEL-28 and HT-29 cells, while gartanine was reported to be effective on both A-431 and HT-29 cells, but not on SK-MEL-28 cells (Han *et al.* 2009). The difference in the effect of the xanthones might lie in the variations in the concentrations used and the cancer cell types tested. The effect of the xanthones on

NFκB subunits of the two types of skin cancer cells can be determined using western blotting analysis in the future.

IκBα is known to play a key role in the NFκB pathway. Phosphorylation of IκBα by IKK and subsequent degradation is required for the activation of NFκB (Ravi & Bedi 2004). Hence, the involvement of IκBα was investigated to understand the NFκB pathway. In the current study, increase in the mRNA level of IκBα were found after treatment with α-mangostin, β-mangostin, 9-hydroxycalabaxanthone, and γ-mangostin on A-431 cells, and only with γ-mangostin on SK-MEL-28 cells (Figure 4-13). These results indicate that IκBα was involved in the inhibitory effect of NFκB induced by compounds α-mangostin, γ-mangostin, and 9-hydroxycalabaxanthone on A-431 cells and γ-mangostin on SK-MEL-28 cells, respectively. Apart from IKK and IκBα, ERK is another important upstream regulator for NFκB (Figure 1-9). Therefore, the ERK pathway might be involved in downregulation of NFκB expression induced by the xanthones tested (e.g. 8-deoxygartanine and gartanine). To clarify this, the mRNA and protein level of these molecular targets warrants further investigation.

2) Akt1 pathway

Akt, a serine/threonine protein kinase, is involved in cell survival and growth, which is constitutively activated through multiple mechanisms in most cancers (Pap & Cooper 1998). Among its three isoforms (Akt1, 2, and 3), Akt1 plays a key role in maintaining cell survival (Chen *et al.* 2001a; Gonzalez & McGraw 2009; Nicholson & Anderson 2002). Therefore, the Akt1 pathway can be an important molecular target for cancer prevention and treatment (Crowell *et al.* 2007). α-Mangostin was

previously reported to downregulate Akt expression on human colon DLD-1 cells (Nakagawa *et al.* 2007), human Chondrosarcoma SW1353 cells (Krajarng *et al.* 2011), and mammary carcinoma both *in vitro* and *in vivo* (Shibata *et al.* 2011). However, the Akt inhibitory effect of this compound on skin cancer cells was not known. Also, apart from α-mangostin, there is limited information available on the effect of other xanthones on the expression of Akt.

In the current study, MPEE and all the tested compounds, except for 8-deoxygartanine, were shown to significantly decrease the mRNA level of Akt1 on A-431 (Figure 4-11A). Inhibition of Akt1 has been reported to activate its downstream targets, including Bax, Bad, Noxa and Puma (Eberle *et al.* 2007b). As mentioned earlier, an increase in the mRNA expression of Bax was found after treatment with xanthones on A-431 (Figure 4-10). These results indicate that downregulation of Akt1 is involved in the apoptotic effect induced by these xanthones on this cell line. Inhibition of Akt1 was also observed on SK-MEL-28 cells after treatment with α-mangostin and γ-mangostin (Figure 4-11B). The mRNA level of Bax was not significantly altered after treatment with these two xanthone compounds in this cell line (data not shown). It is possible that inhibition of Akt1 may activate other downstream targets (e.g. Bad, Noxa and Puma) instead of Bax. To clarify this, the expression of these molecular targets at both mRNA and protein levels needs to be investigated in the future. In order to elucidate which steps in this survival pathway are involved, additional upstream (e.g. PI3K) and downstream (e.g. Hdm-2) targets of Akt need to be studied.

3) MAPK pathway

MAPK pathway has been shown to correlate with the cell survival and chemoresistance in a range of human cancers, including melanoma and head and neck squamous cell carcinoma (Smalley & Eisen 2003; Wagner & Nebreda 2009). BRAF, a cytoplasmic serine/threonine kinase, plays a predominant role in the MAPK pathway by transducing signals from RAS to MEK (Mercer & Pritchard 2003). BRAF gene mutations have been reported in most malignant melanomas (Davies *et al.* 2002; Gorden *et al.* 2003). BRAF V600E mutation accounts for 89-90% of all the detected mutations. This mutation is a single transversion in exon 15, corresponding to an amino-acid swap of glutamate for valine at residue 600 (Kumar *et al.* 2003). BRAF V600E mutation leads to constituent activation of the MEK/ERK pathway, and thus promotes cancer cell survival and proliferation (Kumar *et al.* 2003). Therefore, BRAF V600E can be an important therapeutic target for melanoma. In the current study, significant downregulation of BRAF V600E was observed on human melanoma SK-MEL-28 cells after treatment with α-mangostin, γ-mangostin, 8-deoxygartanine, gartanine, and 9-hydroxycalabaxanthone (Figure 4-14). Indeed, RG7204 (PLX4032), a selective BRAF V600E inhibitor, has shown potent inhibitory effect on the growth of melanoma harboring this mutation both *in vitro* and *in vivo* (Yang *et al.* 2010). It is currently in phase II and phase III clinical test (Yang *et al.* 2010). GSK2118436 is another successful example of treating melanoma by targeting BRAF mutation (Kefford *et al.* 2010). The current result indicates that xanthones show the potential as anti-melanoma drugs by selectively targeting the BRAF V600E mutation.

To the best of my knowledge, this is the first demonstration of the inhibitory effect of

xanthone compounds on BRAF V600E mutation, although α-mangostin was reported to downregulate MAPK pathway by inhibiting ERK and JNK on human colon DLD-1 cells (Nakagawa *et al.* 2007), and human Chondrosarcoma SW1353 cells (Krajarng *et al.* 2011). Therefore, this study provides important information about the novel mechanisms of anti-cancer activity of xanthone compounds on skin cancer cells. In the future, BRAF V600E inhibitor can be applied in the study of xanthone inhibition on melanoma survival. Aslo, BRAF may also be a contributor to squamous cell carcinoma, although not through direct mutations as is common in melanomas. Therefore, it would be interesting to test the alteration in the protein level of total BRAF after treatment with xanthones for both A-431 and SK-MEL-28 cell lines.

4.4.4 General discussion of the variation of results

As shown in the method sections in this Chapter, the methodology was validated and both reproducibility and sensitivity were achieved as evidenced by the inter-assay CV and intra-assay CV. All experiments were repeated on at least three independent occasions. Therefore, the variations seen in the results are believed to be from biological variations. Some of the results show large error bars. One example is as shown in Figure 4-9B, treatment of SK-MEL-28 cells with γ-mangostin (10 µg/ml) induced a 14.1-fold increase in the mRNA expression in cytochrome c when compared with the untreated control. However, this difference was not statistically significant ($P > 0.05$) due to the large error bar. Each treatment condition was performed with three technical replicates. The inter-assay CV from the three replicates for this treatment condition (10 µg/ml of γ-mangostin) was acceptable with values of less than 20%, indicating good reliability and reproducibility of the assay. The change from the three independent experiments was 16.0, 21.0, and 5.3 fold, respectively. Apparently, the data from the third experiment resulted in the large

standard deviation. Therefore, additional replicates are needed to reduce error associated with biological variation and clarify the statistical significance of these results. However, due to the time constraint and the availability of resources, additional experiments have not been carried out in the current study but should be in the future.

4.5 Summary

The anti-skin cancer activities of xanthones are *via* induction of cell cycle arrest in G_1 phase, induction of apoptosis through extrinsic and/or intrinsic pathways, and/or inhibition of survival pathways. The effect of the compounds on A431 and SKMEL28 was fundamentally different, promoting extensive apoptosis in the former and essentially cell cycle arrest in the latter. It is not likely to be related to the rate of cycling because A-431 and SK-MEL-28 cells showed similar rate of cycling as stated in Chapter 3. The difference might be due to different genetic backgrounds of these two cell lines. However, it needs to be confirmed by carrying out experiments using a broad range of cell lines with different genetic backgrounds.

Extensive interactions among the different survival pathways are shown to be activated in skin cancer, especially melanoma, contributing to the high frequency of chemoresistance (Figure 1-9) (Eberle *et al.* 2007b). For example, the NFκB pathway is closely associated with both MAPK and Akt pathways in melanoma cells (Dhawan & Richmond 2002; Dhawan *et al.* 2002). Activation of either MAPK or Akt is sufficient to activate NFκB. Thus, NFκB activation could only be suppressed by blocking both pathways. Therefore, it is of importance to block multiple pathways to treat skin cancer. In terms of targeting multiple pathways, this study shows highly promising results. Because the cellular and molecular response to the tested

xanthones can fall into one or more pathways, with α-mangostin being the most potent one. Furthermore, the results demonstrate that different cell lines exhibit different responses to each specific xanthone compound, as evidenced by different mechanisms observed in our study and in the literature.

CHAPTER 5
POTENTIAL SYNERGISTIC EFFECTS OF COMBINING XANTHONES WITH COMMERCIAL DRUGS OR WITH α-MANGOSTIN

5.1 Introduction

A synergistic effect is one where the effect of two or more agents combined is greater than the sum of the individual effects. Therefore, drugs are widely used in combination to treat cancer and other diseases to achieve a synergistic effect, to enhance their therapeutic response and reduce harmful side effects and drug resistance (Chou 2006).

Recently, natural compounds from plants have been reported to enhance the efficacy of anti-cancer drugs and their metabolism (Bava *et al.* 2005). 5-FU is a commonly used drug for squamous cell carcinoma and colorectal adenocarcinoma (de Mulder 1999). A synergistic effect on cell growth of human colon cancer DLD-1 was found when 5-FU was combined with α-mangostin (Nakagawa *et al.* 2007). However, the synergistic effect of this combination on skin cancer cell lines was not known. Such synergy is not able to be predicted without being tested (Chou 2010). Cisplatin is a chemotherapeutic drug used against malignant solid tumours (Kelland 2007). A synergistic effect on human bladder carcinoma NTUB1 cell growth was observed when cisplatin was combined with one synthetic xanthone compound (Cheng *et al.* 2011). DTIC is a commonly used drug for melanoma (Serrone *et al.* 2000). A strong synergy between DTIC and plitidepsin (a marine agent isolated from the Mediterranean tunicate *Aplidium albicans*) was observed for the inhibition of human melanoma SK-MEL-28 cell proliferation (Muñoz-Alonso *et al.* 2008). Therefore, combining of natural compounds with anti-cancer drugs can be an effective strategy to improve the therapeutic efficacy of these drugs (Bava *et al.* 2005).

Studies have also reported that combinations of some natural compounds originating

from different plants, or from different parts within single plants, demonstrate synergistic effect against cancer (Gilbert & Alves 2003; Williamson 2001). For example, ovarian carcinoma cell growth was synergistically inhibited by a combination of quercetin (e.g. from onions) and genistein (e.g. from soya) (Shen & Weber 1997). When flavonoids (e.g. from orange juice) were used together with tocotrienols (e.g. from palm oil), breast cancer growth was synergistically inhibited both *in vitro* and *in vivo* (Guthrie & Carroll 1998). A combination of extracts from different parts of the pomegranate (juice, pericarp, and seed) synergistically inhibited the growth and invasion of human prostate PC-3 cell line (Lansky *et al.* 2005). Furthermore, the results in Chapter 3 indicate that there might be synergistic effects among the individual xanthone compounds and this needs to be determined.

The aims of this chapter are therefore to evaluate the potential synergistic effect between xanthones and commercial drugs as well as between individual xanthones on human squamous cell carcinoma A-431 cell line and human melanoma SK-MEL-28 cell line and to investigate the underlying mechanisms of the effects observed.

5.2 Materials and Methods

5.2.1 Materials

Information on the materials used in this Chapter is described in Section 3.2.

5.2.2 Crystal Violet assay

Crystal Violet assay was used to investigate the cell proliferation of human skin cancer cells after treatment with individual compounds as well as different combinations. The detail of this method is described in Section 3.2.6.

5.2.3 Cell cycle analysis and apoptosis analysis

Cell cycle analysis and apoptosis analysis were used to investigate the underlying mechanism of the cytotoxicity induced by different combinations. For the details of these two methods refer to Sections 4.2.3 & 4.2.4.

5.2.4 Experimental design for screening of potential synergistic cytotoxic effect

5.2.4.1 Combinations of xanthones with commercial drugs (5-FU & DTIC)

The killing curve for individual drug or xanthone compound was obtained across six different concentrations (Table 5-1). The combinations were set up as non-constant ratio: two concentrations were selected for the commercial drugs (one was the IC_{50} value and the other one was half the IC_{50} value) and three concentrations were selected for the xanthones. The individual drug/compound killing curve was set up each time with the combinations. Concentrations used for these experiments are shown in Table 5-1. The experiments were repeated on three independent occasions with six technical replicates per condition.

Table 5-1
Experimental design for the combination of commercial drug with individual xanthones.

Compound / Drug	Concentration (µg/ml)
Individual:	
5-FU	0, 0.3125, 0.625, 1.25, 2.5, 5
DTIC	0, 25, 50, 100, 200, 400
Xanthone	0, 1.25, 2.5, 5, 10, 20
Combination:	
5-FU/Xanthone	0.625/1.25, 0.625/2.5, 0.625/5, 1.25/1.25, 1.25/2.5, 1.25/5
DTIC/Xanthone	50/1.25, 50/2.5, 50/5, 100/1.25, 100/2.5, 100/5

5.2.4.2 Combinations of α-mangostin with individual xanthone compounds

Individual compound killing curves were obtained across six different concentrations. The combinations were set up as non-constant ratio: two

concentrations were selected for the α-mangostin (one was IC_{50} value and the other one lower) and three concentrations were selected for the other xanthones. The individual compound killing curve was set up each time with the combinations. Concentrations used for these experiments are shown in Table 5-2. The experiments were repeated on three independent occasions with six technical replicates per condition.

Table 5-2
Experimental design for the combination of α-mangostin and another xanthone.

Compounds	Concentration (μg/ml)
Individual xanthone:	0, 1.25, 2.5, 5, 10, 20
α-Mangostin /another Xanthone:	
On A-431	1.25/1.25, 1.25/2.5, 1.25/5, 2.5/1.25, 2.5/2.5, 2.5/5
On SK-MEL-28	2.5/1.25, 2.5/2.5, 2.5/5, 5/1.25, 5/2.5, 5/5

The only xanthone combinations tested were between α-mangostin and the other individual xanthones, due to α-mangostin showing the most promise (see Chapters 3 & 4 for individual results) and time constraints.

5.2.5 Statistical analysis

The synergy of different combinations on cell proliferation was determined according to the median-effect principle analysis of Chou and Talalay (Chou and Talalay, 1983) using the CalcuSyn Software (Biosoft, Ferguson, MO). The program calculates the combination index (CI), which reflects the nature of the interaction between drugs - the lower the CI value, the stronger the synergism. A CI value of 0.9-1.1 indicates an additive effect between two drugs, a CI < 0.9 indicates synergism. Values < 0.1 represent a very strong synergism whereas a range of CI values of 0.1-0.3, 0.3-0.7, 0.7-0.85 and 0.85-0.9 represents strong synergism, synergism, moderate synergism and slight synergism, respectively. A CI >1.1

indicates antagonism. Values of 1.1-1.2, 1.2-1.45, 1.45-3.3, 3.3-10, >10 represent slight antagonism, moderate antagonism, antagonism, strong antagonism, and very strong antagonism, respectively.

The interaction between drug and / or xanthone compound on cell cycle arrest and apoptosis induction was tested by Two way ANOVA test using the General Linear Model, Univariate analysis. These tests were performed using SPSS software (version 17). Percent cell distribution (for cell cycle analysis) or apoptotic population (for apoptosis analysis) was chosen as the dependent variable while the treatments were the fixed variables. This method compares the expected additive response of two treatments with the actual response. Therefore, responses were considered non-additive (either synergistic or antagonistic) when the *P*-value of the term treatment1*treatment 2 was less than 0.05 (significant) or 0.01 (highly significant).

5.3 Results

5.3.1 Combinations with commercial drugs

No synergistic effects were observed between 5-FU or DTIC and xanthones under all the tested conditions (Table 5-1). The results for combination of α-mangostin with 5-FU or DTIC are presented in Figures 5-1 and 5-2 as examples.
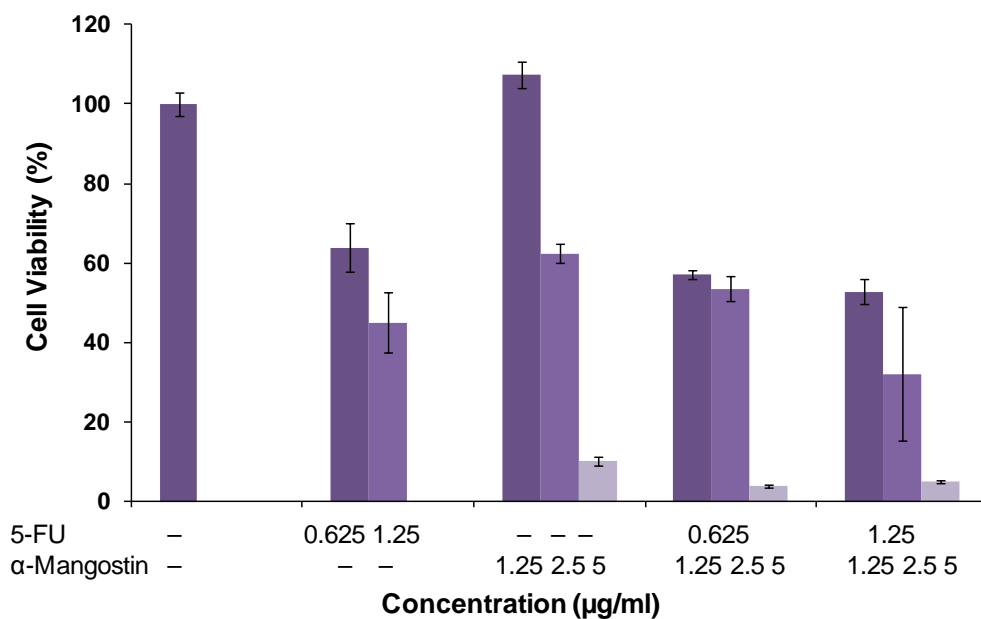
Figure 5-1
Cell viability of A-431 cells was investigated using the Crystal Violet assay after 48-h treatment in the presence of the indicated concentrations of an individual α-mangostin / 5-fluorouracil (5-FU) alone or in combination of α-mangostin with 5-FU. Data are presented as mean ± SEM of three independent experiments performed in six replicates.
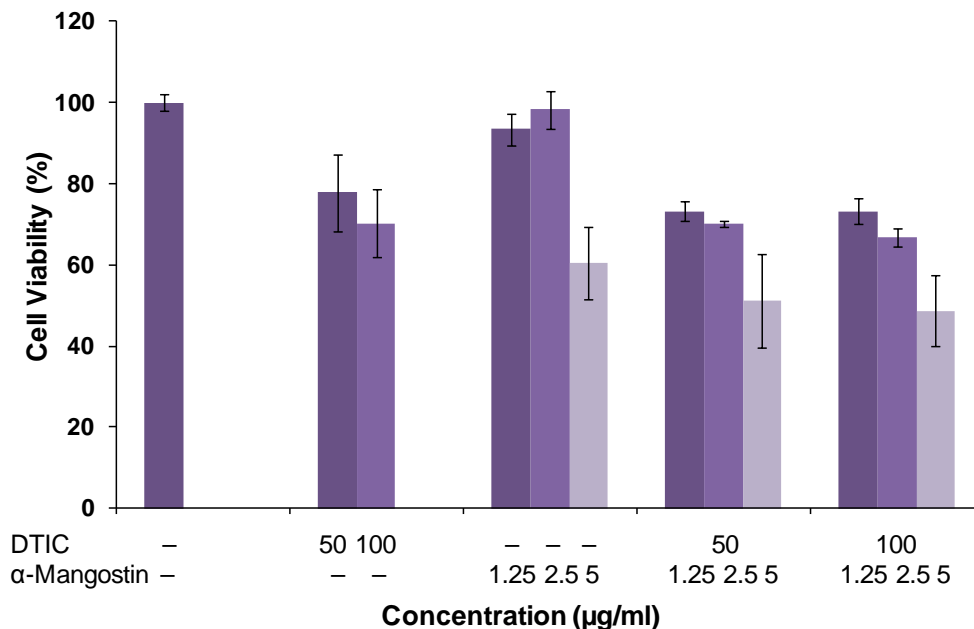
Figure 5-2
Cell viability of SK-MEL-28 cells was investigated using the Crystal Violet assay after 48-h treatment in the presence of the indicated concentrations of an individual α-mangostin / dacarbazine (DTIC) alone or in combination of α-mangostin with DTIC. Data are presented as mean ± SEM of three independent experiments performed in six replicates.

5.3.2 Combinations of α-mangostin with another xanthone compound

5.3.2.1 Effects of combinations of α-mangostin with another xanthone on human squamous cell carcinoma A-431 cells

Figure 5-3 shows the effect on A-431 cell proliferation after 48-h treatment with combinations of α-mangostin (1.25 and 2.5 µg/ml) and another xanthone compound (1.25, 2.5 and 5 µg/ml). Synergistic antiproliferative effect was observed when α-mangostin was used with some of the xanthones at specific concentrations as shown in Figure 5-3. The most marked combination was found to be α-mangostin and β-mangostin (Figure 5-3B). Synergy to different extents was observed at all combinations tested. α-Mangostin at 1.25 µg/ml and β-mangostin at 1.25 and 2.5 µg/ml showed no significant effect on A-431 cell proliferation when used separately. However, the combination of two xanthones synergistically enhanced the cytotoxic effect, as evidenced by 70 and 75% cell killing observed after treatment with these combinations. The synergy was confirmed by the CalcuSyn median effect analysis (Table 5-3).

The greatest synergy was found when combining an individual xanthone with α-mangostin at a higher concentration (2.5 µg/ml) rather than a lower one (1.25 µg/ml). In contrast, when an individual xanthone was used with 1.25 µg/ml of α-mangostin, for example, α-mangostin (1.25 µg/ml) with gartanine (1.25, 2.5 and 5 µg/ml) (Figure 5-3E), antagonism to different extent was observed at some of these combinations. When α-mangostin was combined with γ-mangostin (Figure 5-3C), only additive effect or slight antagonism was found.
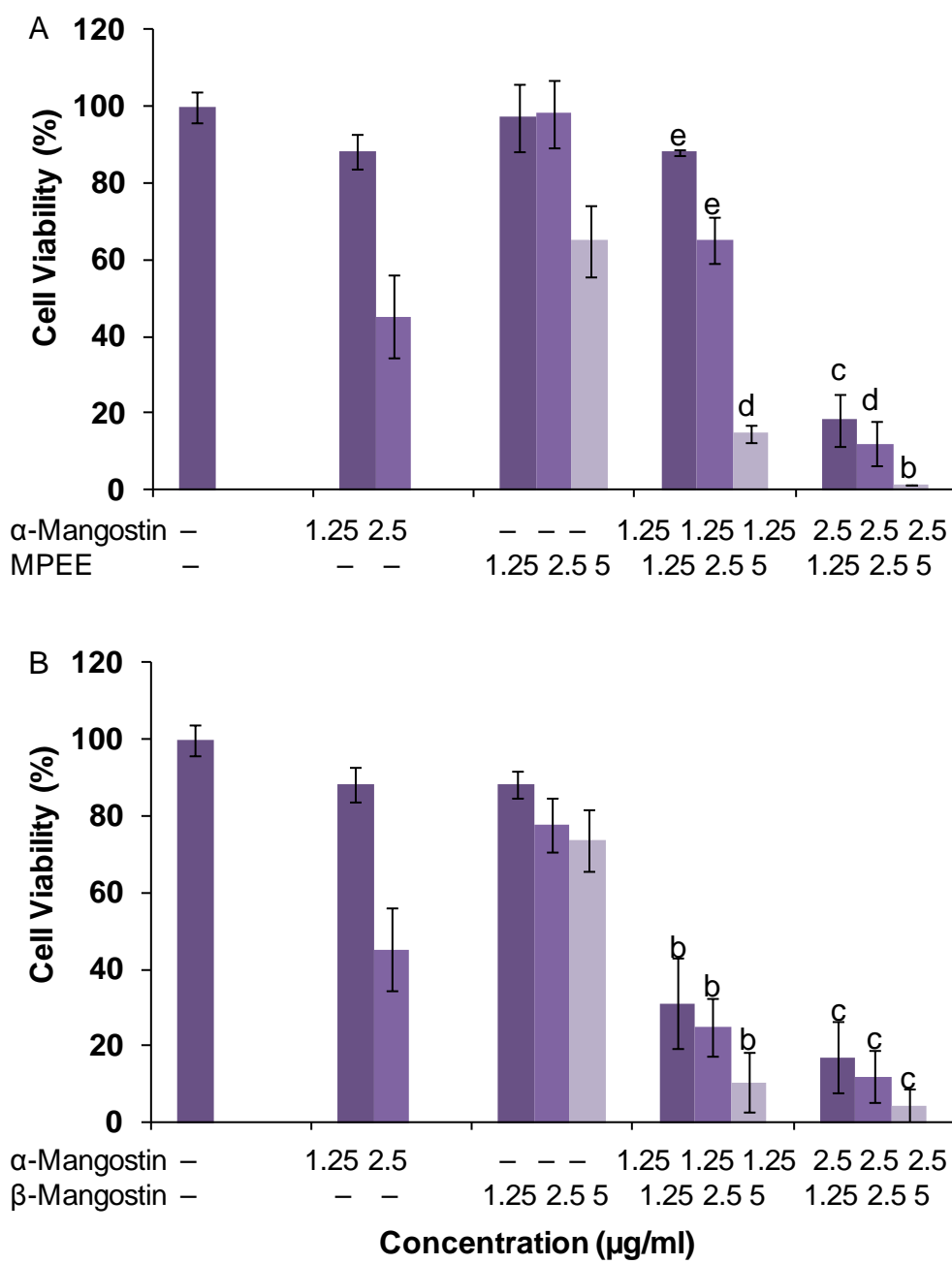
Figure 5-3

(Continued)
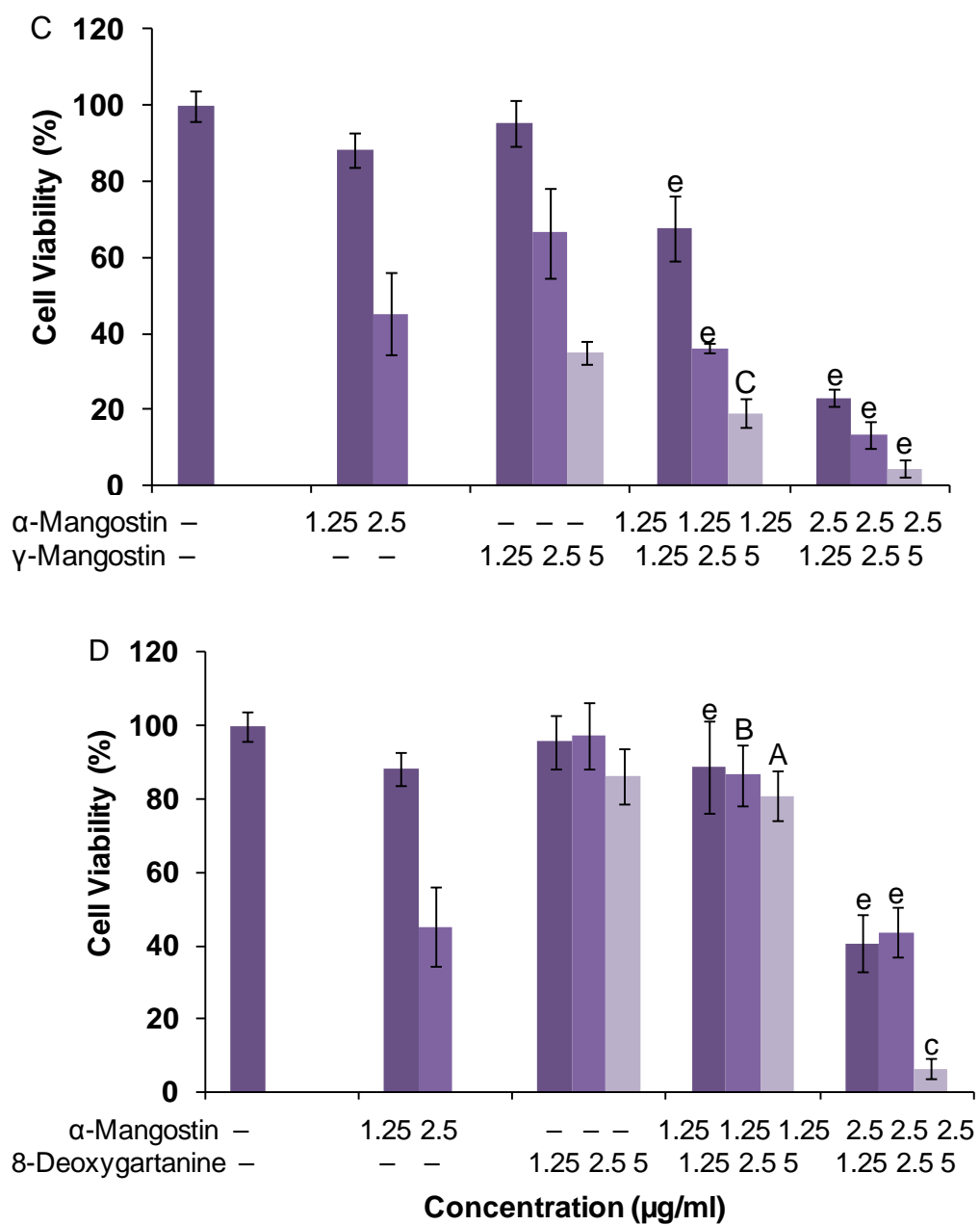
Figure 5-3

(Continued)
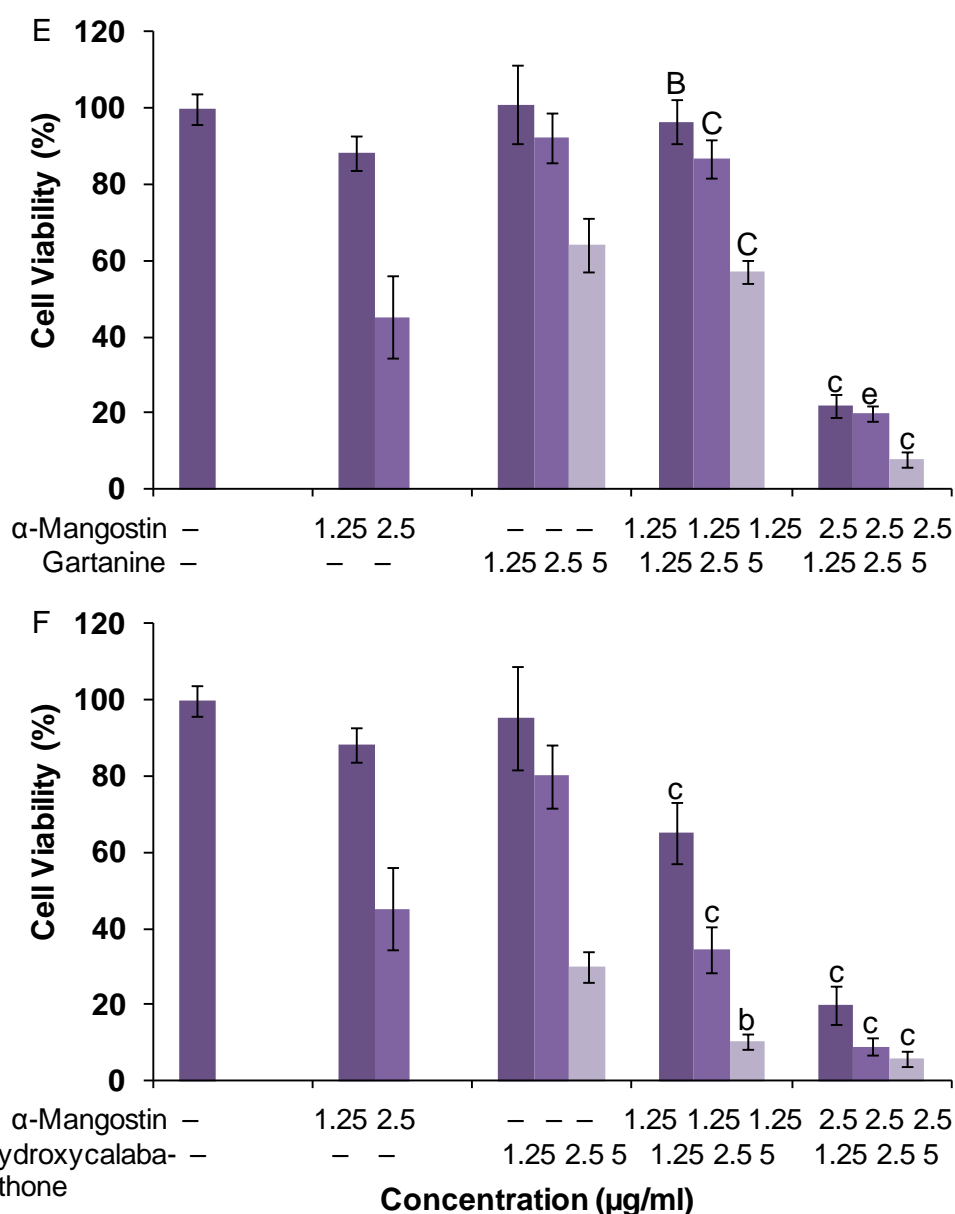
Figure 5-3
Cell viability of A-431 cells was investigated using the Crystal Violet assay after 48-h treatment in the presence of the indicated concentrations of an individual xanthone alone or in combination of α-mangostin with: A. MPEE; B. β-mangostin; C. γ-mangostin; D. 8-deoxygartanine; E. gartanine; F: 9-hydroxycalabaxanthone. Data are presented as mean ± SEM of three independent experiments performed in six replicates. The interaction effect of the combination was analysed using CalcuSyn (Section 1.2.6). The degree of different interaction effect was indicated by the combination index (CI) value as labeled with different letters: range of CI values of 0.1-0.3 (a. strong synergism), 0.3-0.7 (b. synergism), 0.7-0.85 (c. moderate synergism), 0.85-0.9 (d. slight synergism), 0.9-1.1 (e. nearly additive), 1.1-1.2 (C. slight antagonism), 1.2-1.45 (B. moderate antagonism), and 1.45-3.3 (A. Antagonism).

5.3.2.2 Effects of combinations α-mangostin with another xanthone on human melanoma SK-MEL-28 cells

As shown in Figure 5-4, synergistic antiproliferative effect on SK-MEL-28 was observed when α-mangostin (5 µg/ml) was used with all the other xanthones tested (1.25, 2.5, 5 µg/ml). For example, when used alone, α-mangostin at 5 µg/ml and MPEE at 1.25, 2.5 and 5 µg/ml induced 35, 14, 12, and 23% of cell killing. However, the combination of α-mangostin (5 µg/ml) and MPEE at 1.25, 2.5 and 5 µg/ml, respectively, induced 92, 98, and 99% of cell killing (Figure 5-4 A). Data analysis using CalcuSyn software confirmed the synergy (CI< 1) across different concentrations and different combinations between α-mangostin and another xanthone (Table 5-3).

Synergistic effect to a lesser extent or an additive effect was found when the other xanthones were used with α-mangostin at 2.5 µg/ml. This finding is similar to that found with A-431 cells.
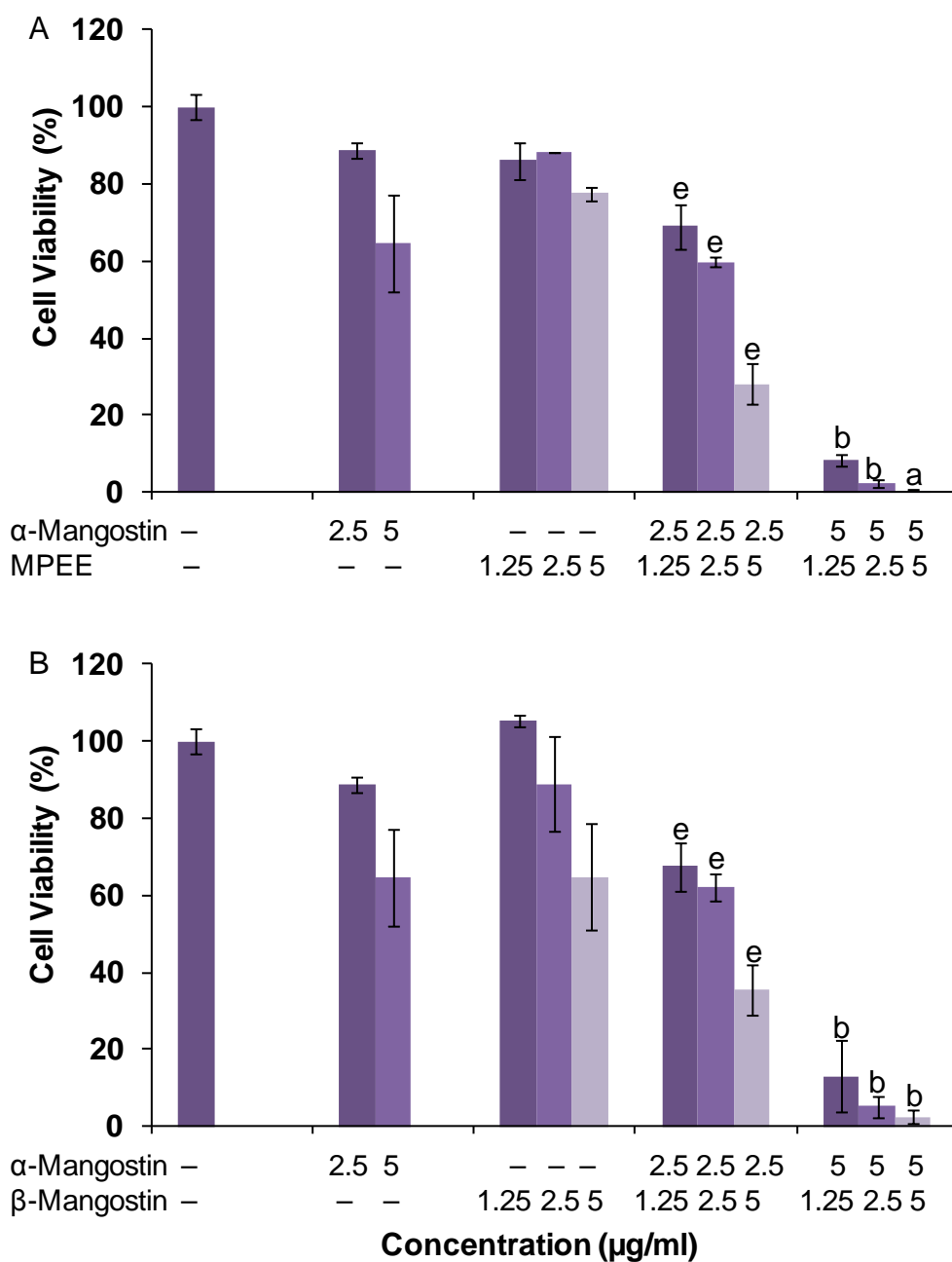
Figure 5-4

(Continued)
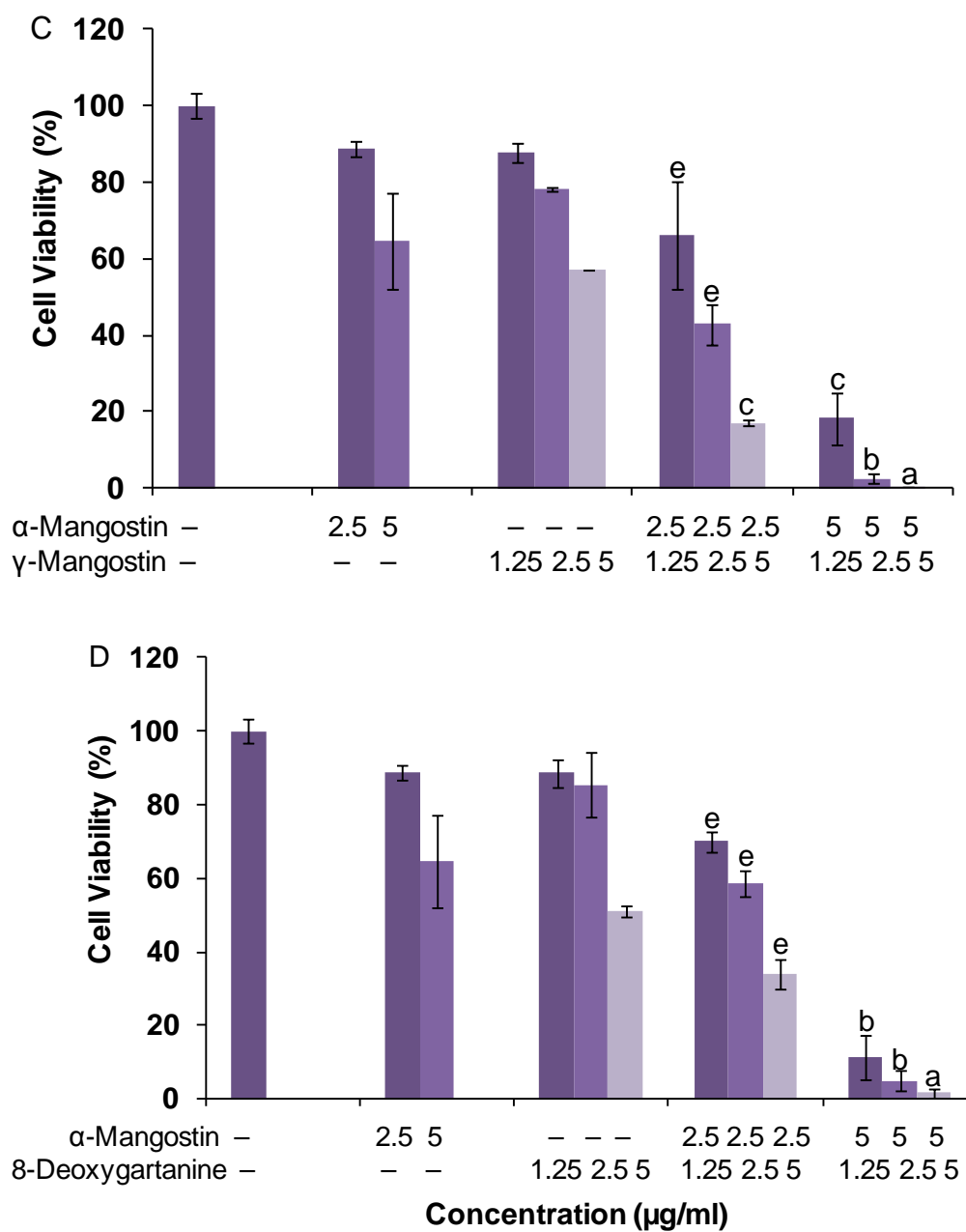
Figure 5-4

(Continued)
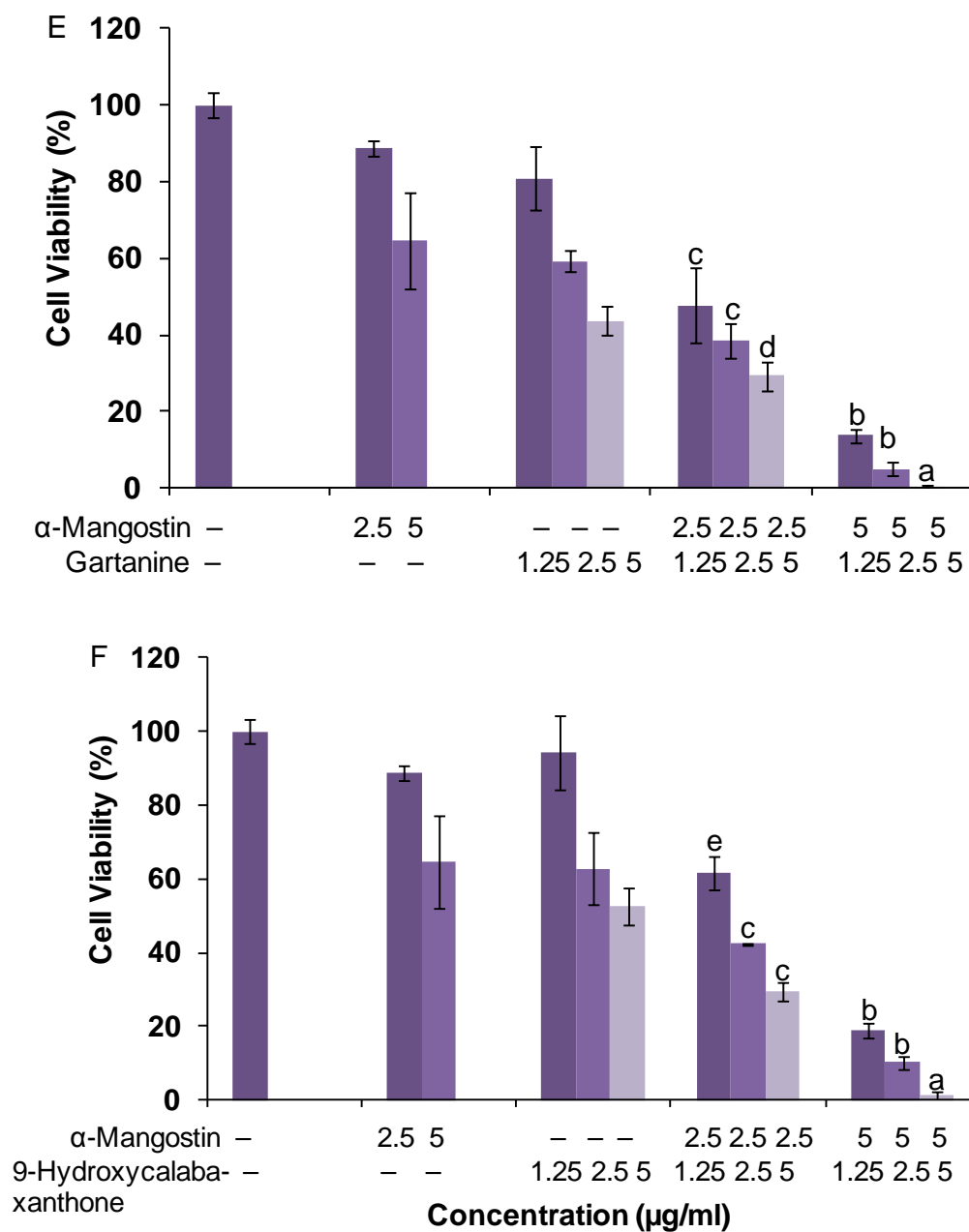
Figure 5-4
Cell viability of SK-MEL-28 cells was investigated using the Crystal Violet assay after 48-h treatment in the presence of the indicated concentrations of an individual xanthone alone or in combination of α-mangostin with: A. MPEE; B. β-mangostin; C. γ-mangostin; D. 8-deoxygartanine; E. gartanine; F: 9-hydroxycalabaxanthone. Data are presented as mean ± SEM of three independent experiments performed in six replicates. The interaction effect of the combination was analysed using CalcuSyn (Section 1.2.6). The degree of different interaction effect was indicated by the combination index (CI) value as labeled with different letters: range of CI values of 0.1-0.3 (a. strong synergism), 0.3-0.7 (b. synergism), 0.7-0.85 (c. moderate synergism), 0.85-0.9 (d. slight synergism), 0.9-1.1 (e. nearly additive), 1.1-1.2 (C. slight antagonism), 1.2-1.45 (B. moderate antagonism), and 1.45-3.3 (A. Antagonism).

Table 5-3

Combination Index (CI) values for the cytotoxicity induced by different combinations of α-mangostin with another xanthones on A) A-431 cells and B) SK-MEL-28 cells. The concentration unit for the xanthones is µg/ml. Combination analyses were performed using CalcuSyn software, as indicated in Section 5.2.5.

A. A-431

	MPEE			β-Mangostin			γ-Mangostin			8-Deoxygartanine			Gartanine			9-hydroxycalabaxanthone		
	1.25	2.5	5	1.25	2.5	5	1.25	2.5	5	1.25	2.5	5	1.25	2.5	5	1.25	2.5	5
α-Mangostin (1.25)	1.05	1.10	0.86	0.57	0.61	0.64	1.02	1.01	1.20	1.03	1.43	1.86	1.42	1.19	1.20	0.84	0.75	0.58
α-Mangostin (2.5)	0.84	0.87	0.61	0.79	0.81	0.70	0.97	1.02	0.99	1.02	1.19	0.75	0.83	0.91	0.85	0.82	0.71	0.72

B. SK-MEL-28

	MPEE			β-Mangostin			γ-Mangostin			8-Deoxygartanine			Gartanine			9-hydroxycalabaxanthone		
	1.25	2.5	5	1.25	2.5	5	1.25	2.5	5	1.25	2.5	5	1.25	2.5	5	1.25	2.5	5
α-Mangostin (2.5)	1.16	1.08	1.04	0.96	1.07	0.93	1.08	0.96	0.73	1.09	1.05	0.93	0.80	0.84	0.89	0.95	0.81	0.79
α-Mangostin (5)	0.55	0.37	0.25	0.60	0.45	0.39	0.74	0.33	0.12	0.55	0.41	0.27	0.60	0.39	0.14	0.70	0.56	0.23

5.3.3 Potential mechanisms of observed synergistic effects

The underlying mechanisms for the synergistic effect of different combinations of xanthone compounds were investigated using cell cycle analysis and apoptosis analysis.

5.3.3.1 The modulatory effect on cell cycle regulation after treatment with combination of α-mangostin with another xanthone in skin cancer cells

For the A-431 cell line, treatment with α-mangostin (2.5 µg/ml) and MPEE (1.25 µg/ml) alone did not show any effect on the cell cycle regulation, while treatment with β-mangostin, γ-mangostin, 8-deoxygartanine, gartanine, and 9-hydroxycalabaxanthone increased the cell distribution in G_0/G_1 phase. α-Mangostin combined with the other tested xanthones did not induce any synergistic effect on the cell cycle arrest in G_0/G_1 phase. However, some of the tested combinations induced a synergistic effect on the sub G_1 peak. These combinations were 2.5 µg/ml of α-mangostin with 1.25 µg/ml of β-mangostin ($P< 0.05$), γ-mangostin ($P< 0.01$), 9-hydroxycalabaxanthone ($P< 0.01$), and gartanine ($P< 0.05$), respectively (Figure 5-5).

For the SK-MEL-28 cell line, treatment with an individual xanthone alone at the indicated concentration had no effect on the cell cycle regulation. However, a significant positive synergistic response on the increase of $subG_1$ phase was found when α-mangostin (5 µg/ml) was used with 1.25 µg/ml of MPEE (Figure 5-6, $P< 0.01$) and γ-mangostin (Figure 5-6; $P< 0.01$), respectively. Additionally, a significant positive synergistic response on the increase of G_0/G_1 phase was found when α-mangostin (5 µg/ml) was combined with 1.25 µg/ml of β-mangostin ($P< 0.05$).
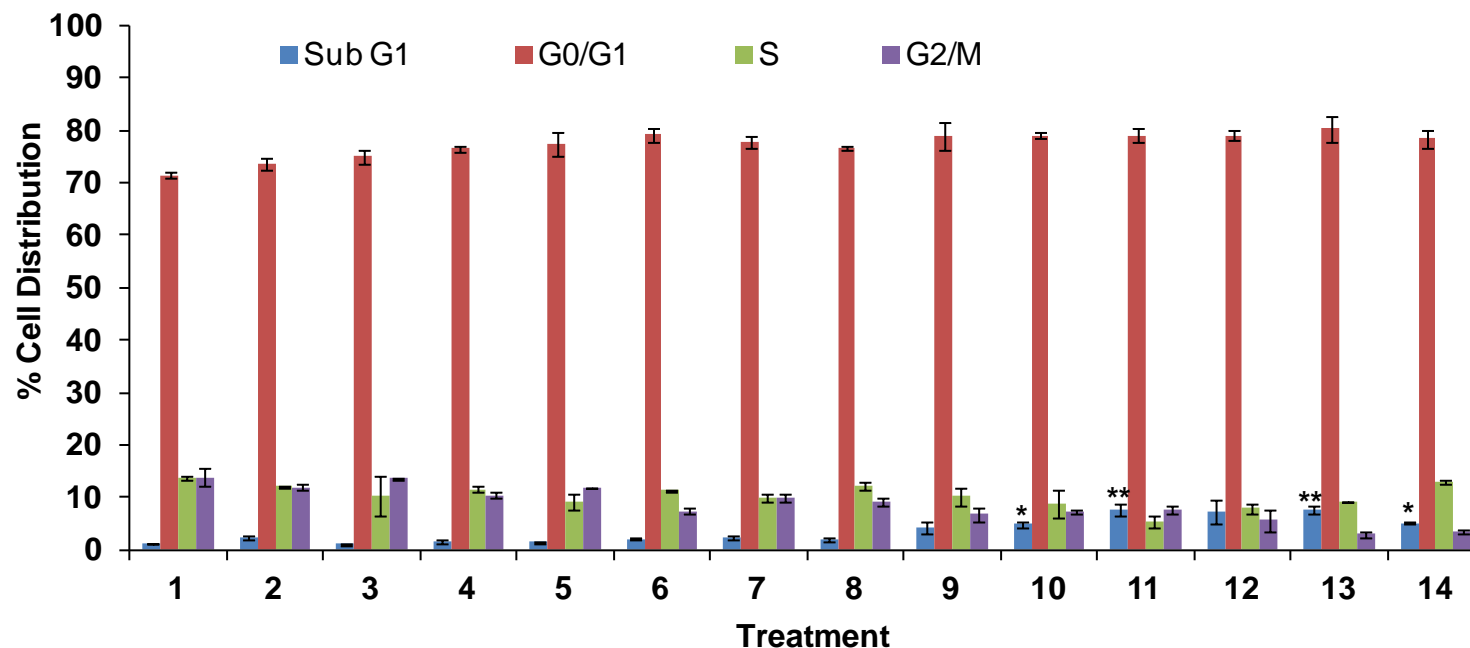
Figure 5-5

Cell distribution (%) in each cell cycle phase of A-431 cells was investigated using prodium iodide staining as detected by flow cytometry after 48-h treatment in the presence of the indicated concentrations of individual xanthone alone or in combination with α-mangostin: 1: untreated control; 2-7: xanthone compound alone (2: α-mangostin (2.5 µg/ml), 3-8: 1.25 µg/ml of MPEE, β-mangostin, γ-mangostin, 8-deoxygartanine, 9-hydroxycalabaxanthone, and gartanine, respectively); 9-14: combination of α-mangostin with MPEE, β-mangostin, γ-mangostin, 8-deoxygartanine, 9-hydroxycalabaxanthone, and gartanine, respectively. The values are shown as the mean ± SEM of 3 independent experiments. Synergy was tested by two-way ANOVA where significance ($P < 0.05$ as * and $P < 0.01$ as **) indicates that the combination produced a non-additive response compared with the individual compound separately.

Figure 5-6

Cell distribution (%) in each cell cycle phase of SK-MEL-28 cells was investigated using prodium iodide staining as detected by flow cytometry after 48-h treatment in the presence of the indicated concentrations of individual xanthone alone or in combination with α-mangostin: 1: untreated control; 2-7: xanthone compound alone (2: α-mangostin (5 µg/ml), 3-8: 1.25 µg/ml of MPEE, β-mangostin, γ-mangostin, 8-deoxygartanine, 9-hydroxycalabaxanthone, and gartanine, respectively); 9-14: combination of α-mangostin with MPEE, β-mangostin, γ-mangostin, 8-deoxygartanine, 9-hydroxycalabaxanthone, and gartanine, respectively. The values are shown as the mean ± SEM of 3 independent experiments. Synergy was tested by Two-way ANOVA where significance ($P< 0.05$ as * and $P< 0.01$ as **) indicates that the combination produced a non-additive response compared with the individual compound separately.

5.3.3.2 Apoptosis-inducing effect after treatment with combinations of α-mangostin with another xanthone in skin cancer cells

In A-431 cells, the apoptotic cells were generally less than 6% when cells were treated with the tested xanthones as single agents at the indicated concentration (Figure 5-7). However, combinations of 2.5 µg/ml α-mangostin with 1.25 µg/ml MPEE, β-mangostin, γ-mangostin, or 9-hydroxycalabaxanthone, synergistically increased the apoptosis when compared to that of cells treated with the corresponding individual xanthone alone. The most significant effect was with the α-mangostin and β-mangostin combination, which induced approximately 30% apoptosis ($P<0.01$; Figure 5-7). In contrast, combinations of 2.5 µg/ml α-mangostin with 1.25 µg/ml 8-deoxygartanine or gartanine did not increase apoptosis synergistically.

Similar results were found on SK-MEL-28 cells. Cells treated with 5 µg/ml of α-mangostin showed significant increases (22.3-38.5 %) in apoptosis in combination with 1.25 µg of separate individual xanthones. Significant synergy was found between α-mangostin and MPEE ($P<0.01$), β-mangostin ($P<0.01$), γ-mangostin ($P<0.01$), and 8-deoxygartanine ($P<0.05$), respectively (Figure 5-8).
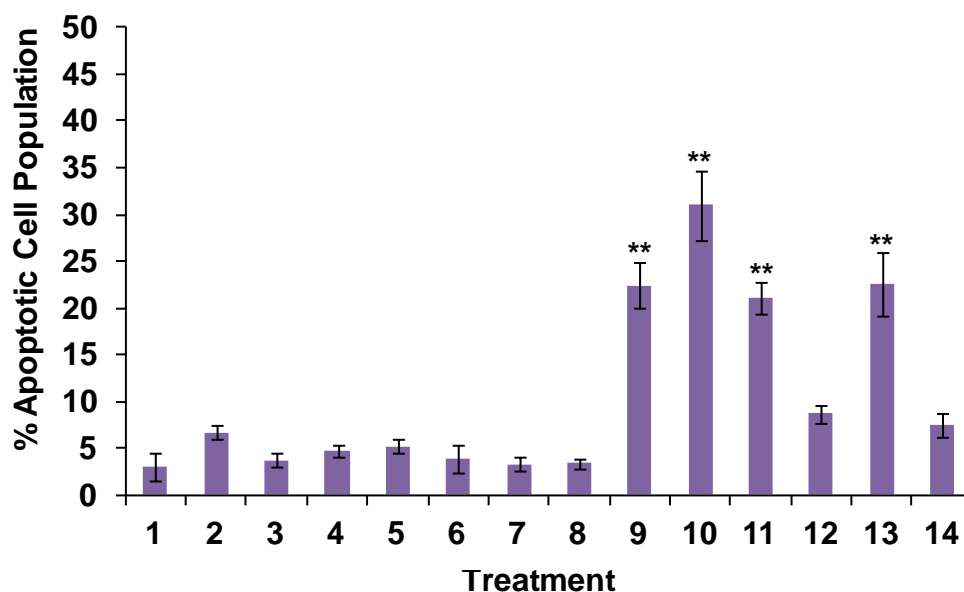
Figure 5-7

Apoptotic cell population induced in A-431 cells was investigated using prodium iodide and Annexin-V FITC staining as detected by flow cytometry after 48-h treatment in the presence of the indicated concentrations of individual xanthone alone or in combination with α-mangostin: 1: untreated control; 2-7: xanthone compound alone (2: α-mangostin (2.5 µg/ml), 3-8: 1.25 µg/ml of MPEE, β-mangostin, γ-mangostin, 8-deoxygartanine, 9-hydroxycalabaxanthone, and gartanine, respectively); 9-14: combination of α-mangostin with MPEE, β-mangostin, γ-mangostin, 8-deoxygartanine, 9-hydroxycalabaxanthone, and gartanine, respectively. The values are shown as the mean ± SEM of 3 independent experiments. Synergy was tested by Two-way ANOVA where significance ($P < 0.05$ as * and $P < 0.01$ as **) indicates that the combination produced a non-additive response compared with the individual compound separately.

Figure 5-8

Apoptotic cell population induced in SK-MEL-28 cells was investigated using prodium iodide and Annexin-V FITC staining as detected by flow cytometry after 48-h treatment in the presence of the indicated concentrations of individual xanthone alone or in combination with α-mangostin: 1: untreated control; 2-7: xanthone compound alone (2: α-mangostin (5 µg/ml), 3-8: 1.25 µg/ml of MPEE, β-mangostin, γ-mangostin, 8-deoxygartanine, 9-hydroxycalabaxanthone, and gartanine, respectively); 9-14: combination of α-mangostin with MPEE, β-mangostin, γ-mangostin, 8-deoxygartanine, 9-hydroxycalabaxanthone, and gartanine, respectively. The values are shown as the mean ± SEM of 3 independent experiments. Synergy was tested by Two-way ANOVA where significance ($P< 0.05$ as * and $P< 0.01$ as **) indicates that the combination produced a non-additive response compared with the individual compound separately.

## 5.4 Discussion

5.4.1 No synergy observed when xanthones in combination with commercial drugs

In the current study, no synergistic effect was observed between xanthone compounds and 5-FU in the two skin cancer cell lines. This might be explained by the cell cycle-mediated drug resistance as proposed by Shah and Schwartz (2001). For example, simultaneous combination of fuorouracil and irinotecan demonstrated anatagonism in HT-29 colon cancer cells (Guichard *et al.* 1997). 5-FU has been reported to be an S phase active agent, with no effect on cells in G_0 or G_1 (Shah & Schwartz 2001). However, irinotecan induced a cell cycle arrest in G_2 phase in HT-

208

29 cells, thus creating resistance to 5-FU (Guichard *et al.* 1997). Similarly, in the current study, MPEE and xanthone compounds induced cell cycle arrest in subG$_1$ phase in A-431 cells (Figure 4-2A), making 5-FU therapy ineffective. In contrast, a synergistic effect was observed between α-mangostin and 5-FU on human colon cancer DLD-1 cells (Nakagawa *et al.* 2007). The authors suggested that the synergy was possible due to cell cycle arrest at the concentrations tested (Nakagawa *et al.* 2007). According to Shah & Schwartz (2001), an antagonism should be expected instead of synergism, since α-mangostin induced a G$_1$ phase arrest in DLD-1 cells (Nakagawa *et al.* 2007). This discrepancy might be explained by the complex of cellular response. As discussed in Chapter 3 & 4, different cell lines exhibit different responses to each specific xanthone compound. Therefore, different anti-proliferative responses of the combinations of xanthone compounds with 5-FU may be expected on different cancer cell lines. Also, in Nakagawa *et al.* (2007) study, it should be noted that the synergy was only found at lower concentrations when the total concentrations were 2 and 5 µM, respectively, and antagonistic effect was found at higher concentrations. This phenomenon suggests that the interaction between compounds is not only associated with their efficacy, but also with their concentrations used (Bava *et al.* 2005).

No synergistic effect was observed between xanthones and DTIC under the tested conditions in the two types of skin cancer cells. A synergy between plitidepsin and DTIC was previously reported to contribute to their different signaling leading to apoptosis. Inhibition of VEGF by plitidepsin could also enhance the effect of DTIC, because DTIC has been shown to induce VEGF expression in melanoma cells (Broggini *et al.* 2003; Lev *et al.* 2003). It was reported that synergy occurs when the

stimuli act through different mechanisms (Schmidt 2008). The tested xanthones have been demonstrated to induce cytotoxicity through inducing cell cycle arrest and apoptosis and inhibiting MAPK, NFκB and Akt survival pathways, as discussed in Chapter 4. The mechanism of action of DTIC is via induction of methylating nucleic acids or direct DNA damage leading to cell death, but the exact mechanism is still not fully understood (Eggermont & Kirkwood 2004; Soengas & Lowe 2003). Xanthones and DTIC may work through a similar mechanism, or they may block each other's pathways. DTIC has been reported to induce transcriptional upregulation of the expression of IL-8 via activation of NFκB and MAPK pathways (Lev *et al.* 2003). Therefore, the inhibitory effect of the tested xanthones on these two pathways is compromised by DTIC, resulting in no synergistic effect. To clarify this, more work on the mechanism of action of each drug and compound needs to be carried out in the future. For example, the changes of protein level of NFκB and Akt can be determined after treatment with individual xanthone, DTIC, and combination of xanthone and DTIC.

5.4.2 Synergy found between α-mangostin and another xanthone in inhibiting skin cancer cell proliferation

Synergistic effects were observed when α-mangostin was used with other xanthones at indicated concentrations on both A-431 and SK-MEL-28 cell lines as shown in the results section (Figures 5-3 & 4). Interestingly, more combinations were found to be synergistic against the SK-MEL-28 compared to the A-431 cell line. The reason for this might be that α-mangostin worked through distinctly different pathways to the other xanthones on SK-MEL-28, i.e. α-mangostin activated both extrinsic and intrinsic pathways, while the other xanthones only activated intrinsic pathways (Figure 4-4B; Figure 4-5B; Figure 4-6B). In contrast, all the xanthones tested worked through similar pathways in A-431 as discussed in Chapter 4. Furthermore, the

synergistic antiproliferative effect was greater when xanthones were combined with a higher concentration of α-mangostin in both skin cancer cell lines. This indicates that the interaction of natural compounds can be influenced by their concentrations (Bava *et al.* 2005).

The underlying mechanism of the observed synergy was investigated using cell cycle analysis and apoptosis analysis. The synergy observed with the combined treatments at tested concentrations was probably due to enhancement of mechanisms leading to apoptosis induction as evidenced by the increase in $subG_1$ peak and apoptosis on A-431 cells and SK-MEL-28 cells. Consistent with the results from the Crystal Violet assay, the synergistic effect was more significant in SK-MEL-28 than in A-431 cell line. For example, the combination of α-mangostin (2.5 µg/ml) and MPEE (1.25 µg/ml) induced 22.5% apoptosis in A-431 cell line (Figure 5-7), while that of α-mangostin (5 µg/ml) and MPEE (1.25 µg/ml) induced 38.5% apoptosis in SK-MEL-28 cell line (Figure 5-8). As shown in Chapter 4, α-mangostin (5 µg/ml) and MPEE (5 µg/ml) alone induced 38.0% and 5.0% apoptosis respectively in A-431 cell line, while α-mangostin (7.5 µg/ml) and MPEE (10 µg/ml) induced 29.3% and 3.3% apoptosis respectively in SK-MEL-28. Therefore, even though the combination of α-mangostin and MPEE induced synergistic apoptotic effect on both skin cancer cell lines, the effect was greater on SK-MEL-28 because the combination of compounds exhibited a larger incremental increase in apoptotic activity than the additive effect of both compounds on SK-MEL-28 than on A-431 cell line. This result suggests that this combination may be promising in the treatment of melanoma. The findings also support the theory that synergy occurs if the compounds work through different mechanisms. For example, on SK-MEL-28 cells, α-mangostin is the only compound

that could induce apoptosis through both intrinsic and extrinsic pathways and inhibit all three tested survival pathways. In contrast, the other tested compounds only could induce cellular and/or molecular responses through one or more pathways. Additionally, the magnitude of apoptosis induced by individual xanthone was remarkably different, with 30% induced by α-mangostin (7.5 µg/ml) and less than 10% by other tested xanthones (10 µg/ml) (Figure 4-3B). This implies that the potential of apoptosis induction between α-mangostin and other tested xanthones are distinctly different, probably contributing to the enhancement of anti-melanoma effect when α-mangostin and another xanthone were used simultaneously. These results from the current study also indicate that even the same combination of compounds could evoke different responses on different cell lines.

5.5 Summary

This study is the first demonstration of synergy between two xanthone compounds on human skin cancer cells. Significant synergistic antiproliferative effect was observed when α-mangostin was combined with some of the tested xanthones at specific concentrations in both skin cancer cell lines. The synergistic effects achieved by this combined treatments are possibly due to the enhancement of the mechanisms of action leading to apoptosis, and the exact underlying mechanism warrants further investigation. Compared to A-431 cell line, the synergistic effect was found to be greater in SK-MEL-28 cell line because the compounds act through different mechanisms in this cell line. Importantly, the response to any one combination of compounds was found to be significantly different with different cell types and concentrations of compounds.

CHAPTER 6
ANTI-METASTATIC EFFECT OF α-MANGOSTIN ON HUMAN SKIN CANCER CELLS

6.1 Introduction

Metastasis is the major cause of cancer treatment failure, responsible for 90% of human cancer deaths (Weigelt *et al.* 2005). Melanoma is aggressive because of its high tendency to metastasise. In patients with advanced metastatic melanoma, the 10-year survival rate for patients is less than 10% (Balch *et al.* 2001; Tarhini & Agarwala 2006; Tsao & Sober 2005). Nonmelanoma skin cancers are also invasive and metastatic even though the metastasis rate is much lower than that of melanoma (Kwa *et al.* 1992; Miller 1991). Therefore, blocking cancer cell invasion and metastasis are critical targets for therapeutic treatment of skin cancers.

Many natural compounds have been reported to possess the capacity to inhibit melanoma metastasis, as discussed in Chapter 1. They include 4-nerolidylcatechol (Brohem *et al.* 2009), γ-tocotrienol (Chang *et al.* 2009), curcumin (Banerji *et al.* 2004; Lin *et al.* 1998), and aqueous extract of the root of *Platycodon grandiflorum* (Lee *et al.* 2006). However, limited information is available on the anti-metastatic activity of natural products on squamous cell carcinoma.

α-Mangostin exhibited anti-metastatic activity on human prostate cancer, lung adenocarcinoma and breast adenocarcinoma cells (Hung *et al.* 2009; Lee *et al.* 2010; Shih *et al.* 2010) (Chapter1 Section 1.3.4.3). This compound and panaxanthone (a mixture of α-mangostin and γ-mangostin) also showed significant suppression of mammary cancer metastasis *in vivo* (Doi *et al.* 2009; Shibata *et al.* 2011) (Section 1.3.4.3). The anti-metastatic activities of α-mangostin have been found to be cancer-cell type dependent because different sensitivities and mechanisms have been observed after treatment with α-mangostin on different cell lines, as discussed in

Chapter1 Section 1.3.4.3. For example, treatment with α-mangostin inhibited JNK1/2 pathway but not ERK1/2 pathway on human prostate cancer PC3 cells (Hung *et al.* 2009). In contrast, treatment with α-mangostin inhibited ERK1/2 pathway but not JNK1/2 pathway in human lung adenocarcinoma A549 (Shih *et al.* 2010) and human breast adenocarcinoma MCF-7 cells (Lee *et al.* 2010). Due to these differences, questions regarding the roles of α-mangostin in the metastasis of human skin cancer cell lines and its potential underlying mechanisms could not be answered based on currently available literature.

The aim of this chapter is therefore to investigate the anti-metastatic effects of α-mangostin on human squamous carcinoma A-431 and melanoma SK-MEL-28 cell lines by examining *in vitro* motility, adhesion, migration, invasion, and the ability to regulate the metastasis-related gene expressions. In orderto ensure the anti-metastatic activity of α-mangostin was not due to its cytotoxicity, non-toxic concentrations as detected by the Crystal Violet assay are applied in the subsequent experiments in this Chapter.

6.2 Materials and methods

6.2.1 Materials

Bovine serum albumin (BSA) and 4′, 6-diamidino-2-phenylindole dihydrochloride (DAPI) were purchased from Sigma-Aldrich. Fibronectin and type I collagen were from BD Biosciences (Bedford, MA, USA). All other the reagents and chemicals used in this chapter were of analytical grade from Merck or tissue culture tested grade from Sigma-Aldrich unless otherwise noted.

6.2.2 Cell lines and cell culture

Human squamous cell carcinoma A-431 and melanoma SK-MEL-28 cell lines were used *in vitro* model in this Chapter. For description of the cell lines and cell culture refer to Section 3.2.2.

6.2.3 Treatment preparation

α-Mangostin was dissolved in absolute ethanol and diluted with medium to the desired treatment concentration. Vehicle volume was consistently kept as 1% (v/v) for each treatment.

6.2.4 Cell viability assay

The Crystal Violet assay (Section 3.2.6) was used to determine what concentrations of α-mangostin are non-toxic to A-431 and SK-MEL-28 cells. Briefly, cells were seeded at 1×10^4 cells/well in 96-well plates and incubated for 24 h. Cells were then treated with α-mangostin at various concentrations (0, 0.3125, 0.625, 1.25 and 2.5 µg/ml) for 48 h exposure duration. After treatment, cell culture medium was removed and cells were stained by 0.5% (w/v) crystal violet and destained with 33% (v/v) acetic acid. The absorbance was recorded on a microplate reader at the wavelength of 570 nm. The cytotoxic effect of α-mangostin was presented as the percentage of cell viability compared to untreated control cells.

The viability of skin cancer cells was above 80% when treated with α-mangostin at a range of low concentrations (from 0 to 2.5 µg/ml for SK-MEL-28 and from 0 to 1.25 µg/ml for A-431) (Figure A-19 in Appendix A12). Therefore, these non-toxic doses were used for all the subsequent experiments on the two types of skin cancer cells for the study of anti-metastatic activities.

6.2.5 Wound healing Assay

A wound healing assay was performed to determine the cell motility as previously described (Valster *et al.* 2005) with minor modification. Briefly, SK-MEL-28 and A-431 cells (5×10^5 cells/well) were seeded in a 6-well tissue culture plate and grown to 80-90% confluence. After the medium was removed, a gap with constant width was created in the centre of cell in each well by scratching the monolayer with a sterile yellow micropipette tip. After that, cells were rinsed with phosphate-buffered saline (PBS) twice to get rid of cellular debris, and then cells were exposed to various concentrations of α-mangostin (0, 0.625 and 1.25 µg/ml for A-431; 0, 1.25 and 2.5 for SK-MEL-28). The wound closure was monitored and photographed at 0, 24, and 48 h with the Olympus 1X71 phase contrast inverted fluorescence microscope and analySIS image capture software (magnification 100 ×). For each well, at least ten different areas of the scratch were photographed.

6.2.6 Boyden chamber invasion and migration assay

An *in vitro* invasion assay was conducted using a 24-well transwell unit (8 µm pore size) with polyvinylpyrrolidone-free polycarbonate filters coated with Matrigel and placed in transwell well chambers according to the manufacturer's instruction. The coated filters were rehydrated using serum-free medium for 2 h in the incubator at 37 ºC before use. Medium containing 10% (v/v) FBS and 10 µg/ml of fibronectin was applied to the lower chamber as chemoattractant. Cells (2×10^4 cells/well) in serum-free medium were seeded in the upper part of the transwell plate and incubated with various concentrations of α-mangostin for 48 h at 37 °C. After incubation, the cells in the upper surface of the membrane filter were carefully removed with a cotton swab and cells that had invaded across the Matrigel to the lower surface of the membrane were fixed with methanol and stained with 1 µg/ml of DAPI. The invasive cells on the lower surface of the membrane filter were recorded with Olympus 1X71 inverted

fluorescence microscope and analySIS image capture software at 200× and the cell number was counted by the Image J software. The data are presented as the average number of cells attached to the bottom surface from 10 randomly chosen fields. The experiments were repeated three times and each experiment was carried out in duplicate.

The migration assay was performed in a similar way to the invasion assay, except that no Matrigel coating was applied to the upper surface of the transwell filters.

6.2.7 Cell-matrix adhesion assay

The cell adhesion assay was performed as previously described (Sakamoto *et al.* 1996). 96-well cell culture plates were coated with type I collagen or fibronectin (200 ng/well) for 2 h at 37 ℃, followed by blocking with BSA (1 mg/ml) in PBS for 2 h at 37 ℃ and rinsing twice with PBS. After pretreatment with α-mangostin for 48 h, cells were detached with trypsin-EDTA. The suspended cells were washed once with DMEM culture medium containing 10% (v/v) FBS and twice with serum-free medium before being added to the wells at a density of 4×10^4 cells/well in 100 µl of serum-free medium. Subsequently, the cells were incubated in the incubator for 1 h. After that, floating cells were removed by PBS washes, and adherent cells were stained with 0.5% (w/v) crystal violet and destained with 33% (v/v) acetic acid. The absorbance was recorded on a microplate reader at the wavelength of 570 nm. The effect of α-mangostin on cell adhesion was presented as the relative percentage of attached cells compared to the untreated control cells.

6.2.8 Real-time polymerase chain reaction (qRT-PCR)

qRT-PCR was performed to determine mRNA expressions of different key genes (MMP-2, MMP-9, Akt1, NFκB, IκBα, and BRAF V600E) involved in the process of

metastasis in the A431 and SK-MEL-28 cells subjected to the indicated treatments. For description of this method refer to Section 4.2.7.

6.2.9 Statistical analysis

Data are expressed as mean (± SEM). The experiments were repeated at least three independent times. Statistical analysis of the data was carried out using ANOVA, followed by Tukey's HSD *post hoc* test (equal variances) or Dunnett's T3 *post hoc* test (unequal variances). These tests were performed using SPSS software (version 17). Difference was considered statistically significant when the *P*-value was less than 0.05 (significant) or 0.01 (highly significant).

6.3 Results

6.3.1 α-Mangostin inhibits the motility of skin cancer cells

α-Mangostin displayed inhibitory effect on cell motility of both A-431 and SK-MEL-28 cells after 24 h and 48 h of co-incubation at two different concentrations (Figure 6-1A&B), as evidenced by the lesser wound closure after treatment, compared with the untreated control. The inhibitory effect was found to be concentration-dependent. This was most marked for the concentration of 1.25 µg/ml for A-431 and 2.5 µg/ml for SK-MEL-28.

Figure 6-1
Effect of α-mangostin on the motility of A) A-431 and B) SK-MEL-28 cells was monitored by the wound healing assay as described in the method (Section 6.2.5). The wound closure was recorded at 0, 24, and 48 h by the Olympus 1X71 inverted fluorescence microscope and analySIS image capture software. The images shown here are from a representative experiment repeated three times with similar results (Scale bar 100 µm).

A) A-431
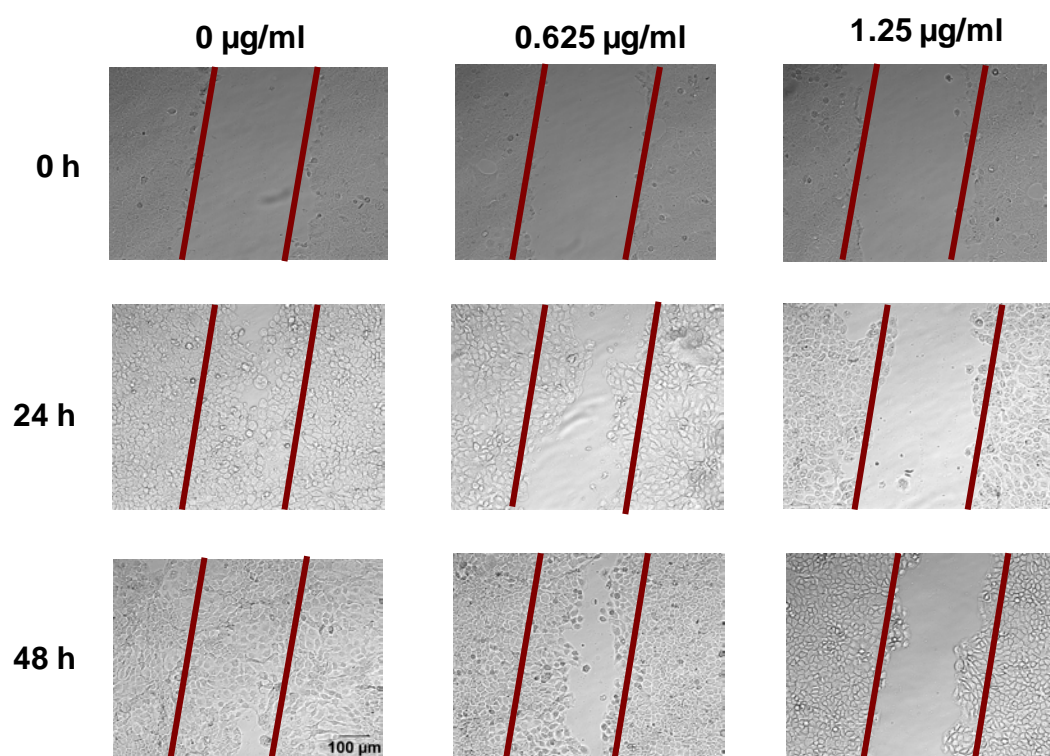
B) SK-MEL-28
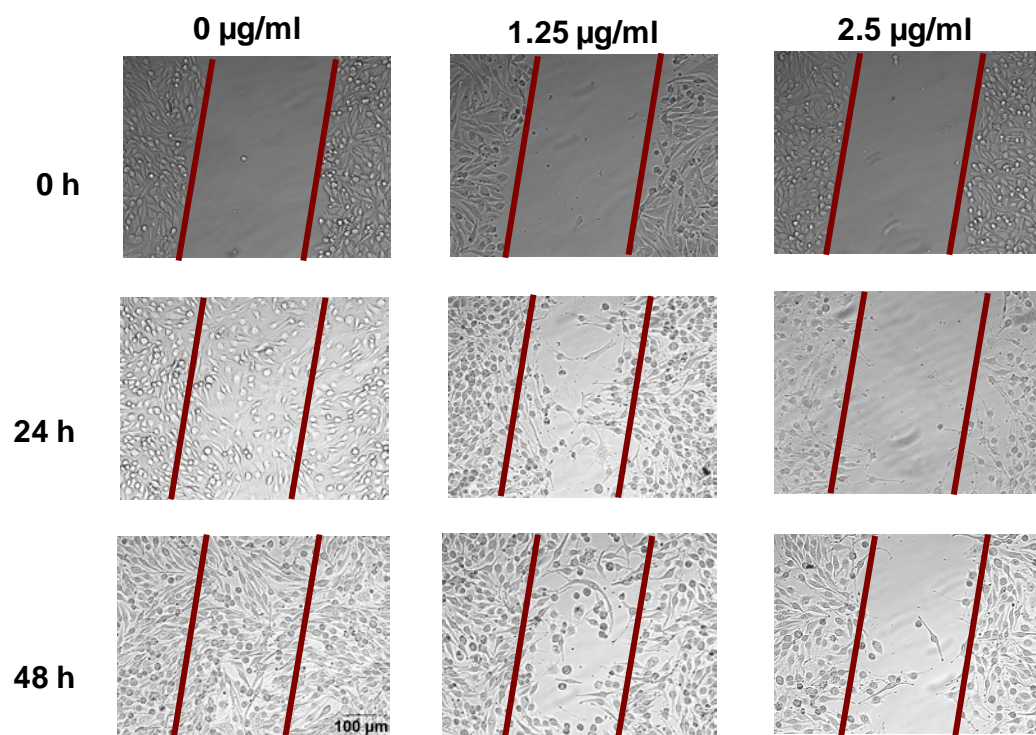
Figure 6-1

6.3.2 α-Mangostin inhibits the migration and invasion of skin cancer cells

Boyden chamber assay was used to measure the migratory and invasive potential of skin cancer cells after treatment with α-mangostin. α-Mangostin induced a dose-dependent decrease in migration and invasion with increasing concentration of α-mangostin on both A-431 and SK-MEL-28 cell lines ($P< 0.01$; Figure 6-2 & Figure 6-3). After treatment of A-431 cells with 1.25 µg/ml of α-mangostin, the migration and the invasion were reduced to 6% and 4% of the untreated control, respectively (Figure 6-2). After treatment of SK-MEL-28 cells with 2.5 µg/ml of α-mangostin, the migration and the invasion were reduced to 23% and 20% of the untreated control (Figure 6-3).
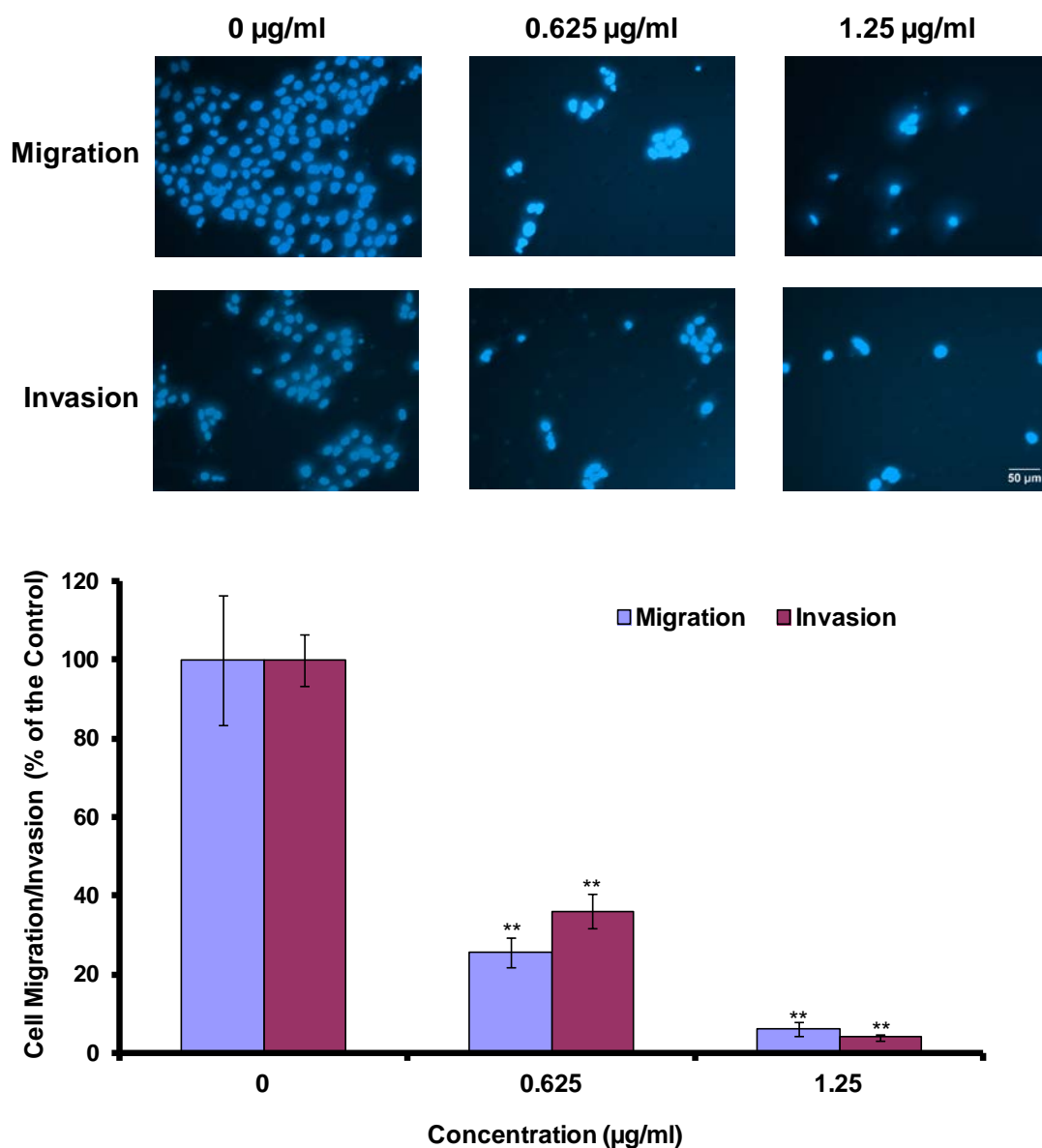
Figure 6-2

Effect of α-mangostin on migration and invasion of A-431 cells was detected by the Boyden Chamber assay as described in the method (Section 6.2.6). The migration and invasion of cells were recorded by the Olympus 1X71 inverted fluorescence microscope and analySIS image capture software and the cell number was counted by the Image J software (Scale bar 50 µm). The values are shown as the mean ± SEM of three independent experiments. Treatments significantly different from the untreated control at $P < 0.05$ are presented as * and at $P < 0.01$ as **.
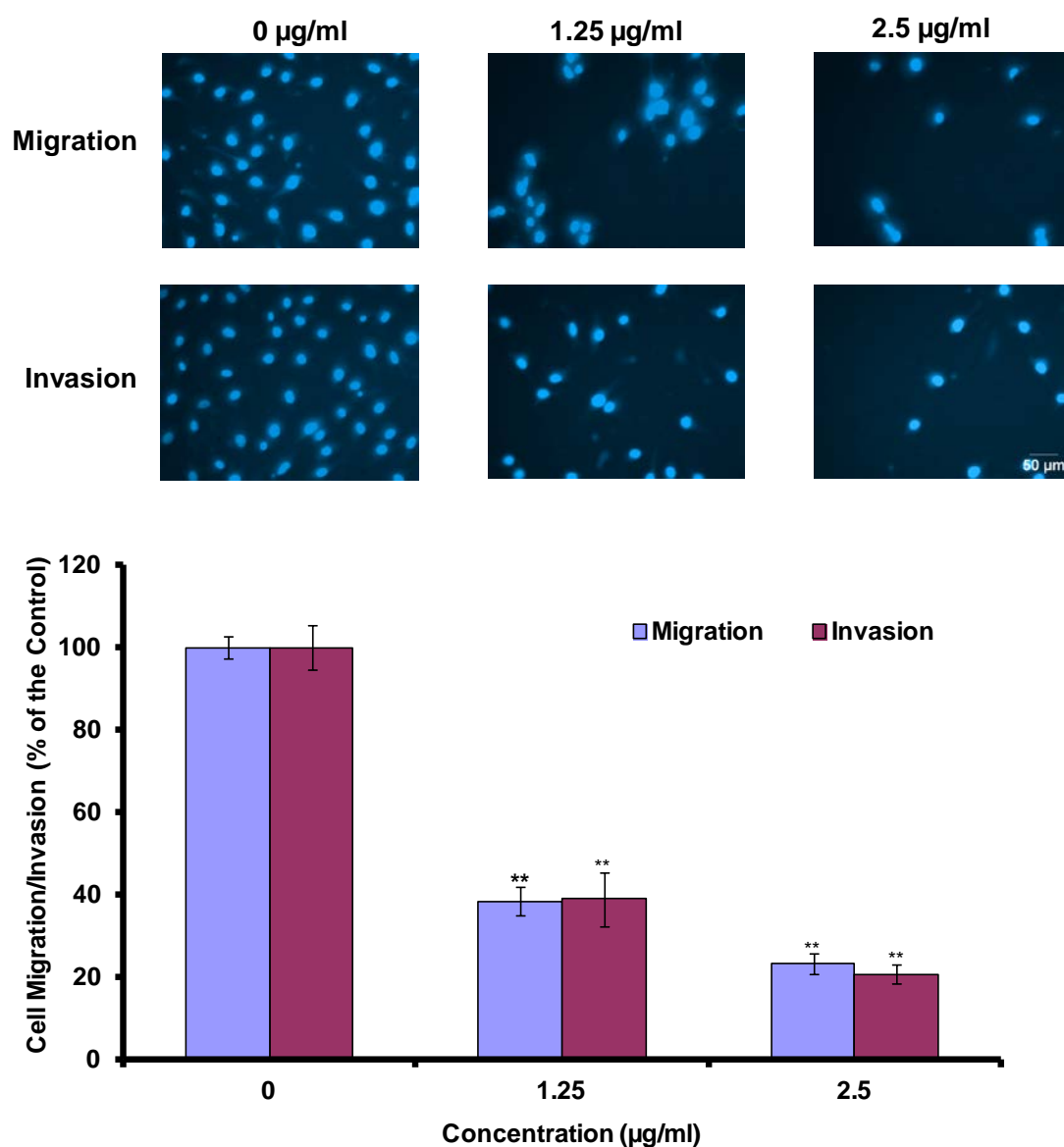
Figure 6-3

Effect of α-mangostin on migration and invasion of SK-MEL-28 cells was detected by the Boyden Chamber assay as described in the method (Section 6.2.6). The migration and invasion of cells were recorded by the Olympus 1X71 inverted fluorescence microscope and analySIS image capture software and the cell number was counted by the Image J software (Scale bar 50 µm). The values are shown as the mean ± SEM of three independent experiments. Treatments significantly different from the untreated control at $P <0.05$ are presented as * and at $P <0.01$ as **.

6.3.3 α-Mangostin inhibits the adhesion of skin cancer cells

As detected by the cell-matrix adhesion assay, α-mangostin was found to decrease the adherence of the skin cancer cells to fibronectin and type I collagen (Figure 6-4). The adhesive capability on fibronectin decreased to 54% for A-431 cells after treatment with 1.25 µg/ml α-mangostin ($P< 0.05$), and 63% for SK-MEL-28 cells after treatment with 2.5 µg/ml α-mangostin ($P< 0.05$). The adhesion ability on type I collagen decreased to 57% at 1.25 µg/ml of α-mangostin for A-431($P> 0.05$) and 59% at 2.5 µg/ml of α-mangostin for SK-MEL-28 ($P< 0.01$), respectively (Figure 6-4).
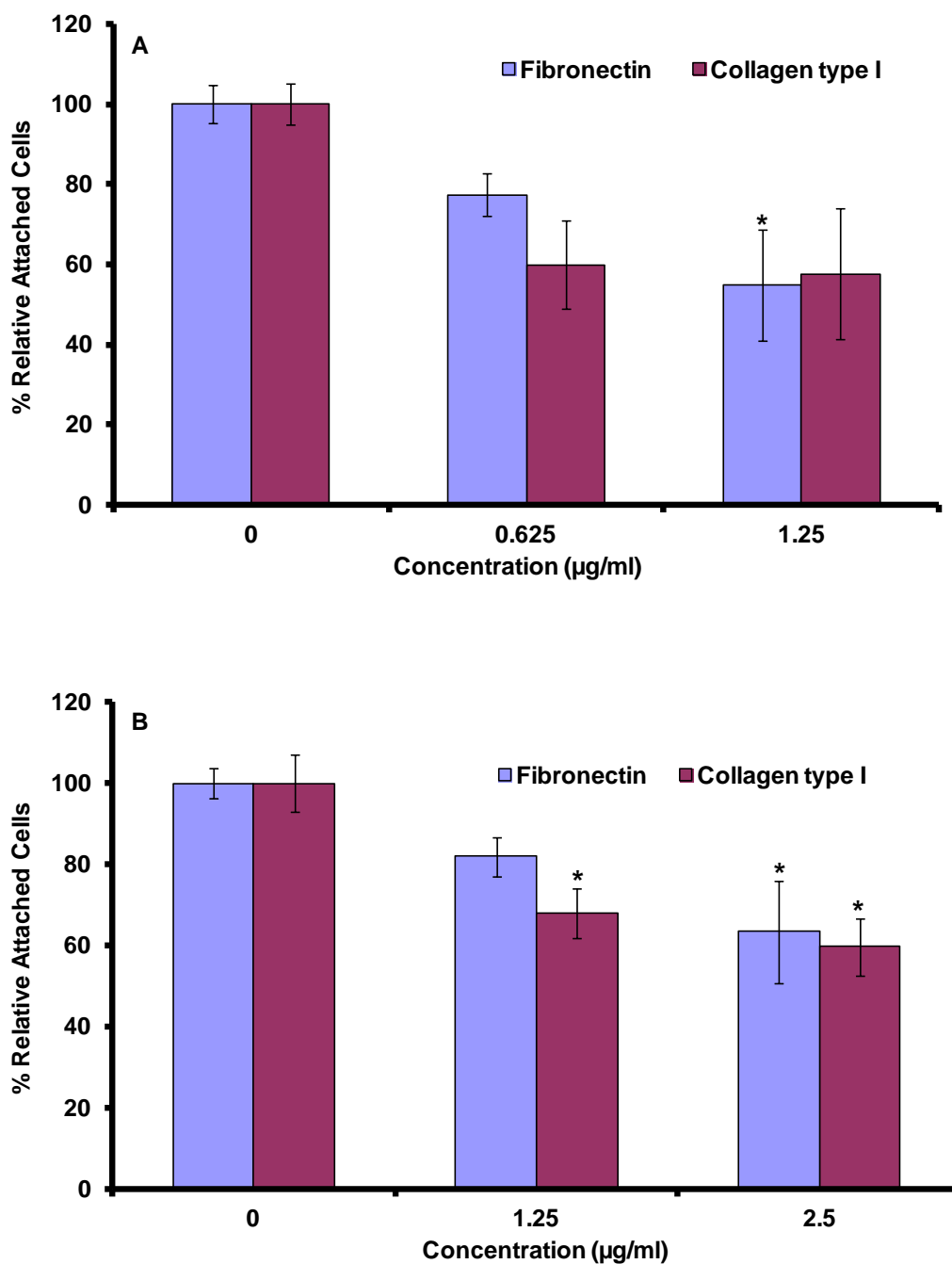
Figure 6-4

Effect of α-mangostin on the adhesion of A) A-431 and B) SK-MEL-28 cells to fibronectin and collagen type I was evaluated by the cell-matrix adhesion assay as described in the method (Section. 6.2.7). The values are shown as the mean ± SEM of three independent experiments. Treatments significantly different from the untreated control at $P <0.05$ are presented as * and at $P <0.01$ as **.

6.3.4 α-Mangostin modulates the metastasis-related genes of skin cancer cells

As detected by qRT-PCR, α-mangostin was observed to inhibit metastasis of the skin cancer cells by downregulating the target genes (Figure 6-5A&B). In A-431 cells, compared with the untreated control, a 1.8-, 2.2-, 1.9-, and 2.8-fold decrease was observed after treatment with α-mangostin in the mRNA expression of MMP-2 ($P<$ 0.05), MMP-9 ($P<$ 0.05), NFκB ($P<$ 0.05), and Akt1 ($P<$ 0.01), respectively (Figure 6-5A). The mRNA expression of IκBα showed an increasing trend after treatment with α-mangostin in this cell line, but not statistically significant (Figure 6-5A). In SK-MEL-28 cells, treatment with α-mangostin induced a 3.6-, 3.2-, and 3.2-fold decrease in the mRNA expression of MMP-2 ($P<$ 0.05), NFκB ($P<$ 0.05), and IκBα ($P<$ 0.05), respectively (Figure 6-5B). α-Mangostin also inhibited the mRNA expression of MMP-9 and Akt1 on this cell line, but not statistically significant (Figure 6-5B). Furthermore, on SK-MEL-28 cells, the gene expression of BRAF V600E decreased in a dose-dependent manner with the increasing concentration of α-mangostin, with a 1.7- ($P<$ 0.01) and 5-fold ($P<$ 0.05) decrease observed at 1.25 and 2.5 µg/ml, respectively(Figure 6-5B).

A) A-431 cell line
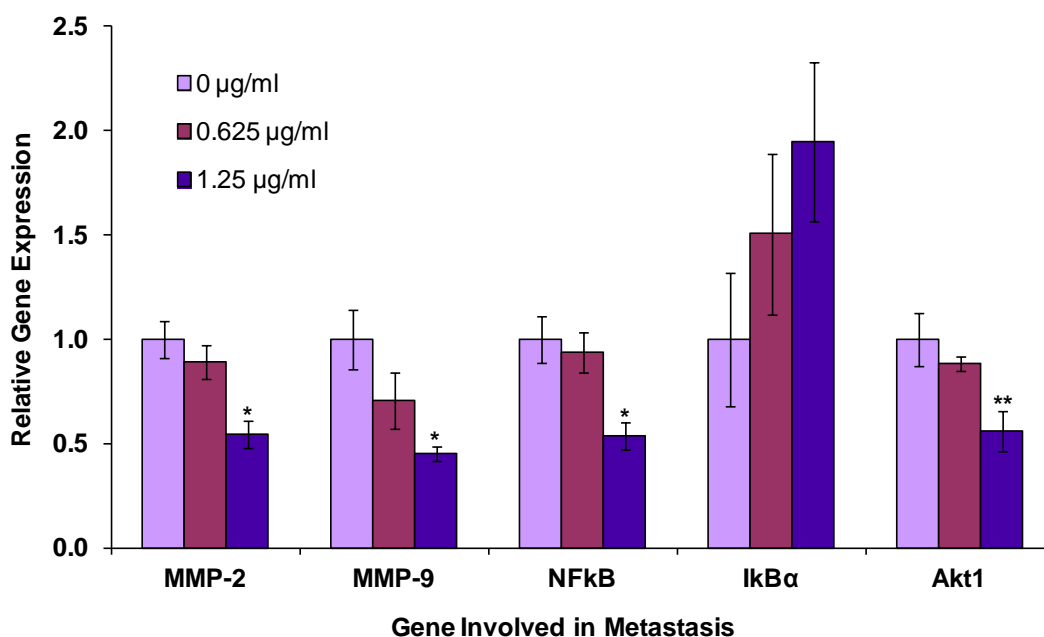
B) SK-MEL-28 cell line
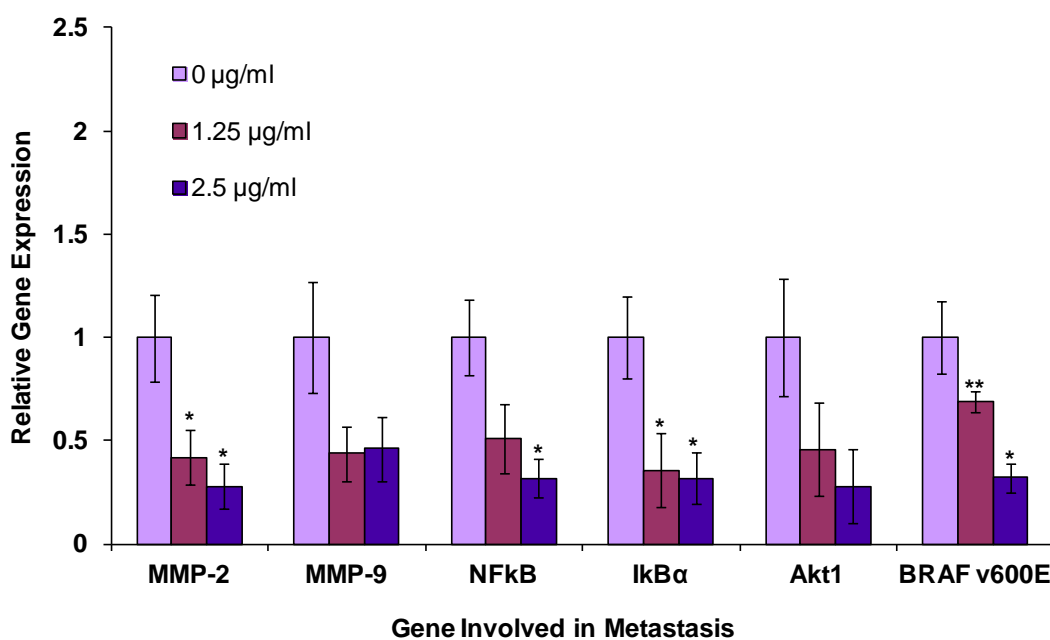
Figure 6-5

Effect of α-mangostin on the metastasis-related gene expression was detected by qRT-PCR after 48-h treatment on A) A-431 and B) SK-MEL-28 cells. The values are shown as the mean ± SEM of three independent experiments. Treatments significantly different from the untreated control at $P < 0.05$ are presented as * and at $P < 0.01$ as **.

6.4 Discussion

As discussed in Section 1.1.7.4 in Chapter 1, the metastasis of cancer cells involves multistep processes, including movement of cancer cells from the primary site, invasion into new blood vessels, altered adhesion ability between cells and the extracellular matrix (ECM), degradation of the environmental ECM and basement membrane, and eventually establishment of a new tumour at distant site (Cavallaro & Christofori 2001; Kawaguchi 2005; Onn & Herbst 2003). Therefore, the aim of the experiments described in this Chapter was to investigate if α-mangostin could disrupt any of these processes. Based on the current results, the potential mechanisms of α-mangostin induced anti-metastatic activity are presented in Figure 6-6.
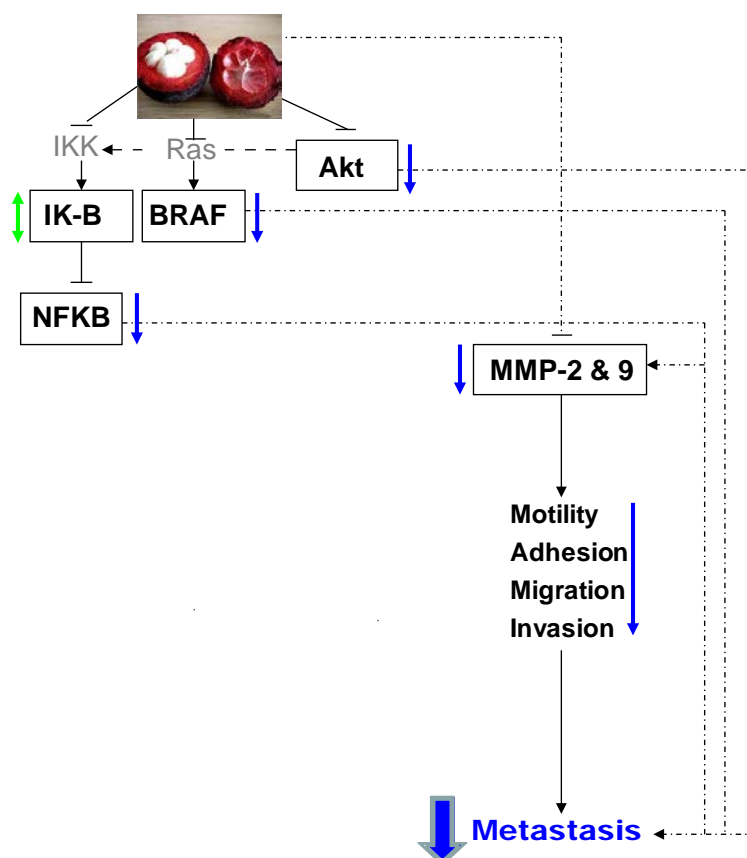
Figure 6-6
Proposed model of mechanisms involved in α-mangostin induced anti-metastatic effect on human squamous cell carcinoma A-431 and melanoma SK-MEL-28 cells. The arrow ↓ represents inhibition or decreased expression, and ↕ represents increased

and decreased expression after treatment with α-mangostin under different conditions.

6.4.1 Inhibition of skin cancer cell motility, migration and invasion by α-mangostin

The present study demonstrated that α-mangostin inhibited the motility, migration and invasion of the two types of skin cancer cells at non-toxic concentrations, in a dose dependent manner (Figures 6-1&2&3). Consistent with our study, α-mangostin inhibits the motility of human prostate cancer PC-3 and breast cancer MCF-7 cells (Hung *et al.* 2009; Lee *et al.* 2010). Migratory and invasive ability is an important characteristic of metastasis of cancer cells. The current results showed that α-mangostin induced a dose dependent decrease in migration and invasion with increasing concentration of α-mangostin (Figures 6-2&3; $P < 0.01$). In agreement with our study, α-mangostin inhibited migration and invasion of human prostate cancer PC-3 cell line, breast cancer MCF-7 cell line, and lung cancer A-549 cell line (Hung *et al.* 2009; Lee *et al.* 2010; Shih *et al.* 2010). However, the extent of these activities was found to be cell-type dependent. For example, in our study, α-mangostin at 1.25 µg/ml reduced the invasion to 4% and migration to 6% in A-431, and at 2.5 µg/ml reduced the invasion to 20% and migration to 23% in SK-MEL-28. In the previous studies, at 2.1 µg/ml (in A-549 cells) reduced the invasion to 20% and migration to 40%, at 5 µg/ml (in PC-3 cells) reduced the invasion to 60% and migration to 40%, and at around 2.5 µg/ml (in MCF-7 cells) reduced the invasion to 55% and migration to 61% compared with the untreated control (Hung *et al.* 2009; Lee *et al.* 2010; Shih *et al.* 2010). Therefore, α-mangostin appears to be more effective on the two skin cancer cells, especially A-431 cells, compared to other cancer cell types.

6.4.2 Inhibition of skin cancer cell adhesion by α-mangostin

The attachment of cancer cells to ECM is an important step in the process of metastasis (Cavallaro & Christofori 2001; Liotta *et al.* 1991). In order to investigate further the possible mechanism of anti-metastatic effects of α-mangostin, the effect of α-mangostin on the ability of A-431 and SK-MEL-28 to adhere to fibronectin and type I collagen, the major components of ECM, was examined. α-Mangostin significantly decreased the adhesive ability on fibronectin on the two skin cancer cell lines. However, on type I collagen, α-mangostin only significantly inhibited the adhesive capability of SK-MEL-28 cells not A-431 cells. Consistent with our study, α-mangostin inhibited the adhesion to type I collagen on PC-3 (Hung *et al.* 2009) and MCF-7 cells (Lee *et al.* 2010) with a decrease to around 75% at 5 µg/ml and around 40% at 2.5 µg/ml, respectively. An increased capacity for collagen binding is one of the important features of metastatic cancer cells (van Muijen *et al.* 1995). Therefore, the inhibition of type I collagen cell adhesion by α-mangostin may involve its anti-invasive effects. Although the role of fibronectin in the metastasis of skin cancer cells is not clear, it is likely that the inhibition of fibronectin cell adhesion contributed to the anti-invasive effects induced by α-mangostin. In the future, the effect of α-mangostin on other ECM proteins (e.g. laminin, type IV collagen, and vitronectin) could be studied and also the integrins which mediate the ECM protein adhesion.

6.4.3 Inhibition of mRNA expression of MMP-2 and MMP-9 by α-mangostin

Degradation of the ECM components is a key step for the metastasis process. MMP-2 and MMP-9 are highly expressed in various malignant tumours and activation of these two enzymes is required for degradation of ECM (Bernhard *et al.* 1994; Itoh & Nagase 2002). Therefore, inhibition of MMPs is an important target for anti-metastatic therapy. To explore further the exact mechanism of α-mangostin for

inhibition of invasion and migration, qRT-PCR was performed to detect the mRNA levels of MMP-2 and MMP- 9. In this study, we found that α-mangostin could significantly downregulate the mRNA level of MMP-2 on both skin cancer cells, while there was an effect on MMP-9 only with A-431 cells. Likewise, inhibition of MMP-2 and MMP-9 by α-mangostin was observed on PC-3, MCF-7, and A549 cells at different concentrations as detected by various methods, such as gelatine zymography, western blotting, and RT-PCR (Hung *et al.* 2009; Lee *et al.* 2010; Shih *et al.* 2010). To confirm the effect of xanthones on MMP activities in the SK-MEL-28 and A-431 cells, western blotting analysis and gelatine zymography can be carried out to determin the protein level of MMP. Also, MMP inhibitors can be applied.

6.4.4 Inhibition of NFκB, Akt1, and BRAF V600E involved in the anti-metastatic activity induced by α-mangostin

NFκB, Akt1, and MAPK signalling pathways are not only involved in cancer cell survival as discussed in Chapter 1 & 4, but also closely associated with invasion and metastasis of cancer cells (Chan-Hui & Weaver 1998; Karin *et al.* 2002; Sun *et al.* 2007). Therefore, the key genes involved in these three pathways were investigated in the current study.

Elevated activity of NFκB was shown to stimulate cell migration and angiogenesis by increasing expression of interleukin-8 and vascular-endothelial growth factor (Huang *et al.* 2000; Karin *et al.* 2002). Additionally, MMP-2 and MMP-9 genes were reported to be regulated through the transcriptional level interaction of NFκB with their binding sequences in the MMP-2 and MMP-9 gene promoter (Surh *et al.* 2001). Therefore, NFκB is an important target for inhibiting metastasis of cancer cells (Bharti & Aggarwal 2002; Surh *et al.* 2001). In the current study, downregulation of NFκB mRNA expression was found after treatment with α-mangostin on both types

of skin cancer cells studied. Similar findings on other cell lines were reported in previous studies (Hung *et al.* 2009; Lee *et al.* 2010; Shih *et al.* 2010). Moreover, increase in the mRNA level of IκBα was found after treatment with α-mangostin on A-431 (Figure 6-5A; $P > 0.05$). This was consistent with the study from Lee *et al.* (2010), which reported that α-mangostin induced an increase in the protein level of IκBα as detected by western blotting. In contrast, a significant decrease in the mRNA expression of IκBα was observed after treatment with α-mangostin on SK-MEL-28 cells (Figure 6-5B; $P < 0.05$). The relationship between NFκB and IκBα is complex (Jenkins *et al.* 2004). IκBα can inhibit activation of NFκB by trapping NFκB in the cytoplasm. Meanwhile, IκBα is one of the major downstream target of NFκB, hence activation of NFκB can switch on IκBα gene expression (Jenkins *et al.* 2004). Therefore, in SK-MEL-28 cells, suppression of NFκB may lead to the downregulation of IκBα. Additionally, regulatory role of ERK in the expression of NFκB has been reported (Eberle *et al.* 2007b). Therefore, apart from IκBα, ERK pathway may also contribute to the downregulation of NFκB expression induced by α-mangostin. This requires further investigation on the alteration of protein levels of ERK after treatment with α-mangostin.

Akt has been reported to be involved in the metastasis of various tumours (Chau & Ashcroft 2004; Sun *et al.* 2007). In particular, activation of Akt is found in approximately two thirds of melanomas and regulates melanoma cell migration, invasion and metastasis (Horst *et al.* 2009; Neudauer & McCarthy 2003; Robertson 2005; Shin *et al.* 2008). In this study, α-mangostin decreased the mRNA level of Akt1 on both A-431 ($P < 0.05$) and SK-MEL-28 ($P > 0.05$) cells. This suggests that the inhibition of Akt1 was involved in the anti-metastatic activities of α-mangostin.

Akt was reported to regulate NFκB via activation of IKK and consequent release of NFκB from the inhibitory complex (Ozes *et al.* 1999; Romashkova & Makarov 1999). The current results indicate that suppression of Akt contributes to the downregulation of NFκB induced by α-mangostin. Likewise, Shibata *et al.* (2011) reported that phospho-Akt-threonine 308 was inhibited after treatment with α-mangostin in human mammary carcinoma MDA-MB231 cells. In contrast, Akt alterations were not found after treatment with α-mangostin on A-549, PC-3, and MCF-7 cells (Hung *et al.* 2009; Lee *et al.* 2010; Shih *et al.* 2010). It is possible that the effects of α-mangostin could partially exert through different molecular targets in different cancer cell lines. This phenomenon needs to be studied further.

Apart from NFκB and Akt pathway, MAPK pathway is another important one involved in cancer invasion and metastasis (Chan-Hui & Weaver 1998). This pathway is highly activated in most melanomas (Cohen *et al.* 2002), with approximately 60% of melanoma expressing BRAF V600E (Davies *et al.* 2002; Kefford *et al.* 2010; Yang *et al.* 2010). The review by Lin *et al.* (2010) hypothesised the involvement of BRAF mutation in the dysregulation of the NFκB/Snail/RKIP/PTEN circuit and in the induction of metastasis. They also implied the possibility of targeting BRAF mutation as a novel therapeutic intervention in the treatment of metastasis (Lin *et al.* 2010). In this study, a dose-dependent decrease in the mRNA expression of BRAF V600E was found after treatment with α-mangostin on melanoma SK-MEL-28 cells (Figure 6-5B). This result indicates that α-mangostin has the potential to inhibit metastasis of melanoma cells. As mentioned earlier, ERK is a key upstream regulator of NFκB (Eberle *et al.* 2007b). Furthermore, downregulation of NFκB was observed after treatment with α-

mangostin in the current study. These results suggest that inhibition of BRAF V600E may contribute to the downregulation of NFκB via suppressing ERK. The role of ERK in the metastasis of skin cancer cells warrants further study.

6.5 Summary

The present study demonstrated that α-mangostin inhibits the metastatic ability of A-431 and SK-MEL-28 cells as reflected in results for cell motility, adhesion, and migration and Matrigel invasion. The anti-metastatic activity of α-mangostin might be via inhibition of Akt1 and NFκB, thereby decreasing the activities of MMP-2 and MMP-9. Additionally, on SK-MEL-28 cells, α-mangostin significantly decreased the mRNA level of BRAF V600E mutation at these non-toxic concentrations, thus potentially inhibiting MAPK pathway. Although there have been a number of studies carried out on the anti-metastatic activities of α-mangostin, significant difference of anti-metastatic activity and mechanism were found between other cancer cell types and those used in our study. Thus, the current study produced novel results that contribute to knowledge in this field by providing important evidences and mechanistic explanation of the anti-metastatic activity of α-mangostin in skin cancer cells. In the future, *in vivo* studies need to be carried out to investigate the therapeutic efficacy.

CHAPTER 7
CONCLUSIONS & FUTURE DIRECTIONS

7.1 Conclusions and future directions

Australia has the highest skin cancer incidence and amongst the highest mortality rates for skin cancer in the world. The resistance of skin cancer to current chemotherapy (e.g. DTIC) requests better therapies for Australians. Many plant secondary metabolites have demonstrated anti-skin cancer activities and therefore they are considered as important sources to screen for a new generation of anti-skin cancer drugs.

This study focused on anti-skin cancer activities of xanthones, the major secondary metabolites derived from the pericarp of a tropical fruit mangosteen. These compounds have shown significant anti-cancer activities on a range of other cancer cell lines, including breast cancer, liver cancer, lung cancer, and leukaemia (Obolskiy *et al.* 2009; Pedraza-Chaverri *et al.* 2008a). The anti-cancer activities of these compounds have been found to be cancer-cell type dependent because different sensitivities and mechanisms were observed after treatment with xanthones on different cell lines. Due to these differences, questions regarding the roles of xanthones in human skin cancer cell lines and their potential underlying mechanisms could not be answered based on currently available literature, highlighting a need for fundamental knowledge in this area.

Therefore, the current study was carried out to test the cytotoxicity and anti-metastatic activities of extracts and xanthone compounds from the mangosteen pericarp on two human skin cancer cell lines, as well as the mechanisms of action and any synergistic effects between xanthones. A detailed study using *in vitro* models, such as presented in this thesis, is a necessary step before moving onto more

expensive and time-consuming *in vivo* models.

7.1.1 Characterisation of standardised crude extracts from the pericarp of mangosteen

To produce consistent and reproducible mangosteen pericarp extracts for this research, a standardised extraction method was developed (Chapter 2). The dried pericarp was extracted with 100% EtOH or water at a pericarp/solvent ratio of 1:10 (w/v) at 75ºC (for EtOH extract) or 100 ºC (for water extract) for 1 h. MPWE and MPEE displayed comparable or higher antioxidant activities than extracts from previous studies using different extraction procedures. Therefore, the extraction method in the current study was efficient to recover the antioxidants from the pericarp of mangosteen.

The antioxidant activities of many xanthone compounds have been previously reported. As discussed in Chapter 1, many plant secondary metabolites present a UV-protective effect mainly due to their antioxidant properties. UV is the major cause of skin cancer. Therefore, xanthones may have UV-protective potential. However, to date, no study has been done in this area. Therefore, in the future, the UVB and UVA-protective effect of xanthone compounds could be studied using human primary skin cell lines (e.g. keratinocytes and melanocytes) for the initial screening to test different end points (e.g. cell viability, DNA damage, and cytokine release), and then using animal models (e.g. SKH-1 hairless mouse model). If these compounds were found to protect normal skin cells from UV-induced damage, they could be added to sunscreen as an active ingredient to help prevent UV-induced skin cancer.

7.1.2 Significant cytotoxicity induced by MPEE and xanthones

The thesis work has demonstrated that MPEE and xanthones have the potential to be anti-skin cancer drug candidates due to their cytotoxic effect on skin cancer cells. MPEE and the six pure xanthone compounds showed significant cytotoxicity on human squamous cell carcinoma A-431 and melanoma SK-MEL-28 cell lines (Chapter 3). The IC_{50} values of xanthones ranged from 2.39 to 7.61 µg/ml on two skin cancer cell lines, which were comparable to that of 5-FU (1.28 µg/ml) but much lower than that of DTIC (IC_{25} value of 100 µg/ml), making xanthones candidates for skin cancer chemotherapy, although more studies need to be conducted. Importantly, MPEE, gartanine, and γ-mangostin demonstrated selectivity against cancer cells, with much lower cytotoxicity on normal skin cells of non-malignant origin (human keratinocyte HaCaT and skin fibroblast CCD-1064Sk). The results indicate that *in vivo* these xanthone compounds might effectively kill cancer cells with less severe side effects than the present drugs. However, non-tumorous counterparts of the cells (e.g. primary melanocyte and keratinocyte cells) should be used to verify the current results.

In the current study, SK-MEL-28 and A-431 cell lines are the cell models to represent melanoma and squamous cell carcinoma to represent the breadth of skin cancer. More work using a broader range of skin cancer cell lines with different genetic backgrounds can be carried out in the future. For example, a broader range of melanoma cell lines with different genetic backgrounds could be used to study the effect of xanthones on melanoma. These cell lines could be one with NRAS mutation (e.g. SK-MEL-2), one with BRAF mutation (e.g. A375), or one without BRAF and NRAS mutation (wt/wt) (e.g. MeWo).

In the future, the mechanisms of the selectivity of these compounds warrant further investigation. Additionally, the selectivity only showed a margin of safety with a maximum of a 4.2-fold difference between cancer and normal cells. Therefore, *in vivo* studies need to be carried out to determine the efficacy and tolerance doses. The first step in this area of assessment could be animal studies.

There are two potential commercial applications of these xanthone compounds: topical and systemic application. For an early stage of skin cancer, topical application could be appropriate, while systemic application could be used for an advanced stage of skin cancer, especially for the metastatic melanoma. In the current study, two normal skin cell lines (HaCaT and CCD-1064Sk) were used as toxicity controls, as is relevant for topical application. However, for the systemic application, the compounds may also be exposed to other tissues and cells, such as colon cells, liver cells, and blood cells. Therefore, the toxicity of xanthone compounds on these cell lines needs to be studied and then *in vivo* studies are also needed.

Furthermore, the cytotoxicity of xanthones has been shown to be structure-related. A future direction could be to modify the structure of xanthone compounds (e.g. alteration of the ring substituent and their position) to improve the specificity of targets and lower toxicity towards normal cells, and hence increase efficacy.

7.1.3 Cytotoxicity induced by MPEE and xanthones via multiple modes of action

MPEE and xanthones exert the cytotoxicity on human skin cancer cells through multiple modes of action (Figure 7-1), as discussed in Chapter 4. Xanthones act to inhibit skin cancer *via*:

1) Cell cycle arrest in G_1 phase by up-regulating the mRNA level of p21^{WAF1}

and down-regulating cyclinD1;

2) Induction of apoptosis by activating the caspase 3/7, 8 or 9 activities, and disrupting the mitochondrial membrane potential. Additionally, an increase in the mRNA expression of cytochrome c and an enhanced ratio of Bax/Bcl-2 are involved in the apoptosis induction by xanthones;

3) Inhibition of three survival pathways by downregulating the mRNA expression of Akt1, BRAF V600E, NFκB, and/or up-regulating IκBα.

The magnitude of response is different for each cell line and each compound tested (Table 7-1). For example, MPEE significantly inhibited the survival pathways of A-431 cells, but not SK-MEL-28 cells. Also, even though 9-hydroxycalabaxanthone significantly induces apoptosis on both A-431 and SK-MEL-28, the magnitude is different: this compound increases the apoptotic population from 1.3% (untreated control) to 6.1% (10 µg/ml) on SK-MEL-28 cells, whereas in A-431 cells increased from 2.4% (untreated control) to as much as 48.6% (10 µg/ml).

In the future, other up- and down- stream targets as presented in Figure 1-9 could be tested to confirm the current cytotoxicity results and further clarify the underlying mechanisms of action (e.g. other Bcl-2 family members and c-kit) (Eberle *et al.* 2007b).

In the current study, the gene expression was tested at 48 h when significant apoptosis occurred. However, if the target gene expression was only examined at this one time point, the alteration of mRNA expression induced by mangosteen compounds may be underestimated. The changes at transcriptional level occur earlier

than those at protein level. Before the apoptosis is manifest at the cellular level, the mRNA expression level of target genes may reach a peak and then decrease. In the future, additional time points early in the process of apoptosis could be studied (e.g. 2, 4, 6, 12, 24 h) to detect the peak of mRNA expression of the target genes.

The mRNA expression patterns as detected by qRT-PCR provide important information for the quantitative description of biological systems (Gygi *et al.* 1999). However, they are not sufficient by themselves (Harford & Morris 1997; Urlinger *et al.* 1997; Varshavsky 1996). For example, Akt1 is only activated in its phosphorylation form. The mRNA level of this gene does not indicate the phosphorylated and non-phosphorylated protein levels. Additionally, NFκB is inactivated in the cytoplasm and only activated to promote cancer cell proliferation and metastasis once it translocates into the nucleus. The mRNA expression of this gene is not indicative of the subcellular location of the protein. Hence, gene analysis in complement with proteome analysis has been suggested to achieve the quantitative description of the state of a biological system (Wilkins *et al.* 1997). Proteome analysis includes the quantity of target protein expression, their subcellular location, and the modification state. Therefore, in the future, the results from the current study can be confirmed and clarified by the proteome analysisusing two-dimensional gel electrophoresis (Garfin, 2003), western blotting, and ELISA. For example, the total protein level of Akt1 and the phosphorated forms Thr308 and Ser473 can be determined by western blotting.

7.1.4 Synergistic effect was found when α-mangostin was combined with another xanthone

One aim of this thesis was to identify treatment combinations that showed a synergistic enhancement of cell death (Chapter 5). In SK-MEL-28 cells, a synergistic

cytotoxic effect was found when α-mangostin was combined with MPEE and any one of the other five xanthone compounds. Likewise, a synergistic cytotoxic effect was found on A-431 cells when α-mangostin was combined with MPEE and each of the other xanthone compounds, except for γ-mangostin. These synergistic effects might be due to the enhancement of the actions leading to apoptosis. Compared to A-431 cell line, the synergistic effect was found to be greater in SK-MEL-28 cell line. This may be because the compounds act through different mechanisms in SK-MEL-28 cell line, whereas they act through similar mechanisms in A-431 cells. This suggests that synergy can only occur if the stimuli act through independent mechanisms. Importantly, the response to any one combination of compounds was found to be significantly different with different cell types and concentrations of compounds. To understand further the mechanisms, the alteration of protein level of targets (e.g. NFκB and Akt) can be determined after treatment with individual xanthone and combination of xanthones. Also, BRAF inhibitor can be applied to elucidate the synergistic effects of xanthone inhibition.

In contrast, no synergistic effect was observed between xanthone compounds and either of 5-FU and DTIC under the tested conditions.

Due to α-mangostin showing the most potent activity and time constraints, the only xanthone combinations tested were between α-mangostin and the other individual xanthones. However, other xanthones were also found to be effective to kill skin cancer cells under the conditions tested in Chapter 3. Therefore, other combinations of xanthones would act synergistically and warrant further investigation, using the model system utilised in this thesis work. In addition to the Crystal Violet assay, the

MTT assay and LDH assay could be used to measure cell survival after treatment with xanthone compounds. Also, the cytotoxicity of the xanthone combinations against the non-cancerous counterpart cell lines should be determined in the future.

7.1.5 Anti-metastatic activity

α-Mangostin, as shown in Chapter 3 & 4, was the most potent compound of those tested on both A-431 and SK-MEL-28 cells. Therefore, it was selected to study for anti-metastatic activity. α-Mangostin shows significant anti-metastatic activity on the two types of skin cancer cells by inhibiting the cancer cell motility, adhesion, migration and invasion (Chapter 6). The molecular mechanism of anti-metastatic activity of α-mangostin was found to be via inhibition of Akt1 and NFκB, thereby decreasing the activities of MMP-2 and MMP-9. Additionally, inhibition of BRAF V600E mutation was found to be involved in the anti-metastatic activity of α-mangostin on SK-MEL-28. It would be interesting to compare the xanthones' effect with the commercially available BRAF inhibitor (e.g. RG7204 and GSK2118436) by measuring the protein level of BRAF after treatment. The model of anti-metastatic activity of α-mangostin on skin cancer cells is presented in Figure 7-1.

As shown in Chapter 4, the other tested xanthones were also able to inhibit Akt1and NFκB pathways under the conditions tested. One of the important functions of these two pathways is in the promotion of cancer cell metastasis. Therefore, one or more of the other xanthones may also be effective as anti-metastatic agents and they warrant future investigation.

The current model for the metastasis assays is a simple two-dimensional one. In the future, a three-dimensional model constructed using isolated cutaneous cell

populations could be used to better mimic the human disease than the two-dimensional invasion assay (Odashiro *et al.* 2005). Additionally, animal models (e.g. metastatic melanoma xenograft) could be used to understand skin cancer progression and spread, because these processes occur only *in vivo*. The available skin cancer models were reviewed by Odashiro *et al.* (2005).

7.2 Overall conclusion

The overall aim of this study was to identify new treatments for skin cancer and investigate the underlying cellular and molecular mechanisms. The ethanol extract of mangosteen pericarp (MPEE) and six pure xanthone compounds tested were found to be effective to inhibit skin cancer cells via multiple modes of action and are predicted to act at various stages of skin cancer cell progression. These effects are more potent in specific combinations. The results have demonstrated that, at high concentrations, xanthones can inhibit skin cancer cell proliferation via cell cycle arrest in G_1 phase, apoptosis induction, and survival pathway suppression. At lower concentrations (non-toxic), α-mangostin can inhibit the metastatic processes of skin cancer cell motility, migration, invasion, and adhesion through a variety of mechanisms, including the inhibition of Akt1 and NFκB signalling pathways. In conclusion, the findings presented in this thesis provide novel evidence andconsiderable insight into its mechanisms of actionof anti-skin cancer activities of xanthones. The current study provides an important basis for further exploration of the possible beneficial effect of mangosteen pericarp extract and xanthones in the prevention and treatment of skin cancer growth and metastasis.
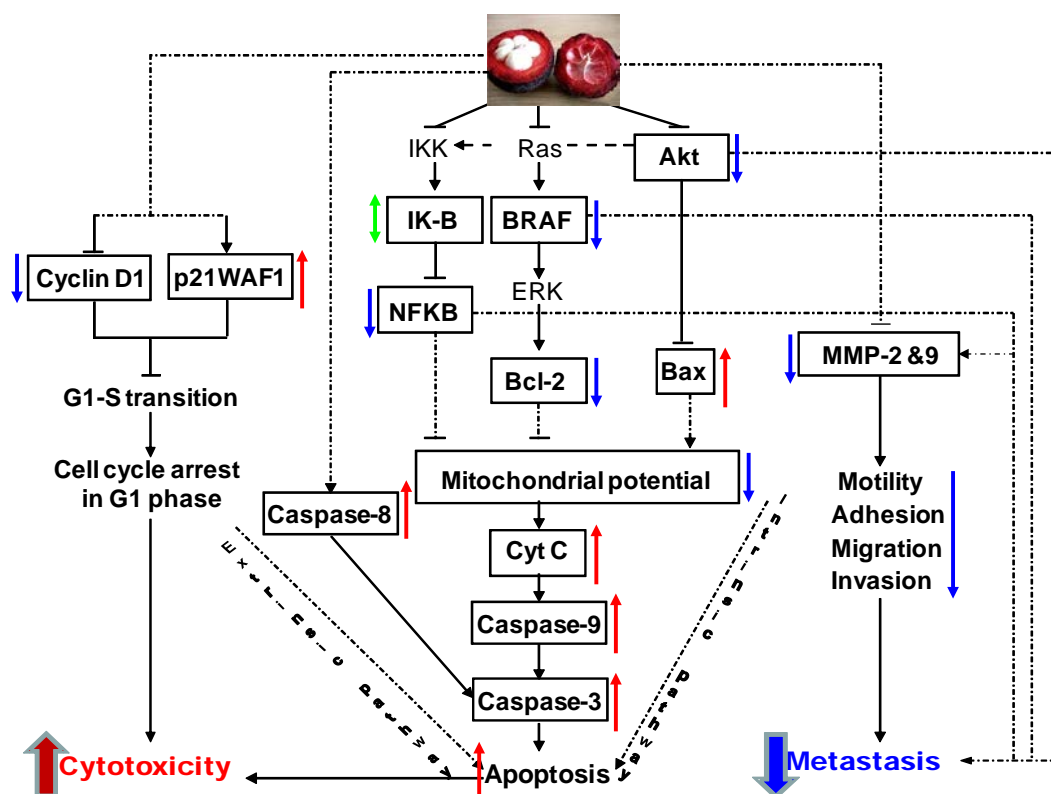
Figure 7-1

Proposed mechanism of multiple signalling pathway involved in xanthones induced anti-skin cancer activities of human squamous cell carcinoma A-431 and melanoma SK-MEL-28 cells. The arrow ↑ represents activation or increased expression, ↓ represents inhibition or decreased expression, and ↕ represents increased and decreased expression after treatment with the same xanthone compound under different conditions.

Table 7-1

Different responses of xanthones on different cell lines.

	Hypotheses	Cell Lines	MPEE	α-Mangostin	β-Mangostin	γ-Mangostin	8-Deoxygartanine	Gartanine	9-Hydroxycala-baxanthone
✓	Inhibition of proliferaton	SCC	✓	✓				✓	✓
		Melanoma	✓	✓		✓	✓	✓	✓
✓	Induction of apoptosis	SCC	✓	✓	✓	✓		✓	✓
		Melanoma	✓	✓	✓		✓	✓	✓
✓	Inhibition of survival pathway	SCC	✓	✓	✓	✓	✓	✓	✓
		Melanoma		✓	✓	✓	✓	✓	✓
✓	*Inhibition of metastasis	SCC		✓					
		Melanoma		✓					

*Only α-mangostin was studied for the anti-metastatic activity

SCC: Squamous Cell Carcinoma; MPEE: Mangosteen Pericarp Ethanol Extract

REFERENCES

Australian Institute of Health and Welfare (AIHW) 2008, Non-melanoma skin cancer: General practice consultations, hospitalisation and mortality, in Cancer Series no. 43. Cat no. 39. Canberra: AIHW.

Adams, JM & Cory, S 1998, The Bcl-2 protein family: arbiters of cell survival, *Science*, 281: 1322-6.

Adams, JM & Cory, S 2001, Life-or-death decisions by the Bcl-2 protein family, *Trends in Biochemical Sciences*, 26: 61-6.

Adhami, VM, Afaq, F & Ahmad, N 2003, Suppression of ultraviolet B exposure-mediated activation of NF-kappaB in normal human keratinocytes by resveratrol, *Neoplasia*, 5: 74-82.

Adil, İH, Çetin, Hİ, Yener, ME & Bayındırlı, A 2007, Subcritical (carbon dioxide + ethanol) extraction of polyphenols from apple and peach pomaces, and determination of the antioxidant activities of the extracts, *The Journal of Supercritical Fluids*, 43: 55-63.

Afaq, F, Adhami, VM & Ahmad, N 2003, Prevention of short-term ultraviolet B radiation-mediated damages by resveratrol in SKH-1 hairless mice, *Toxicology and Applied Pharmacology*, 186: 28-37.

Afaq, F, Adhami, VM, Ahmad, N & Mukhtar, H 2002, Botanical antioxidants for chemoprevention of photocarcinogenesis, *Frontiers in Bioscience*, 7: 784-92.

Afaq, F & Mukhtar, H 2001, Effects of solar radiation on cutaneous detoxification pathways, *Journal of Photochemistry and Photobiology B*, 63: 61-9.

Afaq, F & Mukhtar, H 2002, Photochemoprevention by botanical antioxidants, *Skin Pharmacology and Applied Skin Physiology*, 15: 297-306.

Ahmad, N, Gupta, S & Mukhtar, H 2000, Green tea polyphenol epigallocatechin-3-gallate differentially modulates nuclear factor κB in cancer cells versus normal cells, *Archives of Biochemistry and Biophysics*, 376: 338-46.

Akao, Y, Nakagawa, Y, Iinuma, M & Nozawa, Y 2008, Anti-cancer effects of xanthones from pericarps of mangosteen, *International Journal of Molecular Sciences*, 9: 355-70.

Amundson, SA, Myers, TG, Scudiero, D, Kitada, S, Reed, JC & Fornace, AJ, Jr. 2000, An informatics approach identifying markers of chemosensitivity in human cancer cell lines, *Cancer Research*, 60: 6101-10.

Anthony, ML 2000, Surgical treatment of nonmelanoma skin cancer, *AORN Journal*, 71: 552-64.

Antonsson, B & Martinou, JC 2000, The Bcl-2 protein family, *Experimental Cell Research*, 256: 50-7.

Aramwit, P, Bang, N & Srichana, T 2010, The properties and stability of anthocyanins in mulberry fruits, *Food Research International*, 43: 1093-7.

Armstrong, BK & Kricker, A 1995, Skin cancer, *Dermatologic Clinics*, 13: 583-94.

Armstrong, BK & Kricker, A 2001, The epidemiology of UV induced skin cancer, *Journal of Photochemistry and Photobiology B: Biology*, 63: 8-18.

Asai, F, Tosa, H, Tanaka, T & Iinuma, M 1995, A xanthone from pericarps of *Garcinia Mangostana.* , *Phytochemistry*, 39: 943-4.

Ashkenazi, A & Dixit, VM 1998, Death receptors: signaling and modulation, *Science*, 281: 1305-8.

Autier, P 2004, Perspectives in melanoma prevention: the case of sunbeds, *European Journal of Cancer*, 40: 2367-76.

Aziz, MH, Afaq, F & Ahmad, N 2005a, Prevention of ultraviolet-B radiation damage by resveratrol in mouse skin is mediated via modulation in survivin, *Photochemistry and Photobiology*, 81: 25-31.

Aziz, MH, Reagan-Shaw, S, Wu, J, Longley, BJ & Ahmad, N 2005b, Chemoprevention of skin cancer by grape constituent resveratrol: relevance to human disease, *The Federation of American Societies for Experimental Biology Journal*, 19: 1193-5.

Bae, EY, Na, M, Njamen, D, Mbafor, JT, Fomum, ZT, Cui, L, Choung, DH, Kim, BY, Oh, WK & Ahn, JS 2006, Inhibition of protein tyrosine phosphatase 1B by prenylated isoflavonoids isolated from the stem bark of *Erythrina addisoniae*, *Planta Medica*, 72: 945-8.

Balaji, R, Rekha, N, Deecaraman, M & Manikandan, L 2009, Antimetastatic and antiproliferative activity of methanolic fraction of *Jatropha curcas* against B16F10 melanoma induced lung metastasis in C57BL/6 mice, *African Journal of Pharmacy and Pharmacology*, 3: 547-55.

Balch, CM, Buzaid, AC, Soong, SJ, Atkins, MB, Cascinelli, N, Coit, DG, Fleming, ID, Gershenwald, JE, Houghton, A, Jr., Kirkwood, JM, McMasters, KM, Mihm, MF, Morton, DL, Reintgen, DS, Ross, MI, Sober, A, Thompson, JA & Thompson, JF 2001, Final version of the American Joint Committee on Cancer staging system for cutaneous melanoma, *Journal of Clinical Oncology*, 19: 3635-48.

Baliga, MS & Katiyar, SK 2006, Chemoprevention of photocarcinogenesis by selected dietary botanicals, *Photochemical & Photobiological Sciences*, 5: 243-53.

Ballard, TS 2008, 'Optimizing the Extraction of Phenolic Antioxidant Compounds from Peanut Skins', PhD thesis, Blacksburg, Virginia Polytechnic Institute and State University.

Balunas, MJ & Kinghorn, AD 2005, Drug discovery from medicinal plants, *Life*

Sciences, 78: 431-41.

Balunas, MJ, Su, B, Brueggemeier, RW & Kinghorn, AD 2008, Xanthones from the botanical dietary supplement mangosteen (*Garcinia mangostana*) with aromatase inhibitory activity, *Journal of Natural Products*, 71: 1161-6.

Banerji, A, Chakrabarti, J, Mitra, A & Chatterjee, A 2004, Effect of curcumin on gelatinase A (MMP-2) activity in B16F10 melanoma cells, *Cancer Letters*, 211: 235-42.

Bava, SV, Puliappadamba, VT, Deepti, A, Nair, A, Karunagaran, D & Anto, RJ 2005, Sensitization of taxol-induced apoptosis by curcumin involves down-regulation of nuclear factor-κB and the serine/threonine kinase Akt and is independent of tubulin polymerization, *Journal of Biological Chemistry*, 280: 6301-8.

Benzie, IF & Strain, JJ 1996, The ferric reducing ability of plasma (FRAP) as a measure of "antioxidant power": the FRAP assay, *Analytical Biochemistry*, 239: 70-6.

Bernhard, EJ, Gruber, SB & Muschel, RJ 1994, Direct evidence linking expression of matrix metalloproteinase 9 (92-kDa gelatinase/collagenase) to the metastatic phenotype in transformed rat embryo cells, *Proceedings of the National Academy of Sciences of the United States of America*, 91: 4293-7.

Berton, TR, Mitchell, DL, Fischer, SM & Locniskar, MF 1997, Epidermal proliferation but not quantity of DNA photodamage is correlated with UV-induced mouse skin carcinogenesis, *Journal of Investigative Dermatology*, 109: 340-7.

Bertram, JS, Kolonel, LN & Meyskens, FL, Jr. 1987, Rationale and strategies for chemoprevention of cancer in humans, *Cancer Research*, 47: 3012-31.

Bharti, AC & Aggarwal, BB 2002, Nuclear factor-kappa B and cancer: its role in prevention and therapy, *Biochemical Pharmacology*, 64: 883-8.

Blois, MS 1958, Antioxidant determinations by the use of a stable free radical, *Nature*, 181: 1199-200.

Bomser, J, Singletary, K & Meline, B 2000, Inhibition of 12-O-tetradecanoylphorbol-13-acetate (TPA)-induced mouse skin ornithine decarboxylase and protein kinase C by polyphenolics from grapes, *Chemico-Biological Interactions*, 127: 45-59.

Boukamp, P, Petrussevska, RT, Breitkreutz, D, Hornung, J, Markham, A & Fusenig, NE 1988, Normal keratinization in a spontaneously immortalized aneuploid human keratinocyte cell line, *Journal of Cell Biology*, 106: 761-71.

Braun, FK, Fecker, LF, Schwarz, C, Walden, P, Assaf, C, Durkop, H, Sterry, W & Eberle, J 2007, Blockade of death receptor-mediated pathways early in the signaling cascade coincides with distinct apoptosis resistance in cutaneous T-cell lymphoma

cells, *Journal of Investigative Dermatology*, 127: 2425-37.

Brazil, DP, Park, J & Hemmings, BA 2002, PKB binding proteins. Getting in on the Akt, *Cell*, 111: 293-303.

Broggini, M, Marchini, SV, Galliera, E, Borsotti, P, Taraboletti, G, Erba, E, Sironi, M, Jimeno, J, Faircloth, GT, Giavazzi, R & D'Incalci, M 2003, Aplidine, a new anticancer agent of marine origin, inhibits vascular endothelial growth factor (VEGF) secretion and blocks VEGF-VEGFR-1 (flt-1) autocrine loop in human leukemia cells MOLT-4, *Leukemia*, 17: 52-9.

Brohem, CA, Sawada, TCH, Massaro, RR, Almeida, RL, Rivelli, DP, Ropke, CD, da Silva, VV, de Lima, TM, Curi, R, Barros, SBM & Maria-Engler, SS 2009, Apoptosis induction by 4-nerolidylcatechol in melanoma cell lines, *Toxicology in Vitro*, 23: 111-9.

Burney, S, Niles, JC, Dedon, PC & Tannenbaum, SR 1999, DNA Damage in Deoxynucleosides and Oligonucleotides Treated with Peroxynitrite, *Chemical Research in Toxicology*, 12: 513-20.

Caius, CF 2003, The medicinal and poisonous plants of India, in Scientific Publishers, Jodhpur, India, p. 527.

Campbell, CT, Prince, M, Landry, GM, Kha, V & Kleiner, HE 2007, Pro-apoptotic effects of 1'-acetoxychavicol acetate in human breast carcinoma cells, *Toxicology Letter*, 173: 151-60.

Cardone, MH, Roy, N, Stennicke, HR, Salvesen, GS, Franke, TF, Stanbridge, E, Frisch, S & Reed, JC 1998, Regulation of cell death protease caspase-9 by phosphorylation, *Science*, 282: 1318-21.

Carsin, AE, Sharp, L & Comber, H 2011, Geographical, urban/rural and socioeconomic variations in nonmelanoma skin cancer incidence: a population-based study in Ireland, *British Journal of Dermatology*, 164: 822-9.

Cavallaro, U & Christofori, G 2001, Cell adhesion in tumor invasion and metastasis: loss of the glue is not enough, *Biochimica et Biophysica Acta*, 1552: 39-45.

Chairungsrilerd, N, Furukawa, KI, Ohta, T, Nozoe, S & Ohizumi, Y 1996, Pharmacological properties of oL-mangostin, a novel histamine H 1
receptor antagonist., *European Journal of Pharmacology*, 314 351-6.

Chandra, D, Liu, JW & Tang, DG 2002, Early mitochondrial activation and cytochrome c up-regulation during apoptosis, *Journal of Biological Chemistry*, 277: 50842-54.

Chan-Hui, PY & Weaver, R 1998, Human mitogen-activated protein kinase kinase kinase mediates the stress-induced activation of mitogen-activated protein kinase cascades, *Biochemical Journal*, 336: 599-609.

Chan, W-H, Wu, C-C & Yu, J-S 2003, Curcumin inhibits UV irradiation-induced oxidative stress and apoptotic biochemical changes in human epidermoid carcinoma A431 cells, *Journal of Cellular Biochemistry*, 90: 327-38.

Chang, HF, Huang, WT, Chen, HJ & Yang, LL 2010, Apoptotic effects of gamma-mangostin from the fruit hull of *Garcinia mangostana* on human malignant glioma cells, *Molecules*, 15: 8953-66.

Chang, PN, Yap, WN, Wing Lee, DT, Ling, MT, Wong, YC & Yap, YL 2009, Evidence of γ-tocotrienol as an apoptosis-inducing, invasion-suppressing, and chemotherapy drug-sensitizing agent in human melanoma cells, *Nutrition and Cancer*, 61: 357-66.

Chatterjee, ML, Agarwal, R & Mukhtar, H 1996, Ultraviolet B radiation-induced DNA lesions in mouse epidermis: an assessment using a novel ^{32}P-postlabelling technique, *Biochemical and Biophysical Research Communications*, 229: 590-5.

Chau, NM & Ashcroft, M 2004, Akt2: a role in breast cancer metastasis, *Breast Cancer Researsh*, 6: 55-7.

Chen, LG, Yang, LL & Wang, CC 2008, Anti-inflammatory activity of mangostins from *Garcinia mangostana*, *Food and Chemical Toxicology*, 46: 688-93.

Chen, WS, Xu, PZ, Gottlob, K, Chen, ML, Sokol, K, Shiyanova, T, Roninson, I, Weng, W, Suzuki, R, Tobe, K, Kadowaki, T & Hay, N 2001a, Growth retardation and increased apoptosis in mice with homozygous disruption of the Akt1 gene, *Genes and Development*, 15: 2203-8.

Chen, X, Wen, WF, Liu, XJ & Sun, LF 2002, The extraction of flavonoids and the determination of their content in the powder of *Artemisia selengensis* Turcz, *Journal of Jiangxi Normal University*, 24: 690-7.

Chen, XH, Miao, YX, Wang, XJ, Yu, Z, Geng, MY, Han, YT & Wang, LX 2011, Effects of *Ginkgo biloba* extract EGb761 on human colon adenocarcinoma cells, *Cellular Physiology and Biochemistry*, 27: 227-32.

Chen, Z, Gibson, TB, Robinson, F, Silvestro, L, Pearson, G, Xu, B, Wright, A, Vanderbilt, C & Cobb, MH 2001b, MAP kinases, *Chemical Reviews*, 101: 2449-76.

Cheng, JH, Huang, AM, Hour, TC, Yang, SC, Pu, YS & Lin, CN 2011, Antioxidant xanthone derivatives induce cell cycle arrest and apoptosis and enhance cell death induced by cisplatin in NTUB1 cells associated with ROS, *European Journal of Medicinal Chemistry*, 46: 1222-31.

Cherpelis, BS, Marcusen, C & Lang, PG 2002, Prognostic factors for metastasis in squamous cell carcinoma of the skin, *Dermatologic Surgery*, 28: 268-73.

Chiang, LC, Cheng, HY, Liu, MC, Chiang, W & Lin, CC 2004, *In vitro* evaluation of antileukemic activity of 17 commonly used fruits and vegetables in Taiwan, *Food Science and Technology*, 37: 539-44.

Chicheportiche, Y, Bourdon, PR, Xu, H, Hsu, Y-M, Scott, H, Hession, C, Garcia, I & Browning, JL 1997, TWEAK, a new secreted ligand in the tumor necrosis factor family that weakly induces apoptosis, *Journal of Biological Chemistry*, 272: 32401-10.

Chin, YW, Jung, HA, Chai, HB, Keller, WJ & Kinghorn, AD 2008, Xanthones with quinone reductase-inducing activity from the fruits of *Garcinia mangostana* (Mangosteen). *Phytochemistry*, 69: 754–8.

Chirinos, R, Rogez, H, Campos, D, Pedreschi, R & Larondelle, Y 2007, Optimization of extraction conditions of antioxidant phenolic compounds from mashua (*Tropaeolum tuberosum* Ruíz; Pavón) tubers, *Separation and Purification Technology*, 55: 217-25.

Chomnawang, MT, Surassmo, S, Nukoolkarn, VS & Gritsanapan, W 2005, Antimicrobial effects of Thai medicinal plants against acne-inducing bacteria, *Journal of Ethnopharmacology*, 101: 330-3.

Chomnawang, MT, Surassmo, S, Nukoolkarn, VS & Gritsanapan, W 2007, Effect of *Garcinia mangostana* on inflammation caused by Propionibacterium acnes, *Fitoterapia*, 78: 401-8.

Chou, TC 2006, Theoretical basis, experimental design, and computerized simulation of synergism and antagonism in drug combination studies, *Pharmacological Reviews*, 58: 621-81.

Chou, TC 2010, Drug combination studies and their synergy quantification using the Chou-Talalay method, *Cancer Research*, 70: 440-6.

Chu, Q, Ling, MT, Feng, H, Cheung, HW, Tsao, SW, Wang, X & Wong, YC 2006, A novel anticancer effect of garlic derivatives: inhibition of cancer cell invasion through restoration of E-cadherin expression, *Carcinogenesis*, 27: 2180-9.

Chu, WF, Wu, DM, Liu, W, Wu, LJ, Li, DZ, Xu, DY & Wang, XF 2009, Sulforaphane induces G_2-M arrest and apoptosis in high metastasis cell line of salivary gland adenoid cystic carcinoma, *Oral Oncology*, 45: 998-1004.

Chun, KS, Keum, YS, Han, SS, Song, YS, Kim, SH & Surh, YJ 2003, Curcumin inhibits phorbol ester-induced expression of cyclooxygenase-2 in mouse skin through suppression of extracellular signal-regulated kinase activity and NF-κB activation, *Carcinogenesis*, 24: 1515-24.

Cimino, F, Cristani, M, Saija, A, Bonina, FP & Virgili, F 2007, Protective effects of a red orange extract on UVB-induced damage in human keratinocytes, *Biofactors*, 30: 129-38.

Clydesdale, GJ, Dandie, GW & Muller, HK 2001, Ultraviolet light induced injury: immunological and inflammatory effects, *Immunology & Cell Biology*, 79: 547-68.

Cohen, C, Zavala-Pompa, A, Sequeira, JH, Shoji, M, Sexton, DG, Cotsonis, G, Cerimele, F, Govindarajan, B, Macaron, N & Arbiser, JL 2002, Mitogen-actived protein kinase activation is an early event in melanoma progression, *Clinical Cancer Research*, 8: 3728-33.

Cole, CA, Forbes, PD & Davies, RE 1986, An action spectrum for UV photocarcinogenesis, *Photochemistry and Photobiology*, 43: 275-84.

Crompton, M 2000, Bax, Bid and the permeabilization of the mitochondrial outer membrane in apoptosis, *Current Opinion in Cell Biology*, 12: 414-9.

Cross, SE, Jiang, R, Benson, HA & Roberts, MS 2001, Can increasing the viscosity of formulations be used to reduce the human skin penetration of the sunscreen oxybenzone?, *Journal of Investigative Dermatology*, 117: 147-50.

Crowell, JA, Steele, VE & Fay, JR 2007, Targeting the AKT protein kinase for cancer chemoprevention, *Molecular Cancer Therapeutics*, 6: 2139-48.

Crowley-Weber, CL, Payne, CM, Gleason-Guzman, M, Watts, GS, Futscher, B, Waltmire, CN, Crowley, C, Dvorakova, K, Bernstein, C, Craven, M, Garewal, H & Bernstein, H 2002, Development and molecular characterization of HCT-116 cell lines resistant to the tumor promoter and multiple stress-inducer, deoxycholate, *Carcinogenesis*, 23: 2063-80.

Crozier, A, Clifford, MN & Ashihara, H (eds) 2006, Plant secondary metabolites: occurence, structure and role in the human diet, Blackwell Publishing Ltd, , Oxford, UK.

Cruz, JM, Dominguez, H & Parajo, JC 2004, Assessment of the production of antioxidants from winemaking waste solids, *Journal of Agricultural and Food Chemistry*, 52: 5612-20.

Cvek, J, Medic-Saric, M, Jasprica, I, Zubcic, S, Vitali, D, Mornar, A, Vedrina-Dragojevic, I & Tomic, S 2007, Optimisation of an extraction procedure and chemical characterisation of Croatian propolis tinctures, *Phytochemical Analysis*, 18: 451-9.

Datta, SR, Dudek, H, Tao, X, Masters, S, Fu, H, Gotoh, Y & Greenberg, ME 1997, Akt phosphorylation of BAD couples survival signals to the cell-intrinsic death machinery, *Cell*, 91: 231-41.

Davies, H, Bignell, GR, Cox, C, Stephens, P, Edkins, S, Clegg, S, Teague, J, Woffendin, H, Garnett, MJ, Bottomley, W, Davis, N, Dicks, E, Ewing, R, Floyd, Y, Gray, K, Hall, S, Hawes, R, Hughes, J, Kosmidou, V, Menzies, A, Mould, C, Parker, A, Stevens, C, Watt, S, Hooper, S, Wilson, R, Jayatilake, H, Gusterson, BA, Cooper, C, Shipley, J, Hargrave, D, Pritchard-Jones, K, Maitland, N, Chenevix-Trench, G, Riggins, GJ, Bigner, DD, Palmieri, G, Cossu, A, Flanagan, A, Nicholson, A, Ho, JW, Leung, SY, Yuen, ST, Weber, BL, Seigler, HF, Darrow, TL, Paterson, H, Marais, R, Marshall, CJ, Wooster, R, Stratton, MR & Futreal, PA 2002, Mutations of the BRAF gene in human cancer, *Nature*, 417: 949-54.

de Gruijl, FR, Sterenborg, HJ, Forbes, PD, Davies, RE, Cole, C, Kelfkens, G, van Weelden, H, Slaper, H & van der Leun, JC 1993, Wavelength dependence of skin cancer induction by ultraviolet irradiation of albino hairless mice, *Cancer Research*, 53: 53-60.

de Gruijl, FR, van Kranen, HJ & van Schanke, A 2005, UV exposure, genetic targets in melanocytic tumors and transgenic mouse models, *Photochemistry and Photobiology*, 81: 52-64.

de Gruijl, RR 2002, Photocarcinogenesis: UVA vs. UVB radiation., *Skin Pharmacology and Applied Skin Physiology*, 15: 316-20.

de Mulder, PH 1999, The chemotherapy of head and neck cancer, *Anticancer Drugs*, 10: 33-7.

Demarchi, F & Brancolini, C 2005, Altering protein turnover in tumor cells: New opportunities for anti-cancer therapies, *Drug resistance updates : reviews and commentaries in antimicrobial and anticancer chemotherapy*, 8: 359-68.

Devi Sampath, P & Vijayaraghavan, K 2007, Cardioprotective effect of α-mangostin, a xanthone derivative from mangosteen on tissue defense system against isoproterenol-induced myocardial infarction in rats, *Journal of Biochemical and Molecular Toxicology*, 21: 336-9.

Dhawan, P & Richmond, A 2002, A novel NF-κ B-inducing kinase-MAPK signaling pathway up-regulates NF-κ B activity in melanoma cells, *The Journal of Biological Chemistry*, 277: 7920-8.

Dhawan, P, Singh, AB, Ellis, DL & Richmond, A 2002, Constitutive activation of Akt/protein kinase B in melanoma leads to up-regulation of nuclear factor-κB and tumor progression, *Cancer Research*, 62: 7335-42.

Dia, VP & Gonzalez de Mejia, E 2011, Lunasin induces apoptosis and modifies the expression of genes associated with extracellular matrix and cell adhesion in human metastatic colon cancer cells, *Molecular Nutrition and Food Research*, 55: 623-34.

DiGiovanni, J 1992, Multistage carcinogenesis in mouse skin, *Pharmacology & Therapeutics*, 54: 63-128.

Doi, H, Shibata, MA, Shibata, E, Morimoto, J, Akao, Y, Iinuma, M, Tanigawa, N & Otsuki, Y 2009, Panaxanthone isolated from pericarp of *Garcinia mangostana* L. suppresses tumor growth and metastasis of a mouse model of mammary cancer, *Anticancer Research*, 29: 2485-95.

Duthie, MS, Kimber, I & Norval, M 1999, The effects of ultraviolet radiation on the human immune system, *British Journal of Dermatology*, 140: 995-1009.

Easton, JB & Houghton, PJ 2006, mTOR and cancer therapy, *Oncogene*, 25: 6436-46.

Eberle, J, Fecker, LF, Forschner, T, Ulrich, C, Rowert-Huber, J & Stockfleth, E 2007a, Apoptosis pathways as promising targets for skin cancer therapy, *British Journal of Dermatology*, 156 Suppl 3: 18-24.

Eberle, J & Hossini, AM 2008, Expression and function of Bcl-2 proteins in melanoma., *Current Genomics*, 9: 409-19.

Eberle, J, Kurbanov, BM, Hossini, AM, Trefzer, U & Fecker, LF 2007b, Overcoming apoptosis deficiency of melanoma-hope for new therapeutic approaches, *Drug Resistance Updates*, 10: 218-34.

Edlundh-Rose, E, Egyha`zi, S, Omholt, K, Mansson-Brahme, E, Platz, A, Hansson, J & Lundeberg, J 2006, NRAS and BRAF mutations in melanoma tumours in relation to clinical characteristics: a study based on mutation screening by pyrosequencing, *Melanoma Research*, 16: 471-8.

Ee, GCL, Daud, S, Izzaddin, SA & Rahmani, M 2008, *Garcinia mangostana*: a source of potential anti-cancer lead compounds against CEM-SS cell line, *Journal of Asian Natural Products Research*, 10: 475-9.

Ee, GCL, Daud, S, Taufiq-yap, YH, Ismail, NH & Rahmani, M 2006, Xanthones from *Garcinia mangostana* (Guttiferae), *Natural Product Research*, 20: 1067-73.

Eggermont, AM & Kirkwood, JM 2004, Re-evaluating the role of dacarbazine in metastatic melanoma: what have we learned in 30 years?, *European Journal of Cancer*, 40: 1825-36.

Eisenmann, KM, VanBrocklin, MW, Staffend, NA, Kitchen, SM & Koo, H-M 2003, Mitogen-Activated Protein Kinase Pathway-Dependent Tumor-Specific Survival Signaling in Melanoma Cells through Inactivation of the Proapoptotic Protein Bad, *Cancer Research*, 63: 8330-7.

Elmore, S 2007, Apoptosis: a review of programmed cell death., *Toxicologic Pathology*, 35: 495-516.

Fan, C & Su, J 1997, Antioxidative mechanism of isolated components from methanol extract of fruit hulls of *Garcinia mangostana* L, *Journal of the Chinese Agricultural Chemical Society*, 35: 540–51.

Fan, C, Yang, J & Engelhardt, JF 2002, Temporal pattern of NFκB activation influences apoptotic cell fate in a stimuli-dependent fashion, *Journal of Cell Science*, 115: 4843-53.

Farina, HG, Pomies, M, Alonso, DF & Gomez, DE 2006, Antitumor and antiangiogenic activity of soy isoflavone genistein in mouse models of melanoma and breast cancer, *Oncology Reports*, 16: 885-91.

Farnsworth, RN & Bunyapraphatsara, N 1992, *Garcinia mangostana* Linn., in *Thai Medicinal Plants*, Prachachon Co., Ltd, Bangkok, pp. 160-2.

Fellows, PJ 2000, *Food Processing Technology - Principles and Practice (2nd Edition)*, Woodhead Publishing, 978-1-85573-533-0, <http://www.knovel.com/web/portal/browse/display?_EXT_KNOVEL_DISPLAY_bookid=213>.

Filip, A, Clichici, S, Daicoviciu, D, Adriana, M, Postescu, ID, Perde-Schrepler, M & Olteanu, D 2009, Photochemoprevention of cutaneous neoplasia through natural products, *Experimental Oncology*, 31: 9-15.

Fotakis, G & Timbrell, JA 2006, In vitro cytotoxicity assays: Comparison of LDH, neutral red, MTT and protein assay in hepatoma cell lines following exposure to cadmium chloride, *Toxicology Letters*, 160: 171-7.

Fridovich, I 1998, Oxygen toxicity: a radical explanation, *The Journal of Experimental Biology*, 201: 1203-9.

Fulda, S & Debatin, KM 2006, Extrinsic versus intrinsic apoptosis pathways in anticancer chemotherapy, *Oncogene*, 25: 4798-811.

Fulda, S, Galluzzi, L & Kroemer, G 2010, Targeting mitochondria for cancer therapy, *Nature Reviews Drug Discovery*, 9: 447-64.

Furuta, E, Bandyopadhyay, S, Iiizumi, M, Mohinta, S, Zhan, R & Watabe, K 2006, The role of tumor metastasis suppressors in cancers of breast and prostate, *Frontiers in Bioscience*, 11: 2845-60.

Gan, J, Papiernik, SK, Koskinen, WC & Yates, SR 1999, Evaluation of accelerated solvent extraction (ASE) for analysis of pesticide residues in soil, *Environmental Science & Technology*, 33: 3249-53.

Garbe, C & Eigentler, TK 2007, Diagnosis and treatment of cutaneous melanoma: state of the art 2006, *Melanoma Research*, 17: 117-27.

Garcia, VV, Magpantay, TO & Escobin, LD 2005, Antioxidant potential of selected Philippine vegetables and fruits., *The Philippine Agricultural Scientist*, 88: 78-83.

Gardai, SJ, Hildeman, DA, Frankel, SK, Whitlock, BB, Frasch, SC, Borregaard, N, Marrack, P, Bratton, DL & Henson, PM 2004, Phosphorylation of Bax Ser184 by Akt regulates its activity and apoptosis in neutrophils, *The Journal of Biological Chemistry*, 279: 21085-95.

Garfin, DE 2003, Two-dimensional gel electrophoresis: an overview, *TrAC Trends in Analytical Chemistry*, 22: 263-72.

Garner, CM, Hubbold, LM & Chakraborti, PR 2000, Mycoplasma detection in cell cultures: a comparison of four methods, *British Journal of Biomedical Science*, 57: 295-301.

Gilbert, B & Alves, LF 2003, Synergy in plant medicines, *Current Medicinal Chemistry*, 10: 13-20.

Gillies, RJ, Didier, N & Denton, M 1986, Determination of cell number in monolayer cultures, *Analytical Biochemistry*, 159: 109-13.

Goette, DK 1981, Topical chemotherapy with 5-fluorouracil. A review, *Journal of the American Academy of Dermatology*, 4: 633-49.

Gonzales, M, Erdei, E & Berwick, M 2008, Epidemiology of skin cancer, in K Nouri (ed.), *Skin cancer*, The McGraw-Hill Company, Miami, Florida.

Gonzalez, E & McGraw, TE 2009, The Akt kinases: Isoform specificity in metabolism and cancer, *Cell Cycle*, 8: 2502-8.

Gopalakrishnan, G, Banumathi, B & Suresh, G 1997, Evaluation of the antifungal activity of natural xanthones from *Garcinia mangostana* and their synthetic derivatives, *Journal of Natural Products*, 60: 519-24.

Gordaliza, M 2007, Natural products as leads to anticancer drugs, *Clinical and Translational Oncology*, 9: 767-76.

Gorden, A, Osman, I, Gai, W, He, D, Huang, W, Davidson, A, Houghton, AN, Busam, K & Polsky, D 2003, Analysis of BRAF and N-RAS mutations in metastatic melanoma tissues, *Cancer Research*, 63: 3955-7.

Gorinstein, S, Zachwieja, Z, Katrich, E, Pawelzik, E, Haruenkit, R, Trakhtenberg, S & Martin-Belloso, O 2004, Comparison of the contents of the main antioxidant compounds and the antioxidant activity of white grapefruit and his new hybrid, *LWT - Food Science and Technology*, 37: 337-43.

Govindachari, TRKP & Muthukumaraswamy, N 1971, Xanthones of *Garcinia mangostana* Linn., *Tetrahedron*, 27: 3919-26.

Grana, X & Reddy, EP 1995, Cell cycle control in mammalian cells: role of cyclins, cyclin dependent kinases (CDKs), growth suppressor genes and cyclin-dependent kinase inhibitors (CKIs), *Oncogene*, 11: 211-9.

Green, AC, Williams, GM, Logan, V & Strutton, GM 2011, Reduced Melanoma After Regular Sunscreen Use: Randomized Trial Follow-Up, *Journal of Clinical Oncology*, 29: 257-63.

Green, DR & Amarante-Mendes, GP 1998, The point of no return: mitochondria, caspases, and the commitment to cell death, *Results & Problems in Cell Differentiation*, 24: 45-61.

Green, DR & Reed, JC 1998, Mitochondria and apoptosis, *Science*, 281: 1309-12.

Gross, A, McDonnell, JM & Korsmeyer, SJ 1999, BCL-2 family members and the mitochondria in apoptosis, *Genes and Development*, 13: 1899-911.

Guertin, DA & Sabatini, DM 2007, Defining the role of mTOR in cancer, *Cancer*

Cell, 12: 9-22.

Guichard, S, Cussac, D, Hennebelle, I, Bugat, R & Canal, P 1997, Sequence-dependent activity of the irinotecan-5FU combination in human colon-cancer model HT-29 *in vitro* and *in vivo*, *International Journal of Cancer*, 73: 729-34.

Gupta, S & Mukhtar, H 2001, Chemoprevention of skin cancer through natural agents, *Skin Pharmacology and Applied Skin Physiology*, 14: 373-85.

Guthrie, N & Carroll, KK 1998, Inhibition of mammary cancer by citrus flavonoids, *Advances in Experimental Medicine and Biology*, 439: 227-36.

Gygi, SP, Rochon, Y, Franza, BR & Aebersold, R 1999, Correlation between protein and mRNA abundance in yeast, *Molecular and Cellular Biology*, 19: 1720-30.

Hacker, SM, Browder, JF & Ramos-Caro, FA 1993, Basal cell carcinoma. Choosing the best method of treatment for a particular lesion, *Postgraduate Medicine*, 93: 101-4, 6-8, 11.

Hahnvajanawong, C, Boonyanugomol, W, Nasomyon, T, Loilome, W, Namwat, N, Anantachoke, N, Tassaneeyakul, W, Sripa, B, Namwat, W & Reutrakul, V 2010, Apoptotic activity of caged xanthones from *Garcinia hanburyi* in cholangiocarcinoma cell lines, *World Journal of Gastroenterology*, 16: 2235-43.

Hall, M & Peters, G 1996, Genetic Alterations of Cyclins, Cyclin-Dependent Kinases, and Cdk Inhibitors in Human Cancer, in FVW, *Advances in Cancer Research*, vol. 68, pp. 67-108.

Han, AR, Kim, JA, Lantvit, DD, Kardono, LB, Riswan, S, Chai, H, Carcache de Blanco, EJ, Farnsworth, NR, Swanson, SM & Kinghorn, AD 2009, Cytotoxic xanthone constituents of the stem bark of *Garcinia mangostana* (mangosteen), *Journal of Natural Products*, 72: 2028-31.

Hanada, M, Feng, J & Hemmings, BA 2004, Structure, regulation and function of PKB/AKT—a major therapeutic target, *Biochimica et Biophysica Acta*, 1697: 3-16.

Hanahan, D & Weinberg, RA 2011, Hallmarks of cancer: the next generation, *Cell*, 144: 646-74.

Hansen, MB, Nielsen, SE & Berg, K 1989, Re-examination and further development of a precise and rapid dye method for measuring cell growth/cell kill, *Journal of Immunological Methods*, 119: 203-10.

Harbone, J, Baxter, H & Moss, G 1999, Phytochemical dictionary- A handbook of bioactive compounds from plants., in Taylor & Francis, London, p. 590.

Harford, JB & Morris, DR 1997, Post-transcriptional gene regulation., in Wiley-Liss, Inc., New York.

Harrison, NLJ 2002, Xanthones from the heartwood of *Garcinia mangostana*,

Phytochemistry, 60: 541-8.

Haruenkit, R, Poovarodom, S, Leontowicz, H, Leontowicz, M, Sajewicz, M, Kowalska, T, Delgado-Licon, E, Rocha-Guzmán, NE, Gallegos-Infante, JA, Trakhtenberg, S & Gorinstein, S 2007, Comparative study of health properties and nutritional value of durian, mangosteen, and snake fruit: experiments *in vitro* and *in vivo*, *Journal of Agricultural and Food Chemistry*, 55: 5842-9.

Hatzivassiliou, G, Song, K, Yen, I, Brandhuber, BJ, Anderson, DJ, Alvarado, R, Ludlam, MJC, Stokoe, D, Gloor, SL, Vigers, G, Morales, T, Aliagas, I, Liu, B, Sideris, S, Hoeflich, KP, Jaiswal, BS, Seshagiri, S, Koeppen, H, Belvin, M, Friedman, LS & Malek, S 2010, RAF inhibitors prime wild-type RAF to activate the MAPK pathway and enhance growth, *Nature*, 464: 431-5.

Hayakawa, S, Tochigi, M, Chishima, F, Shiraishi, H, Takahashi, N, Watanabe, K, Fujii, KT & Satoh, K 1996, Expression of the recombinase-activating gene (RAG-1) in murine early embryogenesis, *Immunology & Cell Biology*, 74: 52-6.

Hedrick, JL, Mulcahey, LJ & Taylor, LT 1992, Supercritical fluid extraction, *Microchimica Acta*, 108: 115-32.

Hemalatha, S, Mandal, V & Mohan, Y 2007, Microwave assisted extraction - An innovative and promising extraction tool for medicinal plant research, *Pharmacognosy Reviews*, 1: 7-18.

Hendricks, WA & Robey, KW 1936, The sampling distribution of the coefficient of variation., *Annals of Mathematical Statistics*, 7: 129-32.

Hennings, H, Shores, R, Mitchell, P, Spangler, EF & Yuspa, SH 1985, Induction of papillomas with a high probability of conversion to malignancy, *Carcinogenesis*, 6: 1607-10.

Henry-Mowatt, J, Dive, C, Martinou, JC & James, D 2004, Role of mitochondrial membrane permeabilization in apoptosis and cancer, *Oncogene*, 23: 2850-60.

Heon Seo, K, Ko, HM, Kim, HA, Choi, J-H, Jun Park, S, Kim, KJ, Lee, HK & Im, SY 2006, Platelet-activating factor induces up-regulation of antiapoptotic factors in a melanoma cell line through nuclear factor-κB activation, *Cancer Research*, 66: 4681-6.

Herrera, MC & de Castro, MD 2005, Ultrasound-assisted extraction of phenolic compounds from strawberries prior to liquid chromatographic separation and photodiode array ultraviolet detection, *Journal of Chromatography A*, 1100: 1-7.

Ho, CK, Huang, YL & Chen, CC 2002, Garcinone E, a xanthone derivative, has potent cytotoxic effect against hepatocellular carcinoma cell lines, *Planta Medica*, 68: 975-9.

Ho, ML, Hsieh, YS, Chen, JY, Chen, KS, Chen, JJ, Kuo, WH, Lin, SJ & Chen, PN 2011, Antimetastatic potentials of *Dioscorea nipponica* on melanoma *in vitro* and *in*

vivo, *Evidence-based Complementary and Alternative Medicine*, 2011: 507920.

Hofmann, UB, Houben, R, Brocker, EB & Becker, JC 2005, Role of matrix metalloproteinases in melanoma cell invasion, *Biochimie*, 87: 307-14.

Hollestein, LM, van den Akker, SA, Nijsten, T, Karim-Kos, HE, Coebergh, JW & de Vries, E 2012, Trends of cutaneous melanoma in The Netherlands: increasing incidence rates among all Breslow thickness categories and rising mortality rates since 1989, *Annals of Oncology*, 23: 524-30.

Horst, B, Gruvberger-Saal, SK, Hopkins, BD, Bordone, L, Yang, Y, Chernoff, KA, Uzoma, I, Schwipper, V, Liebau, J, Nowak, NJ, Brunner, G, Owens, D, Rimm, DL, Parsons, R & Celebi, JT 2009, Gab2-mediated signaling promotes melanoma metastasis, *The American Journal of Pathology*, 174: 1524-33.

Hossini, AM, Eberle, J, Fecker, LF, Orfanos, CE & Geilen, CC 2003, Conditional expression of exogenous Bcl-XS triggers apoptosis in human melanoma cells *in vitro* and delays growth of melanoma xenografts, *Federation of European Biochemists letters*, 553: 250-6.

Housman, TS, Feldman, SR, Williford, PM, Fleischer, AB, Jr., Goldman, ND, Acostamadiedo, JM & Chen, GJ 2003, Skin cancer is among the most costly of all cancers to treat for the Medicare population, *Journal of the American Academy of Dermatology*, 48: 425-9.

Hsu, CY, Chan, YP & Chang, JL 2007, Antioxidant activity of extract from *Polygonum cuspidatum*, *Biological Research*, 40: 13-21.

Hsu, H, Xiong, J & Goeddel, DV 1995, The TNF receptor 1-associated protein TRADD signals cell death and NF-kB activation, *Cell*, 81: 495-504.

http://www.doubling-time.com

Huang, D, Ou, B & Prior, RL 2005, The chemistry behind antioxidant capacity assays, *Journal of Agricultural and Food Chemistry*, 53: 1841-56.

Huang, DC & Strasser, A 2000, BH3-only proteins-essential initiators of apoptotic cell death, *Cell*, 103: 839-42.

Huang, S, Robinson, JB, Deguzman, A, Bucana, CD & Fidler, IJ 2000, Blockade of nuclear factor-kappaB signaling inhibits angiogenesis and tumorigenicity of human ovarian cancer cells by suppressing expression of vascular endothelial growth factor and interleukin 8, *Cancer Research*, 60: 5334-9.

Huang, YL, Chen, CC, Chen, YJ, Huang, RL & Shieh, BJ 2001, Three xanthones and a benzophenone from *Garcinia mangostana*, *Journal of Natural Products*, 64: 903-6.

Hung, SH, Shen, KH, Wu, CH, Liu, CL & Shih, YW 2009, α-Mangostin suppresses PC-3 human prostate carcinoma cell metastasis by inhibiting matrix

metalloproteinase-2/9 and urokinase-plasminogen expression through the JNK signaling pathway, *Journal of Agricultural and Food Chemistry*, 57: 1291-8.

Iiizumi, M, Liu, W, Pai, SK, Furuta, E & Watabe, K 2008, Drug development against metastasis-related genes and their pathways: a rationale for cancer therapy, *Biochimica et Biophysica Acta*, 1786: 87-104.

Ishiyama, M, Tominaga, H, Shiga, M, Sasamoto, K, Ohkura, Y & Ueno, K 1996, A combined assay of cell viability and in vitro cytotoxicity with a highly water-soluble tetrazolium salt, neutral red and crystal violet, *Biological & Pharmaceutical Bulletin*, 19: 1518-20.

Itoh, Y & Nagase, H 2002, Matrix metalloproteinases in cancer, *Essays in Biochemistry*, 38: 21-36.

Ivanov, VN, Bhoumik, A & Ronai, Z 2003, Death receptors and melanoma resistance to apoptosis, *Oncogene*, 22: 3152-61.

Jarry, A, Masson, D, Cassagnau, E, Parois, S, Laboisse, C & Denis, MG 2004, Real-time allele-specific amplification for sensitive detection of the BRAF mutation V600E, *Molecular and Cellular Probes*, 18: 349-52.

Javanmardi, J, Stushnoff, C, Locke, E & Vivanco, JM 2003, Antioxidant activity and total phenolic content of Iranian Ocimum accessions, *Food Chemistry*, 83: 547-50.

Jemal, A, Murray, T, Ward, E, Samuels, A, Tiwari, RC, Ghafoor, A, Feuer, EJ & Thun, MJ 2005, Cancer statistics, 2005, *CA - A Cancer Journal for Clinicians*, 55: 10-30.

Jemal, A, Siegel, R, Ward, E, Murray, T, Xu, J, Smigal, C & Thun, MJ 2006, Cancer statistics, 2006, *CA - A Cancer Journal for Clinicians*, 56: 106-30.

Jenkins, GJS, Harries, K, Doak, SH, Wilmes, A, Griffiths, AP, Baxter, JN & Parry, JM 2004, The bile acid deoxycholic acid (DCA) at neutral pH activates NF-κB and induces IL-8 expression in oesophageal cells *in vitro*, *Carcinogenesis*, 25: 317-23.

Ji, X, Avula, B & Khan, IA 2007, Quantitative and qualitative determination of six xanthones in *Garcinia mangostana* L. by LC–PDA and LC–ESI-MS, *Journal of Pharmaceutical and Biomedical Analysis* 43: 1270–6.

Jinsart, W, Ternai, B, Buddhasukh, D & Polya, GM 1992, Inhibition of wheat embryo calcium-dependent protein kinase and other kinases by mangostin and γ-mangostin, *Phytochemistry*, 31: 3711-3.

Johnson, TM, Dolan, OM, Hamilton, TA, Lu, MC, Swanson, NA & Lowe, L 1998, Clinical and histologic trends of melanoma, *Journal of the American Academy of Dermatology*, 38: 681-6.

Johnstone, RW, Ruefli, AA & Lowe, SW 2002, Apoptosis: a link between cancer genetics and chemotherapy, *Cell*, 108: 153-64.

Jung, HA, Su, BN, Keller, WJ, Mehta, RG & Kinghorn, AD 2006, Antioxidant xanthones from the pericarp of *Garcinia mangostana* (Mangosteen), *Journal of Agriculture Food Chemistry*, 54: 2077-82.

Kalia, K, Sharma, K, Singh, HP & Singh, B 2008a, Effects of extraction methods on phenolic contents and antioxidant activity in aerial parts of *Potentilla atrosanguinea Lodd*. and quantification of its phenolic constituents by RP-HPLC, *Journal of Agriculture Food Chemistry*, 56: 10129-34.

Karin, M, Cao, Y, Greten, FR & Li, ZW 2002, NF-kappaB in cancer: from innocent bystander to major culprit, *Nature Reviews Cancer*, 2: 301-10.

Kaur, J, Sharma, M, Sharma, PD & Bansal, MP 2010, Antitumor activity of Lantadenes in DMBA/TPA induced skin tumors in mice: expression of transcription factors, *American Journal of Biomedical Sciences*, 2: 79-90.

Kaur, M, Agarwal, C, Singh, RP, Guan, X, Dwivedi, C & Agarwal, R 2005, Skin cancer chemopreventive agent, α-santalol, induces apoptotic death of human epidermoid carcinoma A431 cells via caspase activation together with dissipation of mitochondrial membrane potential and cytochrome c release, *Carcinogenesis*, 26: 369-80.

Kawaguchi, T 2005, Cancer metastasis: characterization and identification of the behavior of metastatic tumor cells and the cell adhesion molecules, including carbohydrates, *Current Drug Targets Cardiovascular & Haematological Disorder*, 5: 39-64.

Kefford, R, Arkenau, H, Brown, MP, Millward, M, Infante, JR, Long, GV, Ouellet, D, Curtis, M, Lebowitz, PF & Falchook, GS 2010, Phase I/II study of GSK2118436, a selective inhibitor of oncogenic mutant BRAF kinase, in patients with metastatic melanoma and other solid tumors., *Journal of Clinical Oncology*, 28:15s, 2010 (suppl; abstr 8503)

Kelland, L 2007, The resurgence of platinum-based cancer chemotherapy, *Nature Reviews Cancer*, 7: 573-84.

Kim, AL, Zhu, Y, Zhu, H, Han, L, Kopelovich, L, Bickers, DR & Athar, M 2006, Resveratrol inhibits proliferation of human epidermoid carcinoma A431 cells by modulating MEK1 and AP-1 signalling pathways, *Experimental Dermatology*, 15: 538-46.

Kischkel, FC, Hellbardt, S, Behrmann, I, Germer, M, Pawlita, M, krammer, PH & Peter, ME 1995, Cytotoxicity-dependent APO-1 (Fas/CD95)-associated proteins form a death-inducing signaling complex (DISC) with the receptor., *The European Molecular Biological Organization Journal*, 14: 5579-88.

Kitchen, CMR 2009, Nonparametric vs parametric tests of location in biomedical research, *American Journal of Ophthalmology*, 147: 571-2.

Kohler, T 1995, Design of suitable primers and competitor fragments for quantitative PCR, in T Kohler, D labner, AK Rost, B Thamm, B Pustowoit & H Remke (eds), *Quantitation of mRNA by polymerase chain reaction*, Springer-Verlag, Berlin, pp. 15-26.

Konczak, I & Zhang, W 2004, Anthocyanins-More than nature's colours, *Journal of Biomedicine and Biotechnology*, 2004: 239-40.

Koopman, G, Reutelingsperger, CP, Kuijten, GA, Keehnen, RM, Pals, ST & van Oers, MH 1994, Annexin V for flow cytometric detection of phosphatidylserine expression on B cells undergoing apoptosis, *Blood*, 84: 1415-20.

Krajarng, A, Nakamura, Y, Suksamrarn, S & Watanapokasin, R 2011, Alpha-Mangostin induces apoptosis in human chondrosarcoma cells through downregulation of ERK/JNK and Akt signaling pathway, *Journal of Agricultural and Food Chemistry*, 59: 5746-54.

Krinsky, NI 1989, Antioxidant functions of carotenoids, *Free Radical Biology & Medicine*, 7: 617-35.

Kroemer, G 2003, Mitochondrial control of apoptosis: an introduction, *Biochemical and Biophysical Research Communications*, 304: 433-5.

Kumar, R, Angelini, S, Czene, K, Sauroja, I, Hahka-Kemppinen, M, Pyrhonen, S & Hemminki, K 2003, BRAF mutations in metastatic melanoma: a possible association with clinical outcome, *Clinical Cancer Research*, 9: 3362-8.

Kwa, RE, Campana, K & Moy, RL 1992, Biology of cutaneous squamous cell carcinoma, *Journal of the American Academy of Dermatology*, 26: 1-26.

Kyriakis, JM & Avruch, J 2001, Mammalian mitogen-activated protein kinase signal transduction pathways activated by stress and inflammation, *Physiological Reviews*, 81: 807-69.

Lansky, EP, Jiang, W, Mo, H, Bravo, L, Froom, P, Yu, W, Harris, NM, Neeman, I & Campbell, MJ 2005, Possible synergistic prostate cancer suppression by anatomically discrete pomegranate fractions, *Investigational New Drugs*, 23: 11-20.

Laphookhieo, S, Syers, JK, Kiattansakul, R & Chantrapromma, K 2006, Cytotoxic and antimalarial prenylated xanthones from *Cratoxylum cochinchinense*, *Chemical and Pharmaceutical Bulletin*, 54: 745-7.

Laroze, L, Soto, C & Zuniga, ME 2010, Phenolic antioxidants extraction from raspberry wastes assisted by-enzymes., *Electronic Journal of Biotechnology*, 13: http://dx.doi.org/10.2225/vol13-issue6-fulltext-12.

Larrosa, M, Tomas-Barberan, FA & Espin, JC 2003, Grape polyphenol resveratrol and the related molecule 4-hydroxystilbene induce growth inhibition, apoptosis, S-phase arrest, and upregulation of cyclins A, E, and B1 in human SK-Mel-28 melanoma cells, *Journal of Agriculture Food Chemistry*, 51: 4576-84.

Le Floch, F, Tena, MT, Rios, A & Valcarcel, M 1998, Supercritical fluid extraction of phenol compounds from olive leaves, *Talanta*, 46: 1123-30.

Lee, KJ, Kim, JY, Choi, JH, Kim, HG, Chung, YC, Roh, SH & Jeong, HG 2006, Inhibition of tumor invasion and metastasis by aqueous extract of the radix of *Platycodon grandiflorum*, *Food and Chemical Toxicology*, 44: 1890-6.

Lee, YB, Ko, KC, Shi, MD, Liao, YC, Chiang, TA, Wu, PF, Shih, YX & Shih, YW 2010, α-Mangostin, a novel dietary xanthone, suppresses TPA-mediated MMP-2 and MMP-9 expressions through the ERK signaling pathway in MCF-7 human breast adenocarcinoma cells, *Journal of Food Science*, 75: 13-23.

Leong, LP & Shui, G 2002, An investigation of antioxidant capacity of fruits in Singapore markets, *Food Chemistry*, 76: 69-75.

Lev, DC, Ruiz, M, Mills, L, McGary, EC, Price, JE & Bar-Eli, M 2003, Dacarbazine causes transcriptional up-regulation of interleukin 8 and vascular endothelial growth factor in melanoma cells: a possible escape mechanism from chemotherapy1, *Molecular Cancer Therapeutics*, 2: 753-63.

Li, G, Kalabis, J, Xu, X, Meier, F, Oka, M, Bogenrieder, T & Herlyn, M 2003, Reciprocal regulation of MelCAM and AKT in human melanoma, *Oncogene*, 22: 6891-9.

Li, G, Mitchell, DL, Ho, VC, Reed, JC & Tron, VA 1996, Decreased DNA repair but normal apoptosis in ultraviolet-irradiated skin of p53-transgenic mice, *American Journal of Pathology*, 148: 1113-23.

Li, JJ, Westergaard, C, Ghosh, P & Colburn, NH 1997, Inhibitors of both nuclear factor-kappaB and activator protein-1 activation block the neoplastic transformation response, *Cancer Research*, 57: 3569-76.

Li, Y, Birnbaumer, L & Teng, CT 2010, Regulation of ERRα gene expression by estrogen receptor agonists and antagonists in SKBR3 breast cancer cells: differential molecular mechanisms mediated by G protein-coupled receptor GPR30/GPER-1, *Molecular Endocrinology*, 24: 969-80.

Li, ZG, Zhao, YL, Wu, X, Ye, HY, Peng, A, Cao, ZX, Mao, YQ, Zheng, YZ, Jiang, PD, Zhao, X, Chen, LJ & Wei, YQ 2009, Barbigerone, a natural isoflavone, induces apoptosis in murine lung-cancer cells via the mitochondrial apoptotic pathway, *Cellular Physiology Biochemistry*, 24: 95-104.

Lillehammer, T, Engesaeter, BO, Prasmickaite, L, Maelandsmo, GM, Fodstad, O & Engebraaten, O 2007, Combined treatment with Ad-hTRAIL and DTIC or SAHA is associated with increased mitochondrial-mediated apoptosis in human melanoma cell lines, *The Journal of Gene Medicine*, 9: 440-51.

Lin, HY, Sun, M, Tang, HY, Simone, TM, Wu, YH, Grandis, JR, Cao, HJ, Davis, PJ & Davis, FB 2008, Resveratrol causes COX-2- and p53-dependent apoptosis in head

and neck squamous cell cancer cells, *Journal of Cellular Biochemistry*, 104: 2131-42.

Lin, K, Baritaki, S, Militello, L, Malaponte, G, Bevelacqua, Y & Bonavida, B 2010, The role of B-RAF mutations in melanoma and the induction of EMT via dysregulation of the NF-κB/Snail/RKIP/PTEN circuit, *Genes & Cancer*, 1: 409-20.

Lin, LI, Ke, YF, Ko, YC & Lin, JK 1998, Curcumin inhibits SK-Hep-1 hepatocellular carcinoma cell invasion *in vitro* and suppresses matrix metalloproteinase-9 secretion, *Oncology*, 55: 349-53.

Liotta, LA, Stetler-Stevenson, WG & Steeg, PS 1991, Cancer invasion and metastasis: positive and negative regulatory elements, *Cancer Investigation Journal*, 9: 543-51.

Lowe, SW, Cepero, E & Evan, G 2004, Intrinsic tumour suppression, *Nature*, 432: 307-15.

Madan, E, Prasad, S, Roy, P, George, J & Shukla, Y 2008, Regulation of apoptosis by resveratrol through JAK/STAT and mitochondria mediated pathway in human epidermoid carcinoma A431 cells, *Biochemical and Biophysical Research Communications*, 377: 1232-7.

Mahabusarakam, W, Proudfoot, J, Taylor, W & Croft, K 2000, Inhibition of lipoprotein oxidation by prenylated xanthones derived from mangostin, *Free Radical Research*, 33: 643-59.

Mahabusarakam, W, Wiriyachitra, P & Taylor, WC 1987, Chemical constituents of *Garcinia mangostana*, *Journal of Natural Products*, 50: 474-8.

Malumbres, M & Carnero, A 2003, Cell cycle deregulation: a common motif in cancer, *Progress in Cell Cycle Research*, 5: 5-18.

Manda, G, Nechifor, MT & Neagu, TM 2009, Reactive oxygen species, cancer and anti-cancer therapies., *Current Chemical Biology*, 3: 342-66.

Manning, BD & Cantley, LC 2007, AKT/PKB signaling: navigating downstream, *Cell*, 129: 1261-74.

Mantena, SK, Sharma, SD & Katiyar, SK 2006, Berberine inhibits growth, induces G_1 arrest and apoptosis in human epidermoid carcinoma A431 cells by regulating Cdki-Cdk-cyclin cascade, disruption of mitochondrial membrane potential and cleavage of caspase 3 and PARP, *Carcinogenesis*, 27: 2018-27.

Matsumoto, K, Akao, Y, Kobayashi, E, Ohguchi, K, Ito, T, Tanaka, T, Iinuma, M & Nozawa, Y 2003, Induction of apoptosis by xanthones from mangosteen in human leukemia cell lines, *Journal of Natural Products*, 66: 1124-7.

Matsumoto, K, Akao, Y, Ohguchi, K, Ito, T, Tanaka, T, Iinuma, M & Nozawa, Y 2005, Xanthones induce cell-cycle arrest and apoptosis in human colon cancer DLD-

1 cells, *Bioorganic & Medicinal Chemistry*, 13: 6064-9.

Matsumoto, K, Akao, Y, Yi, H, Ohguchi, K, Ito, T, Tanaka, T, Kobayashi, E, Iinuma, M & Nozawa, Y 2004, Preferential target is mitochondria in alpha-mangostin-induced apoptosis in human leukemia HL60 cells, *Bioorganic & Medicinal Chemistry*, 12: 5799-806.

Mazurkiewicz, M & Peszynski, J 1998, Acute radiation reaction and its healing time after skin cancer radiotherapy in elderly patients, *Polski Merkuriusz Lekarski*, 4: 199-201.

McDonald, ER, 3rd & El-Deiry, WS 2000, Cell cycle control as a basis for cancer drug development (Review), *International Journal of Oncology*, 16: 871-86.

Meeran, SM & Katiyar, SK 2007, Grape seed proanthocyanidins promote apoptosis in human epidermoid carcinoma A431 cells through alterations in Cdki-Cdk-cyclin cascade, and caspase-3 activation via loss of mitochondrial membrane potential, *Experimental Dermatology*, 16: 405-15.

Mercer, KE & Pritchard, CA 2003, Raf proteins and cancer: B-Raf is identified as a mutational target, *Biochimica et Biophysica Acta*, 1653: 25-40.

Miller, DL & Weinstock, MA 1994, Nonmelanoma skin cancer in the United States: incidence, *Journal of the American Academy of Dermatology*, 30: 774-8.

Miller, SJ 1991, Biology of basal cell carcinoma (Part I), *Journal of the American Academy of Dermatology*, 24: 1-13.

Mirmohammadsadegh, A, Mota, R, Gustrau, A, Hassan, M, Nambiar, S, Marini, A, Bojar, H, Tannapfel, A & Hengge, UR 2007, ERK1/2 is highly phosphorylated in melanoma metastases and protects melanoma cells from cisplatin-mediated apoptosis, *Journal of Investigative Dermatology*, 127: 2207-15.

Mohapatra, S, Coppola, D, Riker, AI & Pledger, WJ 2007, Roscovitine inhibits differentiation and invasion in a three-dimensional skin reconstruction model of metastatic melanoma, *Molecular Cancer Research*, 5: 145-51.

Molinari, M 2000, Cell cycle checkpoints and their inactivation in human cancer, *Cell Proliferation*, 33: 261-74.

Moongkarndi, P, Kosem, N, Kaslungka, S, Luanratana, O, Pongpan, N & Neungton, N 2004, Antiproliferation, antioxidation and induction of apoptosis by *Garcinia mangostana* (mangosteen) on SKBR3 human breast cancer cell line, *Journal of Ethnopharmacology*, 90: 161-6.

Moongkarndi, P, Kosem, N, Luanratana, O, Jongsomboonkusol, S & Pongpan, N 2004c, Antiproliferative activity of Thai medicinal plant extracts on human breast adenocarcinoma cell line, *Fitoterapia*, 75: 375-7.

Morgan, DO 1995, Principles of CDK regulation, *Nature*, 374: 131-4.

Morton, JF 1987, Fruits of warm climates, in Creative Resource System Inc., Miami, USA, p. 304.

Mosmann, T 1983, Rapid colorimetric assay for cellular growth and survival: application to proliferation and cytotoxicity assays, *Journal of Immunological Methods*, 65: 55-63.

Mukhtar, H & Elmets, CA 1996, Photocarcinogenesis: mechanisms, models and human health implications, *Photochemistry and Photobiology*, 63: 356-7.

Müller, M, Schleithoff, ES, Stremmel, W, Melino, G, Krammer, PH & Schilling, T 2006, One, two, three-p53, p63, p73 and chemosensitivity, *Drug resistance updates : reviews and commentaries in antimicrobial and anticancer chemotherapy*, 9: 288-306.

Muñoz-Alonso, MJ, González-Santiago, L, Zarich, N, Martínez, T, Alvarez, E, Rojas, JM & Muñoz, A 2008, Plitidepsin has a dual effect inhibiting cell cycle and inducing apoptosis via Rac1/c-Jun NH2-terminal kinase activation in human melanoma cells, *Journal of Pharmacology and Experimental Therapeutics*, 324: 1093-101.

Munshi, A, Kurland, JF, Nishikawa, T, Chiao, PJ, Andreeff, M & Meyn, RE 2004, Inhibition of constitutively activated nuclear factor-kappaB radiosensitizes human melanoma cells, *Molecular Cancer Therapeutics*, 3: 985-92.

Murphy, GF, Sellheyer, K & Mihm, MC 2004, The skin, in Robbins & Cotran Pathologic Basis of Disease (V Kumar, AK Abbas, N Fausto, eds), 7th ed. Elsevier-Saunders, Philadelphia, p. 1227-72.

Na, Y 2009, Recent cancer drug development with xanthone structures, *Journal of Pharmacy and Pharmacology*, 61: 707-12.

Nabandith, V, Suzui, M, Morioka, T, Kaneshiro, T, Kinjo, T, Matsumoto, K, Akao, Y, Iinuma, M & Yoshimi, N 2004, Inhibitory effects of crude alpha-mangostin, a xanthone derivative, on two different categories of colon preoplastic lesions induced by 1, 2-dimethylhydrazine in the rat, *Asian Pacific Journal of Cancer Prevention*, 5: 433-8.

Nakagawa, Y, Iinuma, M, Naoe, T, Nozawa, Y & Akao, Y 2007, Characterized mechanism of α-mangostin-induced cell death: caspase-independent apoptosis with release of endonuclease-G from mitochondria and increased miR-143 expression in human colorectal cancer DLD-1 cells, *Bioorganic & Medicinal Chemistry*, 15: 5620-8.

Nakamura, K, Nagata, C, Oba, S, Takatsuka, N & Shimizu, H 2008, Fruit and vegetable intake and mortality from cardiovascular disease are inversely associated in Japanese women but not in men, *Journal of Nutrition*, 138: 1129-34.

Nakayama, H, Ikebe, T, Beppu, M & Shirasuna, K 2001, High expression levels of nuclear factor B, I B kinase , and Akt kinase in squamous cell carcinoma of the oral

cavity, *Cancer (Phila.)*, 92: 3037–44.

Neudauer, CL & McCarthy, JB 2003, Insulin-like growth factor I-stimulated melanoma cell migration requires phosphoinositide 3-kinase but not extracellular-regulated kinase activation, *Experimental Cell Research*, 286: 128-37.

Newman, DJ, Cragg, GM & Snader, KM 2003, Natural products as sources of new drugs over the period 1981-2002, *Journal of Natural Products*, 66: 1022-37.

Nicholson, KM & Anderson, NG 2002, The protein kinase B/Akt signalling pathway in human malignancy, *Cellular Signalling*, 14: 381-95.

Nicoletti, I, Migliorati, G, Pagliacci, MC, Grignani, F & Riccardi, C 1991, A rapid and simple method for measuring thymocyte apoptosis by propidium iodide staining and flow cytometry, *Journal of Immunological Methods*, 139: 271-9.

Nirmala, MJ, Samundeeswari, A & Sankar, PD 2011, Natural plant resources in anti-cancer therapy - A review, *Research in Plant Biology*, 1: 1-14.

Norbury, C & Nurse, P 1992, Animal cell cycles and their control, *Annual Review of Biochemistry*, 61: 441-70.

Nouri, K (ed.) 2008, Skin cancer, McGraw-Hill Medical, New York.

Nuijen, B, Bouma, M, Manada, C, Jimeno, JM, Schellens, JH, Bult, A & Beijnen, JH 2000, Pharmaceutical development of anticancer agents derived from marine sources, *Anticancer Drugs*, 11: 793-811.

Obolskiy, D, Pischel, I, Siriwatanametanon, N & Heinrich, M 2009, *Garcinia mangostana* L.: a phytochemical and pharmacological review, *Phytotherapy Research*, 23: 1047-65.

Odashiro, AN, Pereira, PR, Marshall, J-C, Godeiro, K & Burnier Jr, MN 2005, Skin cancer models, *Drug Discovery Today: Disease Models*, 2: 71-5.

Ogbourne, SM, Suhrbier, A, Jones, B, Cozzi, SJ, Boyle, GM, Morris, M, McAlpine, D, Johns, J, Scott, TM, Sutherland, KP, Gardner, JM, Le, TT, Lenarczyk, A, Aylward, JH & Parsons, PG 2004, Antitumor activity of 3-ingenyl angelate: plasma membrane and mitochondrial disruption and necrotic cell death, *Cancer Research*, 64: 2833-9.

Onn, A & Herbst, RS 2003, Angiogenesis, metastasis, and lung cancer. An overview, *Methods in Molecular Medicine*, 74: 329-48.

Ouhtit, A & Ananthaswamy, HN 2001, A model for UV-induction of skin cancer, *Journal of Biomedicine and Biotechnology*, 1: 5-6.

Ozes, ON, Mayo, LD, Gustin, JA, Pfeffer, SR, Pfeffer, LM & Donner, DB 1999, NF-κB activation by tumour necrosis factor requires the Akt serine-threonine kinase, *Nature*, 401: 82-5.

Padda, MS & Picha, DH 2007, Methodology optimization for quantification of total phenolics and individual phenolic acids in sweetpotato (*Ipomoea batatas* L.) roots, *Journal of Food Science*, 72: 412-6.

Panka, DJ, Atkins, MB & Mier, JW 2006, Targeting the Mitogen-Activated Protein Kinase pathway in the treatment of malignant melanoma, *Clinical Cancer Research*, 12: 2371-5.

Pap, M & Cooper, GM 1998, Role of glycogen synthase kinase-3 in the phosphatidylinositol 3-Kinase/Akt cell survival pathway, *The Journal of Biological Chemistry*, 273: 19929-32.

Parkin, DM, Bray, F, Ferlay, J & Pisani, P 2005, Global cancer statistics, 2002, *CA-A Cancer Journal for Clinicians*, 55: 74-108.

Patthamakanokporn, O, Puwastien, P, Nitithamyong, A & Sirichakwal, PP 2008, Changes of antioxidant activity and total phenolic compounds during storage of selected fruits, *Journal of Food Composition and Analysis*, 21: 241-8.

Pavletich, NP 1999, Mechanisms of cyclin-dependent kinase regulation: structures of Cdks, their cyclin activators, and Cip and INK4 inhibitors, *Journal of Molecular Biology*, 287: 821-8.

Peak, MJ, Ito, A, Foote, CS & Peak, JG 1988, Photosensitized inactivation of DNA by monochromatic 334-nm radiation in the presence of 2-thiouracil: genetic activity and backbone breaks, *Photochemistry and Photobiology*, 47: 809-13.

Pedraza-Chaverri, J, Cardenas-Rodriguez, N, Orozco-Ibarra, M & Perez-Rojas, JM 2008a, Medicinal properties of mangosteen (*Garcinia mangostana*), *Food and Chemical Toxicology*, 46: 3227-39.

Pedraza-Chaverri, J, Reyes-Fermin, LM, Nolasco-Amaya, EG, Orozco-Ibarra, M, Medina-Campos, ON, Gonzalez-Cuahutencos, O, Rivero-Cruz, I & Mata, R 2008b, ROS scavenging capacity and neuroprotective effect of α-mangostin against 3-nitropropionic acid in cerebellar granule neurons, *Experimental and Toxicologic Pathology*, 61: 491-501

Pedro, M, Cerqueira, F, Sousa, ME, Nascimento, MS & Pinto, M 2002, Xanthones as inhibitors of growth of human cancer cell lines and their effects on the proliferation of human lymphocytes *in vitro*, *Bioorganic & Medicinal Chemistry*, 10: 3725-30.

Peres, V, Nagem, TJ & de Oliveira, FF 2000, Tetraoxygenated naturally occurring xanthones, *Phytochemistry*, 55: 683-710.

Peter, ME & Krammer, PH 1998, Mechanisms of CD95 (APO-1/Fas)-mediated apoptosis, *Current Opinion in Immunology*, 10: 545-51.

Petit, JY, Avril, MF, Margulis, A, Chassagne, D, Gerbaulet, A, Duvillard, P, Auperin, A & Rietjens, M 2000, Evaluation of cosmetic results of a randomized trial

comparing surgery and radiotherapy in the treatment of basal cell carcinoma of the face, *Plastic and Reconstructive Surgery*, 105: 2544-51.

Petty, RD, Sutherland, LA, Hunter, EM & Cree, IA 1995, Comparison of MTT and ATP-based assays for the measurement of viable cell number, *Journal of Bioluminescence and Chemiluminescence*, 10: 29-34.

Pfaffl, MW, Georgieva, TM, Georgiev, IP, Ontsouka, E, Hageleit, M & Blum, JW 2002, Real-time RT-PCR quantification of insulin-like growth factor (IGF)-1, IGF-1 receptor, IGF-2, IGF-2 receptor, insulin receptor, growth hormone receptor, IGF-binding proteins 1, 2 and 3 in the bovine species, *Domestic Animal Endocrinology*, 22: 91-102.

Pierce, SC 2003, A Thai herbal, in Findhorn Press, Forres, UK, p. 118.

Pines, J 1995, Cyclins and cyclin-dependent kinases: theme and variations, *Advances in Cancer Research*, 66: 181-212.

Pinto, MM, Sousa, ME & Nascimento, MS 2005, Xanthone derivatives: new insights in biological activities, *Current Medicinal Chemistry*, 12: 2517-38.

Plumb, JA, Milroy, R & Kaye, SB 1989, Effects of the pH dependence of 3-(4,5-dimethylthiazol-2-yl)-2,5-diphenyl-tetrazolium bromide-formazan absorption on chemosensitivity determined by a novel tetrazolium-based assay, *Cancer Research*, 49: 4435-40.

Pourmortazavi, SM & Hajimirsadeghi, SS 2007, Supercritical fluid extraction in plant essential and volatile oil analysis, *Journal of Chromatography A*, 1163: 2-24.

Prakash, J, Gupta, SK & Dinda, AK 2002, *Withania somnifera* root extract prevents DMBA-induced squamous cell carcinoma of skin in Swiss albino mice, *Nutrition and Cancer*, 42: 91-7.

Prasad, S, Madan, E, Nigam, N, Roy, P, George, J & Shukla, Y 2009, Induction of apoptosis by lupeol in human epidermoid carcinoma A431 cells through regulation of mitochondrial, Akt/PKB and NFκB signaling pathways, *Cancer Biology & Therapy*, 8: 1632-9.

Prashar, R, Kumar, A, Banerjee, S & Rao, AR 1994, Chemopreventive action by an extract from Ocimum sanctum on mouse skin papillomagenesis and its enhancement of skin glutathione S-transferase activity and acid soluble sulfydryl level, *Anti-cancer Drugs*, 5: 567-72.

Puripattanavong, JKW, Khajorndetkun, W & Chansathirapanich, W 2006, Improved isolation of alpha-mangostin from the fruit hull of *Garcinia mangostana* and its antioxidant and antifungal activitiy, *Planta Medica*, 72: 1078.

Pyrzynska, K & Biesaga, M 2009, Analysis of phenolic acids and flavonoids in honey, *TrAC Trends in Analytical Chemistry*, 28: 893-902.

Raisova, M, Bektas, M, Wieder, T, Daniel, P, Eberle, J, Orfanos, CE & Geilen, CC 2000, Resistance to CD95/Fas-induced and ceramide-mediated apoptosis of human melanoma cells is caused by a defective mitochondrial cytochrome c release, *FEBS letters*, 473: 27-32.

Raisova, M, Hossini, AM, Eberle, J, Riebeling, C, Wieder, T, Sturm, I, Daniel, PT, Orfanos, CE & Geilen, CC 2001, The Bax/Bcl-2 ratio determines the susceptibility of human melanoma cells to CD95/Fas-mediated apoptosis, *Journal of Investigative Dermatology*, 117: 333-40.

Rajkumar, V, Guha, G & Ashok Kumar, R 2011, Antioxidant and anti-cancer potentials of *Rheum emodi* rhizome extracts, *Evidence Based Complement and Alternative Medicine*, 697986.

Rajkumar, V, Guha, G & Kumar, RA 2011, Antioxidant and anti-neoplastic activities of *Picrorhiza kurroa* extracts, *Food and Chemical Toxicology*, 49: 363-9.

Ramírez, P, Fornari, T, Señoráns, FJ, Ibañez, E & Reglero, G 2005, Isolation of phenolic antioxidant compounds by SFC, *The Journal of Supercritical Fluids*, 35: 128-32.

Rass, K & Reichrath, J 2008, UV damage and DNA repair in malignant melanoma and nonmelanoma skin cancer, *Advances in Experimental Medicine and Biology*, 624: 162-78.

Ravi, R & Bedi, A 2004, NF-κB in cancer—a friend turned foe, *Drug resistance updates : reviews and commentaries in antimicrobial and anticancer chemotherapy*, 7: 53-67.

Rawadi, G & Dussurget, O 1995, Advances in PCR-based detection of mycoplasmas contaminating cell cultures, *PCR Methods and Applications*, 4: 199-208.

Rayet, B & Gelinas, C 1999, Aberrant *rel/nfkb* genes and activity in human cancer, *Oncogene*, 18: 6938-47.

Reagan-Shaw, S, Afaq, F, Aziz, MH & Ahmad, N 2004, Modulations of critical cell cycle regulatory events during chemoprevention of ultraviolet B-mediated responses by resveratrol in SKH-1 hairless mouse skin, *Oncogene*, 23: 5151-60.

Rehm, M, Düßmann, H, Jänicke, RU 2002, Single-cell fluorescence resonance energy transfer analysis demonstrates that caspase activation during apoptosis is a rapid process, *Journal of Biological Chemistry*, 277: 24506-14.

Robertson, GP 2005, Functional and therapeutic significance of Akt deregulation in malignant melanoma, *Cancer and Metastasis Reviews*, 24: 273-85.

Rodriguez, J & Lazebnik, Y 1999, Caspase-9 and APAF-1 form an active holoenzyme, *Genes and Development*, 13: 3179-84.

Romano, MF, Avellino, R, Petrella, A, Bisogni, R, Romano, S & Venuta, S 2004,

Rapamycin inhibits doxorubicin-induced NF-κB/Rel nuclear activity and enhances the apoptosis of melanoma cells, *European Journal of Cancer*, 40: 2829-36.

Romashkova, JA & Makarov, SS 1999, NF-κB is a target of AKT in anti-apoptotic PDGF signalling, *Nature*, 401: 86-90.

Ropke, CD, da Silva, VV, Kera, CZ, Miranda, DV, de Almeida, RL, Sawada, TC & Barros, SB 2006, *In vitro* and *in vivo* inhibition of skin matrix metalloproteinases by *Pothomorphe umbellata* root extract, *Photochemistry and Photobiology*, 82: 439-42.

Ross, DT, Scherf, U, Eisen, MB, Perou, CM, Rees, C, Spellman, P, Iyer, V, Jeffrey, SS, Van de Rijn, M, Waltham, M, Pergamenschikov, A, Lee, JC, Lashkari, D, Shalon, D, Myers, TG, Weinstein, JN, Botstein, D & Brown, PO 2000, Systematic variation in gene expression patterns in human cancer cell lines, *Nature Genetics*, 24: 227-35.

Roulland-Dussoix, D, Henry, A & Lemercier, B 1994, Detection of mycoplasmas in cell cultures by PCR: a one year study, *Journal of Microbiological Methods*, 19: 127-34.

Rubio-Moscardo, F, Blesa, D, Mestre, C, Siebert, R, Balasas, T, Benito, A, Rosenwald, A, Climent, J, Martinez, JI, Schilhabel, M, Karran, EL, Gesk, S, Esteller, M, deLeeuw, R, Staudt, LM, Fernandez-Luna, JL, Pinkel, D, Dyer, MJS & Martinez-Climent, JA 2005, Characterization of 8p21.3 chromosomal deletions in B-cell lymphoma: TRAIL-R1 and TRAIL-R2 as candidate dosage-dependent tumor suppressor genes, *Blood*, 106: 3214-22.

Sakagami, Y, Iinuma, M, Piyasena, KG & Dharmaratne, HR 2005, Antibacterial activity of alpha-mangostin against vancomycin resistant Enterococci (VRE) and synergism with antibiotics, *Phytomedicine*, 12: 203-8.

Sakamoto, H, Broekelmann, T, Cheresh, DA, Ramirez, F, Rosenbloom, J & Mecham, RP 1996, Cell-type specific recognition of RGD- and non-RGD-containing cell binding domains in fibrillin-1, *The Journal of Biological Chemistry*, 271: 4916-22.

Salado, C, Olaso, E, Gallot, N, Valcarcel, M, Egilegor, E, Mendoza, L & Vidal-Vanaclocha, F 2011, Resveratrol prevents inflammation-dependent hepatic melanoma metastasis by inhibiting the secretion and effects of interleukin-18, *Journal of Translational Medicine*, 9: 59.

Sander, CS, Chang, H, Hamm, F, Elsner, P & Thiele, JJ 2004, Role of oxidative stress and the antioxidant network in cutaneous carcinogenesis, *International Journal of Dermatology*, 43: 326-35.

Saralamp, P, Chuakul, W, Temsirirkkul, R & Clayton, T 1996, Medicinal plants in Thailand., vol. 1, Department of Pharmaceutical Botany, Faculty of Pharmacy, Mahidol University, Bangkok, Thailand.

Sato, A, Fujiwara, H, Oku, H, Ishiguro, K & Ohizumi, Y 2004, Alpha-Mangostin

induces Ca^{2+}-ATPase-dependent apoptosis via mitochondrial pathway in PC12 cells, *Journal of Pharmacological Sciences*, 95: 33-40.

Scheid, MP & Woodgett, JR 2003, Unravelling the activation mechanisms of protein kinase B/Akt, *FEBS Letters*, 546: 108-12.

Schlesier, K, Harwat, M, Bohm, V & Bitsch, R 2002, Assessment of antioxidant activity by using different *in vitro* methods, *Free Radical Research*, 36: 177-87.

Schmidt, L 2008, 'Novel fatty acids as potential therapeutic agents for prostate cancer', PhD thesis, Flinders University, Adelaide.

Sellappan, S, Akoh, CC & Krewer, G 2002, Phenolic compounds and antioxidant capacity of Georgia-Grown blueberries and blackberries, *Journal of Agricultural and Food Chemistry*, 50: 2432-8.

Selzer, E, Schlagbauer-Wadl, H, Okamoto, I, Pehamberger, H, Potter, R & Jansen, B 1998, Expression of Bcl-2 family members in human melanocytes, in melanoma metastases and in melanoma cell lines, *Melanoma Research*, 8: 197-203.

Senderowicz, AM 2003, Novel small molecule cyclin-dependent kinases modulators in human clinical trials, *Cancer Biology & Therapy*, 2: S84-95.

Serrone, L, Zeuli, M, Sega, FM & Cognetti, F 2000, Dacarbazine-based chemotherapy for metastatic melanoma: thirty-year experience overview, *Journal of Experimental & Clinical Cancer Research*, 19: 21-34.

Shah, MA & Schwartz, GK 2001, Cell cycle-mediated drug resistance: an emerging concept in cancer therapy, *Clinical Cancer Research*, 7: 2168-81.

Shan, B, Zhuo, Y, Chin, D, Morris, CA, Morris, GF & Lasky, JA 2005, Cyclin-dependent kinase 9 is required for tumor necrosis factor-α-stimulated matrix metalloproteinase-9 expression in human lung adenocarcinoma cells, *The Journal of Biological Chemistry*, 280: 1103-11.

Shan, T, Ma, Q, Guo, K, Liu, J, Li, W, Wang, F & Wu, E 2011, Xanthones from mangosteen extracts as natural chemopreventive agents: potential anticancer drugs, *Current Molecular Medicine*, 11: 666-77.

Shan, Y & Zhang, W 2010, Preparative separation of major xanthones from mangosteen pericarp using high-performance centrifugal partition chromatography, *Journal of Separation Science*, 33: 1274-8.

Shen, F & Weber, G 1997, Synergistic action of quercetin and genistein in human ovarian carcinoma cells, *Oncology Research*, 9: 597-602.

Sherr, CJ 1996, Cancer cell cycles, *Science*, 274: 1672-7.

Shibata, M-A, Iinuma, M, Morimoto, J, Kurose, H, Akamatsu, K, Okuno, Y, Akao, Y & Otsuki, Y 2011, alpha-Mangostin extracted from the pericarp of the mangosteen

(*Garcinia mangostana* Linn) reduces tumor growth and lymph node metastasis in an immunocompetent xenograft model of metastatic mammary cancer carrying a p53 mutation, *BMC Medicine*, 9: 69.

Shih, YW, Chien, ST, Chen, PS, Lee, JH, Wu, SH & Yin, LT 2010, α-Mangostin suppresses phorbol 12-myristate 13-acetate-induced MMP-2/MMP-9 expressions via αvβ3 integrin/FAK/ERK and NFkB signaling pathway in human lung adenocarcinoma A549 cells, *Cell Biochemistry and Biophysics*, 58: 31-44.

Shin, DH, Kim, OH, Jun, HS & Kang, MK 2008, Inhibitory effect of capsaicin on B16-F10 melanoma cell migration via the phosphatidylinositol 3-kinase/Akt/Rac1 signal pathway, *Experimental and Molecular Medicine*, 40: 486-94.

Siddiqui, EJ, Shabbir, MA, Mikhailidis, DP, Mumtaz, FH & Thompson, CS 2006, The effect of serotonin and serotonin antagonists on bladder cancer cell proliferation, *BJU International*, 97: 634-9.

Sies, H 1991, Oxidative stress: from basic research to clinical application, *The American Journal of Medicine*, 91: 31S-8S.

Sies, H 1993, Strategies of antioxidant defense, *European Journal of Biochemistry*, 215: 213-9.

Siller, G, Gebauer, K, Welburn, P, Katsamas, J & Ogbourne, SM 2009, PEP005 (ingenol mebutate) gel, a novel agent for the treatment of actinic keratosis: results of a randomized, double-blind, vehicle-controlled, multicentre, phase IIa study, *Australasian Journal Dermatology*, 50: 16-22.

Simon, P 2003, Q-Gene: processing quantitative real-time RT-PCR data, *Bioinformatics*, 19: 1439-40.

Sinclair, C & Foley, P 2009, Skin cancer prevention in Australia, *British Journal of Dermatology*, 161: 116-23.

Singh, A, Singh, SP & Bamezai, R 1999, Modulatory potential of Clocimum oil on mouse skin papillomagenesis and the xenobiotic detoxication system, *Food and Chemical Toxicology*, 37: 663-70.

Singh, RP, Dhanalakshmi, S & Agarwal, R 2002, Phytochemicals as cell cycle modulators--a less toxic approach in halting human cancers, *Cell Cycle*, 1: 156-61.

Singleton, VL & Rossi, JA 1965, Colorimetry of total phenolics with phosphomolybdic-phostungstic acid reagents, *American Journal of Enology and Viticulture*, 16: 144-58.

Skovlund, E & Fenstad, GU 2001, Should we always choose a nonparametric test when comparing two apparently nonnormal distributions?, *Journal of Clinical Epidemiology*, 54: 86-92.

Smalley, KSM & Eisen, TG 2003, Farnesyl transferase inhibitor SCH66336 is

cytostatic, pro-apoptotic and enhances chemosensitivity to cisplatin in melanoma cells, *International Journal of Cancer*, 105: 165-75.

Soengas, MS, Capodieci, P, Polsky, D, Mora, J, Esteller, M, Opitz-Araya, X, McCombie, R, Herman, JG, Gerald, WL, Lazebnik, YA, Cordon-Cardo, C & Lowe, SW 2001, Inactivation of the apoptosis effector Apaf-1 in malignant melanoma, *Nature*, 409: 207-11.

Soengas, MS & Lowe, SW 2003, Apoptosis and melanoma chemoresistance, *Oncogene*, 22: 3138-51.

Soudamini, KK & Kuttan, R 1989, Inhibition of chemical carcinogenesis by curcumin, *Journal of Ethnopharmacology*, 27: 227-33.

Stahl, JM, Sharma, A, Cheung, M, Zimmerman, M, Cheng, JQ, Bosenberg, MW, Kester, M, Sandirasegarane, L & Robertson, GP 2004, Deregulated Akt3 activity promotes development of malignant melanoma, *Cancer Research*, 64: 7002-10.

Staples, MP, Elwood, M, Burton, RC, Williams, JL, Marks, R & Giles, GG 2006, Non-melanoma skin cancer in Australia: the 2002 national survey and trends since 1985, *The Medical Journal of Australia*, 184: 6-10.

Stuffness, M & Pezzuto, JM (eds) 1990, Assays related to cancer drug discovery., vol. 6, Methods in Plant Biochemistry: Assays for Bioactivity, Academic Press, London.

Suksamrarn, S, Komutiban, O, Ratananukul, P, Chimnoi, N, Lartpornmatulee, N & Suksamrarn, A 2006, Cytotoxic prenylated xanthones from the young fruit of *Garcinia mangostana.*, *Chemical & Pharmaceutical Bulletin*, 54: 301-5.

Suksamrarn, S, Suwannapoch, N, Phakhodee, W, Thanuhiranlert, J, Ratananukul, P, Chimnoi, N & Suksamrarn, A 2003, Antimycobacterial activity of prenylated xanthones from the fruits of *Garcinia mangostana*, *Chemical & Pharmaceutical Bulletin*, 51: 857-9.

Suksamrarn, S, Suwannapoch, N, Ratananukul, P, Aroonlerk, N & Suksamrarn, A 2002, Xanthones from the green fruit hulls of *Garcinia mangostana*, *Journal of Natural Products*, 65: 761-3.

Suliman, A, Lam, A, Datta, R & Srivastava, RK 2001, Intracellular mechanisms of TRAIL: apoptosis through mitochondrial-dependent and -independent pathways, *Oncogene*, 20: 2122-33.

Sultanbawa, MUS 1980, Xanthonoids of tropical plants, *Tetrahedron*, 36: 1465-506.

Sun, LC, Luo, J, Mackey, LV, Fuselier, JA & Coy, DH 2007, A conjugate of camptothecin and a somatostatin analog against prostate cancer cell invasion via a possible signaling pathway involving PI3K/Akt, $\alpha v \beta 3/\alpha v \beta 5$ and MMP-2/-9, *Cancer Letters*, 246: 157-66.

Sun, SY, Hail, N, Jr. & Lotan, R 2004, Apoptosis as a novel target for cancer chemoprevention, *Journal of the National Cancer Institute*, 96: 662-72.

Surh, YJ, Na, HK, Lee, JY & Keum, YS 2001, Molecular mechanisms underlying anti-tumor promoting activities of heat-processed Panax ginseng C.A. Meyer, *Journal of Korean Medical Science*, 16: 38-41.

Suzuki, T, Higgins, PJ & Crawford, DR 2000, Control selection for RNA quantitation, *Biotechniques*, 29: 332-7.

Svobodova, A, Psotova, J & Walterova, D 2003, Natural phenolics in the prevention of UV-induced skin damage. A review, *Biomedical Papers of the Medical Faculty of University Palacky Olomouc Czech Republic*, 147: 137-45.

Tan, G, Gyllenhaal, C & Soejarto, DD 2006, Biodiversity as a source of anticancer drugs, *Current Drug Targets*, 7: 265-77.

Tarhini, AA & Agarwala, SS 2006, Cutaneous melanoma: available therapy for metastatic disease, *Dermatology and Therapy*, 19: 19-25.

Testa, JR & Bellacosa, A 2001, AKT plays a central role in tumorigenesis, *Proceedings of the National Academy of Sciences of the United States of America*, 98: 10983–5.

Tomaino, A, Cristani, M, Cimino, F, Speciale, A, Trombetta, D, Bonina, F & Saija, A 2006, *In vitro* protective effect of a Jacquez grapes wine extract on UVB-induced skin damage, *Toxicology in Vitro*, 20: 1395-402.

Trabelsi, N, Megdiche, W, Ksouri, R, Falleh, H, Oueslati, S, Soumaya, B, Hajlaoui, H & Abdelly, C 2010, Solvent effects on phenolic contents and biological activities of the halophyte *Limoniastrum monopetalum* leaves, *LWT - Food Science and Technology*, 43: 632-9.

Trautinger, F 2001, Mechanisms of photodamage of the skin and its functional consequences for skin ageing, *Clinical and Experimental Dermatology*, 26: 573-7.

Tsao, H, Atkins, MB & Sober, AJ 2004, Management of cutaneous melanoma, *The New England Journal of Medicine*, 351: 998-1012.

Tsao, H & Sober, AJ 2005, Melanoma treatment update, *Dermatologic Clinics*, 23: 323-33.

Tsao, R & Deng, Z 2004, Separation procedures for naturally occurring antioxidant phytochemicals, *Journal of Chromatography B*, 812: 85-99.

Urbach, F 1991, Incidence of nonmelanoma skin cancer, *Dermatologic Clinics*, 9: 751-5.

Urlinger, S, Kuchler, K, Meyer, TH, Uebel, S & Tampé, R 1997, Intracellular location, complex formation, and function of the transporter associated with antigen

processing in yeast, *European Journal of Biochemistry*, 245: 266-72.

Valster, A, Tran, NL, Nakada, M, Berens, ME, Chan, AY & Symons, M 2005, Cell migration and invasion assays, *Methods*, 37: 208-15.

van Kuppeveld, FJ, van der Logt, JT, Angulo, AF, van Zoest, MJ, Quint, WG, Niesters, HG, Galama, JM & Melchers, WJ 1992, Genus- and species-specific identification of mycoplasmas by 16S rRNA amplification, *Applied and Environmental Microbiology*, 58: 2606-15.

van Muijen, GN, Danen, EH, de Vries, TJ, Quax, PH, Verheijen, JH & Ruiter, DJ 1995, Properties of metastasizing and nonmetastasizing human melanoma cells, *Recent Results in Cancer Research*, 139: 105-22.

Varshavsky, A 1996, The N-end rule: functions, mysteries, uses, *Proceedings of the National Academy of Sciences of the United States of America*, 93: 12142-9.

Vayalil, PK, Elmets, CA & Katiyar, SK 2003, Treatment of green tea polyphenols in hydrophilic cream prevents UVB-induced oxidation of lipids and proteins, depletion of antioxidant enzymes and phosphorylation of MAPK proteins in SKH-1 hairless mouse skin, *Carcinogenesis*, 24: 927-36.

Vermes, I, Haanen, C, Steffens-Nakken, H & Reutelingsperger, C 1995, A novel assay for apoptosis. Flow cytometric detection of phosphatidylserine expression on early apoptotic cells using fluorescein labelled Annexin V, *Journal of Immunological Methods*, 184: 39-51.

Vermeulen, K, Van Bockstaele, DR & Berneman, ZN 2003, The cell cycle: a review of regulation, deregulation and therapeutic targets in cancer, *Cell Proliferation*, 36: 131-49.

Vieira, LMM & Kijjoa, A 2005, Naturally-occurring xanthones: recent developments, *Current Medicinal Chemistry*, 12: 2413-46.

Vinokur, Y, Rodov, V, Reznick, N, Goldman, G, Horev, B, Umiel, N & Friedman, H 2006, Rose petal tea as an antioxidant-rich beverage: cultivar effects, *Journal of Food Science*, 71: S42-S7.

Vultur, A, Villanueva, J & Herlyn, M 2010, BRAF Inhibitor Unveils Its Potential against Advanced Melanoma, *Cancer Cell*, 18: 301-2.

Vuong, E 2009, 'Screening natural antioxidants and anti-skin cancer activities from Australian native plant leaves ', Honours thesis, Flinders University, Adelaide.

Wagner, EF & Nebreda, AR 2009, Signal integration by JNK and p38 MAPK pathways in cancer development, *Nature Reviews Cancer*, 9: 537-49.

Wajant, H 2002, The Fas signaling pathway: more than a paradigm, *Science*, 296: 1635-6.

Wang, L, Yang, B, Du, X & Yi, C 2008, Optimisation of supercritical fluid extraction of flavonoids from *Pueraria lobata*, *Food Chemistry*, 108: 737-41.

Wang, S & El-Deiry, WS 2003, TRAIL and apoptosis induction by TNF-family death receptors, *Oncogene*, 22: 8628-33.

Wang, YF, Jiang, CC, Kiejda, KA, Gillespie, S, Zhang, XD & Hersey, P 2007, Apoptosis Induction in human melanoma cells by inhibition of MEK Is caspase-independent and mediated by the Bcl-2 family members PUMA, Bim, and Mcl-1, *Clinical Cancer Research*, 13: 4934-42.

Wasserman, DI & Gilchrest, BA 2008, Chemoprevention of skin cancer., in K Nouri (ed.), *Skin cancer*, McGraw-Hill Medical New York, pp. 622-34.

Watanapokasin, R, Jarinthanan, F, Jerusalmi, A, Suksamrarn, S, Nakamura, Y, Sukseree, S, Uthaisang-Tanethpongtamb, W, Ratananukul, P & Sano, T 2010, Potential of xanthones from tropical fruit mangosteen as anti-cancer agents: caspase-dependent apoptosis induction in vitro and in mice, *Applied Biochemistry and Biotechnology*, 162: 1080-94.

Watanapokasin, R, Jarinthanan, F, Nakamura, Y, Sawasjirakij, N, Jaratrungtawee, A & Suksamrarn, S 2011, Effects of α-mangostin on apoptosis induction of human colon cancer, *World Journal of Gastroenterology*, 17: 2086-95.

Watjen, W, Weber, N, Lou, YJ, Wang, ZQ, Chovolou, Y, Kampkotter, A, Kahl, R & Proksch, P 2007, Prenylation enhances cytotoxicity of apigenin and liquiritigenin in rat H4IIE hepatoma and C6 glioma cells, *Food and Chemical Toxicology*, 45: 119-24.

Wattenberg, LW 1985, Chemoprevention of cancer, *Cancer Research*, 45: 1-8.

Weecharangsan, W, Opanasopit, P, Sukma, M, Ngawhirunpat, T, Sotanaphun, U & Siripong, P 2006, Antioxidative and neuroprotective activities of extracts from the fruit hull of mangosteen (*Garcinia mangostana* Linn.), *Medical Principles and Practice*, 15: 281-7.

Weigelt, B, Peterse, JL & van't Veer, LJ 2005, Breast cancer metastasis: markers and models, *Nature Reviews Cancer*, 5: 591-602.

Weisburger, JH 1999, Mechanisms of action of antioxidants as exemplified in vegetables, tomatoes and tea, *Food and Chemical Toxicology*, 37: 943-8.

Wilkins, MR, Williams, KL, Appel, RD & Hochstrasser, DF 1997, Proteome research: new frontiers in functional genomics, Springer-Verlag, Berlin, Germany.

Williams, P, Ongsakul, M, Proudfoot, J, Croft, K & Beilin, L 1995, Mangostin inhibits the oxidative modification of human low density lipoprotein, *Free Radical Research*, 23: 175-84.

Williamson, EM 2001, Synergy and other interactions in phytomedicines, *Phytomedicine*, 8: 401-9.

Wölfel, T, Hauer, M, Schneider, J, Serrano, M, Wölfel, C, Klehmann-Hieb, E, De Plaen, E, Hankeln, T, Meyer zum Büschenfelde, KH & Beach, D 1995, A p16INK4a-insensitive CDK4 mutant targeted by cytolytic T lymphocytes in a human melanoma, *Science*, 269: 1281-4.

Wolter, KG, Verhaegen, M, Fernandez, Y, Nikolovska-Coleska, Z, Riblett, M, Martin de la Vega, C, Wang, S & Soengas, MS 2007, Therapeutic window for melanoma treatment provided by selective effects of the proteasome on Bcl-2 proteins, *Cell Death & Differentiation*, 14: 1605-16.

Wu, X, Cao, S, Goh, S, Hsu, A & Tan, BK 2002, Mitochondrial destabilisation and caspase-3 activation are involved in the apoptosis of Jurkat cells induced by gaudichaudione A, a cytotoxic xanthone, *Planta Medica*, 68: 198-203.

Xu, C, Green, A, Parisi, A & Parsons, PG 2001, Photosensitization of the sunscreen octyl p-dimethylaminobenzoate by UVA in human melanocytes but not in keratinocytes, *Photochemistry and Photobiology*, 73: 600-4.

Yamakuni, T, Aoki, K, Nakatani, K, Kondo, N, Oku, H, Ishiguro, K & Ohizumi, Y 2006, Garcinone B reduces prostaglandin E2 release and NF-κB-mediated transcription in C6 rat glioma cells, *Neuroscience Letters*, 394: 206-10.

Yang, H, Higgins, B, Kolinsky, K, Packman, K, Go, Z, Iyer, R, Kolis, S, Zhao, S, Lee, R, Grippo, JF, Schostack, K, Simcox, ME, Heimbrook, D, Bollag, G & Su, F 2010, RG7204 (PLX4032), a selective BRAF V600E inhibitor, displays potent antitumor activity in preclinical melanoma models, *Cancer Research*, 70: 5518-27.

Yaoshikawa, M, Harada, E, Miki, A, Tsukamoto, K, Si Qian, L, Yamahara, J & Murakami, N 1994, Antioxidant constituents from the fruit hulls of mangosteen (*Garcinia mangostana* L.) originating in Vietnam, *Yakugaku Zasshi*, 114: 129-33.

Yates, P & Stout, GH 1958, The structure of mangostin1, *Journal of the American Chemical Society*, 80: 1691-700.

Young, FM, Phungtamdet, W & Sanderson, BJ 2005, Modification of MTT assay conditions to examine the cytotoxic effects of amitraz on the human lymphoblastoid cell line, WIL2NS, *Toxicology In Vitro*, 19: 1051-9.

Yu, L, Zhao, M, Yang, B, Zhao, Q & Jiang, Y 2007, Phenolics from hull of *Garcinia mangostana* fruit and their antioxidant activities, *Food Chemistry*, 104: 176-81.

Yu, Q 2006, Restoring p53-mediated apoptosis in cancer cells: New opportunities for cancer therapy, *Drug resistance updates : reviews and commentaries in antimicrobial and anticancer chemotherapy*, 9: 19-25.

Zhao, J, Wang, J, Chen, Y & Agarwal, R 1999, Anti-tumor-promoting activity of a polyphenolic fraction isolated from grape seeds in the mouse skin two-stage

initiation–promotion protocol and identification of procyanidin B5-3′-gallate as the most effective antioxidant constituent, *Carcinogenesis*, 20: 1737-45.

Zimmermann, KC, Bonzon, C, & Green, DR 2001, The machinery of programmed cell death, *Pharmacology & Therapeutics*, 92: 57-70.

Zou, H, Henzel, WJ, Liu, X, Lutschg, A & Wang, X 1997, Apaf-1, a human protein homologous to C. elegans CED-4, participates in cytochrome c-dependent activation of caspase-3, *Cell*, 90: 405-13.

APPENDIX

A1 Stock solutions

Phosphate Buffered Saline (PBS) (10×) per Litre

KCl   2 g

KH_2PO_4 2 g

NaCl   80 g

Na_2HPO_4 11.5 g

Stored at room temperature

MTT Solution (5 mg/ml)

Dissolve 500 mg in 100 ml 1× PBS

Filter sterilised

Stored at -20°C

Trypan Blue

Dissolve 0.9 g NaCl in 90 ml MQ H_2O

Dissolve 0.2 g Trypan Blue in salt solution as above

Made up to 100 ml and filtered

Stored at room temperature

20% (w/v) Sodium Dodecyl Solution (SDS) in 0.2 M HCl

Dissolve 20 g of SDS in 100 ml 0.2 M HCl (with gentle heating)

Stored at room temperature

0.5% (w/v) Crystal Violet

Dissolve 0.5 g crystal violet in 100 ml of 50% (v/v) methanol (1:1 methanol and H$_2$O)

Stored at room temperature

33% Acetic Acid Destain Solution

Mix 33 ml of acetic acid with 67 ml of MQ H$_2$O

Stored at room temperature

5× TBE Buffer

54 g Tris base

27.5 g Boric acid

20 ml of 0.5 M EDTA (pH 8.0)

Made up to 1 l with MQ water (pH should be ~8.3)

6× DNA Loading Dye (10 ml)

Add 25 mg of bromophenol blue to 6.7 ml of ddH$_2$O and mix.

Add 25 mg of xylene cyanol FF and mix.

Add 3.3 ml of glycerol and mix.

Aliquot and freeze at -20 °C for long-term storage.

A2 Identification and quantification of xanthones in the mangosteen pericarp ethanol extract

A2.1 HPLC profile of mangosteen pericarp ethanol extract
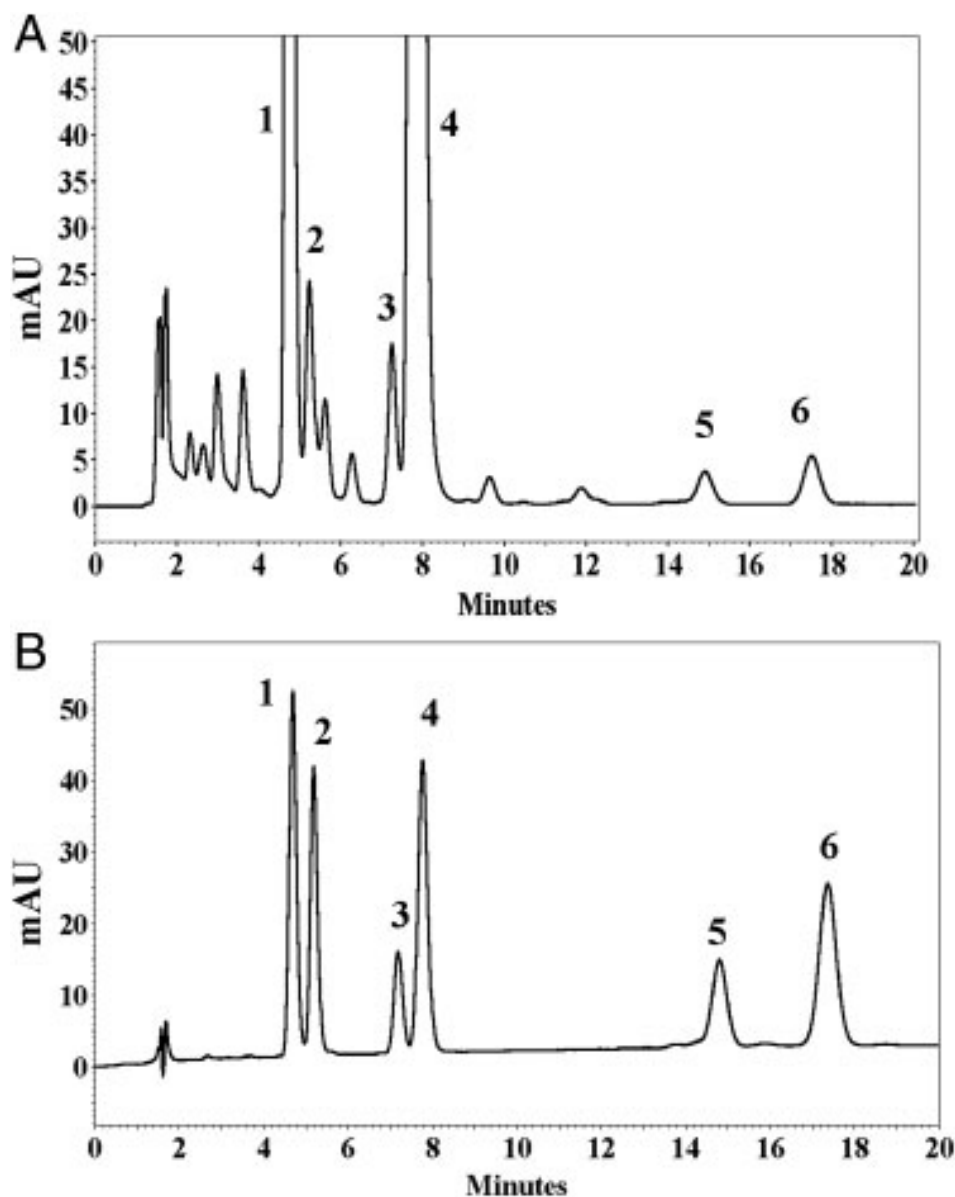
Figure A-1

Identification of characteristic compounds in mangosteen ethanol extract using HPLC: (A) chromatograms of mangosteen ethanol extract. (B) Chromatograms of standard (1: γ-mangostin; 2: 8-desoxygartanin; 3: gartanin; 4: α-mangostin; 5: 9-hydroxycalabaxanthone; 6: β-mangostin). Chromatographic conditions are the same as in Section 2. Standard: 0.01 mg/ml of each standard with injection volume of 10 ml; sample: 0.6 mg/ml mangosteen ethanol extract with injection volume of 20 ml. (Taken from (Shan & Zhang 2010))

A2.2 Molecular weight and composition of xanthones in the mangosteen pericarp ethanol extract

Table A-1

Molecular weight and composition of major xanthones in the mangosteen pericarp ethanol extract (Taken from (Shan & Zhang 2010)).

Xanthone compounds	Molecular weight	Concentration (mg/g extract)
α-Mangostin	410.46	321.0 ± 20.5
β-Mangostin	424.49	3.88 ± 0.3
γ-Mangostin	396.43	81.3 ± 4.2
8-Desoxygartanine	380.43	10.7 ± 0.5
Gartanine	396.44	18.7 ± 1.1
9-Hydroxycalabaxanthone	408.44	4.84 ± 0.63

A3 Mycoplasma detection using PCR

A3.1 Master mix and primer sequences for PCR

Master Mix:

$10 \times$ PE II PCR buffer	2.5 µl
50 mM $MgCl_2$	1.0 µl
10 mM d(T)NTPs	0.5 µl
100 ng/ µl GPO-1	1.0 µl
100 ng/ µl MGSO	1.0 µl
100 ng/ µl HRAG1-F	0.5 µl
100 ng/ µl HRAG1-R	0.5 µl
H_2O	15.8 µl
Taq Gold	0.2 µl
Total	23 µl

Primer sequence (5′-3′):

MGSO: TGCACCATCTGTCACTCTGTTAACCTC

GPO-1: ACTCCTACGGGAGGCAGCAGTA

A3.2 Result for the mycoplasma test
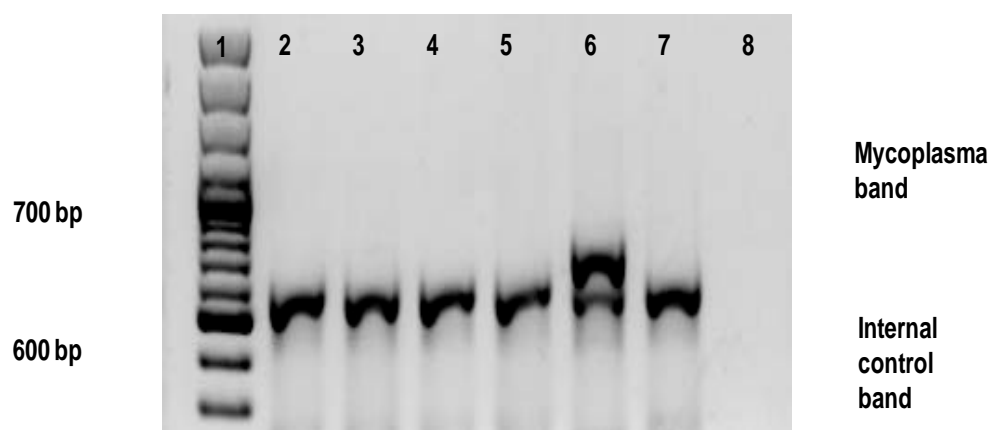
Figure A-2

Potential mycoplasma contamination was tested using PCR. The PCR products were visualised on 1.5% agarose gel containing 0.01% (v/v) gel red staining using a LAS-4000 imager. Lane 1: GeneRulerTM (100-3000bp) (Thermo Scientific, Australia); Lane 2: A-431 cell line; Lane 3: SK-MEL-28 cell line; Lane 4: HaCaT cell line; Lane 5: CCD-1064Sk; Lane 6: mycoplasma positive control; Lane 7: mycoplasma negative control; Lane 8: water only.

A4 Cell growth curve as determined by the Trypan Blue assay over the period of 144 h
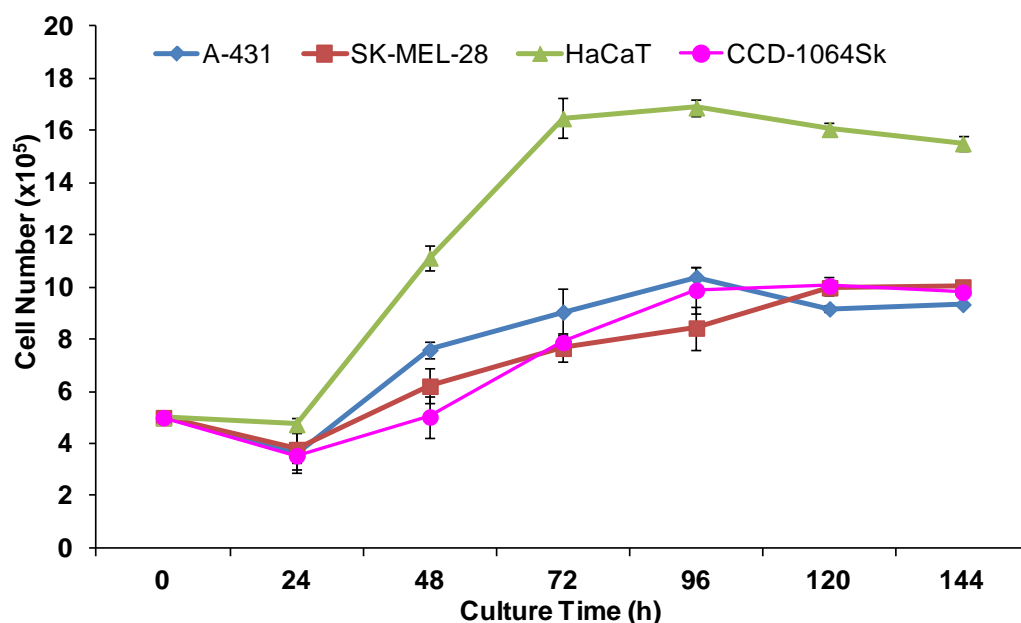
Figure A-3

Cell growth curves of four different cell lines. Cell number was counted by the Trypan Blue assay after each time point (24, 48, 72, 96, 120, and 144 h). Data are presented as the mean ± SEM of three independent experiments.

A5 Comparison of the MTT and Crystal Violet assay
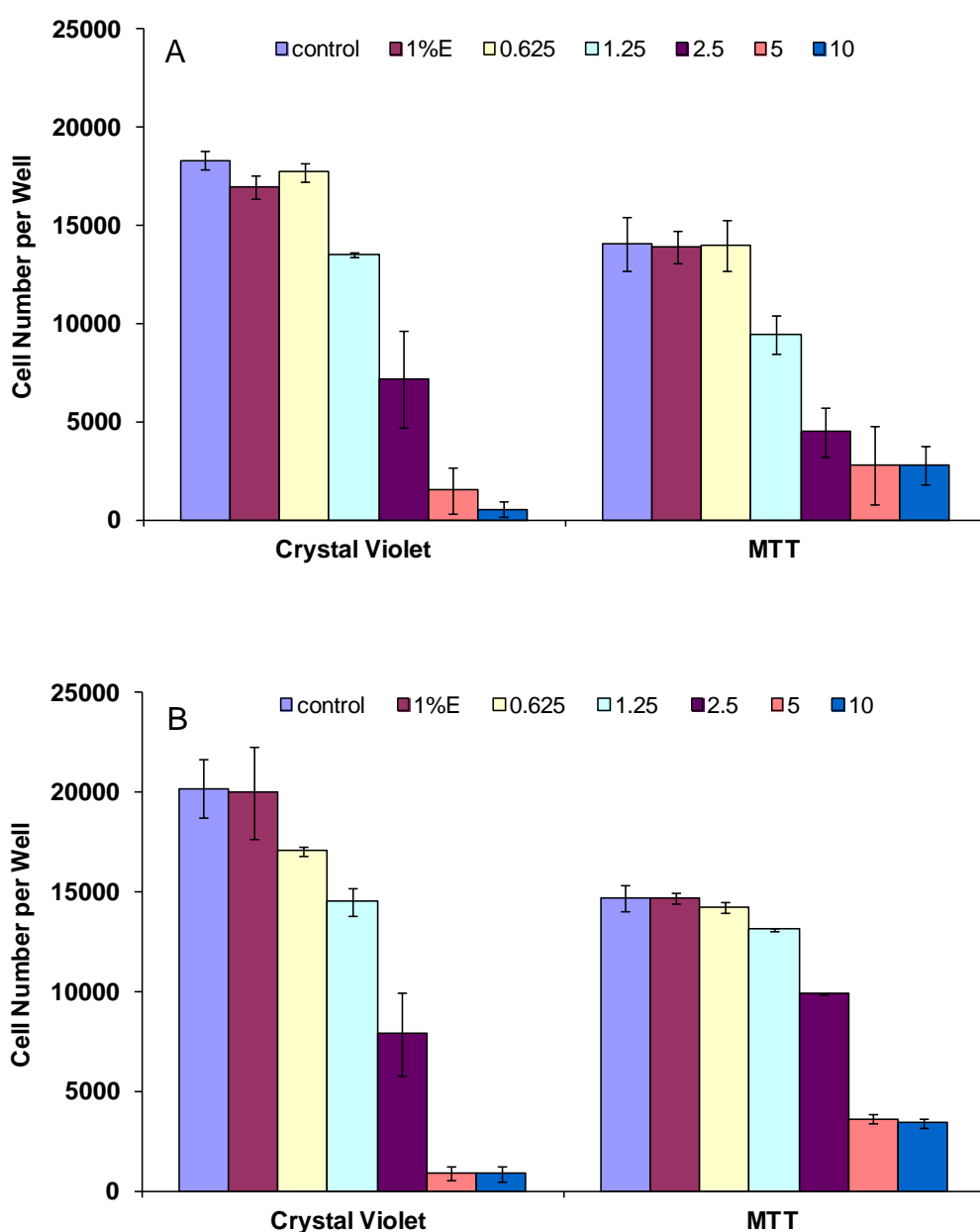
Figure A-4

Comparison of the MTT and the Crystal Violet assay based on the cell number calculated by these two assays. A-431 (A) and SK-MEL-28 (B) cells were cultured at 1×10^4 cells/well in DMEM media. Cells were treated with crude mangosteen pericarp ethanol extract (MPEE) (0-10 µg/ml of total phenolics). Ethanol (1%E; v/v) was used as vehicle control. After 48 h treatment, the MTT and Crystal Violet assay were carried out and the absorbance was read as described in the method (3.2.5 &3.2.6). The absorbance was used to calculate the number of viable cells from the 24 h adherence linear regression equation. The experiment was repeated three times and the data were represented as mean ± SEM.

A6   Cytotoxicity of 5-FU and DTIC on human skin cell lines
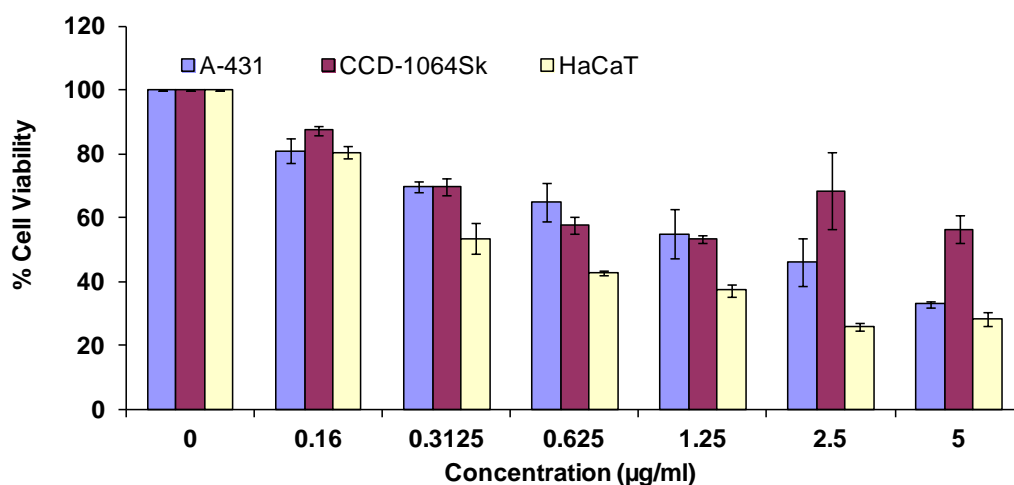
Figure A-5

Cell viability measured by the Crystal Violet assay after 48 h treatment with 5-fluorouracil (5-FU) on human squamous cell carcinoma A-431 cell line, normal skin fibroblast CCD-1064Sk cell line and keratinocyte HaCaT cell line. Data are shown as % viability compared to the untreated control and are presented as the mean ± SEM of three independent experiments.
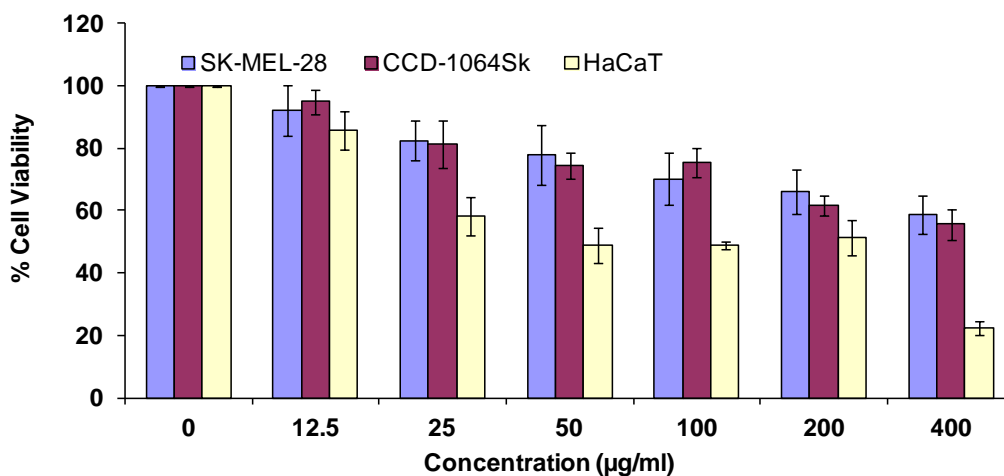
Figure A-6

Cell viability measured by the Crystal Violet assay after 48 h treatment with dacarbazine (DTIC) on human melanoma SK-MEL-28 cell line, normal skin fibroblast CCD-1064Sk cell line and keratinocyte HaCaT cell line. Data are shown as % viability compared to the untreated control and are presented as the mean ± SEM of three independent experiments.

A7 One example of histogram for cell cycle analysis

Untreated control:
SubG$_1$: 0.7%
G$_0$/G$_1$: 77.98%
S: 7.25%
G$_2$/M: 14.85%

Treatment with
MPEE (10 µg/ml):
SubG$_1$: 0.51%
G$_0$/G$_1$: 92.3%
S: 1.88%
G$_2$/M: 5.58%
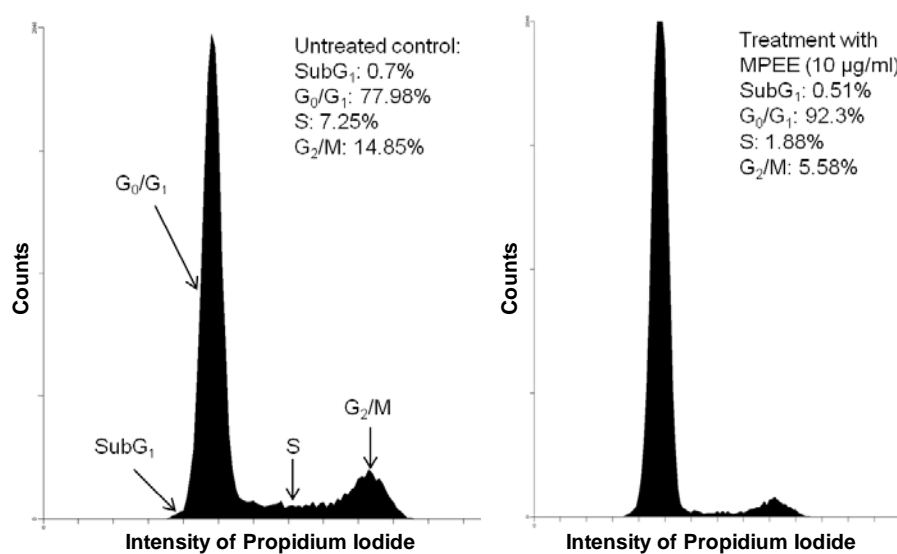
Figure A-7
One example of histogram for cell cycle analysis as analysed by Cell Quest software. After 48-h treatment with 0 or 10 µg/ml of mangosteen pericarp ethanol extract (MPEE), SK-MEL-28 cells were harvested, lysed, and stained with propidium iodide (Section 4.2.3). The cell distribution (%) in each phase of subG$_1$, G$_0$/G$_1$, S, G$_2$/M was detected by flow cytometry.

A8 Supplementary data for apoptosis analysis

A8.1 Late apoptotic or necrotic cell population after treatment with xanthones in two skin cancer cell lines
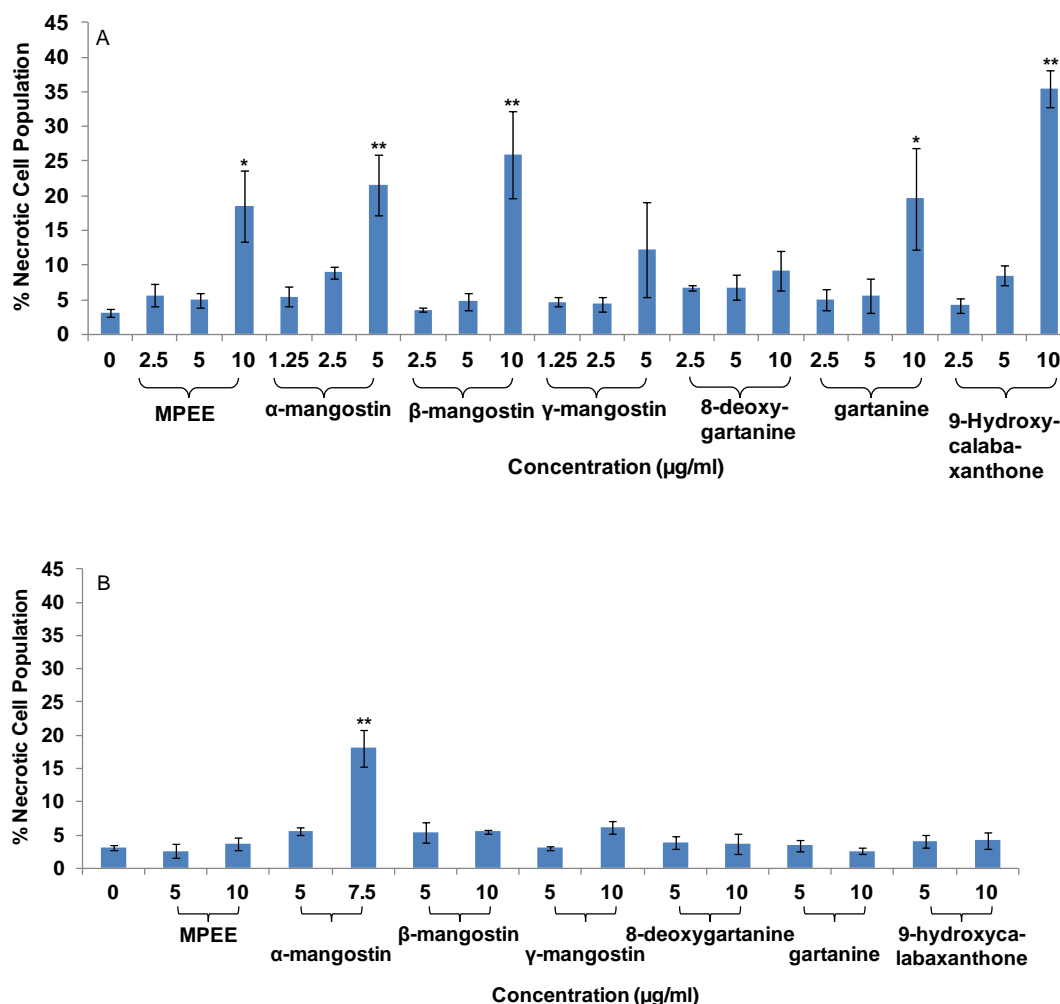
Figure A-8

Late apoptosis or necrosis induced by xanthones on human squamous carcinoma A-431 (A) and human melanoma SK-MEK-28 cells (B) was determined by Annexin V-conjugated PI staining through flow cytometry. Data were obtained from 20,000 events and presented as the percentage of necrotic cells (Annexin positive/PI positive). The values are shown as the mean ± SEM of 3 independent experiments. Treatments significantly different from the untreated control at $P < 0.05$ are presented as * and $P < 0.01$ as **.

A8.2 One example of dot plot for apoptosis analysis
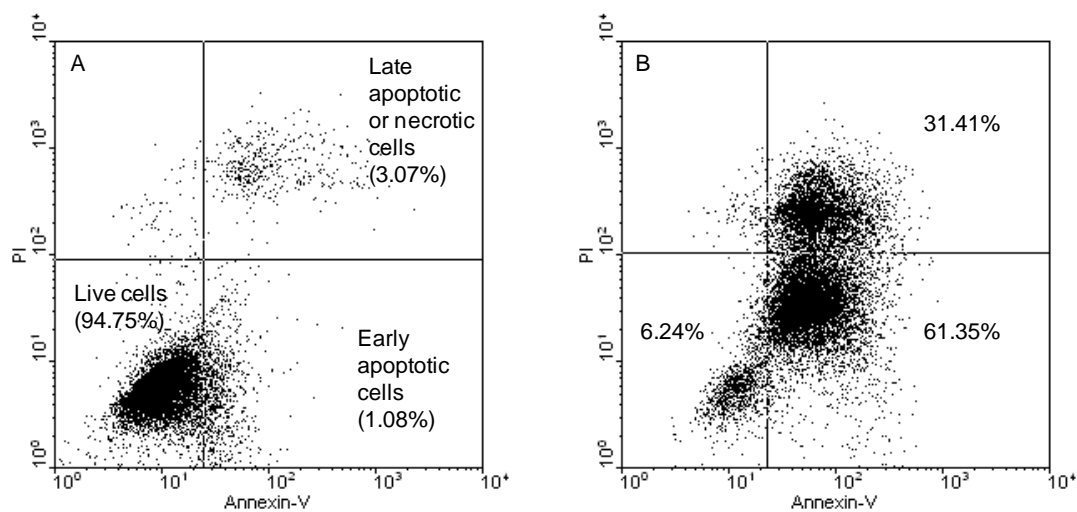
Figure A-9

One example of dot plot for apoptosis analysis. After 48-h treatment with 0 (A) or 10 µg/ml (B) of α-mangostin, SK-MEL-28 cells were harvested and stained with propidium iodide (PI) and Annexin-V (Section 4.2.4). The apoptotic cell population (%) was detected by flow cytometry. The lower left corner of each plot represents the live cells (negative for both PI and Annexin-V). The lower right corner represents the early apoptotic cells (negative for PI and positive for Annexin-V). The upper right corner represents the late apoptotic or necrotic cells (positive for both PI and Annexin-V). The figures show the percentage of cells in each population.

A9 Principle of caspase 3/7, 8, and 9 assays
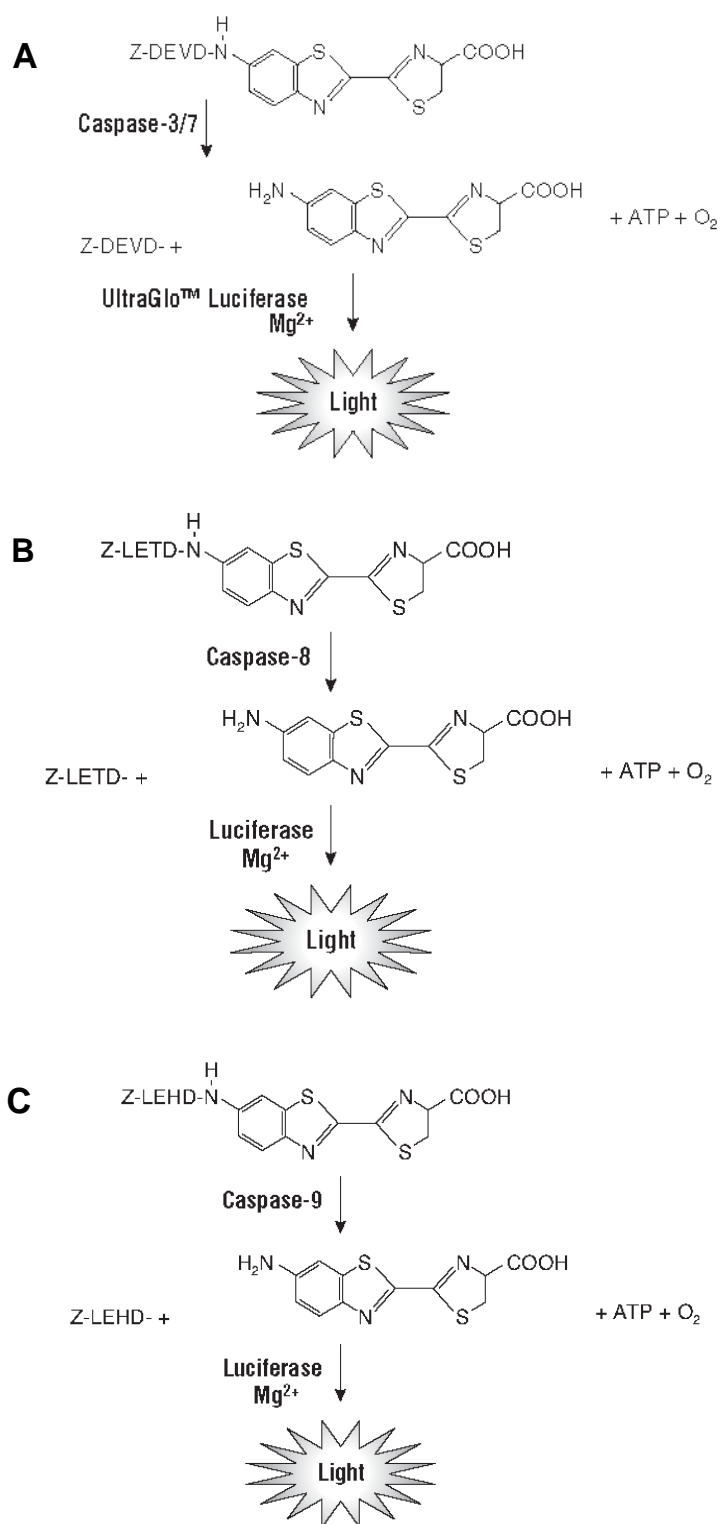
Figure A-10
Caspase-3/7 (A), 8 (B) and 9 (C) cleavage of the specific luminogenic substrate. Following caspase cleavage, a substrate for luciferase (aminoluciferin) is released, resulting in the luciferase reaction and the production of light. The diagrams were taken from the manufacturer's instruction.

A10 One example of dot plot for the mitochondrial membrane potential detection assay
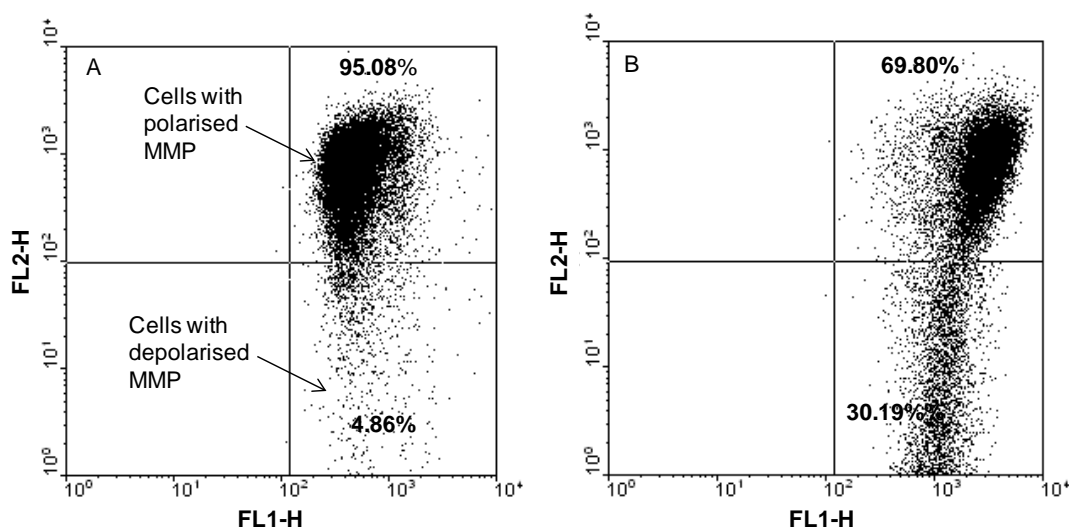
Figure A-11

One example of dot plot for mitochondrial membrane potential (MMP; Δψ) detection assay. After 48-h treatment with (A) or without 10 µg/ml (B) of mangosteen pericarp ethanol extract (MPEE), A-431 cells were harvested and stained with JC-1 according to the protocol and analysed by flow cytometry as described in Section 4.2.6. Cells with polarised Δψ are shown to fluoresce in both the FL-1 and FL-2 channels (upper right corner). In contrast, those with depolarised Δψ are shown to fluoresce only in the FL-1 channel (lower right corner), indicating apoptosis induction.

A11 Supplementary data for qRT-PCR

A11.1 Efficacy of DNase treatment

Figure A-12
Agarose gel of total RNA (A) before DNase treatment and (B) after DNase treatment. Lane 1 and 3: RNA sample extracted from human squamous cell carcinoma A-431 cells; Lane 2 and 4: RNA sample extracted from human melanoma SK-MEL-28 cells.

A11.2 Detection of genomic DNA contamination by PCR
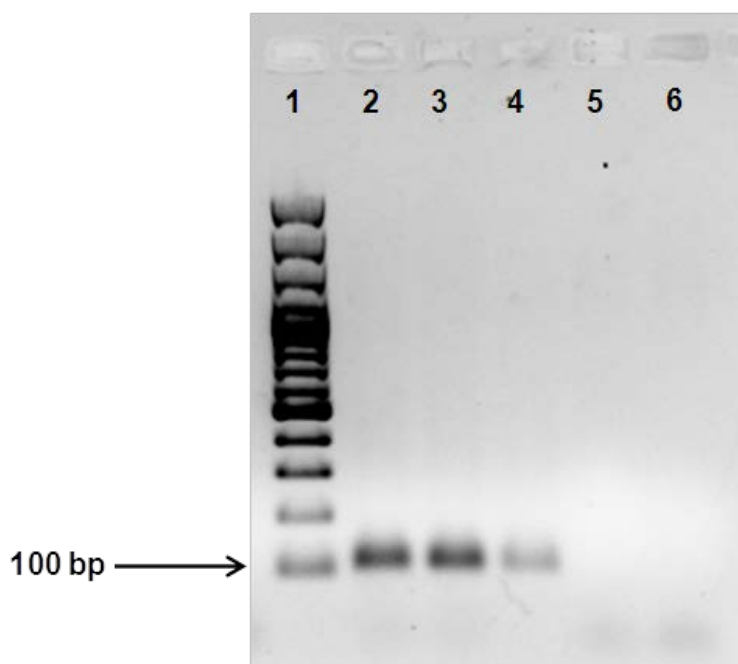
Figure A-13
Detection of genomic DNA contamination by running PCR using different templates: lane 2: cDNA from total RNA; lane 3: cDNA from DNased treated RNA; lane 4: total RNA; lane 5: DNased treated RNA; lane 6; nuclease free water; lane 1: GeneRulerTM (100-3000bp) (Thermo Scientific, Australia).

A11.3 Comparison of three different commercial master mixes

Table A-2

Comparison of qRT-PCR results using three different commercial master mixes.

Master mix (Company)	Price for 25 ml	Standard curve		
		R^2 value	Amplification efficiency	CV (%)
Quantitect SYBR-green master mix (Qiagen)	$2788	0.99716	2.01	1.1
GoTaq® qPCR Master Mix (Promega)	$990	0.99925	1.93	0.892
PerfeCTa® SYBR® Green FastMix® (Quanta Biosciences)	$1970	0.99536	1.97	1.3

A11.4 Optimisation of qRT-PCR conditions

Table A-3

Optimisation of qRT-PCR conditions including the ratio of forward and reverse primers and the annealing temperatures, based on the optimal amplification efficiency.

Primers	Forward / Reverse (nM / nM)	Annealing Temperature (ºC)	Amplification efficiency
Bax	150/150	60	1.89
Bcl-2	150/150	60	1.87
Cytochrome C	150/150	60	1.95
Cyclin D1	500/500	60	1.98
P21WAF1	500/500	62	2.01
Akt1	150/150	60	1.82
NFκB	500/500	60	1.89
IκBα	500/500	60	1.87
MMP-2	500/500	58	1.85
MMP-9	500/500	60	1.86
BRAF V600E	500/500	66	1.94
Beta-actin (House-keeping gene)	150/100	60	1.99

A11.5 Verification of PCR product size by running agarose gel
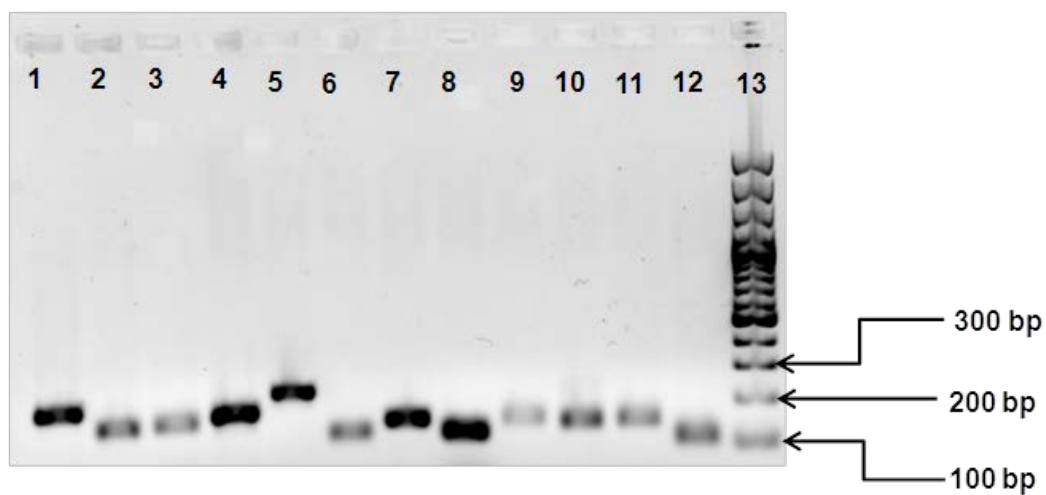
Figure A-14
Agarose gel electrophoretic analysis was used to verify the size of the PCR amplification products. Lane 1-13: 1) MMP-2, 2) MMP-9, 3) BRAF V600E, 4) p21WAF1, 5) cyclin D1, 6) Akt1, 7) NFκB, 8) IκBa, 9) Bcl-2, 10) Bax, 11) cytochrome c, 12) β-actin, 13) GeneRulerTM (100-3000bp).

A11.6 Stability of housekeeping gene (β-actin) expression
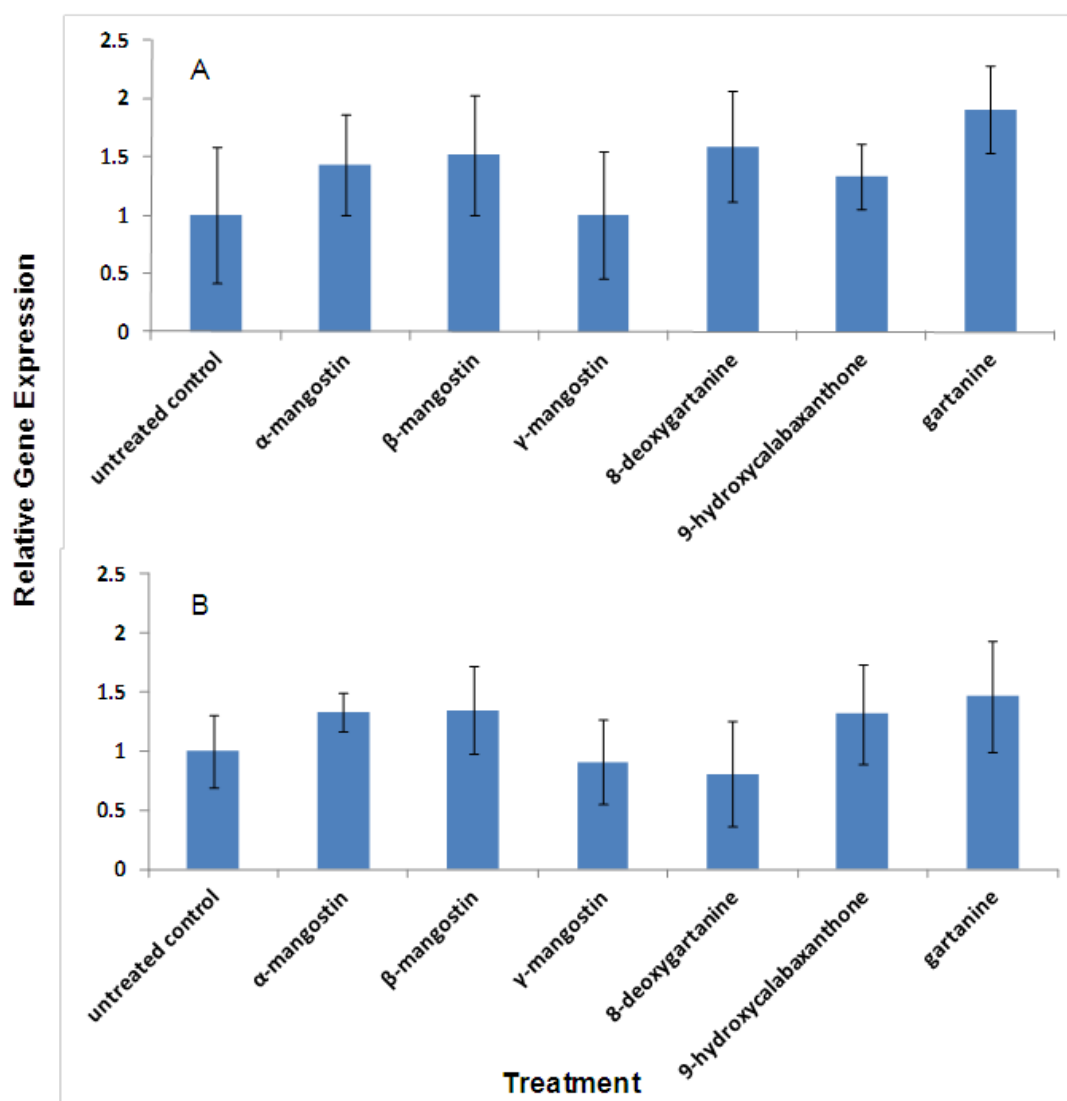
Figure A-15

Expression of β-actin in (A) human melanoma SK-MEL-28 and (B) human squamous cell carcinoma A-431 cells after 48 h treatment with 0 µg/ml (untreated control) or 5 µg/ml of α-mangostin, β-mangostin, γ-mangostin, 8-deoxygartanine, 9-hydroxycalabaxanthone, and gartanine, respectively. Quantitative data calculated using Q-gene software, normalised against untreated control. The data are presented as mean ± SEM of 4 independent experiments with 3 technical replicates for each condition.

A11.7 Reproducibility of qRT-PCR

Table A-4

Intra- and inter-run coefficients of variation (CV) of qRT-PCR.

Primers	Intra-run CV (%)	Inter-run CV (%)
Cytochrome c	15.3	16.3
Bcl-2	11.2	31.6
Bax	7.3	22.7
P21WAF1	8.1	13.5
Cyclin D1	13.9	24.4
NFκB	16.4	23.3
IκBα	4.4	12.1
BRAF V600E	9.8	29.2
Akt1	12.3	20.4
MMP-2	18.9	26.2
MMP-9	17.2	21.7
β-Actin	12.7	26.2

A11.8 One example of qRT-PCR standard curve

A11.8.1 Standard curve

$$y = -1.412\ln(x) + 13.527$$
$$R^2 = 0.9971$$
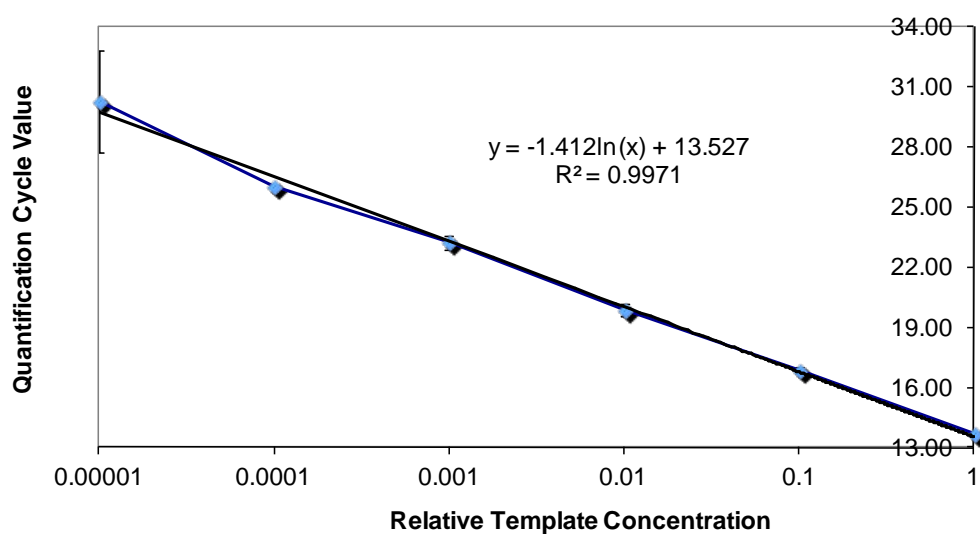
Figure A-16

One example of standard curve derived from qRT-PCR for β-actin. Assays run in triplicates for each dilution of cDNA over 6 orders of magnitude. No template control in triplicates was also included. Results are shown as mean ± SEM.

A11.8.2 Amplification efficiency (AE)

AE=EXP (-1/slope of standard curve)
   =EXP (-1/-1.412)
   =2.03

A11.9 One example of raw data of qRT-PCR standard curve
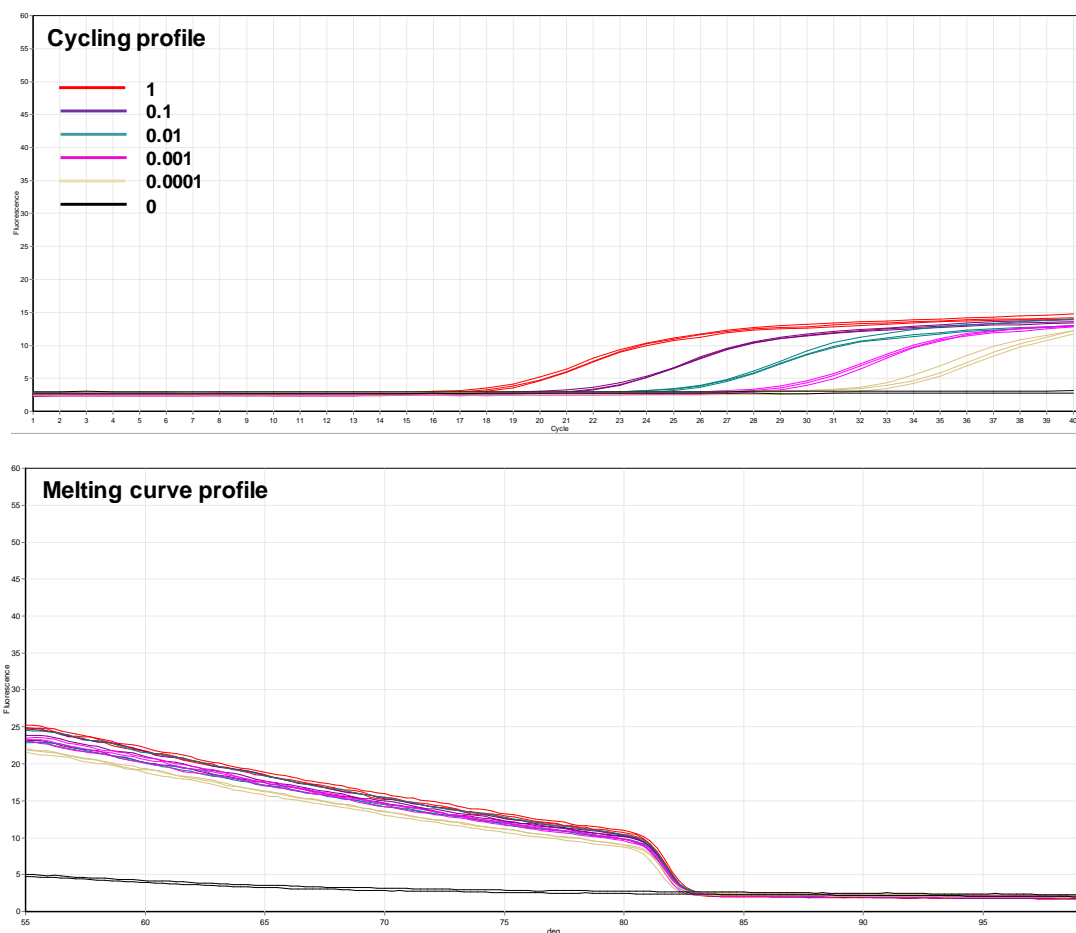
Figure A-17
One example of raw data of qRT-PCR standard curve for β-actin using untreated SK-MEL-28 cells. Assays run in triplicates for each dilution of cDNA over 5 orders of magnitude. No template control in triplicates was also included.

A11.10   qRT-PCR melt curve for each gene
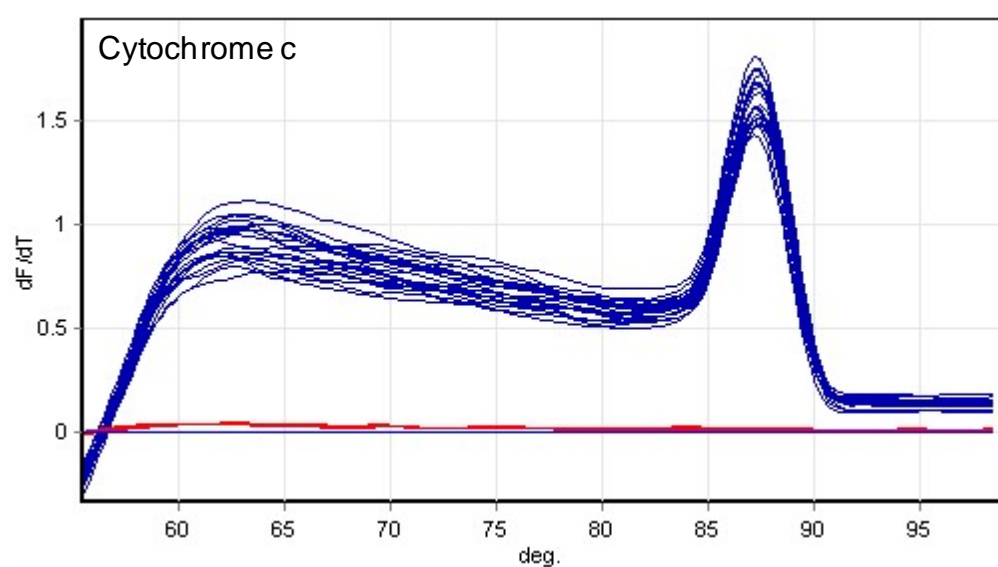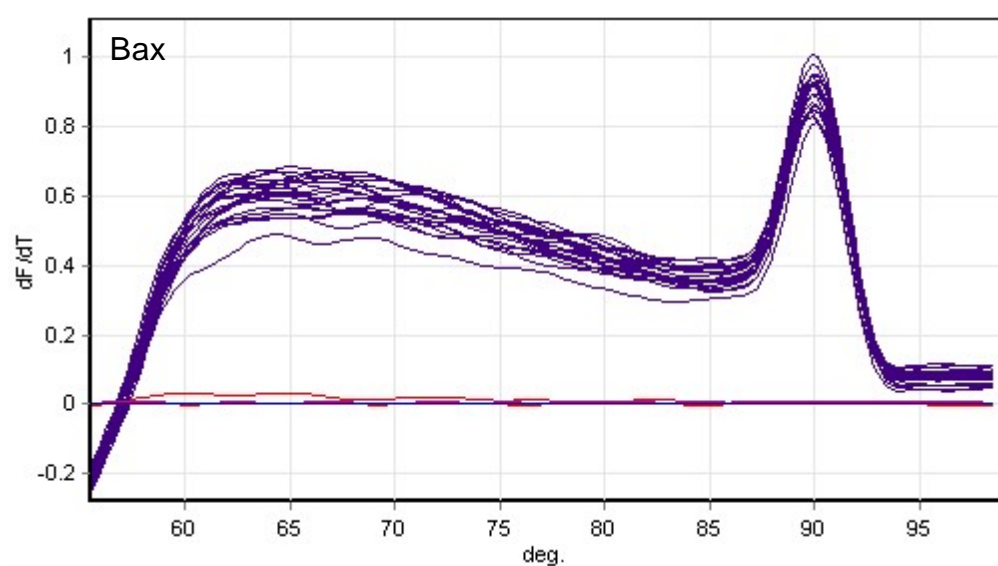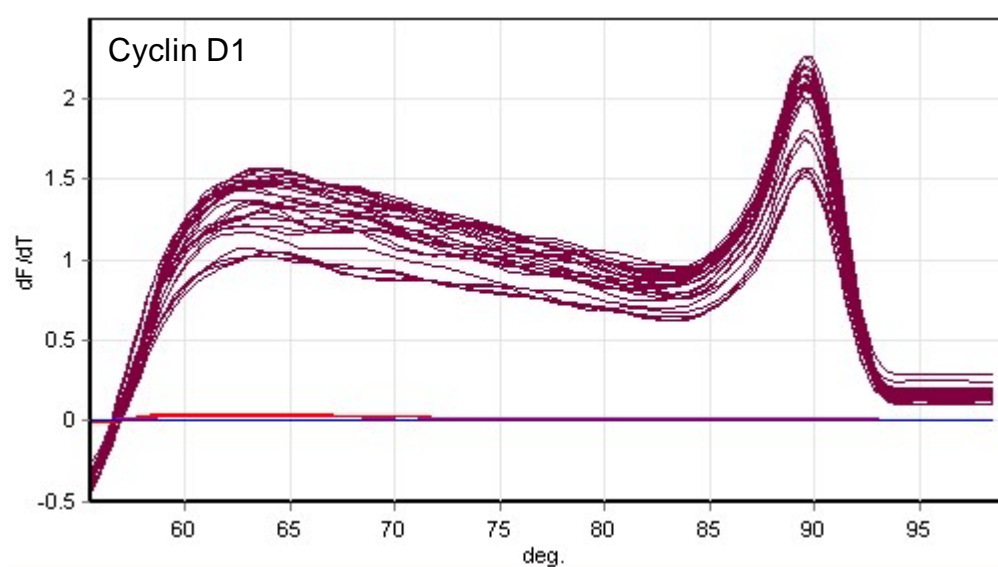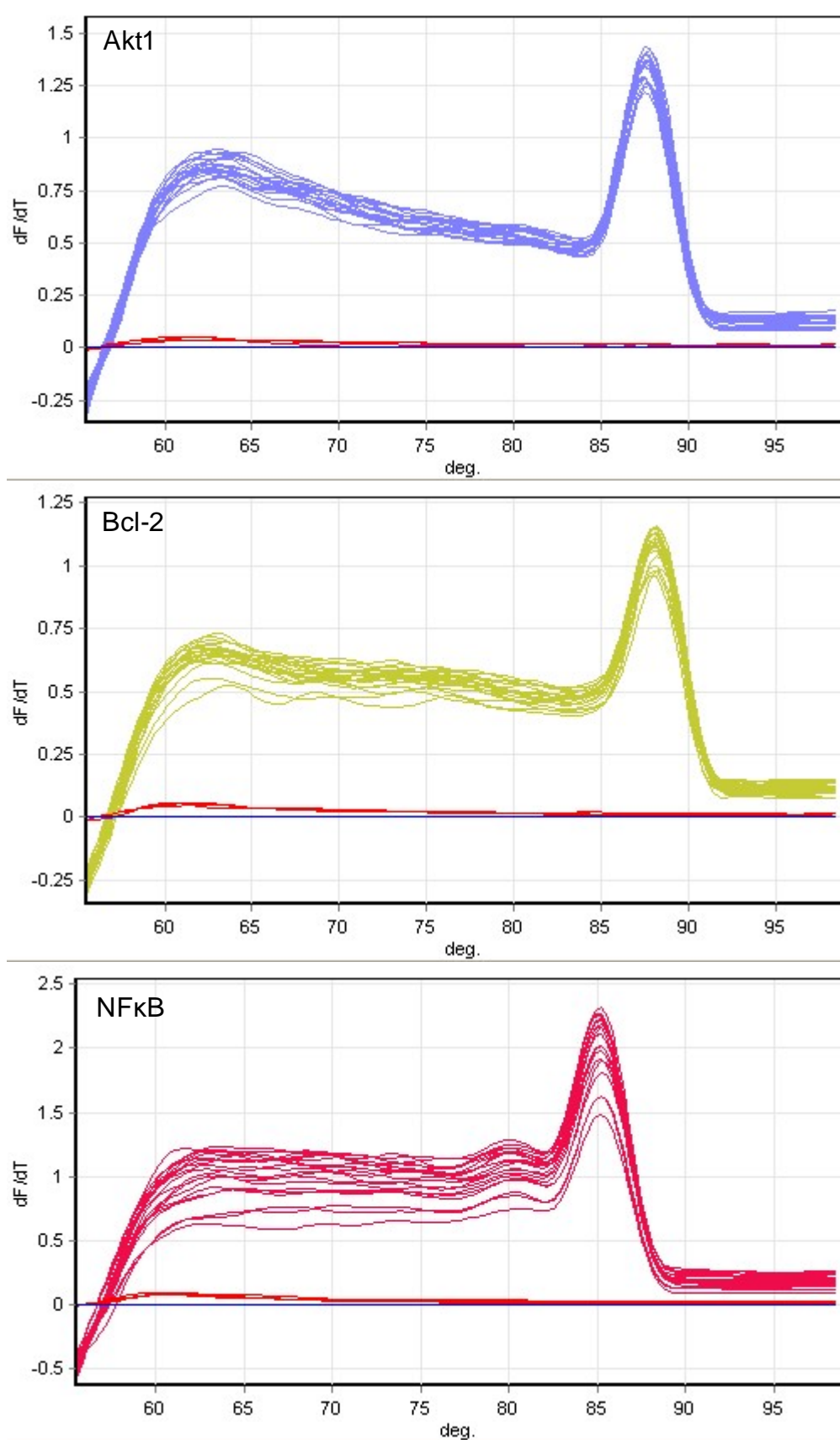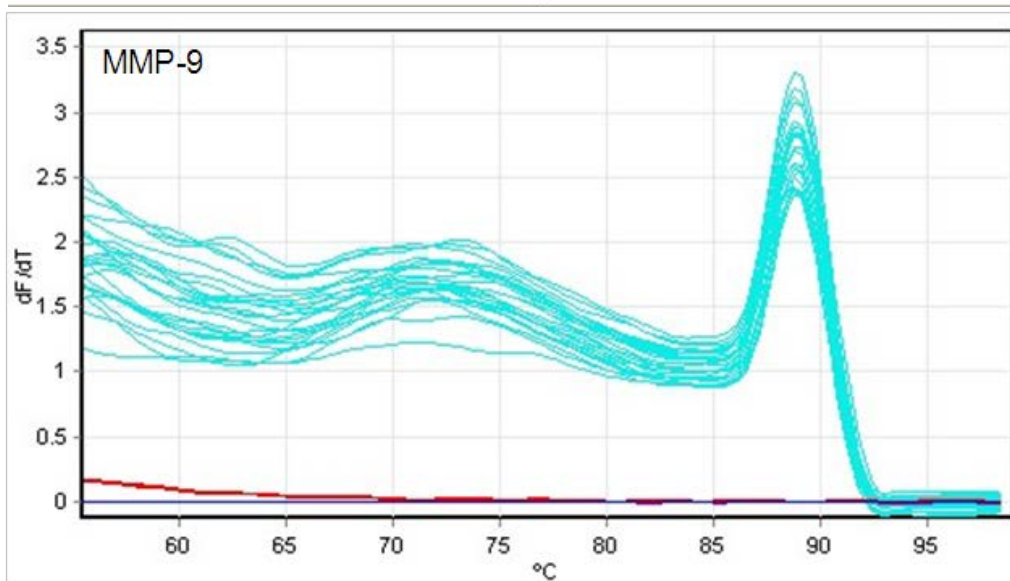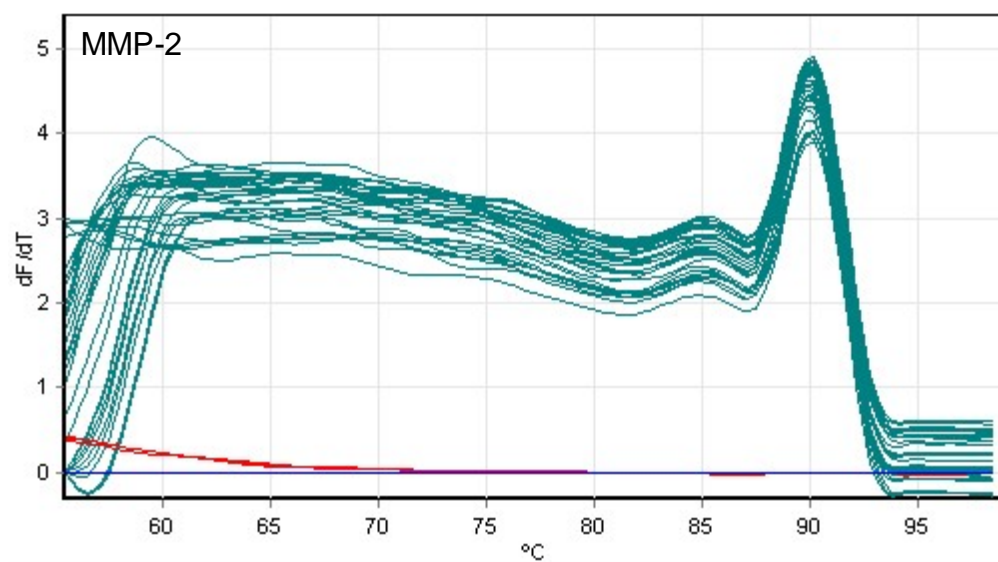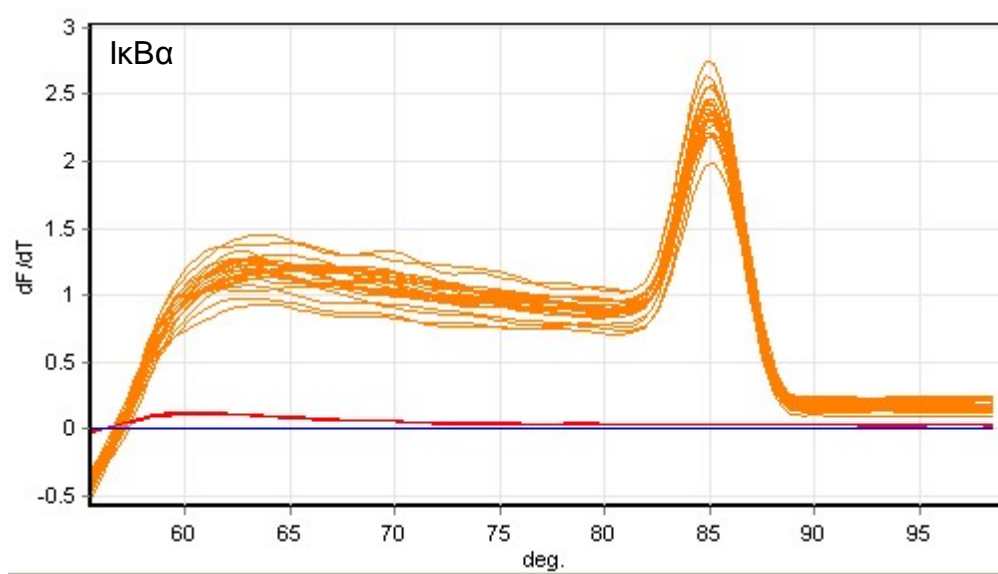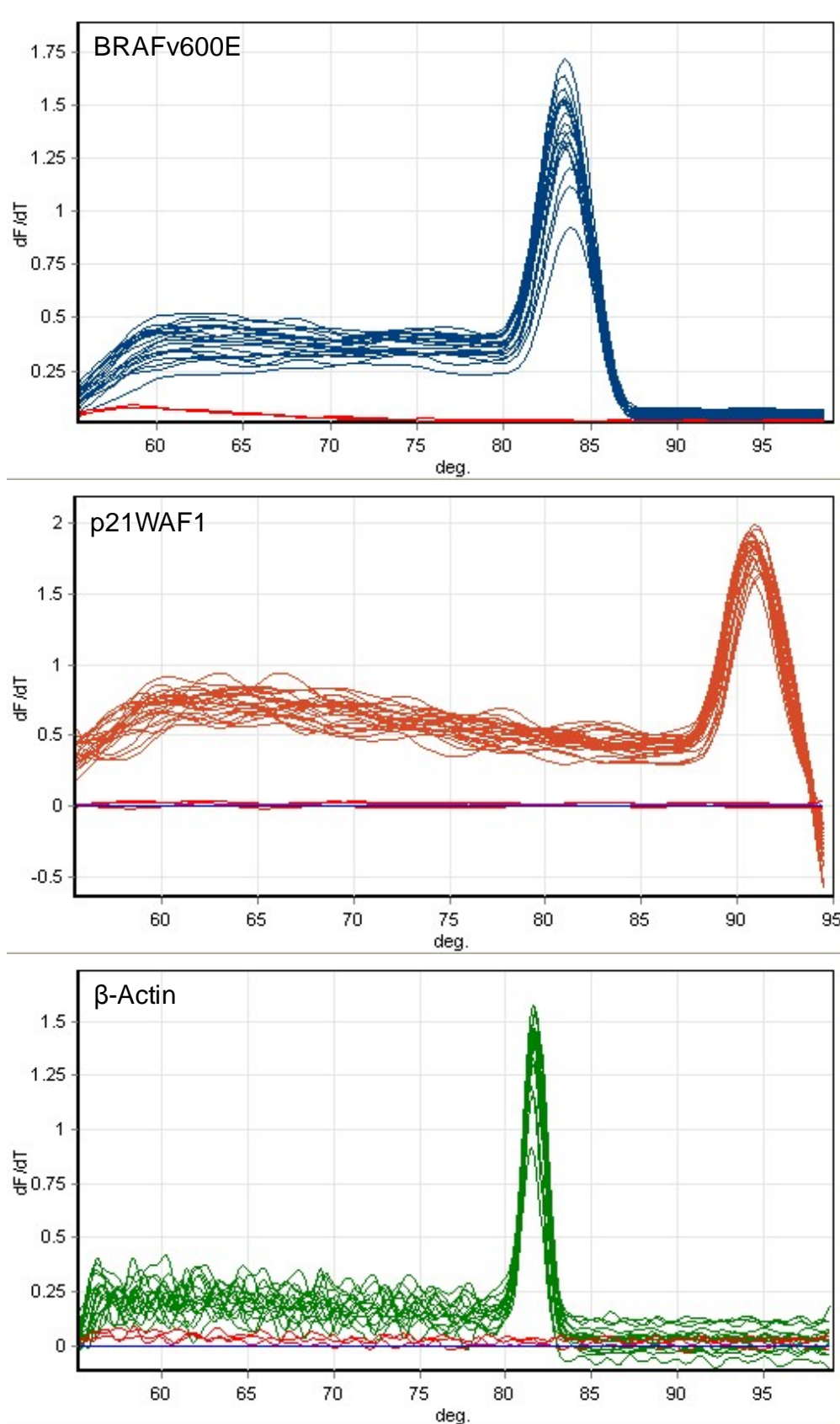
Figure A-18

Melt curve analysis of each gene amplicon as analysed using the Rotergene 3000 software. A no-template control (NTC) was included in the qRT-PCR assay for each primer set. NTC produced no amplicon or primer dimerisation (NTC).

## A12 Cytotoxicity of α-mangostin at low concentrations on A-431 and SK-MEL-28 cells
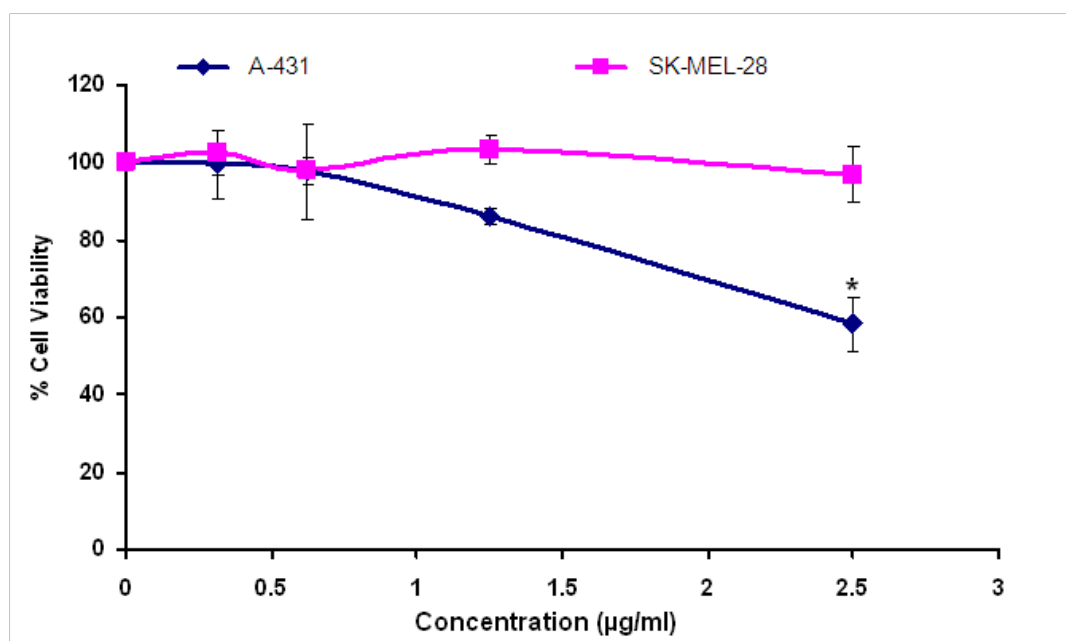
Figure A-19

Effect of α-mangostin on the cell viability was determined by the Crystal Violet assay after 48 h treatment of A-431 and SK-MEL-28 cells with various concentrations of α-mangostin. Data are shown as % viability compared to the untreated control and are presented as the mean ± SEM of three independent experiments. Treatments significantly different from the untreated control at $P < 0.05$ are presented as * and at $P < 0.01$ as **.